DISSERTATION

REVEALING THE CONTROLS OF MICROBIAL NITROUS OXIDE (N_2O) PRODUCTION AND CONSUMPTION USING STABLE ISOTOPE METHODS

Submitted by

Emily R. Stuchiner

Graduate Degree Program in Ecology

In partial fulfillment of the requirements

For the Degree of Doctor of Philosophy

Colorado State University

Fort Collins, Colorado

Fall 2021

Doctoral Committee:

Advisor: Joseph C. von Fischer

Jill Baron
M. Francesca Cotrufo
Alan Knapp

ABSTRACT

REVEALING THE CONTROLS OF MICROBIAL NITROUS OXIDE (N_2O) PRODUCTION AND CONSUMPTION USING STABLE ISOTOPE METHODS

Of the three primary anthropogenic greenhouse gases that contribute to climate change, carbon dioxide (CO_2), methane (CH_4), and nitrous oxide (N_2O), N_2O remains the most understudied. While N_2O is the least abundant greenhouse gas of the three, it is also the most potent. N_2O has a warming potential ~300x greater than CO_2 and ~34x greater than CH_4, and it is the primary stratospheric ozone depleting substance. Globally, the majority of N_2O is emitted from soils through abiotic and microbial processes, but primarily through microbial metabolism. Microbes oxidize or reduce inorganic N as an energy source through different metabolic processes; they emit N_2O as a byproduct of these processes. Microbes can also consume N_2O by biochemically reducing it to N_2, a harmless non greenhouse gas. However, the factors that regulate N_2O production and consumption processes are diverse, interactive, and subject to rapid spatial and temporal changes. Drivers of N_2O production and consumption include climate features, edaphic properties, and soil microbial community composition and activity. Characterizing these properties in relation to N_2O flux behaviors requires a suite of measurements, and the way these factors interact to effect N_2O production and consumption remain elusive. Furthermore, isotopic strategies exist to measure different N_2O production processes and N_2O consumption, but these strategies have been limited in their scope and capacity due to analytical constraints. Together, these challenges have limited our understanding of N_2O production and consumption processes. These limitations have made it difficult to

robustly disentangle the sources of N_2O and understand the importance of N_2O consumption in different soils. However, to curtail N_2O emissions, we must be able to better understand and anticipate the drivers of N_2O fluxes.

In my dissertation, I seek to better understand what drives N_2O production and consumption in diverse soils. In this work, I deploy innovative methods to measure different N_2O production processes, and I seek to more granularly understand what controls N_2O consumption. In Chapter 2 I develop a calibration algorithm for a high-throughput, novel, laser-based N_2O isotopic analyzer. This allows for direct measurement of diverse microbial N_2O-generating source processes. In Chapter 3 I use paired natural abundance and isotopic enrichment approaches to disentangle among N_2O production processes more robustly. It will be useful for researchers to deploy paired isotopic strategies to discern more precisely which microbial process(es) are generating N_2O. In Chapter 4, I shifted focus from N_2O production to better understanding N_2O consumption. Here, I sought to stimulate N_2O consumption by amending soils with a specific blend of organic acids, and using isotope pool dilution, I learned that microbes consume more N_2O when they are freed from electron donor limitation. In Chapter 5, I amended soils with different amounts of organic acids to further explore this electron donor limitation to N_2O consumption. I learned that a variety of N_2O flux responses can emerge from OC amendment, suggesting that perhaps our understanding of the drivers of N_2O reduction are less resolved then we previously might have thought.

Human activities have only exacerbated, and are poised to continue to exacerbate, N_2O emissions through agricultural practices and industrial activities. There is burgeoning recognition of the importance in managing CO_2 and CH_4 emissions to mitigate the worst impacts of climate change, but the urgency for N_2O, despite its potency and increasing atmospheric emissions, still

lags. We must continue to advance understanding of the drivers of N_2O production and consumption from soils, and my research makes strides to do this. This will be critical to effectively managing this highly potent greenhouse gas in a global climate that needs to make immediate, and dramatic, greenhouse gas reductions. A proposed Global Denitrification Research Network offers the potential for concerted, coordinated, and systematic N_2O research to address the challenge of decreasing N_2O emissions.

ACKNOWLEDGEMENTS

First and foremost, I'd like to thank my advisor, Joe von Fischer for being the best advisor I could possibly have asked for. Thank you for always making yourself available to me, even when we didn't have a meeting scheduled. Thank you for regularly letting me stick around and continue to bombard you with questions even after our scheduled meeting time was over. Thank you for *answering* all my questions, assuaging my fears that my project would come to fruition, and always convincing me that we would figure out the problems plaguing the LGR. Thank you for helping me become a better writer and public speaker. Thank you so much for teaching me about work-life balance and thank you for always reminding me that prioritizing my work over myself is a choice. Thank you for driving your convertible to the field that one time with the FREUDE license plate because that is indelibly seared into my brain now. Things like that have taught me how to imbue joy into the scientific process. You have taught me how to be a scientist and I am proud that moving forward in my career, I will think more like you.

I would also like to thank my wonderful committee, Francesca Cotrufo, Jill Baron, and Alan Knapp for your support, feedback on my work, help coordinating access to field sites, and so much more. Your support has been instrumental to my success, and through taking your classes and in conversations, you have all taught me so much, and made me a sharper scientist. And truly, many of my soil samples could never have been collected without your logistical help. Thank you all so much.

To my fantastic undergraduates Kelly Nelson, Torrey Stephenson, Jacob Peress, and Collin Coon, you've all been amazing. Thank you for tolerating my anal-retentive needs to stack funnels a particular way and effectively fumigate the lab space with ethanol. You have sieved my

soils, washed countless dishes, woken up at 3am for soil campaigns, and made my ability to do research so much easier. You've all been wonderful, and I am so grateful. I would like to give a particular shoutout to my very good friend Torrey Stephenson. Torrey, thank you for working tirelessly beside me for a year, thank you for asking me if I was nourishing myself on things besides coffee, and thank you for being a really wonderful friend. You have taught me what it means to be a friend and a mentor at the same time, and I'm glad that with you, I can do both. And thank you for writing me literal poetry when I was in the throes of dissertation-writing. If my eventual lab comes to fruition, I can't wait to sip green tea with you.

To my von Fischer lab-mates, though our time together was short, you were all great and you taught me so much in the year we did have together. Thank you to Charlotte Alster, Sam Dunn, and Paul Brewer. Thank you, Sam, for showing me around when I started grad school. You took your senior grad student role seriously, and I am tremendously grateful. Thank you, Paul, for showing me how to use the GC, and thank you for answering all, all, all, of my emails. Endless thanks to Charlotte for all the feedback, words of wisdom, and to this day sending me periodic texts to check in about how things are going. I am endlessly grateful to former postdoc Zach Weller, who seemed to enjoy being in the lab so much that he stuck around (now Professor Zach Weller). My calibration model chapter would not have been possible without you, and you have helped create the foundation for so much that I know about doing statistics and using statistical analysis software. Thank you.

None of my genetic research would have been possible without the support of the Trivedi lab. I am endlessly grateful to Pankaj Trivedi, Kristen Otto, and Abbey Thompson. Thank you all for patiently showing me pretty much how to do genetic work, thank you for answering all my questions, and answering my (many) emails. My work has been enriched because of your help,

and I am forever grateful for the lab skills you have taught me along the way. I am also endlessly thankful for the incredibly helpful folks at the USDA-ARS who facilitated my field work at ARDEC. In particular, thank you to Mary Smith (I always really appreciated all the kitten photos!!), Cathy Stewart, Liz Pruessner, and Steve Del Grosso. I have run countless samples for various soil assays at EcoCore, and I could never have done any of this work if it were not for the support of Guy Beresford and Dan Reuss. Thank you, Guy, for running more KCl extracts than I can imagine, and thank you for the laughs in the sample prep room. Thank you, Dan, for always bringing me back to reality about the analytical precision of an instrument and thank you for always knowing what was wrong with a piece of equipment and how to fix it. I also thank Nora Flynn and Tim Weinmann for bringing me out to your field sites. You've been instrumental to me. Some of my dissertation chapters would not have happened without your field support and know-how, and thank you, so much, for letting me collect gallons of soil. And thanks for not being weird about it when I tried to tent the soil to collect N_2O flux data (didn't work), or when I carried 50 lbs of bicycle chains up a mountain (unnecessary). Thank you so much.

I am so, so, so, grateful to the wonderful women mentors I've gotten to have while in graduate school. Meena Balgopal, Colleen Webb, and Jennifer Neuwald really took me under their wings, and I am so appreciative of the advice, thoughtful feedback, and the wonderful collaborations we've shared. Participating in Research Mentoring to Advance Inclusivity in STEM (RMAIS) was one of the greatest decisions I made, and it has expanded my way of thinking about teaching and mentoring irrevocably. Dani Lin Hunter, words will never be enough. The mentoring paper would not have been possible without you. Thank you for teaching me how to do social science research and expanding my way of thinking. You have taught me so much. And Meena, endless thanks to you. Thank you for inviting me to participate in the Science

Education Research Group (SERG) lab meetings and thank you for all the formal and informal mentoring. You have been a beacon of support.

To my caring, supportive, and highly forgiving graduate school friends – thank you. Thank you for not caring that it took me around three years to want to hang out with you guys. That's my bad. You have all been such uplifting and positive presences in my life, and whether we struggled through a class together, did research or field work together, hung out at the climbing gym, skied, hiked, biked, walked around, went on trips, generally hung out, you have all been amazing. You made graduate school fun; you really did. I would like to especially thank Amanda Cicchino, Erika Peirce, Katie Rocci, Leena Vilonen, Jenna Parker, Craig Marshall, Vincent (Vinny) Landau, Lydia Baldwin, Melissa Booher, Dani Lin Hunter, Nathan Hahn, Julian Cassano, Nathan Phipps, Carrie Tait, Olivia Hajek, Maddy Scheer, Mary Linabury, Grace Morgan, and Nico Matallana-Meja for being such great friends. You have taught me the meaning of disciplined, rigorous, work, and balancing those efforts with some amazingly fun times.

Colin, I think you were one of the best things to come out of all of this. I know you know I'm not usually at a loss for words, but the words here can't do it justice.

To my Mountain Misfits: I love you all. Thank you for facilitating ~200 days of skiing, countless desert trips, thousands of miles driven, gallons of Bloody Mary's consumed, endless laughter, and so, so, so much love. You have grounded me and kept me sane throughout this entire graduate school journey. Not a day goes by that I don't thank the universe that Walking Mountains Science Center brought us together. I don't think words can adequately express how much you all mean to me. To McCale Carter (Cale), Natalie Fioretti (Natty), Rachel Barfield (Rach), Marshall Kohls (Marshy), and Laura Robison – my OG crew, the Girls with Altitude. I love you immeasurably. To Kaylor Lodge, Alessandro ("Sandro") Molina, Kira Koppel, Josh

Pipkin, Paul Leininger, Teddy Jones, Alex Reich, Emory Strawn, and Ed Moore, I am so grateful that you moved to the Vail Valley and that we all got to become friends. You are so dear to me. Special thanks to Timmy "to try to hold on."

To mom and dad: I think we finally did it. Thank you for the countless multi-hour phone calls, thank you for always picking me up when I doubted myself, thank you for supporting me staunchly, even when you weren't quite sure what I was doing. Thank you for always telling me that I could do it, and thank you for making me feel so, so, so loved. I wouldn't be me if it weren't for you. Thank you, Jacob, for supporting me in your way. Many thanks to my wonderful and supportive family, but I especially want to thank Aunt Ida, Uncle Geoff, and Aunt Eve. Thank you for the phone calls, texts, emails, embroidery, cards, and endless support. Thanks so much for caring so much about what I've been up to these past five years. Uncle David, thank you endlessly for the countless, and also muti-hour, phone calls. Thanks for the inspiration to write that final chapter. You have helped me more than you know.

This work would not have been possible without the generous support from the Environmental Defense Fund and Graduate Degree Program in Ecology Small Research Grants.

DEDICATION

To my mom, Judy Stuchiner, who truly taught me what it means to get a PhD. Because of you, I think I did it the right way. And to my dad, Robert Stuchiner, because you had Siri read my first published paper out loud to you, all the way through.

TABLE OF CONTENTS

CHAPTER 1: INTRODUCTION

Nitrous oxide (N_2O) is a powerful greenhouse gas that has proven uniquely difficult to manage. Though N_2O currently accounts for only 6% of the net radiative forcing that warms earth's atmosphere, it is a formidable force (Ciais et al. 2013). On a per molecule basis, N_2O has a warming potential ~300x greater than carbon dioxide (CO_2) and ~34x greater than methane (CH_4) over a 100-year period (Ciais et al. 2013). It is also the primary stratospheric ozone depleting substance following the 1987 Montreal Protocol (Ravishankara et al. 2009, Kanter et al. 2012). Furthermore, N_2O comes from diffuse and diverse natural and anthropogenic sources (Butterbach-Bahl et al. 2013). Natural sources include soils, freshwater, and oceans. Anthropogenic sources include industry, transportation, biomass burning, runoff, and agriculture (Kanter et al. 2014). Globally, more than 60% of N_2O is emitted from soils, and of those emissions, more than half of them come from agriculture (Smith 2017). In fact, atmospheric N_2O emissions are projected to increase up to 30% by 2050 from agricultural sources alone (Kanter et al. 2014). As such, managing N_2O emissions from soils, especially agricultural soils, is likely to have the greatest potential for N_2O emissions reduction moving forward. Consequently, this dissertation focuses on understanding the controls over N_2O production and consumption in soils. My work aims to better understand these controls so we can develop strategies to effectively manage N_2O emissions.

Not only is N_2O a powerful greenhouse gas that comes from a multitude of different places, but it is also produced by a suite of biotic and abiotic pathways (Butterbach-Bahl et al. 2013, Heil et al. 2014, Heil et al. 2015). Biotic pathways include the microbial metabolic processes autotrophic nitrification, heterotrophic nitrification, nitrifier-denitrification,

denitrification, co-denitrification, dissimilatory nitrate reduction to ammonium (DNRA), and anaerobic ammonium oxidation (anammox; Butterbach-Bahl et al. 2013). There are also several abiotic N_2O-generating pathways, including non-microbial chemodenitrification, spontaneous hydroxylamine (NH_2OH) oxidation, chemical decomposition of nitrite (NO_2^-), and chemical decomposition of NH_2OH that is fixed to soil organic matter, although this dissertation primarily focuses on microbial sources of N_2O (Heil et al. 2014, Heil et al. 2015). To further complicate matters, microbial and abiotic processes can co-occur in soils, sometimes over fine spatial and temporal scales (Kuypers et al. 2018, McTigue et al. 2016). It can be difficult to discern which processes are responsible for collective N_2O emissions because each process is governed by an array of drivers. These drivers include climate, soil chemical and physical properties, and microbial community composition (Jenny 1980, Wrage et al. 2004, Park et al. 2011, Toyoda et al. 2015, van Groenigen et al. 2015, Congreves et al. 2019, Denk et al. 2019). Furthermore, soils are heterogeneous mixtures riddled with anoxic microsites, nutrient concentration gradients, and variations in underlying topography or landforms (Wang et al. 2019, Sihi et al. 2020). These subtle differences can contribute to variations in the amount of N_2O emitted from biotic and/or abiotic processes, which can make it difficult to discern the important sources of N_2O from a given soil. Microbial metabolism can also consume N_2O from soil pores by biochemically reducing it to N_2 gas as the final step in denitrification (Chapuis-Lardy et al. 2007). The fact that microbes can consume N_2O in addition to producing it adds complexity to the driving forces that regulate how much N_2O a given soil or ecosystem emits. In sum, N_2O emitted from a given soil could be derived from a vast array of processes, and the variability in flux rates could be driven by N_2O production *and* N_2O consumption.

This complexity has allowed a number of basic and applied questions to persist regarding N_2O emissions, leaving variation in the emission rates difficult to predict and to manage. I address some of these questions in my dissertation. Notably, I hope to better elucidate which processes are responsible for N_2O emissions and how does this vary with soil moisture; what are the drivers of N_2O consumption; if N_2O consumption can be stimulated to reduce net N_2O emissions; and what controls the response of N_2O consumption and emission to additions of organic carbon.

To address these questions, there need to be tools in place to measure all these different biotic and abiotic pathways that can produce or consume N_2O. Natural abundance stable isotope approaches have been used for a long time to measure broad sources of N_2O. The bulk ^{15}N isotopic composition of N_2O has been measured for decades to identify if the source of the gas is natural or anthropogenic, or microbially derived (Hogberg et al. 1997). In the last twenty years, researchers have begun taking advantage of the isotopic complexity of N_2O to partition among microbial and abiotic sources (Yoshida and Toyoda 2000, Ostrom and Ostrom 2017). If researchers can determine the unique isotopic fingerprint of each N_2O-generating process, they can more effectively disentangle these processes and better understand what drives N_2O emissions from different soils. Although N_2O is a simple linear molecule – a nitrogen (N) atom attached to an N atom attached to an oxygen (O) atom – it possesses great potential for isotopic complexity because N has two stable isotopes and O has three. The central position N atom is referred to as the α position, whereas the terminal position N atom is referred to as the β position, and either of these atoms can have the abundant ^{14}N atom or the rarer ^{15}N. Similarly, the O atom can be the common ^{16}O isotope, the rarer ^{18}O, or the very rare ^{17}O. Together, this generates 12 possible isotopic versions, or isotopocules, of N_2O (Ostrom and Ostrom 2017). The relative

abundances of these isotopic versions of N_2O can be influenced by biotic and abiotic reactions associated with N_2O production and consumption (Decock and Six 2013). When the masses of the different isotopic versions of N_2O are the same, we refer to these as isotopomers ($^{15}N^{14}N^{16}O$ vs. $^{14}N^{15}N^{16}O$), and when the masses of the different isotopic versions differ, we refer to those as isotopologues ($^{14}N^{14}N^{16}O$ vs. $^{15}N^{14}N^{16}O$). Though very rare, there are also multiply substituted ("clumped") isotopes, in which more than one isotopically heavy atom is contained in the N_2O molecule (e.g., $^{15}N^{14}N^{18}O$; Ostrom and Ostrom 2017).

Despite the potential to gain information about N_2O transformations from these isotopic patterns, the challenge lies in measuring these different isotopic versions of N_2O, particularly since many of them are present at very low abundances in nature (Yamamoto et al. 2014). There are several different analytical approaches for determining natural abundance N_2O isotopes. Researchers measure the bulk ^{15}N or ^{18}O abundances in emitted N_2O (Yoshinari and Wahlen 1985, Yoshida et al. 1989), or they measure position-specific enrichment, the abundance of ^{15}N enrichment in the α or β position of the emitted N_2O (Yoshida and Toyoda 2000). Position specific measurements can be used to calculate intramolecular site preference (SP), which is the difference in $^{15}N^{\alpha}$ and $^{15}N^{\beta}$ enrichment in the emitted N_2O (Yoshida and Toyoda 2000). A growing body of literature has shown that certain microbial N_2O-generating processes reliably yield consistent SP values, and that we can use these SP signatures to infer which microbial process(es) generated N_2O from a given soil (Sutka et al. 2006, Baggs 2008, Heil et al. 2014, Maeda et al. 2015). Some efforts have been made to quantify abundances of clumped isotopes, but this requires very high instrumental analytical precision and is still a developing area of research (Eiler et al. 2007, Ostrom and Ostrom 2017).

Alternatively, isotopic enrichment has proved to be a robust strategy for quantifying both N_2O production and consumption processes (Groffman et al. 2006, Schmidt et al. 2011). Enrichment can be used to partition between two of the broadest classes of N_2O-generating processes: nitrification and denitrification (Well et al. 2006). By amending soils with either ^{15}N-labelled ammonium (NH_4^+) or ^{15}N-labelled nitrate (NO_3^-), one can trace the label into the emitted N_2O and determine if the N_2O was emitted via NH_4^+ oxidation (nitrification) or NO_3^- reduction (denitrification). While this has the advantage of being relatively unambiguous, it presents an important tradeoff with natural abundance measurements. Low atmospheric N_2O concentrations contribute to even lower natural abundance isotopic signatures, which can make natural abundance quantification noisy and less robust, but the capacity to measure multiple N_2O production pathways is greater (Stuchiner et al. 2020). Dissimilarly, isotopic enrichment can only partition between nitrification and denitrification, just two N_2O production processes (Wrage et al. 2004, Wrage et al. 2018). However, this increases the precedent for doing more paired natural abundance and isotopically enriched work, to better understand the amount of information these methods solely and in conjunction can provide. Nonetheless, a strength of isotopic enrichment is that it can be used to measure the lesser studied process N_2O consumption. By injecting isotopically labelled $^{15}N_2O$ into the headspace of an incubation system, one can measure the disappearance of the bulk $^{15}N_2O$ to directly quantify N_2O consumption (von Fischer and Hedin 2002, Yang et al. 2011).

There are two primary instrumental approaches to quantifying isotopocules of N_2O: gas chromatography isotope ratio mass spectrometry (GC-IRMS), and laser-based spectroscopy. GC-IRMS involves the combustion and reduction of N_2O to N_2, in addition to several N_2O ionization steps to determine SP. This method is usually robust, but it suffers from analytical challenges

related to ion “rearrangement” and numerous mass overlap corrections, in addition to onerous sample preparation, which can make these measurements, particularly for isotopomers or clumped isotopes, prohibitively expensive (Ostrom and Ostrom 2017). Laser-based analyzers use absorption spectroscopy to quantify different isotopocules of N_2O. As Beer’s law states, the concentration of a particular isotopocule of N_2O is proportional to the strength of absorption of a specific wavelength of laser light through the gas. Laser-based analyzers have become more broadly available in the last decade, which is ideal for streamlining the N_2O isotope research pipeline, as these instruments are high throughput and tend to have greater ease of measurement than GC approaches (Ostrom and Ostrom 2017, Stuchiner et al. 2020). Laser-based instruments do have analytical precision issues that have hindered their use and popularity, such as optical peak broadening from other greenhouse gases in the sample stream and weak absorption from samples with low N_2O concentrations, but these issues are being addressed (Stuchiner et al. 2020). Fortunately, isotopically enriched samples have fewer of these analytical precision issues, owing to higher signal to noise ratios compared to natural abundance samples, but unfortunately, studies using isotopic enrichment to quantify different isotopocules of N_2O remain rare (Bracken et al. 2021).

For my research, I have used diverse (natural abundance, isotopic enrichment, and isotope pool dilution) approaches to disentangle among microbial sources of N_2O, and I have used novel laser-based instrumentation to carry out this work. In addressing the specific questions listed above, my research contributes to the investigation of three broad questions: (1) What strategies do we have to robustly measure N_2O production and consumption processes? (2) What are the most important processes driving N_2O fluxes from soils? (3) How can we effectively manage N_2O emissions, given its diffuse and diverse sources?

I address these broad questions in my four dissertation chapters. In Chapter 2, I developed a calibration algorithm for a laser-based N_2O isotopic analyzer. This analyzer was used to quantify and disentangle different microbial N_2O-producing and consuming processes in my subsequent chapters. I determined that calibrating bulk N_2O and isotopocule concentrations in ranges helped give rise to high-precision calibration. In Chapter 3 I address the specific question of which processes drive N_2O emissions from soils. Specifically, I used a dual-isotopic approach to determine which microbial process(es) were generating N_2O emissions from different soils. I measured emitted N_2O from soils amended with ^{15}N labelled NH_4^+ or NO_3^- and I measured intramolecular SP from emitted N_2O of soils held at natural abundance. I determined that denitrification was pervasive among soils, and I join the growing body of literature in supporting the idea that denitrification is the most prevalent microbial N_2O-generating source process (Harris et al. 2021). I addressed which processes drive N_2O fluxes in Chapters 4 and 5 by studying the microbial process N_2O consumption. In Chapter 4 I focused on amending soils with electron donors in the form of organic acids to stimulate N_2O consumption. Given that denitrification is such a ubiquitous process in soils, it would be ideal from a greenhouse gas management perspective to be able to control its terminal step, $N_2O \rightarrow N_2$ reduction. I learned that certain soils could increase N_2O consumption and decrease N_2O emissions if they attained an appropriate electron donor-acceptor balance. However, certain soils might be electron-donor limited and could require additional organic acids to show this behavior. My fifth chapter followed up on this, and I amended soils with successively more organic acids to release all soils tested from electron donor limitation to N_2O consumption. I learned that the balance of electron donors and acceptors must accommodate complete denitrification, in that if soils are amended

with electron donors but are not limited by electron acceptors, N_2O consumption will be less likely to occur. Throughout chapters 2-5, I strive to address the question, how can we effectively manage N_2O emissions?

This dissertation makes strides towards improving our capacity to measure, predict, and manage N_2O production and consumption processes. I address which microbial processes are important to manage to curtail N_2O emissions, and I discuss which environmental and microbial properties govern these processes. In my efforts to make this work broadly available to the scientific community, I have published Chapter 2 in Rapid Communications in Mass Spectrometry. Chapter 3 is in revision at JGR: Biogeosciences. Chapter 4 was recently submitted to Global Change Biology, and I intend to submit Chapter 5 for publication shortly. In sum, wading through the complexity that underpins N_2O production and consumption processes is critical for moving towards a future with reduced anthropogenic greenhouse gas emissions.

CHAPTER 1 REFERENCES

Baggs, E. M. (2008). A review of stable isotope techniques for N2O source partitioning in soils: recent progress, remaining challenges, and future considerations. *Rapid Communications in Mass Spectrometry : RCM*, *22*(22), 1664–1672. https://doi.org/10.1002/rcm

Bracken, C. J., Lanigan, G. J., Richards, K. G., Müller, C., Tracy, S. R., Grant, J., … Murphy, P. N. C. (2021). Source partitioning using N2O isotopomers and soil WFPS to establish dominant N2O production pathways from different pasture sward compositions. *Science of the Total Environment*, *781*, 146515. https://doi.org/10.1016/j.scitotenv.2021.146515

Butterbach-Bahl, K., Baggs, E. M., Dannenmann, M., Kiese, R., & Zechmeister-Boltenstern, S. (2013). Nitrous oxide emissions from soils: how well do we understand the processes and their controls? *Philosophical Transactions of the Royal Society of London.*, *368*(1621), 20130122. https://doi.org/10.1098/rstb.2013.0122

Ciais, P., Sabine, C., Bala, G., Bopp, L., Brovkin, V., Canadell, J., … Thornton, P. (2013). The physical science basis. Contribution of working group I to the fifth assessment report of the intergovernmental panel on climate change. *Change, IPCC Climate*, 465–570. https://doi.org/10.1017/CBO9781107415324.015

Decock, C., & Six, J. (2013). How reliable is the intramolecular distribution of 15N in N2O to source partition N2O emitted from soil? *Soil Biology and Biochemistry*, *65*(2), 114–127. https://doi.org/10.1016/j.soilbio.2013.05.012

Denk, T. R. A., Kraus, D., Kiese, R., Butterbach-Bahl, K., & Wolf, B. (2019). Constraining N cycling in the ecosystem model LandscapeDNDC with the stable isotope model SIMONE. *Ecology*, *100*(5), 1–15. https://doi.org/10.1002/ecy.2675

Eiler, J. M. (2007). "Clumped-isotope" geochemistry-The study of naturally-occurring, multiply-substituted isotopologues. *Earth and Planetary Science Letters*, *262*(3–4), 309–327. https://doi.org/10.1016/j.epsl.2007.08.020

Groffman, P. M., Altabet, M. a., Bohlke, J. K., Butterbach-Bahl, K., David, M. B., Firestone, M. K., … Voyteck, M. a. (2006). Methods for Measuring Denitrification : *Ecological Applications*, *16*(December), 2091–2122.

Heil, J., Liu, S., Vereecken, H., & Brüggemann, N. (2015). Abiotic nitrous oxide production from hydroxylamine in soils and their dependence on soil properties. *Soil Biology and Biochemistry*, *84*, 107–115. https://doi.org/10.1016/j.soilbio.2015.02.022

Heil, J., Wolf, B., Brüggemann, N., Emmenegger, L., Tuzson, B., Vereecken, H., & Mohn, J. (2014). Site-specific< sup> 15</sup> N isotopic signatures of abiotically produced N< sub> 2</sub> O. *Geochimica et Cosmochimica Acta*, *139*, 72–82.

Hogberg, P. (1997). Tansley Review No. 95 15N natural abundance in soil-plant systems. *New Phytologist*, *137*(2), 179–203.

Jenny, H. (1980). *The soil resource*.

Maeda, K., Spor, A., Edel-Hermann, V., Heraud, C., Breuil, M.-C., Bizouard, F., … Philippot, L. (2015). N2O production, a widespread trait in fungi. *Scientific Reports*, *5*(1), 9697. https://doi.org/10.1038/srep09697

McTigue, N. D., Gardner, W. S., Dunton, K. H., & Hardison, A. K. (2016). Biotic and abiotic controls on co-occurring nitrogen cycling processes in shallow Arctic shelf sediments. *Nature Communications*, *7*, 13145. https://doi.org/10.1038/ncomms13145

Ostrom, N. E., & Ostrom, P. H. (2017). Mining the isotopic complexity of nitrous oxide: a review of challenges and opportunities. *Biogeochemistry*, *132*(3), 359–372. https://doi.org/10.1007/s10533-017-0301-5

Park, S., Perez, T., Boering, K. A., Trumbore, S. E., Gil, J., Marquina, S., & Tyler, S. C. (2011). Can N2O stable isotopes and isotopomers be useful tools to characterize sources and microbial pathways of N2O production and consumption in tropical soils? *Global Biogeochemical Cycles*, *25*(1), 1–16. https://doi.org/10.1029/2009GB003615

Schmidt, C. S., Richardson, D. J., & Baggs, E. M. (2011). Constraining the conditions conducive to dissimilatory nitrate reduction to ammonium in temperate arable soils. *Soil Biology and Biochemistry*, *43*(7), 1607–1611. https://doi.org/10.1016/j.soilbio.2011.02.015

Smith, K. A. (2017). Changing views of nitrous oxide emissions from agricultural soil: key controlling processes and assessment at different spatial scales. *European Journal of Soil Science*, *68*(2), 137–155. https://doi.org/10.1111/ejss.12409

Stuchiner, E. R., Weller, Z. D., & Fischer, J. C. (2020). An approach for calibrating laser-based N 2 O isotopic analyzers for soil biogeochemistry research . *Rapid Communications in Mass Spectrometry*, (June 2020), 1–14. https://doi.org/10.1002/rcm.8978

Sutka, R. L., Ostrom, N. E., Ostrom, P. H., Breznak, J. A., Gandhi, H., Pitt, A. J., & Li, F. (2006). Distinguishing Nitrous Oxide Production from Nitrification and Denitrification on the Basis of Isotopomer Abundances. *Applied and Environmental Microbiology*, *72*(1), 638–644. https://doi.org/10.1128/AEM.72.1.638

Toyoda, S., Yoshida, N., & Koba, K. (2015). Isotopocule analysis of biologically produced nitrous oxide in various environments. *Mass Spectrometry Reviews*, *36*, 135–160. https://doi.org/10.1002/mas

Van Groenigen, J. W., Huygens, D., Boeckx, P., Kuyper, T. W., Lubbers, I. M., Rütting, T., & Groffman, P. M. (2015). The soil n cycle: New insights and key challenges. *Soil*, *1*(1), 235–256. https://doi.org/10.5194/soil-1-235-2015

von Fischer, J. C., & Hedin, L. O. (2002). Separating methane production and consumption with a field-based isotope pool dilution technique. *Global Biogeochemical Cycles*, *16*(3), 8-1-8–13. https://doi.org/10.1029/2001gb001448

Well, R., & Flessa, H. (2009). Isotopologue signatures of N2O produced by denitrification in soils. *Journal of Geophysical Research: Biogeosciences*, *114*(2), 1–11. https://doi.org/10.1029/2008JG000804

Well, R., Kurganova, I., De Gerenyu, V. L., & Flessa, H. (2006). Isotopomer signatures of soil-emitted N2O under different moisture conditions - A microcosm study with arable loess soil. *Soil Biology and Biochemistry*, *38*(9), 2923–2933. https://doi.org/10.1016/j.soilbio.2006.05.003

Wrage-Mönnig, N., Horn, M. A., Well, R., Müller, C., Velthof, G., & Oenema, O. (2018). The role of nitrifier denitrification in the production of nitrous oxide revisited. *Soil Biology and Biochemistry*, *123*(April), A3–A16. https://doi.org/10.1016/j.soilbio.2018.03.020

Wrage, N., Lauf, J., del Prado, A., Pinto, M., Pietrzak, S., Yamulki, S., … Gebauer, G. (2004). Distinguishing sources of N2O in European grasslands by stable isotope analysis. *Rapid Communications in Mass Spectrometry*, *18*(11), 1201–1207. https://doi.org/10.1002/rcm.1461

Yamamoto, A., Uchida, Y., Akiyama, H., & Nakajima, Y. (2014). Continuous and unattended measurements of the site preference of nitrous oxide emitted from an agricultural soil using quantum cascade laser spectrometry with intercomparison with isotope ratio mass

spectrometry. *Rapid Communications in Mass Spectrometry*, *28*(13), 1444–1452. https://doi.org/10.1002/rcm.6916

Yang, W. H., Teh, Y. A., & Silver, W. L. (2011). A test of a field-based 15N-nitrous oxide pool dilution technique to measure gross N2O production in soil. *Global Change Biology*, *17*(12), 3577–3588. https://doi.org/10.1111/j.1365-2486.2011.02481.x

Yoshida, N., & Toyoda, S. (2000). Constraining the atmospheric N2O budget from intramolecular site preference in N2O isotopomers. *Nature*, *405*(6784), 330–334. https://doi.org/10.1038/35012558

Yoshida, N., Morimoto, H., Hirano, M., Koike, I., Matsuo, S., Wada, E., … Hattori, A. (1989). Nitrification rates and 15N abundances of N2O and NO3- in the western North Pacific. *Nature*, *342*(6252), 895–897. https://doi.org/10.1038/342895a0

Yoshinari, T., & Wahlen, M. (1985). Oxygen isotope ratios in N2 bO from nitrification at a wastewater treatment facility. *Nature*, *317*(6035), 349–350. https://doi.org/10.1038/317349a0

CHAPTER 2: AN APPROACH FOR CALIBRATING LASER-BASED N_2O ISOTOPIC ANALYZERS FOR SOIL BIOGEOCHEMISTRY RESEARCH[1]

1. Summary

Rationale: Technological advances have motivated researchers to transition from traditional gas chromatography/isotope ratio mass spectrometry to rapid, high- throughput, laser-based instrumentation for N_2O isotopic research. However, calibrating laser-based instruments to yield accurate and precise isotope ratios has been an ongoing challenge. To streamline the N_2O isotope research pipeline, I developed the calibration protocol for laser-based analyzers described here. While my approach is targeted at laboratory soil incubations, I anticipate that it will be broadly applicable for diverse types of stable isotope research.

Methods: I prepared standards diluted from USGS52 and from a commercial cylinder to develop a calibration curve spanning from 0.3 to 300 ppm N2O. To calibrate over this broad range, I binned each isotopocule (N_2O, $N^{15}NO$, ^{15}NNO, and $NN^{18}O$) into low, medium, and high concentration ranges and then used mathematically similar polynomial functions to calibrate the isotopocules within each concentration range. I also assessed the temporal stability of the instrument and the capacity for my calibration approach to work with isotopically enriched gas samples.

Results: My calibration approach yielded generally accurate and precise data when isotopocules were calibrated in concentration ranges, and the measurements appeared to be temporally stable. For all isotopocules at natural abundance, the residual percentage error was smallest in the

[1] Stuchiner, E.R., et al. (2020). "An approach for calibrating laser-based N_2O isotopic analyzers for soil biogeochemistry research." Rapid Communications in Mass Spectrometry. https://doi.org/10.1002/rcm.8978

medium N_2O range. There was more noise in the corrected isotopomers and isotopologue at natural abundance in samples with the lowest and highest N_2O concentrations. Corrected isotopomer results from isotopically enriched samples were very precise.

Conclusions: Developing my calibration strategy involved learning several key lessons: (1) calibrate isotopocules in distinct concentration ranges, (2) use mathematically similar models to calibrate the isotopocules in each range, (3) calibrated N_2O concentrations and δ values tend to be most accurate and precise in the medium N_2O range, and (4) I encourage users to take advantage of isotopic enrichment to capitalize on laser-based instrument strengths.

2. Introduction

Nitrous oxide (N_2O) is a powerful greenhouse gas (GHG) with a warming potential ~300 times that of CO_2, and it is the primary stratospheric ozone depleting substance (Ravishankara et al. 2009, Cias et al. 2013). Developing strategies to reduce N_2O emissions is an active area of research, but the myriad sources of N_2O have made this GHG particularly difficult to manage (Davidson et al. 2014, Sinder et al. 2015). N_2O is emitted naturally from all terrestrial, marine, and freshwater ecosystems, but humans also contribute to emissions. Humans add excess N to ecosystems primarily through agriculture and fossil fuel burning, which gives rise to often disproportionately greater N_2O emissions than those from natural systems (Galloway et al. 2003). Furthermore, quantification of N_2O emissions has been an ongoing challenge, as they are much harder to detect relative to other more abundant greenhouse gases, such as CO_2 and CH_4 (Groffman et al. 2001, Bowling et al. 2003, Bouwman et al. 2013, Ostrom and Ostrom 2017).

Soils are an especially important source of N_2O. Natural and agricultural soils are estimated to contribute approximately 70% of total N_2O emissions, with approximately half of these emissions attributed to agriculture (Shcherbak et al. 2014). Given that soils are such an

important source of N_2O, substantial effort has been put towards reducing their emissions (Galloway et al. 2008, Reay et al. 2012). However, these efforts have proven challenging given the diversity of biotic and abiotic processes that generate N_2O.

N_2O is emitted from soils through multiple microbial processes, including nitrification, dissimilatory nitrate reduction to ammonium (DNRA), denitrification (bacterial and heterotrophic), nitrifier-denitrification, co-denitrification, and anaerobic ammonia oxidation (ANNAMOX; Butterbach-Bahl et al. 2013). In addition, non-microbial pathways also emit N_2O, including non-microbial chemodenitrification, spontaneous NH_2OH oxidation, chemical decomposition of NO_2^-, and chemical decomposition of NH_2OH that is fixed to soil organic matter (SOM; Heil et al. 2014, Heil et al. 2015). These diverse biotic and abiotic processes can co-occur over space and time in soils, and multiple processes can be performed by the same individual microbe (Kuypers et al. 2018). Thus, identifying and disentangling the sources of N_2O from ecosystems in order to mitigate emissions has been non-trivial.

Stable isotope techniques have been used to attribute N_2O emissions to different processes, and over the past two decades their use has come to the forefront as a promising tool for N_2O source partitioning (Yoshida and Toyoda 2000, Baggs 2008, Baggs 2011, Ostrom and Ostrom 2017, Yu et al. 2020). In this paper, I describe measurements of different isotopic versions of the N_2O molecule using isotopic terminology as defined by Coplen (2011): isotopocules, isotopomers, and isotopologues. Isotopocules are molecules that differ either in position or mass of enriched elements. Here, I use "isotopocules" to mean the set of all the isotopic molecules I measured: $^{14}N^{14}N^{16}O$, $^{14}N^{15}N^{16}O$, $^{15}N^{14}N^{16}O$, $^{14}N^{14}N^{18}O$, hereafter referred to as N_2O, $N^{15}NO$, ^{15}NNO, and $NN^{18}O$, respectively. Isotopomers are molecules that differ in position of the enriched element, but not in mass. The isotopomers described here are $^{14}N^{15}N^{16}O$

and $^{15}N^{14}N^{16}O$. Lastly, isotopologues differ in both isotopic composition and mass ($^{14}N^{14}N^{16}O$ and $^{14}N^{14}N^{18}O$), and the isotopologue described here is $^{14}N^{14}N^{18}O$.

Studies have shown that different microbial and abiotic processes yield site-specific enrichment in either the central (alpha, α) or terminal (beta, β) nitrogen (N) atoms in the linear N-N-O molecule (Sutka et al. 2006, Heil et al. 2015, Maeda et al. 2015). Microbial N-transformations can also yield site-specific enrichment in the ^{18}O composition of the oxygen atom, and while there have been some advances in characterizing this behavior, it remains less well understood (Kool et al. 2009, Lewicka-Szczebak et al. 2016). A large and growing body of literature is documenting patterns and processes in the site specific N_2O isotopic composition associated with soils. These studies rely on both natural abundance and enriched isotope approaches (Wrage et al. 2004, Perez et al. 2006, Ostrom et al. 2007, Yang et al. 2011, Decock and Six 2013, Denk et al. 2017).

Site specific analyses of N_2O stable isotopes have historically been made using gas chromatography isotope ratio mass spectrometer (GC-IRMS) systems, but these instruments are expensive to purchase and maintain, and the quantifications are laborious (Röckmann et al. 2003). Recently, laser-based analyzers have become commercially available for site specific measurements of the isotopic composition of N_2O, using cavity-enhanced absorption spectroscopy without preconcentration to provide simpler, lower cost systems for analysis of ambient air samples (Koster et al. 2013, Wolf et al. 2015, Ibraim et al. 2019, Yu et al. 2019). Further, this innovation also enables the possibility of in situ field measurements (Yu et al. 2020). However, despite the general power of laser-based analyzers for quantifying N_2O concentrations, their use in stable isotope determination raises unique challenges in calibration. At ambient concentrations (0.3 to 3 ppmv), the absorption signal of natural abundance isotopes is

weak (Ye et al. 2016, Fu et al. 2017). Thus, with noisy calibration for each of the isotopocules, there is potential for the resulting isotopic ratios to carry both significant variability and bias. As adoption of laser-based analyses for N_2O isotopes becomes more common, there exists a need to develop robust methods for calibration (Harris et al. 2020).

My research has used an ABB-Los Gatos Research Inc. (LGR) N_2O Isotopic Analyzer (Model 914-0027; ABB-Los Gatos Research, Mountain View, CA, USA) to measure N_2O from incubation experiments, without pre-concentration of the incoming N_2O. To better understand sources and kinetics of N_2O biogeochemistry, I regularly incubate soils at isotopic natural abundance or amended with isotopically enriched material. The calibration work described here became necessary when I determined that the factory calibration of the analyzer yielded inaccurate stable isotope ratios across broadly ranging incubation N_2O concentrations. Further, there is no published multi-point calibration protocol in the scientific literature that spans the N_2O concentration range often observed in soil incubations (0.3-300 ppm). In response, I developed the calibration approach described here. I anticipate that a standardized calibration strategy will help to streamline the N_2O isotope research pipeline, particularly because laser-based instruments, when properly calibrated, have much higher throughput than IRMS (Mohn et al. 2012, Ostrom et al. 2018).

The work presented here accounts for both changes in the instrument response function for each isotopocule (e.g., linearity) and instrument drift. These changes are inherent in a wide array of optical analyzers and are due to small changes in the laser tuning curve, detector response, and cavity response function. Thus, a strength of this calibration approach is that it can be applied to a wide variety of laser-based systems that measure the concentration of each isotopocule independently. For example, this algorithm can be used with instruments that

measure N_2O, CO_2, or CH_4, and should be able to work for any commercially available laser-based system (e.g., LGR, Picarro Inc., Aerodyne Research Inc.), because in each case the isotope ratio is calculated from concentrations of each independently measured isotopocule.

Here I present methods for calibrating a laser-based N_2O isotopic analyzer. My calibration approach identifies a robust relationship between observed and expected isotopocule concentrations. In particular, I evaluate analytical challenges unique to incubation studies, including: (1) calibration of isotope ratios when the total N_2O concentration spans a broad range; (2) calibration for a broad range of N_2O isotope ratios, which can happen with the addition of isotopically enriched materials; and (3) the need for mathematically similar corrections for all of the isotopocules.

3. Materials and Equipment

My calibration of the LGR instrument depended on use of primary and secondary standard gases, admitted to the instrument through a customized inlet system. Here, I describe the gases and their preparation for use as calibrants, and I also describe the instrument, its configuration, basic operation, and performance metrics.

3.1 Calibration gases

I relied upon both a primary standard, calibrated at an external lab, and a secondary working lab standard that I calibrated against the primary standard. My primary standard is USGS52, supplied from the USGS Reston Stable Isotope Lab (U.S. Geological Survey, Reston, VA, USA) in a 6mm borosilicate tube containing approximately 200 μmol of N_2O. Extensive details on the origin of this material and its isotopic properties are provided in Ostrom et al. (2018). I prepared the standard for laboratory use by diluting it into commercially prepared zero-grade air (synthetic 80:20 N_2:O_2 blend, Airgas Inc., Radford, VA, USA). Dilution was achieved

by breaking the glass tube of standard inside an evacuated 20L cylinder. The cylinder containing the standard gas was then pressurized to 350 kPa with zero-grade air. Details of this preparation can be found in Appendix 1. The diluted concentration of the standard in the 20 L cylinder was approximately 80 ppmv. In light of the limited volume of my primary standard, I developed a secondary standard for everyday laboratory use. This commercially prepared standard (Airgas Industries) contains 500ppm N_2O in an 80:20 N_2 and O_2 blend (analytical uncertainty ± 1%).

3.2 Preparation of standards for concentration and isotopic calibration

I developed calibration standards via dilution of the primary and secondary standards. To capture the breadth of gas concentrations that may be observed in soil incubations, I prepared a wide range of custom N_2O standards from 0.3 ppm to 300 ppm. Calibration standards were prepared from both the primary and secondary standards, as constrained by the stock concentrations (80ppm and 500ppm, respectively).

Standards were prepared into ~1 L gastight (Tedlar or mylar) bags (hereafter "gas bags"). Gas bags were prepared by diluting N_2O primary or secondary standards into zero-grade air. A constant volume of zero-grade air was added to all gas bags with an Alicat Scientific mass flow controller (MFC; model: MC-10SLPM-D/5M, Alicat Scientific Inc., Tucson, AZ, USA) and then an appropriate amount of N_2O standard was injected by hand using a syringe. Details for this procedure can be found in Appendix 1.

3.3 ^{15}N-enriched N_2O

The aim of my approach was to produce a calibration algorithm that could be applied to both natural abundance or ^{15}N enriched measurements across an environmentally relevant span of N_2O concentrations. Thus, my instrument required calibration verification with a $^{15}N_2O$ isotopically enriched standard. I obtained a 1 L cylinder of 99 atom percent (AP) $^{15}N_2O$ (both N

atoms labelled with ^{15}N) from Cambridge Isotope Labs Inc. (Andover, MA, USA) to validate my calibration approach for enriched samples. Standards were prepared by diluting 1 mL aliquots of 99 AP $^{15}N_2O$ into a synthetic atmosphere-like blend (450ppm N_2O, 20% O_2, 1% Argon, and balance N_2) in 1 L Ball jars. This atmosphere-like blend was custom-made by Airgas Inc., and it intentionally omitted CO_2, CH_4, and other common atmospheric gases to minimize the optical peak-broadening effects that are inherent with laser-based analyses. Sample air that reaches the instrument cell is likewise freed of CO_2 and other gases using a scrubber (described below). Due to cost constraints, I was not able to perform tests with ^{18}O-enriched N_2O.

3.4 Inlet and contaminant gas scrubber system

Sample air was admitted to the analyzer via continuous flow from a ~1L gas bag. An internal pump within the analyzer drew sample air at 42 mL/min through a gas scrubber system, into the analytical cell and out to waste. All inlet tubing was ¼" OD polyethylene, connected using Swagelok fittings. Although this configuration allows up to ~23 minutes of instrument analysis for each ~1L gas sample bag, samples were typically analyzed for ~15 minutes, as described in Section 3.6 below.

To scrub the sample stream of gases that could spectroscopically interfere with N_2O, I used traps to remove CO_2, water vapor, and other impurities. The design for my scrubbing system was adapted from Nathaniel Ostrom and Hasand Gandhi (pers. comm.).

The scrubbing system was ordered in the following sequence: gas sample, in-line particulate filter (7 μm; Swagelok, Denver, CO, USA), Nafion water-vapor trap (Perma Pure LLC, Lakewood Township, NJ, USA), CO_2 sorbent trap (Carbosorb; Elemental Microanalysis, Okehampton, England, UK), silica gel/activated charcoal trap (Sigma-Aldrich, Saint Louis, MO, USA) , in-line particulate filter (7 μm; Swagelok), and finally the analyzer inlet. Details of these

traps are provided in Appendix 1. I positioned the first in-line particulate filter to prevent soil particles from blocking the Nafion dryer. The Nafion was dried using a counter-flow of UHP N_2 gas at 400 mL/minute. The silica gel/activated charcoal trap, was regularly re-conditioned by heating only the silica gel portion to approximately 180 °C while being flushed with UHP N_2 at a flow rate of 100 mL/minute for 24-36 hours. Afterwards the silica gel is cooled for 1-2 hours by flushing with UHP N_2 at a flow rate of 100 mL/minute. The final in-line particulate filter protected the LGR inlet. Flow rates were considerably lower when the scrubbing system was in place (72 mL/min without the scrubber and 42 with), due to flow restriction. The internal pressure of the analytical cell was also somewhat lower with scrubbers (45 Torr without scrubbers, and 33-37 Torr with scrubbers, depending on how "packed" the silica gel became over time). However, all calibration and measurement procedures took place with scrubbers and at similar pressures.

To evaluate the efficacy of the scrubber system for removing contaminant gases, I admitted room air to the inlet system and measured the outflowing concentrations of CO_2 and water vapor using an LGR Greenhouse Gas Analyzer (Model 907-0010). The analyzer reported CO_2 concentrations <10ppm and water vapor levels below 1000ppm, indicating a successful removal of these contaminants. My study of the instrument spectroscopy indicated that measures of N_2O isotopes were unaffected by water vapor at concentrations below 1000ppm.

While the scrubbing system described above seemed adequate, I anticipate that other groups might wish to implement a different setup or develop a scrubbing setup that improves upon ours. Adequately scrubbing background gases from the sampling matrix is a dynamic area of research for laser-based instruments (e.g., Harris et al 2020), and I would like to underscore

that the purpose of this paper is to offer a roadmap for laser-based instrument calibration, not guidance on how to best scrub the sample stream of contaminant gases.

3.5 Instrument description

The LGR N_2O Isotopic Analyzer uses mid-infrared Off-Axis Integrated Cavity Output Spectroscopy (ICOS) near 4.5 microns to simultaneously measure the concentrations (ppmv) of $^{14}N^{14}N^{16}O$, $^{15}N^{14}N^{16}O$, $^{14}N^{15}N^{16}O$, and $^{14}N^{14}N^{18}O$ (Provencal et al. 2005). Briefly, a thermoelectrically cooled distributed feedback (DFB) quantum cascade laser is collimated and directed into a high-finesse optical cavity in an off-axis fashion. The cavity is comprised of two highly reflective mirrors (R > 99.95 % at 4.5 microns), and light transmitted through the cavity is focused onto a thermoelectrically-cooled, highly-amplified HgCdTe detector. The laser is continuously current-tuned over the N_2O isotope absorption features, and repeated scans are averaged to yield a cavity-enhanced absorption spectrum. This spectrum is then fit to a baseline function and sum of Voigt profiles to yield the concentrations of the aforementioned isotopocules. The measured concentrations for each isotopocule are corrected for non-linear effects using empirically determined data that are measured before the instrument leaves the factory. Finally, the reported isotope ratios are calculated from the measured isotopocule concentrations.

The analyses described here were for an instrument at a pre-commercial stage of development, manufactured for research use in 2013. Factory recalibration of the instrument was cost prohibitive in 2016, and so I undertook the calibration exercise described here. Subsequent commercial versions of the instrument may account for some errors that I encountered, but I anticipate that the calibration approach outlined below will be appropriate for studies where sample air contains a wide range of N_2O concentrations.

3.6 Instrument performance metrics

When a new sample was connected to the inlet and scrubber system, the reported concentration approached a new steady state value, as the new sample air replaced the air from the prior sample in the inlet system and in the analytical cell within the instrument. Typically, this equilibration period was on the order of 10 minutes. I then collected data for five minutes after the new steady state concentration was reached. This ~15-minute sampling period did not drain gas bags, as it would take ~20 minutes to drain a 1 L bag at my analyzer's flow rate, but additional analysis did not improve the quality of the concentration data. With data reporting at 0.5Hz, this yielded approximately 150 data points that were averaged to yield the reported concentrations of the measured isotopocules: N_2O, $N^{15}NO$ (α), ^{15}NNO (β) and $NN^{18}O$. Under rare circumstances, (n = 13 of 257 data points), highly anomalous samples were removed from analyses when their reported values fell five or more standard deviations (SD) from the expected calibration values. In every case, the anomalous readings were from the rarer isotopocules ($N^{15}NO$, ^{15}NNO, or $NN^{18}O$).

3.7 Mathematical and statistical calculations

I developed my calibration algorithm using RStudio Software (Version 1.1.453 – © 2009-2018 RStudio, Inc.). The R code is available on GitHub (https://github.com/emilystuchiner/calmodel). In Section 4, below, I describe the calibration approach used to develop this code.

4. Calibration approach

4. 1 General strategy

My calibration approach was informed by preliminary tests of the LGR N_2O Isotopic Analyzer where I analyzed dilutions of the primary standard (n = 20) and of the secondary

standard (n = 72) over the wide range of N_2O concentrations that I anticipated for soil incubations (0.3-300ppm). Analysis of these standards revealed persistent, non-linear patterns in the relationship between expected vs. observed concentrations of the four measured isotopocules (Figure 2.1B for N_2O; Figure 2.2A-C for isotopomers and isotopologue). Expected concentrations were estimated by rearranging the δ equation to solve for the concentration of $N^{15}NO$, ^{15}NNO, or $NN^{18}O$ at a given N_2O concentration. For example, the expected $[N^{15}NO] = (\delta^{15}N^{\alpha}_{std}+1)*(R_{std})*[\text{corrected } N_2O]$ where $\delta^{15}N^{\alpha}_{std}$ is the known $\delta^{15}N^{\alpha}$ value for the standard and R_{std} is the $^{15}N/^{14}N$ ratio of standard air (i.e. 0.0036765). Thus, my aims were to (1) determine the calibration algorithms needed to convert raw instrument output to calibrated values (2) determine the isotopic composition of my secondary standard, and (3) apply the calibration algorithm to headspace gas samples from soil incubations.

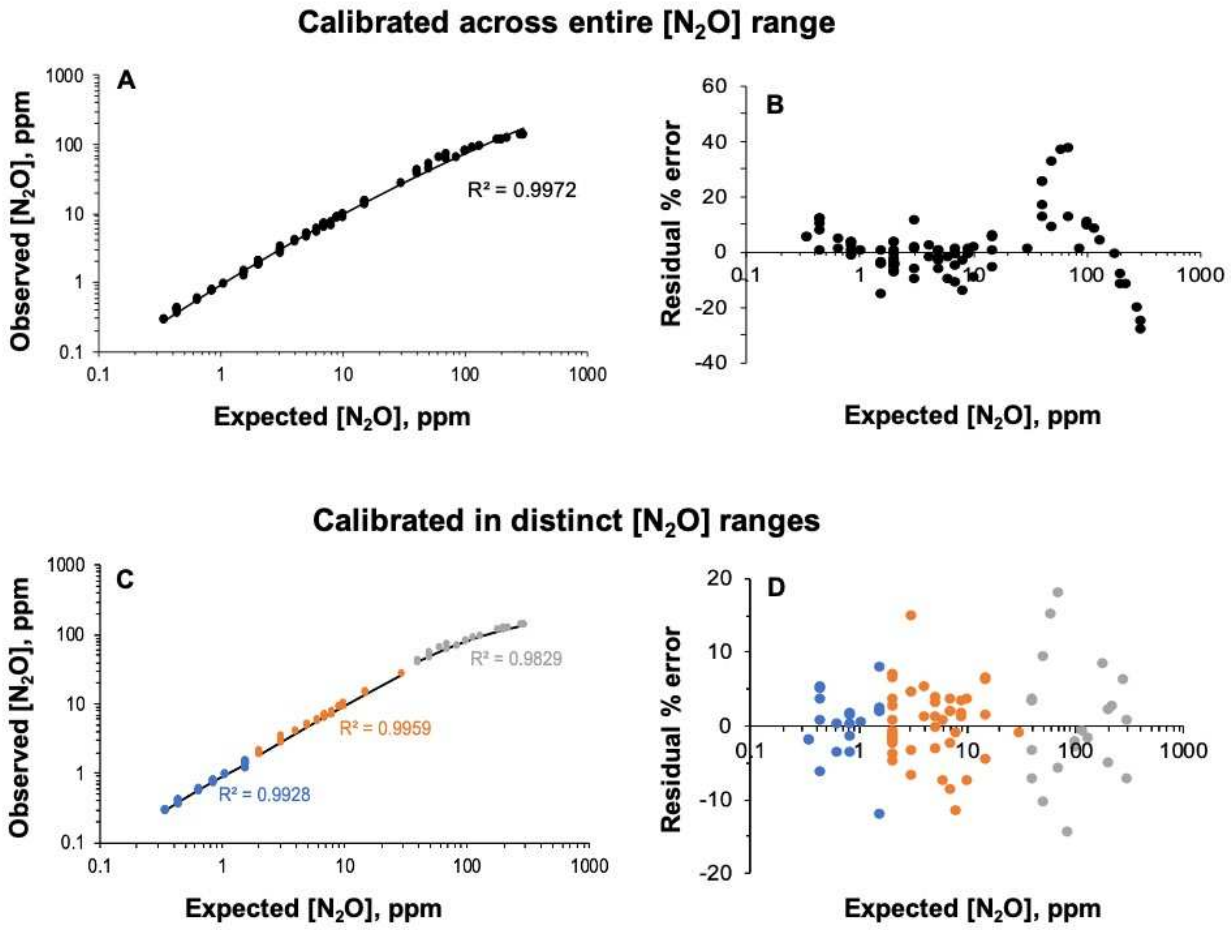

Figure 2.1. Second-order polynomial fit(s) used to calibrate raw N_2O data to expected values, and the residual error from those fits. The top panel shows all N_2O data in log-log space calibrated with a single second-order polynomial and the corresponding residual percent error (**A-B**), whereas the bottom panel shows the N_2O data in log-log space calibrated with three unique second-order polynomials in low, medium, and high data ranges (**C-D**). Colors in the bottom panel correspond to distinct N_2O concentration ranges (see Table 1). As the residual percent error illustrates, error was minimized when multiple polynomial fits were used to calibrate N_2O in distinct N_2O concentration ranges (**D**). While the one model fit is stronger in **A** than the three model fits in **C**, residual error notably decreases when N_2O is calibrated in distinct ranges.

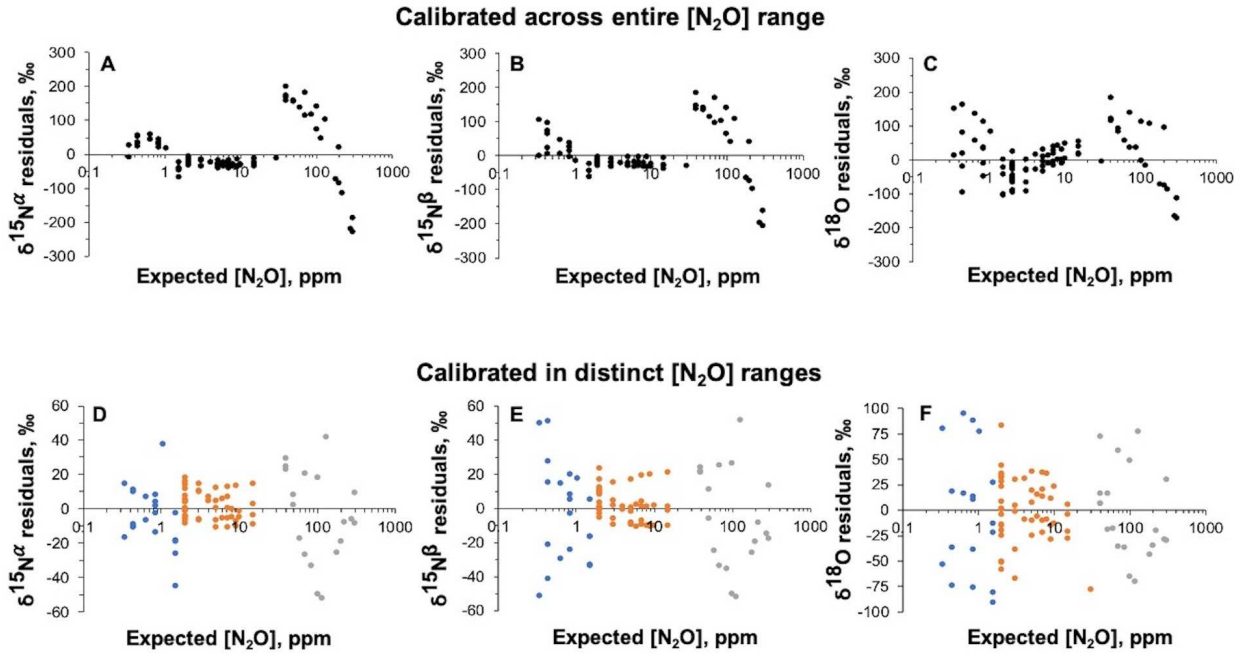

Figure 2.2. A comparison of residuals of N_2O isotope ratios when calibrated with a single curve fit across the entire log-transformed N_2O range **(A-C)** vs. calibrated with distinct curve fits for each log-transformed N_2O concentration range **(D-F)**. Colors in the bottom panel correspond to distinct N_2O concentration ranges (see Table 1). For all three isotopomers, the residuals were minimized when data was calibrated in distinct concentration ranges. Residuals are consistently smallest in the medium N_2O range for all isotopomers.

I determined that applying a mathematically similar correction to all the measured isotopocules is necessary. For example, when I used a spline fit for the N_2O correction and polynomial fits for the other isotopocules, this resulted in systematic errors in the corrected isotope ratios because the calibration curve shapes differ markedly for the spline vs. polynomial fits. As a result, I chose to calibrate all isotopocules using second-order polynomial fits. One benefit of the polynomial fit is it permits limited extrapolation outside of the calibration range, which could be useful if samples occasionally have concentrations outside of the calibration range. Another benefit is that the second-order polynomial allowed for inversion of the y = f(x) relationship, which is not always possible with other mathematical forms of the relationship (e.g., with cubic polynomial or with a spline basis).

Although the isotopic composition of my primary standard was known, it had a limited concentration range (max [N_2O] ~80ppm) and so I needed to use the secondary standard in building the calibration model up to the 300ppm desired maximum concentration. When the calibration approach was complete, it provided estimated mean δ-values for my secondary standard ±1 standard error (SE; $\delta^{15}N^{\alpha}$: 20.69‰ ± 3.18, $\delta^{15}N^{\beta}$: -12.59‰ ±3.48, and $\delta^{18}O$: 44.25‰ ±5.48). The calibration approach I outline below omits discussion of estimating the isotopic composition of the secondary standard and focuses on using the primary and secondary standards post-isotopic characterization, assuming that most future users of this model will have standards of known isotopic composition. However, I have the code for calibrating the secondary standard available on my GitHub site (https://github.com/emilystuchiner/secondarystd_calmodel).

4.2 Calibration of N_2O

Throughout my calibration, I worked with log-transformed concentration values. This was necessary for visualizing patterns in variation across the 1000-fold dilution range (0.3-300 ppm). Likewise, my statistical analyses relied on log-transformed concentration values to reduce the leverage of large concentration values, and to meet the assumptions of normally distributed error in the statistical models. Hereafter, I refer to "raw" concentration values as those derived directly from the instrument, and "corrected" concentration values as those that have been corrected using the calibration approaches described above.

Initial raw vs. expected N_2O values exhibited evidence of a non-zero y-intercept, indicating the presence of a small (~43 ppb) and previously unknown level of N_2O contamination in the zero-grade air that was used in dilutions. Although this concentration was below the reliable detection limits of the instrument, direct analysis of the zero air with the instrument reported values near this magnitude. I accounted for the contamination by adding its

concentration to the expected N_2O values, and then the subsequent regression of raw vs. expected showed no evidence of a non-zero intercept.

Looking broadly at all N_2O data from 0.3-300 ppm, there was a distinct non-linear response that was well fit with a 2nd order polynomial curve, which tracked the saturation response of the analyzer (Figure 2.1A). However, the residuals showed patterns in lack of fit through different N_2O concentration ranges (Figure 2.1B). Based on visual inspection, I hypothesized that breaking the data into three concentration ranges would remove the patterns in the residuals and I found this to be true. Thus, I calibrated the N_2O data in three distinct concentration ranges to capture range-specific differences in instrument behavior and to improve model fits. This was achieved by dividing the N_2O data into low (0-1.49 ppm), medium (1.49-33.12 ppm), and high (33.12-300 ppm) concentration ranges and fitting each "bin" with its own unique second-order polynomial equation. These bins were established based on behaviors unique to each N_2O range: positive residuals in 0-1.49 ppm, no discernable residual trend in 1.49-33.12 ppm, and strong positive and negative residuals in 33.12-300 ppm. This substantially improved the residual diagnostics across the entire calibration dataset (Figure 2.1C-D).

4.3 Calibration of $N^{15}NO$, ^{15}NNO, and $NN^{18}O$

As with N_2O, I calibrated the other measured isotopocules using second-order polynomial equations, binned into ranges that correspond to the low, medium, or high concentration range break points that I established for N_2O (Table 2.1). These break points correspond to the expected concentrations of the isotopocules at natural abundance when $\delta^{15}N = 0‰$ or $\delta^{18}O = 0‰$.

Although I did not calibrate the model with isotopically enriched N_2O, I did analyze standards with high (and known) concentrations of ^{15}NNO, $N^{15}NO$ and $NN^{18}O$ in the form of

natural abundance N_2O at very high concentrations. For example, there is the same concentration of $^{15}N_2O$ in both a 400ppb sample of N_2O at 5 AP enrichment and a 5400ppb sample at natural abundance. Likewise, my 300ppm N_2O calibration standard at natural abundance would allow us to measure a 22ppm N_2O sample that was 5 AP enriched in $^{15}N_2O$. Using this calibration algorithm with isotopically enriched samples is elaborated upon in Section 5.5.

Table 2.1. Concentration break points for each isotopocule of N_2O that designated which calibration curve to use when correcting raw values. Colors corresponding to each break point are the same throughout all calibration procedures. The break point concentrations for the isotopomers and isotopologue of N_2O were calculated by multiplying the break point [N_2O] (1.49 and 33.1) by the natural abundance ratios for $^{15}N/^{14}N$ or $^{18}O/^{16}O$ concentration (0.0036765 or 0.00200052, respectively). All values are in ppm.

Break points	**N_2O**	**$N^{15}NO$ and ^{15}NNO**	**$NN^{18}O$**
Low (blue)	$0 \leq 1.49$	$0 \leq 0.00548$	$0 \leq 0.00299$
Medium (orange)	≤ 33.1	≤ 0.122	≤ 0.0664
High (grey)	> 33.1	> 0.122	> 0.0664
Maximum	300.	1.10	0.602

While I could not precisely quantify the contaminant in zero air for the rarer isotopocules because it was far below the instrument detection limit, my instrument reported approximate contaminant values of 0.0001 ppm for $N^{15}NO$ and 0.0003 ppm for both ^{15}NNO and $NN^{18}O$. To correct for this, I assumed the contamination had an isotopic composition of 0‰ for $\delta^{15}N^{\alpha}$, $\delta^{15}N^{\beta}$, and $\delta^{18}O$. Then, I estimated the expected $N^{15}NO$, ^{15}NNO and $NN^{18}O$ concentrations using R_{sample} values of 0.00374 for $N^{15}NO$ and ^{15}NNO and 0.00209 for $NN^{18}O$, and the estimated [N_2O] for the contaminant of 0.043 ppm. After this correction, regression of observed vs. expected isotopocules did not show a significant y-intercept, indicating that the mixing model correction was successful.

I calculated the δ values from all corrected concentration data using standard δ notation and using the $^{15}N/^{14}N$ ratio of atmospheric N_2 (0.0036765) or $^{18}O/^{16}O$ in VSMOW (0.0020052).

All δ values are reported in ‰ and note again that "N_2O" in the below equations refers to $^{14}N^{14}N^{16}O$ concentrations.

The $\delta^{15}N^{\alpha}$ was calculated as

$$\delta^{15}\mathrm{N}^{\alpha} = \frac{(N^{15}NO/N_2O)_{sample}}{(N^{15}NO/N_2O)_{std}} - 1 \quad (1)$$

and $\delta^{15}N^{\beta}$ was calculated as

$$\delta^{15}\mathrm{N}^{\beta} = \frac{(^{15}NNO/N_2O)_{sample}}{(^{15}NNO/N_2O)_{std}} - 1 \quad (2)$$

and $\delta^{18}O$ was calculated as

$$\delta^{18}\mathrm{O} = \frac{(NN^{18}O/N_2O)_{sample}}{(NN^{18}O/N_2O)_{std}} - 1 \quad (3)$$

I also calculated site preference (SP), the difference in the amount of N_2O enriched in the α or β position:

$$SP = \delta^{15}\mathrm{N}^{\alpha} - \delta^{15}\mathrm{N}^{\beta} \quad (4)$$

5. Features of the final calibration

Here I discuss the accuracy and precision of corrected isotopocule concentrations and δ values following calibration. To characterize the accuracy and precision of these measures, I calculated the residual error between corrected and expected values. I then calculated the means and variances of these errors to understand the analytical accuracy and precision of my calibration.

5.1 Accuracy and precision of N_2O across concentration ranges

My initial calibration efforts did not break the N_2O data into concentration ranges, which resulted in large residual error (Figure 2.1A-B). Following calibration in low, medium, and high N_2O concentration ranges, my estimations of N_2O concentration were much better (Figure 2.1C-D). Across the whole data range (0.3-300 ppm), the residual percent error was ±5.46% (Figure 2.1D). Looking at finer ranges of calibration, residual percent error for the low and medium N_2O concentrations were comparably precise (±4.39% and ±4.63%, respectively; Figure 2.1D). Precision was weakest for the high N_2O concentrations (±7.85%; Figure 2.1C-D). These percent error calculations were derived from ~150 data points for each measured N_2O concentration averaged over a five-minute sampling period (see Section 3.6 for details).

Precision was likely impacted by several factors at all N_2O concentration ranges. First, preparing standards using a MFC and by-hand dilutions with a syringe are susceptible to error. The Alicat Scientific MFC I used reports ±0.5% error in flow rate, and by-hand dilution can also result in discrepancies in precision. Second, there was greater uncertainty in the N_2O concentration of the primary standard compared to the secondary standard. While the secondary standard was commercially prepared by Airgas, the method for diluting the primary standard in the lab led to some uncertainty in its final concentration (see Section 3.1 and Appendix 1). Cumulatively, the overall precision of my calibration may have been affected by these uncertainties in primary and secondary standards. The relative contributions of uncertainty in primary vs. secondary standards is illustrated in Appendix 1.

Further, based on spectroscopic principles, the instrument precision in the low and medium N_2O ranges is likely on the order of ~1%, but in the high N_2O range it is likely greater than 1%. This suggests that most uncertainty in the low and medium ranges is due to human

error diluting the concentration standards. However, in the high range, where spectroscopic saturation is more prominent, I see a flattening of the N_2O correction curve. This would make the calibration less sensitive to changes in the true concentration, and likely helps to explain why precision was notably worse in the high N_2O range. Yet, precision remained relatively good across all N_2O concentrations and even at the lowest N_2O concentrations, which can be difficult to quantify without preconcentration (Figure 2.1C-D; Ibraim et al. 2018). As I illustrate in Figure 2.1D, there was no evidence of residual bias in concentration determination, once the calibration was broken into the three N_2O concentration ranges. Overall, I anticipate that these levels of precision and accuracy for N_2O concentration determination would be acceptable for field application of non-preconcentrating lasers analyzers, because field-sample levels of N_2O are typically near ambient but can spike up to 10's or 100's of ppm, depending on the study.

5.2 Accuracy and precision of $N^{15}NO$, ^{15}NNO, and $NN^{18}O$ across concentration ranges

Like the N_2O calibration, characterizations of the natural abundance isotope ratios were more precise when the data was broken into low, medium, and high N_2O concentration ranges (Figure 2.2). Plots of residual $\delta^{15}N^{\alpha}$, $\delta^{15}N^{\beta}$, and $\delta^{18}O$ vs. N_2O are considerably noisier with the laser-based analyzer as compared to conventional IRMS analyzers (Mohn et al. 2014, Ostrom and Ostrom 2017). However, this noise is most acute at the lower and higher N_2O concentrations and less pronounced at medium N_2O concentrations (Figure 2.2D-F). I also demonstrate that corrected isotopomer, isotopologue, and SP values for the primary standard were accurate. Paired t-tests demonstrate that the corrected values were not significantly different from the known primary standard values (Table 2.2; $p > 0.05$ in all cases). Evidence of good precision in the medium N_2O concentration range, coupled with accurate δ values, suggests that isotopic

analyses can be robust with a laser-based analyzer when constrained to certain N_2O concentrations (Figure 2.2D-F; Table 2.2).

Table 2.2. Primary standard known and estimated mean $\delta^{15}N^{\alpha}$, $\delta^{15}N^{\beta}$, and SP values. Estimated means are averaged from the entire primary standard dataset (n = 20). ± corresponds to SE from the mean. All values are in ‰.

Standard	$\delta^{15}N^{\alpha}$, ‰		$\delta^{15}N^{\beta}$, ‰		SP, ‰		$\delta^{18}O$, ‰	
	Known	**Estimated**	**Known**	**Estimated**	**Known**	**Estimated**	**Known**	**Estimated**
Primary standard (USGS52)	13.52 (±0.04)[a]	10.51 (±5.02)	-12.64 (±0.05)[a]	-15.21 (±5.18)	26.16[b]	25.72 (±2.26)	40.64 (±0.03)[a]	40.38 (±5.71)

[a]uncertainty in known values relative to N_2-AIR or VSMOW from Reston Stable Isotope laboratory.
[b]SE for SP not specified by Reston Stable Isotope laboratory.

Generally, $\delta^{15}N^{\alpha}$ and $\delta^{15}N^{\beta}$ calibrations were more precise and had lower mean residual error than the $\delta^{18}O$ calibration (Table 2.3). Also, precision was consistently best for both isotopomers and SP in the medium N_2O concentration range compared to the low and high N_2O concentration ranges (Table 2.3). At this time, I cannot explain the poorer precision for $NN^{18}O$ compared to $N^{15}NO$ and ^{15}NNO across all N_2O concentrations. It may be that this isotopologue is simply more challenging to quantify from an optical perspective. It also may be that its optical features are more sensitive to interference from co-occurring gases in the sample, despite my best efforts to remove them via scrubbers. Further, it is well understood that ^{18}O in N_2O exchanges with ^{18}O in water vapor, and while I deemed water vapor concentrations satisfactory post-scrubbing, perhaps they were inadequate for entirely eliminating ^{18}O exchange (Kool et al. 2009). Indeed, recent work by Harris et al. (2020) shows that the co-occurring gases can impact N_2O isotopic determinations, underscoring the importance of developing good scrubber systems.

Table 2.3. SD of mean error and SD of error for each N_2O concentration range for all measured isotopocules and SP. SD was lowest (e.g., highest precision) in the medium N_2O concentration range.

SD of error	$\delta^{15}N^{\alpha}$, ‰	$\delta^{15}N^{\beta}$, ‰	$\delta^{18}O$, ‰	SP, ‰
Mean SD of error	± 16.08	± 20.43	± 41.30	± 8.13
Low [N_2O] SD of error	± 17.49	± 29.11	± 60.87	± 13.61
Medium [N_2O] SD of error	± 8.07	± 9.38	± 31.63	± 2.54
Large [N_2O] SD of error	± 26.74	± 29.09	± 43.61	± 3.90

It is also notable that greater precision in $\delta^{15}N^{\alpha}$ and $\delta^{15}N^{\beta}$ resulted in increased precision in SP across all concentration ranges. Thus, SP precision was best in the medium N_2O concentration range and poorer in the low and high N_2O concentration ranges (Table 2.3). Interestingly, the estimated SP precision is consistently better than the estimated precision for $\delta^{15}N^{\alpha}$ and $\delta^{15}N^{\beta}$ (Table 2.3). It appears that errors in $\delta^{15}N^{\alpha}$ and $\delta^{15}N^{\beta}$ are correlated, in that when one isotopomer is over-estimated so is the other, and vice versa. Through calculating SP, this causes the errors to appear to cancel each other out, resulting in greater SP precision than the precision of each isotopomer. From the perspective of using SP to characterize microbial N_2O-generating processes in soils, this could be advantageous.

Overall, I hypothesize that these patterns in isotopomer and isotopologue precision across N_2O concentrations are likely due to a weak optical signal at low N_2O concentrations and optical saturation at high N_2O concentrations. Further, I propose that the isotopomers and isotopologues from the lowest and highest N_2O values are responsible for the poorer precision in the low and high concentration ranges (Figure 2.2). Thus, the outcomes of this calibration suggest that I can best perform isotopic analyses at N_2O concentrations ranging from 1.5-75 ppm (Figure 2.2D-F).

5.3 Using SP to evaluate the accuracy of the calibration approach

I found that I was able to estimate SP values with relatively good precision and accuracy, thus providing further support for the efficacy of my calibration approach (Table 2.2, Figure 2.3).

This is a significant achievement because SP is a focal value of interest for partitioning among microbial and abiotic sources of N_2O. SP is also a uniquely useful metric for identifying possible systematic biases in my calibration because its derivation is sensitive to errors in either of the isotopomer values. That is, SP values carry a legacy effect from over or underestimating either $\delta^{15}N^{\alpha}$ or $\delta^{15}N^{\beta}$.

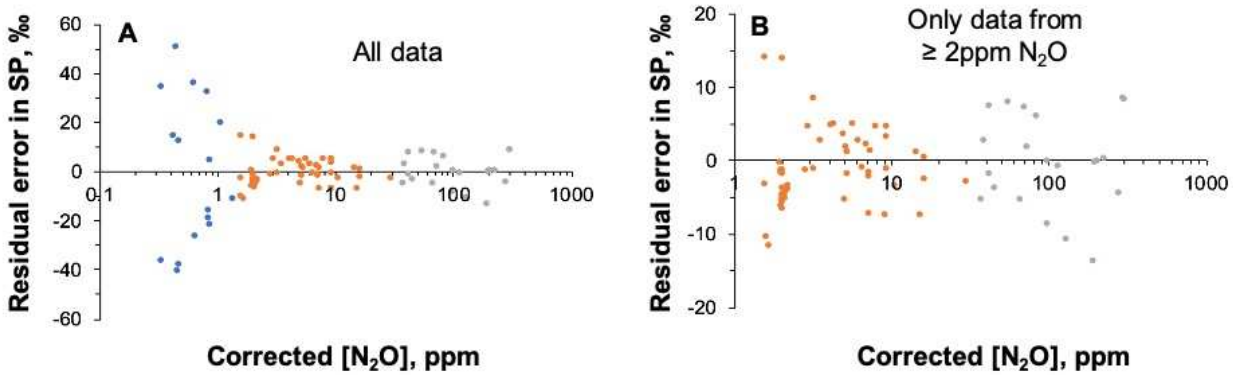

Figure 2.3. The relationship between corrected N_2O and the residual error in SP. Panel **A** shows all data across the entire calibration range, whereas panel **B** is zoomed in to only show residual error in SP from ≥2ppm. *Note the difference in y-axis scale.* While there is still some fanning in residual error vs. N_2O from 0-2ppm following calibration **(A)**, the magnitude of this effect diminishes greatly when N_2O concentration is constrained to ≥2ppm (**B**).

The plot of error in SP vs. corrected N_2O concentrations shows that over and underestimation in $\delta^{15}N^{\alpha}$ and $\delta^{15}N^{\beta}$ are most prevalent at N_2O concentrations less than 2 ppm (Figure 2.3). Note that I am discussing error in SP in the context of individual data points, rather than in reference to the whole population of SP values (e.g., to what degree was each SP value over or underestimated?). To discern whether it is $\delta^{15}N^{\alpha}$ or $\delta^{15}N^{\beta}$ that is being over or underestimated, I can reference back to Figure 2.2D-E. A side-by-side comparison of error for $\delta^{15}N^{\alpha}$ and $\delta^{15}N^{\beta}$ show that the over and under estimations are larger in $\delta^{15}N^{\beta}$ than in $\delta^{15}N^{\alpha}$ (Figure 2.2D-E). This suggests that any over or underestimation I observe in SP is due to a greater magnitude error in ^{15}NNO estimation rather than $N^{15}NO$ estimation. This is not to say

there is no error in $N^{15}NO$ estimation, but that the isotopomer with the greater magnitude error will be responsible for the direction of error in SP calculations.

However, it is worth noting that the error in SP is most dramatic only at the lowest N_2O concentrations in the calibration range (Figure 2.3). Also, while the error in SP < 2ppm is nontrivial, it is notable that the direction of variation is both positive and negative. This suggests that error in SP < 2ppm is due to noise in isotopic data at low N_2O concentrations, which I acknowledge is a limitation to the instrument's precision, rather than the calibration approach itself. However, when the N_2O concentration range is truncated to not include N_2O concentrations < 2ppm, the mean residual error becomes closer to zero (±3.02 ‰) and more homoscedastic, suggesting that (1) error is minimized in $\delta^{15}N^{\alpha}$ and $\delta^{15}N^{\beta}$ corrections ≥ 2ppm, or (2) error in $\delta^{15}N^{\alpha}$ and $\delta^{15}N^{\beta}$ are comparable in magnitude but opposite in direction ≥ 2ppm N_2O and cancel each other out. Whichever the mechanism, my measures of SP validate my calibration approach because I demonstrate small residual error in SP over approximately a 100-fold N_2O dilution range, which is reflective of my accurate and precise calibrations of N_2O, $N^{15}NO$, and ^{15}NNO. I acknowledge that this validation does not account for $NN^{18}O$, but I hypothesize that the instrument behaves similarly for all isotopocules and if three of four isotopocules exhibit good calibration, the fourth is likely well-calibrated too.

5.4 Evaluation of instrument drift over time

Full calibration is an intensive process requiring many analyses and types of diluted standards. During regular operations, I ran check standards of the calibration gases to assure that the instrument had not drifted in calibration over time. I presumed that it would not drift significantly because cavity-enhanced absorption spectroscopy is a first-principles technique in which all the critical factors (e.g., absorption, gas pressure, gas temperature, and optical

pathlength) are measured. Moreover, the instrument temperature, gas pressure, and laser wavelength are actively stabilized, helping to further minimize long-term drift.

I evaluated the tendency for the instrument to drift over time and determine the necessary frequency of re-calibration. To test the rate of drift, I ran dilutions of the secondary standard spanning from 0.3-300ppm N_2O in June 2018 (n = 72), October 2018 (n = 68), and October 2019 (n =14) and performed a series of one-way ANOVAs comparing mean $\delta^{15}N^{\alpha}$, $\delta^{15}N^{\beta}$, SP, and $\delta^{18}O$ from each time point. Dilutions of the primary standard were not run for this test due to its limited volume. All mean values overlapped, indicating little evidence to suggest drift in the instrument over the 17-month period of operations ($p > 0.05$ for $\delta^{15}N^{\alpha}$, $\delta^{15}N^{\beta}$, SP, and $\delta^{18}O$; Figure 2.4).

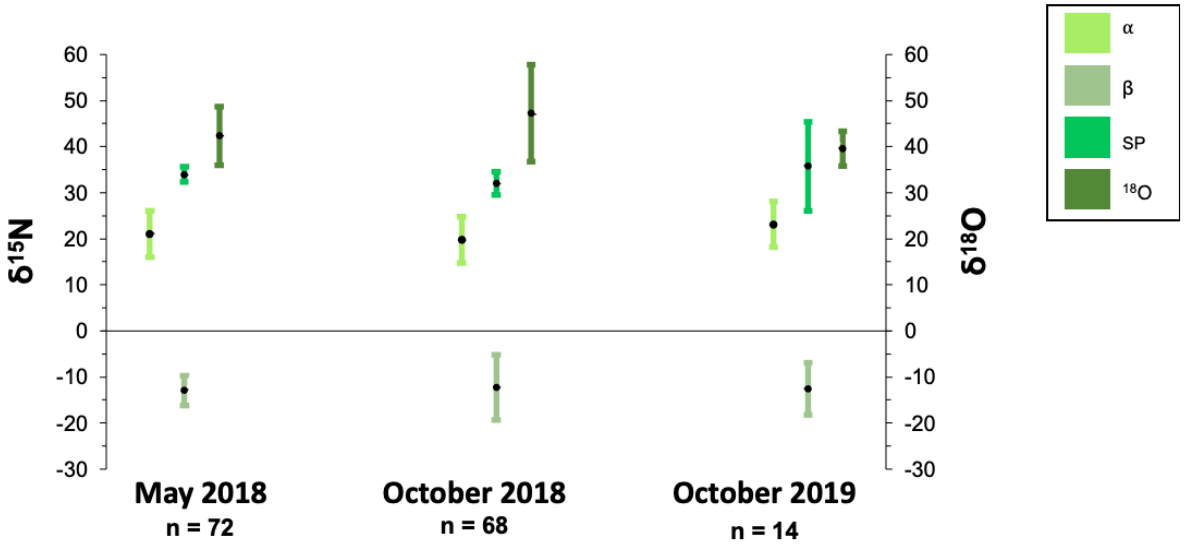

Figure 2.4. Mean and standard error in $\delta^{15}N^{\alpha}$, $\delta^{15}N^{\beta}$, SP, and $\delta^{18}O$ from different sampling periods. Differences among δ values and for SP are not significant ($p > 0.05$ in all cases).

Following this test, I do see that the SE for SP declined somewhat markedly from October 2018 to October 2019 (SE ±2.48 to SE ±9.69, respectively; Figure 2.4). However, the decrease in SE precision is likely due to having much smaller sample size in October 2019 vs.

October 2018. Despite this, I see generally consistent mean isotopomer, isotopologue, and SP values over time (Figure 2.4).

Thus, I recommend updating the calibration model parameters periodically to keep the correction functions robust. The instrument does not appear to require re-calibration more than once annually, which is ideal for instrument use over broad temporal scales. I also recommend running frequent standards to ensure that the instrument is not displaying erratic behavior or drifting at a different rate. Specifically, I recommend running a set of check standards that fall into each concentration range, and not just using a single check standard. That is, run check standards that fall in the low, medium, and high N_2O concentration ranges. This will allow users to evaluate drift across all N_2O concentrations and the need for recalibration. While I think it is unlikely, based on the features of cavity-enhanced absorption spectroscopy described above, it is possible that isotopocule concentrations could drift in one concentration range but remain stable in another. To account for that, running regular check standards will be useful. In my own work, I balance the need for sample throughput vs. calibration checks by running two check standards daily in each of my three concentration ranges, and then looking for evidence of drift on weekly time scales. In sum, I encourage readers to run at least weekly standards that span the full calibration range to assess the need for updating calibration parameters.

5.5 Results of $^{15}N_2O$-enriched validation of calibration approach

An important aspect of using my laser-based analyzer is my ability to run isotopically enriched samples. Isotopic enrichment has the advantage of measuring large changes in $^{15}N_2O$ (high signal) and thus results are more robust and less ambiguous than measurements performed at natural abundance. However, I needed to validate that 1) I could calibrate isotopically enriched

samples using the same methodology as natural abundance samples, and 2) that I could measure isotopically enriched samples with minimal noise to ensure robustness of this method.

I performed two rounds of $^{15}N_2O$-enriched repeated measurements (n = 6 and n = 5) by adding 1 mL of 99 AP $^{15}N_2O$ to incubation jars that were prepared as described in Section 3.3. My aims were to assess if my calibration algorithm would appropriately estimate $^{15}N_2O$-enriched concentrations and examine the analytical precision of the instrument for $^{15}N_2O$-enriched samples. Unfortunately, I was not able to test the calibration algorithm or analytical precision for ^{18}O-enriched N_2O. Groups wishing to use N_2O enriched in ^{18}O should consider running tests on its behavior, although I postulate that since $NN^{18}O$ appears to behave like $N^{15}NO$ and ^{15}NNO at natural abundance, this should be consistent in isotopically enriched material as well.

Both sets of repeated measures yielded excellent analytical precision (Table 2.4). Although SD was greater for all AP values for the first round of samples compared to the second round, SD was comparable in both cases (Table 2.4). I posit that this discrepancy in SD was likely due to the nature of by-hand dilution, as adding 1mL of highly enriched $^{15}N_2O$ to jars with the same degree of precision is a non-trivial task. Further, the second round of samples indicates improved consistency with adding the same volume of enriched gas, as by-hand dilution tends to improve with practice.

Table 2.4. Reported means (±SD) and percent error for $^{15}N_2O$-enriched samples. N_2O concentration and atom percent (AP) abundances of isotopomers are reported. $^{15}N^{bulk} = ([N^{15}NO] + [^{15}NNO])/2$.

Test 1 (n = 6)			**Test 2 (n = 5)**		
	Mean (±SD)	**% Error**		**Mean (±SD)**	**% Error**
N_2O (ppm)	0.501 ppm (±0.001)	0.17%	**N_2O (ppm)**	0.501 ppm (±0.001)	0.22%
$^{15}N^{\alpha}$ (AP)	2.22% (± 0.03)	1.07%	**$^{15}N^{\alpha}$ (AP)**	2.45% (±0.02)	0.51%
$^{15}N^{\beta}$ (AP)	2.78% (±0.04)	1.13%	**$^{15}N^{\beta}$ (AP)**	2.67% (±0.02)	0.52%
$^{15}N^{bulk}$ (AP)	2.48% (±0.04)	1.10%	**$^{15}N^{bulk}$ (AP)**	2.56% (±0.02)	0.52%

Both sets of repeated measures also responded appropriately to the calibration algorithm. Even though N_2O concentrations were small and isotopomer concentrations were large, the calibration algorithm appropriately corrected N_2O, $N^{15}NO$, and ^{15}NNO. This shows that while N_2O and its isotopomers typically fall within the same concentration range (small, medium, or large) at natural abundance, N_2O and its isotopomers can fall into two completely different concentration ranges (e.g., small N_2O and large $N^{15}NO$ or ^{15}NNO) under isotopically enriched conditions and still get calibrated correctly. Since each isotopomer is measured independently, I have the flexibility to calibrate isotopomers in the same sample that fall into different concentration ranges.

Overall, this test illustrates that the calibration algorithm is appropriate for use with isotopically enriched material, and that the LGR N_2O Isotopic Analyzer generates robust measurements (high signal:noise ratio) with isotopically enriched samples. I suggest taking advantage of this feature of the instrument and performing isotopically enriched studies when possible. Enriched studies typically have very large changes in $^{15}N_2O$ concentration (high signal), which makes the level of noise I measured trivial for application in enriched work. Since these data tend to be far less ambiguous than natural abundance data, I propose that performing enriched experiments will require fewer technical replicates than natural abundance experiments, which should contribute to more efficient data collection and interpretation.

5.6 Comparison of LGR precision with IRMS devices

I have demonstrated that my LGR N_2O Isotopic Analyzer can be calibrated to measure N_2O, $N^{15}NO$, ^{15}NNO, and $NN^{18}O$ at natural abundance or under isotopically enriched conditions, but the analytical precision of this instrument is notably lower than the analytical precision of a traditional GC-IRMS for natural abundance measurements. Traditional GC-IRMS often report

analytical error less than 1‰, but the error I observed for samples at natural abundance was greater (Table 2.2, Table 2.3). At this time, the LGR instrument manufacturers report instrument precision better than 1‰ at ambient N_2O concentrations, but to my knowledge only one lab has currently confirmed that (Ostrom and Ostrom 2017). However, it is worth pointing out that the instrument I used for this study was the original prototype for the now commercially available LGR N_2O Isotopic Analyzer (see Section 3.5). Perhaps versions of this instrument manufactured later have improved hardware and software, making them capable of greater analytical precision. There have also been reports of variability attributed to instrument-specific behavior, which could be a factor here, too (Soto et al. 2015).

Additionally, given the inherent noisiness of natural abundance isotopomer data, I argue that the variability I observe in my calibrated natural abundance data may be manageable, with appropriate experimental design and replication. In the literature there is already a large range of possible SP values that are generally agreed upon to correspond to a given microbial or abiotic N-transformation (Baggs 2008, Decock and Six 2013, Hu et al. 2015, Denk et al. 2017, Harris et al. 2017). For example, SP values corresponding to bacterial denitrification range from -15 to 25‰ (Park et al. 2011, Hu et al. 2015). While these broadly ranging SP values should be interpreted with caution, for now the convention is to assume that an SP value within a given range corresponds to a particular process. So, if data are collected in the medium N_2O range, SD of error should be less than 3‰ for SP after calibration (Table 2.3). I think that is a reasonable degree of error for SP measurements, especially as a springboard for using these novel analyzers to characterize N_2O-generating processes.

It is also worth pointing out that there is consensus in the literature about the disparity in analytical precision for $\delta^{15}N^{bulk}$ vs. SP (Koster et al. 2013, Ostrom and Ostrom 2017). GC-IRMS

tends to achieve greater precision for bulk measurements whereas laser-based analyzers tend to achieve greater precision for SP measurements. Lasers circumvent the ion scrambling issue idiosyncratic to mass spectrometry by measuring each isotopomer independently and thus report more precise SP values (Harris et al. 2014, Mohn et al. 2014, Ostrom and Ostrom 2017). I assert that depending on the N_2O measurements a group is most interested in, one instrument might better suit the group's need than another. However, throughput is arguably higher for lasers, which is a factor to weigh despite the onerous calibration challenges.

6. Conclusions and general lessons from calibration approach

As technology for isotopic measurements continues to develop, there is concern that its adoption will move faster than my capacity to generate accurate and appropriately referenced isotopic datasets (Ostrom and Ostrom 2017). There is great potential in high throughput laser-based analyzers, but it is paramount that I use them effectively to improve understanding rather than to produce datasets of ambiguous calibration. By developing this calibration approach, I seek to couple precise and accurate isotopic measurements with technological advancements. Further, this calibration approach can be applied to any laser-based system where the isotope ratios are determined from direct measurement of each isotopocule concentration. Thus, I hope this calibration algorithm can be used to advance not only laser-based N_2O isotopic research, but laser-based isotopic research more generally. Here, I explicitly outline some key suggestions for future calibration efforts.

1. Calibrate isotopocules in N_2O concentration ranges

Calibrate isotopocules of N_2O in ranges to reduce the statistical leverage induced by the very wide concentration spread. The breakpoints for the N_2O concentration ranges should be established by examining plots of residuals vs. known N_2O concentrations. These range

breakpoints can then be established for the concentration of each isotopomer or isotopologue by multiplying the endpoints of the range by the atmospheric $^{15}N/^{14}N$ or $^{18}O/^{16}O$ ratio (see Section 4.2 for details on this procedure). I established that calibrating all isotopocules in concentration ranges yielded more accurate and precisely calibrated values than calibrating isotopocules across the entire calibration range (0.3-300 ppm).

2. Use a mathematically similar calibration for all isotopocules

I determined that using the same type of correction function for all isotopocules of N_2O eliminated systematic bias when calculating δ values. For example, using a spline fit to calibrate N_2O and then using polynomial regressions to calibrate the isotopomers and isotopologue yielded systematic discrepancies in isotope ratios and subsequently in the δ values I calculated. I reduced bias substantially in calculated δ values when all isotopocules were calibrated in the same fashion.

I recommend using 2nd order polynomial regressions for estimating all isotopocules. I found that polynomial regressions fit my data better than any other model excluding spline fits. However, 2nd order polynomial fits were superior to spline fits because the error structure of a spline could differ across isotopocule concentrations, even within a defined N_2O concentration range. This led to poorer isotope ratio determinations, whereas the less flexible polynomial fit did not have this issue. I acknowledge that data from another instrument might be better fit with a different model, but regardless, I recommend being consistent and fitting the same type of model to all data.

3. Natural abundance analytical precision is best in the medium N_2O concentration range

I have empirically determined that natural abundance isotopomer and isotopologue data from my laser-based analyzer is most precise in the medium N_2O concentration range. To that

end, I encourage striving to collect N_2O data that falls within the ~1.5-33 ppm N_2O concentration range. I acknowledge that the endpoints of this range could vary by instrument, but in general instrumental error was greatest at the lowest and highest N_2O concentrations within my calibration range (e.g., below 1.5 ppm and above 75 ppm, Figure 2.2). Thus, although my calibration shows that I can correct natural abundance N_2O and isotopic data relatively accurately and precisely between 2-75 ppm, consider increasing the number of technical replicates if users choose to analyze N_2O data that falls outside of the medium N_2O range (Figure 2.1B; Figure 2.2D-F, Figure 2.3).

4. Isotopically enriched measurements are robust

My repeated measures test of $^{15}N_2O$-enriched samples demonstrates that measuring isotopically enriched isotopomers of N_2O is robust (Table 4). I have determined that the current laser-based technology is ready for high-precision N_2O research once a concentration-specific offline calibration is applied when using isotopically enriched material. I encourage groups aiming to use these laser-based instruments to ask research questions that can be addressed using isotopically enriched material. This will allow our field to continue to study N_2O and its isotopomers while the scientific community works to improve the analytical precision necessary for natural abundance measurements with these laser-based instruments.

CHAPTER 2 REFERENCES

Baggs EM. A review of stable isotope techniques for N_2O source partitioning in soils: recent progress, remaining challenges, and future considerations. *Rapid Commun Mass Spectrom*. 2008;22(22):1664-1672. doi:10.1002/rcm

Baggs EM. Soil microbial sources of nitrous oxide: Recent advances in knowledge, emerging challenges and future direction. *Curr Opin Environ Sustain*. 2011;3(5):321-327. doi:10.1016/j.cosust.2011.08.011

Bowling DR, Sargent SD, Tanner BD, Ehleringer JR. Tunable diode laser absorption spectroscopy for stable isotope studies of ecosystem-atmosphere CO2 exchange. *Agric For Meteorol*. 2003;118(1-2):1-19. doi:10.1016/S0168-1923(03)00074-1

Bowling DR, Burns SP, Conway TJ, Monson RK, White JWC. Extensive observations of CO2 carbon isotope content in and above a high-elevation subalpine forest. *Global Biogeochem Cycles*. 2005;19(3):1-15. doi:10.1029/2004GB002394

Bouwman AF, Beusen AHW, Griffioen J, et al. Global trends and uncertainties in terrestrial denitrification and N_2O emissions. *Philos Trans R Soc B Biol Sci*. 2013;368(1621). doi:10.1098/rstb.2013.0112

Butterbach-Bahl K, Baggs EM, Dannenmann M, Kiese R, Zechmeister-Boltenstern S. Nitrous oxide emissions from soils: how well do we understand the processes and their controls? *Philos Trans R Soc London*. 2013;368(1621):20130122. doi:10.1098/rstb.2013.0122

Ciais P, Sabine C, Bala G, et al. The physical science basis. Contribution of working group I to the fifth assessment report of the intergovernmental panel on climate change. *Chang IPCC Clim*. 2013:465-570. doi:10.1017/CBO9781107415324.015

Coplen, TB. Guidelines and recommended terms for expression of stable-isotope-ratio and gas-ratio measurement results. *Rapid Commun Mass Spectrom*. 2011: 25(17):2538-2560. doi:10.1002/rcm.5129

Davidson EA, Kanter D. Inventories and scenarios of nitrous oxide emissions. *Environ Res Lett*. 2014: 9(10). doi:10.1088/1748-9326/9/10/105012

Decock C, Six J. How reliable is the intramolecular distribution of ^{15}N in N_2O to source partition N_2O emitted from soil? *Soil Biol Biochem*. 2013: 65(2):114-127. doi:10.1016/j.soilbio.2013.05.012

Denk TRA, Mohn J, Decock C, et al. The nitrogen cycle: A review of isotope effects and isotope modeling approaches. *Soil Biol Biochem*. 2017;105:121-137. doi:10.1016/j.soilbio.2016.11.015

Fu C, Lee X, Griffis TJ, Dlugokencky EJ, Andrews AE. Investigation of the N_2O emission strength in the U. S. Corn Belt. *Atmos Res*. 2017;194(January):66-77. doi:10.1016/j.atmosres.2017.04.027

Galloway JN, Aber JD, Erisman JW, et al. The Nitrogen Cascade. *Bioscience*. 2003;53(4):341. doi:10.1641/0006-3568(2003)053[0341:TNC]2.0.CO;2

Galloway JN, Townsend AR, Erisman JW, et al. Transformation of the Nitrogen Cycle: Recent Trends, Questions, and Potential Solutions. *Science (80-)*. 2008;320(May):889-892. doi:10.1126/science.1136674

Groffman PM, Driscoll CT, Fahey TJ, Hardy JP, Fitzhugh RD, Tierney GL. Effects of mild winter freezing on soil nitrogen and carbon dynamics in a northern hardwood forest.

Biogeochemistry. 2001;56(2):191-213. doi:10.1023/A:1013024603959
Harris E, Nelson DD, Olszewski W, et al. Development of a spectroscopic technique for continuous online monitoring of oxygen and site-specific nitrogen isotopic composition of atmospheric nitrous oxide. *Anal Chem*. 2014;86(3):1726-1734. doi:10.1021/ac403606u
Harris E, Henne S, Hüglin C, et al. Tracking nitrous oxide emission processes at a suburban site with semicontinuous, in situmeasurements of isotopic composition. *J Geophys Res*. 2017;122(3):1850-1870. doi:10.1002/2016JD025906
Harris SJ, Liisberg J, Xia L, et al. N2O isotopocule measurements using laser spectroscopy: Analyzer characterization and intercomparison. *Atmos Meas Tech*. 2020;13(5):2797-2831. doi:10.5194/amt-13-2797-2020
Heil J, Wolf B, Brüggemann N, et al. Site-specific ^{15}N isotopic signatures of abiotically produced N_2O. *Geochim Cosmochim Acta*. 2014;139:72-82.
Heil J, Liu S, Vereecken H, Brüggemann N. Abiotic nitrous oxide production from hydroxylamine in soils and their dependence on soil properties. *Soil Biol Biochem*. 2015;84:107-115. doi:10.1016/j.soilbio.2015.02.022
Hu HW, Chen D, He JZ. Microbial regulation of terrestrial nitrous oxide formation: Understanding the biological pathways for prediction of emission rates. *FEMS Microbiol Rev*. 2015;39(5):729-749. doi:10.1093/femsre/fuv021
Ibraim E, Harris E, Eyer S, et al. Development of a field-deployable method for simultaneous, real-time measurements of the four most abundant N2O isotopocules. *Isotopes Environ Health Stud*. 2018;54(1):1-15. doi:10.1080/10256016.2017.1345902
Ibraim E, Wolf B, Harris E, et al. Attribution of N_2O sources in a grassland soil with laser spectroscopy based isotopocule analysis. *Biogeosciences*. 2019;16:3247-3266. doi:10.5194/bg-2018-426
Kool DM, Wrage N, Oenema O, Harris D, Van Groenigen JW. The ^{18}O signature of biogenic nitrous oxide is determined by O exchange with water. *Rapid Commun Mass Spectrom*. 2009;23:104-108. doi:10.1002/rcm
Koster JR, Well R, Tuzson B, et al. Novel laser spectroscopic technique for continuous analysis of N_2O isotopomers - application and intercomparison with isotope ratio mass spectrometry. *Rapid Commun Mass Spectrom*. 2013;27:216-222. doi:10.1002/rcm.6434
Kuypers MMM, Marchant HK, Kartal B. The microbial nitrogen-cycling network. *Nat Rev Microbiol*. 2018;16(5):263-276. doi:10.1038/nrmicro.2018.9
Lewicka-Szczebak D, Dyckmans J, Kaiser J, Marca A, Augustin J, Well R. Oxygen isotope fractionation during N_2O production by soil denitrification. *Biogeosciences*. 2016;13(4):1129-1144. doi:10.5194/bg-13-1129-2016
Maeda K, Spor A, Edel-Hermann V, et al. N_2O production, a widespread trait in fungi. *Sci Rep*. 2015;5(1):9697. doi:10.1038/srep09697
Mohn J, Tuzson B, Manninen A, et al. Site selective real-time measurements of atmospheric N_2O isotopomers by laser spectroscopy. *Atmos Meas Tech*. 2012;5(7):1601-1609. doi:10.5194/amt-5-1601-2012
Mohn J, Wolf B, Toyoda S, et al. Interlaboratory assessment of nitrous oxide isotopomer analysis by isotope ratio mass spectrometry and laser spectroscopy: Current status and perspectives. *Rapid Commun Mass Spectrom*. 2014;28(18):1995-2007. doi:10.1002/rcm.6982
Ostrom NE, Piit A, Sutka R, et al. Isotopologue effects during N_2O reduction in soils and in pure cultures of denitrifiers. *J Geophys Res Biogeosciences*. 2007;112(2):1-12.

doi:10.1029/2006JG000287
Ostrom NE, Ostrom PH. Mining the isotopic complexity of nitrous oxide: a review of challenges and opportunities. *Biogeochemistry*. 2017;132(3):359-372. doi:10.1007/s10533-017-0301-5
Ostrom NE, Gandhi H, Coplen TB, et al. Preliminary assessment of stable nitrogen and oxygen isotopic composition of USGS51 and USGS52 nitrous oxide reference gases and perspectives on calibration needs. *Rapid Commun Mass Spectrom*. 2018;32(15):1207-1214. doi:10.1002/rcm.8157
Park S, Perez T, Boering KA, et al. Can N2O stable isotopes and isotopomers be useful tools to characterize sources and microbial pathways of N2O production and consumption in tropical soils? *Global Biogeochem Cycles*. 2011;25(1):1-16. doi:10.1029/2009GB003615
Perez T, Garcia-Montiel D, Trumbore SE, et al. Nitrous oxide nitrification and denitrification ^{15}N enrichment factors from Amazon forest soils. *Ecol Appl.* 2006;16(6):2153-2167.
Provencal R, Gupta M, Owano TG, et al. Cavity-enhanced quantum-cascade laser-based instrument for carbon monoxide measurements. *Appl Opt*. 2005;44(31):6712-6717. doi:10.1364/AO.44.006712
Ravishankara AR, Daniel JS, Portmann RW. Nitrous oxide (N_2O): The dominant ozone-depleting substance emitted in the 21st century. *Science (80-)*. 2009;326(5949):123-125. doi:10.1126/science.1176985
Reay DS, Davidson E a., Smith K a., et al. Global agriculture and nitrous oxide emissions. *Nat Clim Chang*. 2012;2(6):410-416. doi:10.1038/nclimate1458
Röckmann T, Kaiser J, Brenninkmeijer CAM. The isotopic fingerprint of the pre-industrial and the anthropogenic N 2O source. *Atmos Chem Phys*. 2003;3(2):315-323. doi:10.5194/acp-3-315-2003
Rohe L, Well R, Lewicka-Szczebak D. Use of oxygen isotopes to differentiate between nitrous oxide produced by fungi or bacteria during denitrification. *Rapid Commun Mass Spectrom*. 2017;31(16):1297-1312. doi:10.1002/rcm.7909
Shcherbak I, Millar N, Robertson GP. Global metaanalysis of the nonlinear response of soil nitrous oxide (N_2O) emissions to fertilizer nitrogen. *Proc Natl Acad Sci U S A*. 2014;111(25):9199-9204. doi:10.1073/pnas.1322434111
Snider DM, Venkiteswaran JJ, Schiff SL, Spoelstra J. From the ground up: Global nitrous oxide sources are constrained by stable isotope values. *PLoS One*. 2015;10(3):1-19. doi:10.1371/journal.pone.0118954
Soto DX, Koehler G, Hobson KA. Combining Denitrifying Bacteria and Laser Spectroscopy for Isotopic Analyses ($\delta^{15}N$, $\delta^{18}O$) of Dissolved Nitrate. *Anal Chem*. 2015;87(14):7000-7005. doi:10.1021/acs.analchem.5b01119
Sutka RL, Ostrom NE, Ostrom PH, et al. Distinguishing Nitrous Oxide Production from Nitrification and Denitrification on the Basis of Isotopomer Abundances. *Appl Environ Microbiol*. 2006;72(1):638-644. doi:10.1128/AEM.72.1.638
Wolf B, Merbold L, Decock C, et al. First on-line isotopic characterization of N_2O above intensively managed grassland. *Biogeosciences*. 2015;12(8):2517-2531. doi:10.5194/bg-12-2517-2015
Wrage N, Lauf J, del Prado A, et al. Distinguishing sources of N_2O in European grasslands by stable isotope analysis. *Rapid Commun Mass Spectrom*. 2004;18(11):1201-1207. doi:10.1002/rcm.1461

Yang WH, Teh YA, Silver WL. A test of a field-based ^{15}N-nitrous oxide pool dilution technique to measure gross N_2O production in soil. *Glob Chang Biol*. 2011;17(12):3577-3588. doi:10.1111/j.1365-2486.2011.02481.x

Ye W, Bian L, Wang C, Zhu R, Zheng X, Ding M. Monitoring atmospheric nitrous oxide background concentrations at Zhongshan Station, east Antarctica. *J Environ Sci (China)*. 2016;47:193-200. doi:10.1016/j.jes.2015.12.038

Yoshida N, Toyoda S. Constraining the atmospheric N_2O budget from intramolecular site preference in N_2O isotopomers. Nature. 2000;405(6784):330-334. doi:10.1038/35012558

Yu L, Harris E, Henne S, et al. The isotopic composition of atmospheric nitrous oxide observed at the high-altitude research station Jungfraujoch, Switzerland. *Atmos Chem Phys Discuss*. 2019;(October):1-51. doi:10.5194/acp-2019-829

Yu L, Harris E, Lewicka-Szczebak D, et al. What can we learn from N 2 O isotope data? - Analytics, processes and modelling . *Rapid Commun Mass Spectrom*. 2020;(June):1-14. doi:10.1002/rcm.8858

CHAPTER 3: CHARACTERIZING THE IMPORTANCE OF DENITRIFICATION FOR N_2O PRODUCTION IN SOILS USING NATURAL ABUNDANCE AND ISOTOPIC LABELLING TECHNIQUES

1. Summary

Nitrous oxide (N_2O), a potent greenhouse gas that contributes significantly to climate change, is emitted mostly from soils by a suite of microbial metabolic pathways that are nontrivial to identify, and subsequently, to manage. Using either natural abundance or enriched stable isotope methods has aided in identifying microbial sources of N_2O, but each approach has limitations. Here, I conducted a novel pairing of natural abundance and enriched assays on two dissimilar soils, hypothesizing this pairing would better constrain microbial sources of N_2O. I incubated paired natural abundance and enriched soils from a corn agroecosystem and a subalpine forest in the laboratory at 10-95% soil saturation for 28 hr. The natural abundance method measured intramolecular site preference (SP) from emitted N_2O, whereas the enriched method measured emitted $^{15}N_2O$ from soils amended with ^{15}N-labelled substrate. The isotopic composition of emitted N_2O was measured using a laser-based N_2O isotopic analyzer, yielding two key findings. First, both methods revealed that denitrification was the primary source of N_2O in all soils: isotopic enrichment revealed clear NO_3^- reduction to N_2O, while SP indicated a likely combination of fungal and bacterial denitrification. Second, I quantified, for the first time to my knowledge, persistent (>50%) β-position-specific enrichment in emitted $^{15}N_2O$, which is far in excess of SP-level fractionation expectations. This counter-intuitive enrichment pattern raises the possibility of previously unrecognized N-transformations in these soils, which warrants further study. Alternatively, this pattern could be indicative of co-denitrification, an understudied but potentially highly important contributor to N_2O emissions.

2. Introduction

Nitrous oxide (N_2O) is a far more potent greenhouse gas (GHG) than other biogenic GHGs (Ravishinkara et al. 2009, Cias et al. 2013). On a per molecule basis, N_2O has a warming potential 298x greater than carbon dioxide (CO_2) and 34x greater than methane (CH_4) (Alvarez et al. 2012, Rector et al. 2018). This is problematic because the atmospheric N_2O concentration has risen an unprecedented 20% since the beginning of the Industrial Revolution (Ciais et al. 2013). Microbial metabolism of synthetic and manure-based nitrogen (N) fertilizers in agricultural soils are largely responsible for this sharp rise in atmospheric N_2O (Davidson 2009, Park et al. 2012, Smith 2017). Approximately 70% of N_2O is emitted from soils, and most of that N_2O is emitted from soils that have surpassed an N-limitation threshold (Aber et al. 1989, Aber et al. 1998, Fenn et al. 2018). In these soils, inorganic N supply exceeds soil carbon (C) availability, which typically manifests in heightened microbial N metabolism and excess N_2O emissions (Davidson 2009).

Multiple microbial metabolic pathways can generate N_2O, and so it can be difficult to identify the process(es) responsible for emissions (Snider 2011, Zhang et al. 2016, Ibraim et al. 2018, Wong et al. 2020). Microbes can emit N_2O via nitrification, dissimilatory nitrate reduction to ammonium (DNRA), denitrification (bacterial and fungal), nitrifier-denitrification, co-denitrification, and anaerobic ammonia oxidation (anammox) (Butterbach-Bahl et al. 2013). However, identifying the microbial source process(es) responsible for emissions is particularly challenging because each process is sensitive to a variety of spatially and temporally variable factors such as soil physical and chemical properties, climate, moisture, availability of N substrate, and microbial community composition and activity (Jenny 1980, Wrage et al. 2004, Park et al. 2011, Toyoda et al. 2015, van Groenigen et al. 2015, Congreves et al. 2019, Denk et

al. 2019). To further complicate matters, processes can co-occur, sometimes even being performed by the same soil microbe (Sanford et al. 2012, Long et al. 2013, McTigue et al. 2016, Wen et al. 2016). Taken together, this consort of variables makes it difficult to comprehensively identify the microbial processes responsible for N_2O emissions over space and time. To manage rising N_2O levels, we must be able to better identify which microbial pathways are responsible for emissions, especially as soils become progressively N-saturated due to human activities.

Stable isotopes have proven central to understanding the biochemical source processes of N_2O (Baggs 2008, Baggs 2011, Snider 2011, Snider et al. 2015, Hu et al. 2015, Yu et al. 2020). Both natural abundance and enriched methods have been used to quantify these sources (Perez et al. 2006, Ostrom and Ostrom 2012, Screiber et al. 2012, Ostrom and Ostrom 2017, Yamamoto et al. 2017). Isotopic enrichment has proved a reliable and robust method for partitioning among the better-studied N_2O-generating processes, nitrification and denitrification (Wrage et al. 2004, Mathieu et al. 2006, Wagner-Riddle et al. 2008, Russow et al. 2009). By amending a given soil with isotopically labelled $^{15}NH_4^+$ or $^{15}NO_3^-$, researchers can reveal when nitrification or denitrification dominates by tracing the emitted enriched N_2O back to the enriched substrate. However, ^{15}N additions are somewhat limiting in that they only partition between the two broad classes of processes.

In contrast, a number of studies have now characterized the natural abundance intramolecular distribution of ^{15}N in the N_2O molecule to delineate among multiple N_2O-producing processes (Sutka et al. 2006, Chen et al. 2016). Like many biochemical transformations, stable isotope fractionation occurs during N_2O production (Menyailo and Hungate 2006, Vieten et al. 2007, Lewicka-Szczebak et al. 2015, Snider et al. 2015). This causes differential accumulation of heavy N in either the central, α-position N, or the terminal, β-

position N, in the linear N_2O molecule ($^{\beta}N=^{\alpha}N=O$, Yoshida and Toyoda 2000). The intramolecular distribution, or difference in $\delta^{15}N$ between $\delta^{15}N^{\alpha}$ and $\delta^{15}N^{\beta}$ isotopomers, is termed site preference (SP, Yoshida and Toyoda 2000). Since the early 2000s, a number of pure culture, lab, and field studies have shown that many N_2O-generating processes reliably yield consistent SP values (Toyoda et al. 2005, Sutka et al. 2006, Well et al. 2006, Perez et al. 2006, Baggs 2008, Park et al., 2011, Snider 2011, Maeda et al., 2015). To date, researchers have used SP to disentangle diverse processes, including: nitrification via ammonium oxidizing Archaea (AOA) or ammonium oxidizing bacteria (AOB), fungal or bacterial denitrification, and nitrifier denitrification (Wrage et al. 2004, Sutka et al. 2006, Wu et al. 2016, Wrage-Mönnig et al. 2018, Rohe et al. 2020). However, there are disagreements in the literature about the robustness of this method for multiple reasons. First, interlaboratory calibration for N_2O isotopic standards remains an ongoing issue (Mohn et al. 2014, Ostrom and Ostrom 2017, Ostrom et al. 2018, Harris et al. 2020). Second, SP values have been reported to overlap among very different source processes (e.g., nitrification and fungal denitrification), or among similar source processes that occur under similar conditions (e.g., denitrification and nitrifier denitrification or nitrification via AOA vs. AOB, Decock and Six 2013, Xia et al. 2013, Hu et al. 2015, Wenk et al. 2016, Yamamoto et al. 2017, Wrage-Mönnig et al. 2018, Yu et al. 2020). And third, $N_2O \rightarrow N_2$ reduction during denitrification enriches $\delta^{15}N^{\alpha}$ and can thus confound SP values (Koster et al. 2013, Mohn et al. 2014, Ostrom and Ostrom 2017, Lewicka-Szczebak et al. 2020, Stuchiner et al. 2020).

To overcome the individual limitations of enriched and natural abundance studies, I paired both methods on the same soils to enable better partitioning among N_2O-generating source processes. I paired these methods on two very different soils, one from a corn agroecosystem and one from a subalpine forest, held at 50-95% saturation to promote diverse

N_2O-generating microbial metabolic pathways. Under these relatively wet conditions, soils have the potential to host a variety of biotic processes, such as bacterial or fungal denitrification, nitrifier denitrification, DNRA, anammox, or codenitrification, and I sought to disentangle overlapping or ambiguous isotopic signatures by using paired enriched and natural abundance approaches. I also measured SP for these soils held at 10-40% saturation because I anticipated primarily nitrification-driven SPs (approximately ≥ 30‰) but wanted to test for other processes or atypical SPs (Sutka et al. 2006). By incubating different soils under both natural abundance and isotopically enriched conditions, I aimed to reveal gaps in our understanding about these isotopic approaches, and better understand the microbial N-transformations occurring in different soils.

3. Materials and Methods

3.1 Field sampling and soil characterization

3.1.1 Site descriptions

I collected soils from two contrasting ecosystems in Colorado: a corn field and a subalpine forest. All soils were collected from the top ~20 cm of the soil profile. Soil properties and treatments for each site are summarized Table 3.1.

Table 3.1. Properties and treatment descriptions (as applicable) for all sites. Percent soil organic C (SOC) and soil organic N (SON), and microbial biomass C and N were measured in June 2018. Growing season irrigation or N application was averaged across all the same agricultural treatments plots, and the subalpine values are for the entire watershed surrounding that subalpine environment. The n-value for soil treatment corresponds to the number of plots that samples were collected from. The n-values for all other measurements correspond to the number of technical replicates from each bulked soil sample. Error bars represent ± one SE from the mean.

Site	Soil treatment	Abbreviated soil name	Irrigation (mm/growing season)	Total N application rate (kg/ha/yr)	% SOC	% SON	Microbial Biomass C (μg C/g dry soil)	Microbial Biomass N (μg N/g dry soil)
Agriculture	High N High Water (n = 4)	HNHW	497	266	1.21 (± 0.162) (n = 4)	0.077 (± 0.003) (n = 4)	4.04 (± 0.271) (n = 4)	0.514 (± 0.192) (n = 4)
Agriculture	High N Low Water (n = 3)	HNLW	441	270	1.36 (± 0.036) (n = 4)	0.098 (± 0.017) (n = 4)	2.67 (± 0.485) (n = 4)	0.169 (± 0.045) (n = 4)
Agriculture	Low N High Water (n = 4)	LNHW	497	172	1.28 (± 0.060) (n = 4)	0.093 (± 0.002) (n = 4)	5.19 (± 1.13) (n = 4)	0.523 (± 0.179) (n = 4)
Agriculture	Low N Low Water (n = 3)	LNLW	441	154	1.47 (± 0.090) (n = 4)	0.102 (± 0.004) (n = 4)	2.96 (±0.788) (n = 4)	0.310 (± 0.218) (n = 4)
Subalpine	None (n = 4)	Subalpine	N/A	3-3.5	7.82 (± 1.20) (n = 4)	0.355 (± 0.086) (n = 4)	8.17 (± 1.42 (n = 3)	0.769 (± 0.275) (n = 3)

Agricultural site

I collected soil from the Limited Irrigation Research Farm located north of Greeley, Colorado (described in detail in Zhang and Yemoto 2018). In 2016, experimental treatments were applied across treatment blocks that measured approximately 6 x 20 m. These treatments manipulated soil irrigation and fertilizer N to assess the impact on corn crop yield (detailed in Table 3.1). These treatments included: high N high water (HNHW, n = 4 plots), high N low water (HNLW, n = 3 plots), low N high water (LNHW, n = 4 plots), and low N low water (LNLW, n = 3 plots). The experimental design used 14 fully randomized treatment blocks with high or low irrigation rates, and high or low additions of urea and NO_3^- fertilizer. The blocks were in an approximately 60 x 60 m field, which included other treatment blocks not included in this study, and there was a 6 m buffer around all sides of the field. The soil at this site is classified as Olney fine sandy loam soil, entailing fine-loamy, mixed, super-active, mesic Ustic Haplargids (Zhang and Yemoto 2018). All soil was sampled from the Loamy Sand surface horizon, as classified by Limited Irrigation Research Farm personnel (Trout and Bausch, 2017).

The high and low irrigation treatments provided crops with sufficient watering to meet 100 and 65% of plant evapotranspiration requirements during the late vegetative and maturation growth stages. The high and low N additions were 250 and 130 kg/ha and were applied as a combination of liquid urea and NO_3^- in the irrigation water. Because I could not control the amount of NO_3^- leached into the groundwater, this resulted in some discrepancies in the amount of fertilizer applied to plots, depending on HW or LW treatment. However, analysis of soil IN (described in detail in Text S1) indicated that all HN soils had greater IN levels than LN soils, but the HNHW soil had higher IN levels than the HNLW soil, and the LNHW soil had higher IN levels than the LNLW soil, albeit not appreciably higher (Table 3.3). However, these differences

in N loading have no material impact on my study because my goal was to incubate soils to identify different microbial N_2O-generating processes, not necessarily assess the impact of each of these field treatments. Liquid urea was applied in ~22 kg/ha drip fertigation aliquots throughout the vegetative growth stages (N. Flynn, *pers comm*).

Subalpine site

The Loch Vale Watershed is located in Rocky Mountain National Park on the eastern edge of the Front Range in Colorado, USA, between 3100 and 4000m elevation (described in detail in Heath and Baron 2014). This watershed is subjected to atmospheric N deposition due to easterly winds carrying inorganic N from agricultural, vehicle, and industrial sources along the Colorado Front Range into the park. The N falls primarily as wet deposition (Baron et al. 2000). The Loch Vale Watershed receives ~3-3.5 kg/ha/y of wet N deposition, which has previously been found to alter ecosystem processes (Baron et al. 2000; Booth et al. 2016; Oleksy et al. 2020). Comparatively, background N deposition in the Front Range is ~1 kg/ha/y of wet N deposition (Baron et al. 2000). The watershed receives ~105 cm of precipitation per year, with ~50 cm falling in the summer months (Heath and Baron 2014).

I collected soils from the subalpine forest at ~3200 m, sampling from four randomly selected GPS coordinates where the conditions appeared undisturbed by human foot traffic. No sampling was conducted on the long-term N fertilization plots (Boot et al. 2016). The subalpine forest soils are classified as cryic spodosols, with rocky sandy-loam textures (Weinman 2020). Soils sampled from the Loch Vale Watershed site were taken from the OA horizon (Jill Baron, *pers comm*).

3.1.2 Soil collection and analyses

All soils were collected either in the second week of June 2018 or the third week of July 2018. Soils were collected using a 5cm-diameter soil auger to a depth of ~20 cm. Six cores were collected randomly throughout each sampling plot and bulked into gallon Ziploc bags. Bags were placed on ice in the field to minimize microbial activity, and then refrigerated at 4 °C upon return to the lab. Within 24 hr after sampling, soils were sieved to 2mm and homogenized by treatment. Ziploc bags containing the processed soil were frozen at -20 °C. All incubations and analyses were performed within three months after soils were collected.

Prior to freezing soils, I performed KCl extractions and calculated soil gravimetric water content. After soils had been frozen, I measured soil pH, soil organic C and N (SOC and SON), and soil microbial biomass C and N (MBC and MBN). Frozen soils were also overnight shipped on ice to Ward Laboratories Inc. (Kearney, NE, USA), where soil phospholipid fatty acids (PLFAs) were extracted and analyzed to determine fungi:bacteria ratios for each soil. All of these methods for measuring properties of fresh and frozen soils are described in detail in Appendix 2 (Appendix 2 Text 1).

3.1.3 Determination of soil saturation

Prior to manipulating soil moisture, I first determined the soil water saturation point. My sieved soils lacked soil pore structures, so % water-filled pore space (WFPS), which is typically used to characterize field capacity, was not relevant (Farquharson and Baldock 2008). Instead, I thawed subsamples of the frozen, field-moist soil and amended them with DI water until fully saturated, or at maximum WHC. Then, I dried samples to a constant weight in a 105 °C oven and calculated saturated water content by dividing the mass of water in the sample by the sample dry

soil mass. I brought soils to desired saturation levels (10-90% saturation) by either air-drying or by wetting soils with DI water, as needed.

3.1.4 Comparison of soil properties at two time points

For my experiments, I incubated soils under isotopically enriched conditions and at natural abundance. Due to the limited volume of soil I was permitted to collect in June 2018, I collected more soil in July 2018. As such, the isotopically enriched incubations were performed on June soils, and only on the subalpine soil and the HNHW soil from the agricultural site. Dissimilarly, the natural abundance incubations were performed on all the soil types (see Table 3.1) I collected in July.

To account for differences in soil properties from June to July that could impact microbial activities, I compared all measured soil properties for the soils used in enriched and natural abundance incubations (subalpine and HNHW) with t-tests. Since the other agricultural soils were not used in June, I did not compare how their properties changed from June to July.

3.2 Soil incubations

3.2.1 Soil amendments and incubation setup

Soils were separated into two treatment groups: those amended with isotopically enriched substrate and those held at natural abundance. For all incubations, the frozen soil equivalent of 50g of dry soil (this varied by site and soil treatment) was weighed into 0.5 L Ball jars and refrigerated overnight to thaw. Prior to amendment, all soils were removed from the refrigerator and brought to room temperature over the course of 2 hours to reduce disruption of microbial cellular membranes (Boot et al. 2016).

Soils that were isotopically enriched were amended with 99 atom percent (AP) excess $^{15}NH_4Cl$ or $Na^{15}NO_3$ at an application rate that aimed to double the amount of ^{15}N in the NH_4^+

and NO_3^- pools in each soil. Because natural abundance ^{15}N comprises only 0.37% of N atoms, this isotopic doubling means that I altered the soil N total pool size by <1%, which should have negligible impact as a fertilizer treatment. Specific amounts of ^{15}N added are presented in Appendix 2 (Appendix 2 Table 4). The stable isotope tracer was dissolved in DI water and pipetted over the soils at a constant application rate, and then additional DI water was distributed by pipette over the soils to bring soils to the desired saturations (10-95% soil saturation). After all liquid was added to a given soil, it was mixed thoroughly to ensure sufficient distribution of stable isotope tracer and homogeneous saturation.

Soils that were held at natural abundance were brought to desired saturations either via additions of DI water or through air drying on ice to reduce microbial activity. For the soils that needed to be air dried, they were weighed periodically (~every 10 min) to track moisture loss until the desired dryness was reached.

After soils were brought to their desired saturation and amended with tracer (if applicable), jars were sealed for incubation (Figure 3.1). It is methodologically challenging to balance the need for a small headspace (thus maximizing final N_2O concentration) with the need to remove large volumes of air for isotopic analysis from a hard-sided incubation jar (more details in Section 3.2.2). I compromised with a design that included a 0.5L jar and a 1L gas bag connected to the jar headspace. The jar lid was drilled to contain two ports with Swagelok bulkhead fittings. One fitting vented to ¼ in Tygon tubing with a two-way stopcock (valve 1) for gas sampling (Figure 3.1). The other fitting vented to a luerslip that could be fitted with a two-way stopcock (valve 2) attached to a 1 L Tedlar gas bag (Figure 3.1).

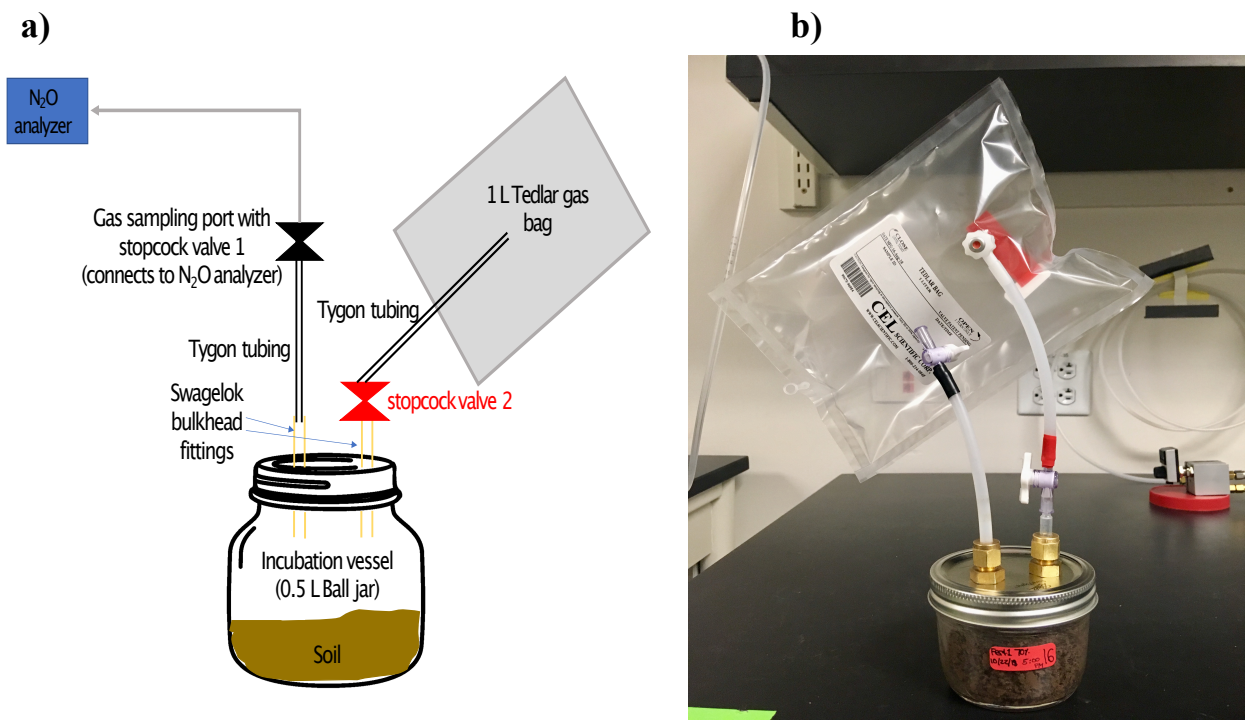

Figure 3.1. Incubation jar-gas bag apparatus. Panel **a** is a conceptual model of the apparatus, and panel **b** shows a photograph of the apparatus.

At the outset of the incubation, I flushed all jars and filled associated gas bags from a cylinder of medical-grade compressed air to provide a uniform starting gas background (Airgas Industries, etc.). Soils were incubated on in an interior lab countertop, at approximately 24 °C for 28 hr. At the end of the incubation period, I mixed each jar and gas bag's air by attaching a 60 mL syringe to the jar's gas sampling port and, by having stopcock valves 1 and 2 open, I pumped the syringe for ~ 60 seconds to homogenize the jar headspace and Tedlar gas bag (Figure 3.1). At the time of sampling, I connected the gas analyzer instrument system directly to the headspace-gas bag apparatus. Removal of jar headspace air thus emptied the gas bag and jar headspaces together, keeping the jar air pressure at atmospheric levels.

3.2.2 Measurements of N_2O concentration and isotopic compositions

After 28 hours, incubation vessels were attached to my laser-based Los Gatos Research (LGR) N_2O isotopic analyzer. Gas was sampled from each incubation vessel for 12-15 minutes

(or until the N_2O concentration stabilized) at a flowrate of 42 mL/min into the analyzer. Samples were attached to the analyzer upstream of a Nafion-Carbosorb-Silica gel scrubbing system to remove CO_2, H_2O vapor, and VOCs from the sampling stream. This measure is taken to minimize the optical peak-broadening effects inherent to laser-based analyzers, as these effects can decrease the accuracy of reported N_2O concentrations. For further details, see Stuchiner et al. (2020).

I previously described the instrumental determination of N_2O concentration and isotopic composition (Stuchiner et al. 2020). Briefly, my analyzer measures concentrations of N_2O ($^{14}N^{14}N^{16}O$) and all its isotopomers ($^{14}N^{15}N^{16}O$, $^{15}N^{14}N^{16}O$, and $^{14}N^{14}N^{18}O$) using cavity enhanced laser absorption spectroscopy (Los Gatos Research N_2O Isotopic Analyzer model 914–0027; ABB-Los Gatos Research, Mountain View, CA, USA) in a continuous flow-through system without pre-concentration of the incoming gas. Calibration, as described in detail in Stuchiner et al. (2020), involves the joint calibration of all isotopomers against dilutions of the USGS52 standard and dilutions of my laboratory working standard. Due to non-linearity in the instrument response, I had best calibration success by breaking the observed data into concentration ranges and using separate polynomial regression to calibrate each range. Check standards interspersed with samples confirmed the accuracy and precision of analyses.

All raw concentration data for each sample was exported to Excel (version 16.46) where it was trimmed to include only the N_2O and isotopomer concentrations after readings had stabilized. Approximately the final ~5 minutes of sampling was used to calculate average N_2O and isotopomer concentrations. The concentrations of N_2O and each isotopomer were calibrated using the model described in Stuchiner et al. (2020), and then isotopomer concentrations were converted to δ notation. I calculated the δ values using standard notation and the $^{15}N/^{14}N$ ratio of

atmospheric N_2 (0.0036765) or the $^{18}O/^{16}O$ in VSMOW (0.0020052). All δ values are in ‰. The $\delta^{18}O$ values are reported in Appendix 2 (Appendix 2 Figure 1).

Equations 1-3 can be used to determine the δ values for the N_2O isotopomers:

$$(\mathbf{1})\ \delta^{15}N^{\alpha} = \frac{(N^{15}NO/N_2O)_{sample}}{(N^{15}NO/N_2O)_{std}} - 1$$

$$(\mathbf{2})\ \delta^{15}N^{\beta} = \frac{(^{15}NNO/N_2O)_{sample}}{(^{15}NNO/N_2O)_{std}} - 1$$

$$(\mathbf{3})\ \delta^{18}O = \frac{(NN^{18}O/N_2O)_{sample}}{(NN^{18}O/N_2O)_{std}} - 1$$

And to determine SP I used Equation 4:

$$(\mathbf{4})\ SP = \delta^{15}N^{\alpha} - \delta^{15}N^{\beta}$$

At low N_2O concentrations the SP data was consistently unreliable or out of the biologically plausible range (e.g., positive hundreds of ‰, Appendix 2 Figure 4), so I did not use any SP data from those incubations. According to Hu et al. (2015), the plausible range goes from -30 to 50‰. To avoid erroneous exclusion of data, I extended the range from -40 to 65‰ because there is uncertainty surrounding the "true" biologically plausible SP range owing to ambiguity in isotopomer calibration and analytical precision (Ostrom and Ostrom 2017, Stuchiner et al. 2020). Thus, I excluded 10 of the 59 samples included in my analysis, where they reported biologically implausible SP values. The complete SP dataset is presented in Appendix 2 Table 1. The majority of these implausible values were associated with relatively low N_2O concentrations (Appendix 2 Figure 3, Appendix 2 Figure 5).

3.2.3 Leak test of incubation apparatus

A separate test was performed to assess the gastight seals of the incubation apparati used in this experiment (Figure 3.1). Twelve incubation apparati were filled with zero-grade air (80:20 N_2:O_2 blend, Airgas Industries) as described in Section 3.2.1 and injected with 1 mL of 99 AP $^{15}N^{15}N$ O using a 3 mL syringe, raising the N_2O concentration to ~500ppb and the $\delta^{15}N^{bulk}$ to ~6300‰. Six apparati were sampled for N_2O and its isotopomer concentrations 1 hr after preparation (T_0) and the remaining six apparati were sampled 48 hr after preparation (T_{48}). All samples were taken on my LGR N_2O isotopic analyzer. Change in total N_2O concentration was not significant, while change in ^{15}N enriched N_2O was < 2.3% for all isotopomers.

3.3 Data analysis

All raw data was collected and collated in Excel, and then all statistical analyses were performed in RStudio (version 4.0.2 (2020-06-22) -- "Taking Off Again" © 2020 The R Foundation for Statistical Computing). Differences among inherent soil properties and treatment effects were examined using ANOVAs and t-tests. Residuals were examined for departure from normality, and all N_2O production data for the enriched incubations were log-transformed to meet assumptions of normality in residuals. All predicted N_2O production data for the natural abundance incubations were also log-transformed to meet assumptions of normality in residuals.

The logistic regressions used to predict N_2O production rates were fitted in RStudio with the package `dr4pl`.

4. Results

4.1 Soil properties

Soils collected from the agricultural and subalpine sites differed sharply in biogeochemical properties in both June and July. The June soils are summarized in Table 3.2.

There were notable differences in most soil properties between the HNHW and subalpine June soils ($p < 0.05$ in all cases), excluding fungi:bacteria ratios, which were not significantly different.

Table 3.2. Biogeochemical properties of HNHW and subalpine soils collected in June 2018. The n-value for each measurement corresponds to the number of technical replicates within each bulked soil treatment. Error bars represent ± one SE from the mean.

Soil treatment	NO_3^- (µg N/g dry soil)	NH_4^+ (µg N/g dry soil)	Fungi:Bacteria (% fungi/% bacteria)	Soil pH
HNHW	80.3 (± 6.51) (n = 10)	3.03 (± 1.09) (n = 10)	0.193 (± 0.035) (n = 4)	7.90 (± 0.06) (n = 8)
Subalpine	1.06 (±0.420) (n = 9)	5.35 (± 1.29) (n =9)	0.192 (± 0.030) (n = 3)	5.14 (± 0.08) (n = 9)

The July soils are summarized in Table 3.3. Pairwise comparisons revealed that all agriculture soils had notably higher NO_3^- concentrations than the subalpine soil-($p < 0.05$ in all cases), but only the HNHW soil had a significantly higher NO_3^- concentration compared to the other agricultural soils ($p < 0.05$ in all cases). Pairwise comparisons also demonstrate that all agricultural soils had significantly less NH_4^+ compared to the subalpine soil ($p < 0.05$ in all cases), but none of the agricultural soils differed in NH_4^+ concentration. There were some differences in fungi:bacteria ratios for soils sampled in July. While there were no differences in fungi:bacteria within the agricultural soils, the HNHW soil had a significantly lower fungi:bacteria ratio from the subalpine soil ($p = 0.0016$), and the HNHW, LNHW, and LNLW soils had borderline significantly lower fungi:bacteria ratios compared to the subalpine soil ($p = 0.045$, $p = 0.056$, $p = 0.071$). Additionally, soil pH was slightly basic for all agricultural soils and slightly acidic for the subalpine soil ($p < 0.001$). There were no significant differences in soil pH among the agricultural soils.

Table 3.3. Biogeochemical properties of agricultural and subalpine soils collected in July 2018. The n-value for each measurement corresponds to the number of technical replicates within each bulked soil treatment. Error bars represent ± one SE from the mean.

Soil treatment	NO_3^- (µg N/g dry soil)	NH_4^+ (µg N/g dry soil)	Fungi:Bacteria (% fungi/% bacteria)	Soil pH
HNHW	77.9 (± 4.74) (n = 12)	1.80 (± 0.23) (n = 12)	0.142 (± 0.008) (n = 4)	8.15 (± 0.03) (n = 8)
HNLW	19.5 (± 6.19) (n = 9)	2.82 (± 0.04) (n = 9)	0.177 (± 0.014) (n = 3)	8.12 (± 0.04) (n = 6)
LNHW	13.3 (± 1.31) (n = 12)	1.80 (± 0.14) (n = 12)	0.188 (± 0.023) (n = 4)	8.16 (± 0.05) (n = 8)
LNLW	8.51 (± 0.74) (n = 9)	2.07 (± 0.07) (n = 9)	0.183 (± 0.013) (n = 3)	8.32 (± 0.04) (n = 6)
Subalpine	0.500 (±0.13) (n = 18)	5.11 (± 0.74) (n =18)	0.267 (± 0.020) (n = 8)	4.72 (± 0.04) (n = 18)

Lastly, I compared the HNHW and subalpine soil properties from June to July. I determined no significant differences in soil NO_3^-, NH_4^+, or fungi:bacteria within each soil from June to July. However, both soils differed in pH from June to July, with the HNHW soil becoming more basic ($p = 0.005$) and the subalpine soil becoming more acidic ($p < 0.001$).

4.2 Soils held at natural abundance

4.2.1 N_2O production rate in natural abundance soils

N_2O production rates showed a clear threshold response to variation in soil moisture (Figure 3.2). At low soil moistures (10-50% soil saturation), N_2O production rate was relatively low and constant. However, at approximately 60% soil saturation, I observed a marked increase in N_2O production rate (Figure 3.2). I fit the following four-parameter logistic model to the data to characterize these response curves (Equation 5):

$$\mathbf{(5)}\ y = d + \frac{a - d}{1 + \left(\frac{x}{c}\right)^b}$$

Where a is the minimum value, b is the slope of the line, c is the inflection point on the line (halfway point between a and d), and d is the maximum value. Each of these values correspond to a biologically relevant N_2O production parameter (Table 3.4).

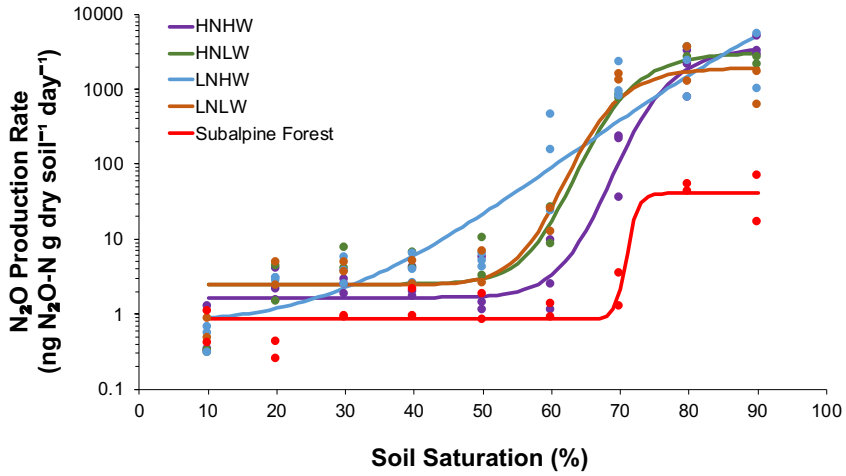

Figure 3.2. N_2O production rates for all soils that were held from 10 to 90% soil saturation. Data points correspond to observed production rate values and fitted lines are modelled predictions of N_2O production rate for all soils. All fits were modelled using logistic regressions. For the observed data, n = 27 for HNHW, n = 26 for LNHW, and n = 18 in all other cases. *Note the log-scaled y-axis*.

The results of these regressions are in Table 3.4. All logistic fits were strong (R^2 range from 0.88 to 0.94). These fits allowed us to compare the mean water content where soil N_2O production rate flipped from low production rates to high production rates (Table 3.4). For most agricultural soils, the transition point (parameter c, Table 3.4) was at approximately 60% soil saturation, and for the subalpine soil the transition point was at approximately 70% soil saturation (Figure 3.2).

Table 3.4. Summary of fit data comparing N_2O production rate data to estimated N_2O production rate data using logistic regressions. The R^2 values correspond to simple linear regressions comparing real production rate data to estimated production rate data, and the p-values correspond to each R^2 value. The values a-d correspond to the parameters estimated from each logistic regression. Parameter values occur from Equation 5. *Note the parameters and R^2 values result from log-transformed N_2O production rate data.*

Site	Treatment	Sample size (n)	R^2	Minimum N_2O production rate (a)	Slope (b)	Soil saturation transition point (c)	Maximum N_2O production rate (d)
Agricultural							
	HNHW	27	0.94	0.511	16.3	69.2	8.22
	HNLW	18	0.92	0.924	15.3	64.0	8.03
	LNHW	26	0.90	-0.170	2.65	83.5	15.8
	LNLW	18	0.94	0.906	15.6	62.3	7.58
Subalpine forest							
	Subalpine	18	0.88	-0.155	89.8	70.9	3.71

It is worth noting that the soil saturation transition point is notably higher for the LNHW soil. The poorer model fit for this soil is likely due to one very high observed N_2O production rate value that pulls the modeled values up, which is why the LNHW curve does not flatten at high soil moistures, as the other curves do.

4.2.2. Intramolecular site preference (SP) at natural abundance

Across all soils, intramolecular SP generally decreased as percent soil saturation increased (Figure 3.3). Linear regression across all data points was significant ($p = 0.01$) with an R^2 of 0.25. However, at 90% saturation, SP increased for HNLW, LNLW, and the subalpine soil (Figure 3.3). Across all soil saturations, HNHW tended to have more enriched SP values than other soils. There is only data for the subalpine soil starting at 60% soil saturation, because below this saturation the N_2O concentrations were very low, making the SP data unreliable (see Section 3.2.2, Appendix 2 Figure 3, and Appendix 2 Table 1 for details), but the subalpine soil also tended to have more enriched SP values. Across all saturations, HNLW, HNLW, and LNLW soils reported SP values between the HNHW and subalpine SP endpoints (Figure 3.3). In some cases n = 1 or 2 replicates per treatment as a consequence of instrument errors leading to biologically implausible SP values (Stuchiner et al. 2020).

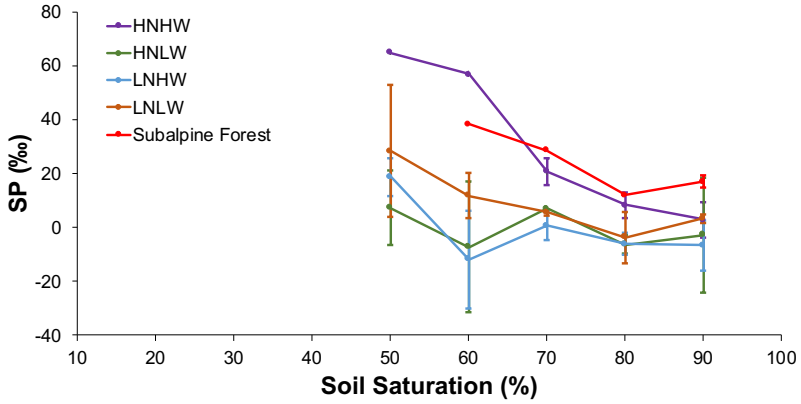

Figure 3.3. Intramolecular SP for all soils from 50-90% soil saturation. SP values were only used from this soil saturation range because values from lower soil saturations were deemed unreliable or not biologically realistic. Error bars represent ± one SE from the mean. *Note not all data points have error bars, as multiple soils have n = 1 at certain soil saturations*. All sample size information is summarized in Appendix 2 Table 2.

While all soils followed the same general patterns with increasing saturation, there was a substantial degree of variability among SP values at each saturation level (Figure 3.3). At 50% soil saturation, SP ranged from 65‰ for HNHW to 7‰ for HNLW. Interestingly, as saturation increased, the degree of difference among SP values decreased, however soils deviated from this trend at 90% saturation (Figure 3.3). At this soil saturation the range of values widened. The subalpine soil had an SP of 17‰, whereas the LNHW soil had an SP of -7‰.

Together, the similar magnitudes and directions of SP values across soils indicate that microbes were likely performing similar N-transformations at each saturation level. However, variation among values within each saturation level could indicate soil-specific differences in microbial behavior. These distinctions may be able to help better elucidate finer-scale differences in microbial metabolism across soils.

4.3 Isotopically amended soils

4.3.1 N_2O production rate in isotopically amended soils

There was no difference in N_2O production rate within each soil saturation level. This indicates that there was no treatment effect from the $^{15}NO_3^-$ vs. $^{15}NH_4^+$ amendments (Figure 3.4). N_2O production rate was highest in the 90% saturation agricultural soils (1650 and 1928 ng N_2O-N/g dry soil/day from soils amended with $^{15}NH_4^+$ and $^{15}NO_3^-$, respectively), but markedly decreased in the 50% saturation soils (3.87 and 3.78 ng N_2O-N/g dry soil/day from soils amended with $^{15}NH_4^+$ and $^{15}NO_3^-$, respectively; Figure 3.4). The subalpine soils had intermediate N_2O production rates (Figure 3.4). N_2O production rate was higher in the 85% saturated soils (451 and 528 ng N_2O-N/g dry soil/day from soils amended with $^{15}NH_4^+$ and $^{15}NO_3^-$, respectively), and lower in the 95% saturated soils (168 and 147 ng N_2O-N/g dry soil/day from soils amended with $^{15}NH_4^+$ and $^{15}NO_3^-$, respectively).

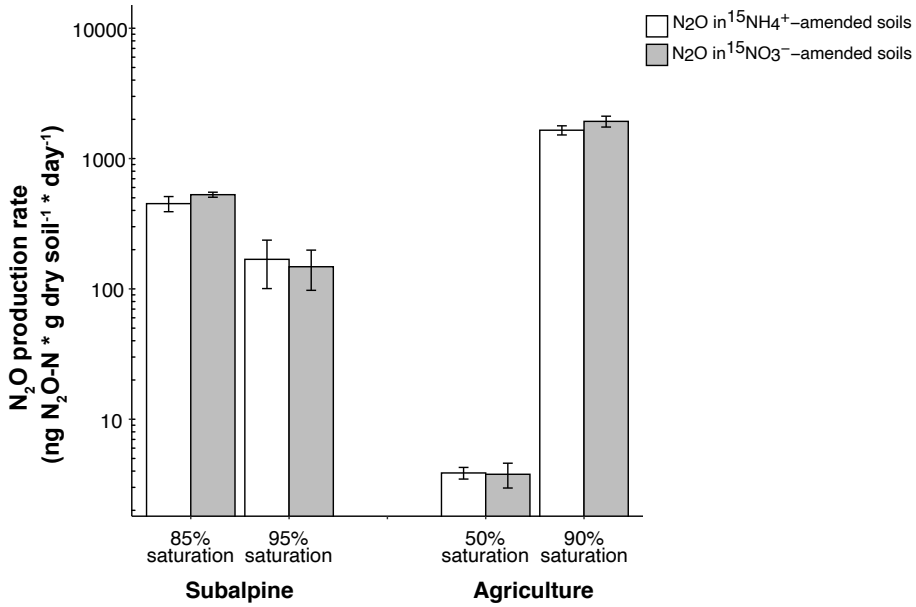

Figure 3.4. N_2O production rates from agricultural and subalpine soils across all soil moisture and isotopic enrichment treatments. In all cases n = 4 except n = 3 for the $^{15}NO_3^-$-amended 50% saturation agricultural soil. Error bars represent ± one SE from the mean. *Note the log scale y-axis.*

4.3.2 Tracing $^{15}N^{bulk}$ signatures to source partition among microbial processes

Across all soil saturations, the majority of ^{15}N-label was emitted from soils amended with $^{15}NO_3^-$ compared to soils amended with $^{15}NH_4^+$ (Figure 3.5a; $p < 0.001$). In the $^{15}NO_3^-$-amended soils, the largest $^{15}N^{bulk}$ signature (AP) was emitted from the 90% saturation agricultural soil, the smallest $^{15}N^{bulk}$ signature was emitted from the 50% saturation agricultural soil, and intermediate between those two were the subalpine soils, with the 95% saturation soil emitting a greater $^{15}N^{bulk}$ signature than the 85% saturation subalpine soil (Figure 3.5a).

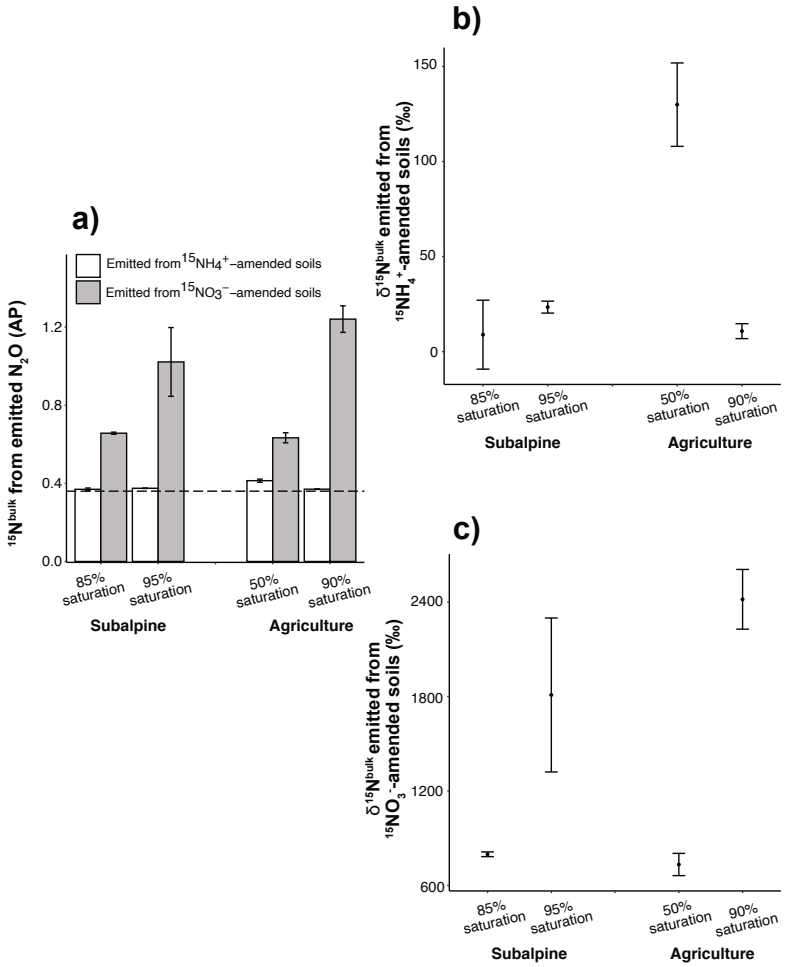

Figure 3.5. *Panel **a***: $^{15}N_2O^{bulk}$ in AP emitted from $^{15}NH_4^+$ or $^{15}NO_3^-$ amended soils. *Panel **b**:* $\delta^{15}N_2O^{bulk}$ emitted from $^{15}NH_4^+$ amended soils. *Panel **c**:* $\delta^{15}N_2O^{bulk}$ emitted from $^{15}NO_3^-$amended soils. In all cases n = 4 except n = 3 for the $^{15}NO_3^-$-amended 50% saturation agricultural soil. Error bars represent ± one SE from the mean. The dashed horizontal line in Panel **a** indicates the AP threshold for isotopic enrichment above natural abundance (0.37 %).

In the $^{15}NH_4^+$-amended soils, the $^{15}N^{bulk}$ δ-values for the two subalpine soils and the 90% saturation agricultural soil were not significantly different and ranged from 3 to 45‰ Figure 3.5b). In contrast, the $^{15}N^{bulk}$ signature for the 50% saturation soil was significantly more enriched than the other $^{15}NH_4^+$-amended soils ($p < 0.001$ in all cases) and reported a mean AP and δ value above ambient (0.41% and 130‰, respectively, Figure 3.5a, 3.5b).

In the $^{15}NO_3^-$-amended soils, the $^{15}N^{bulk}$ δ-values ranged from ~730 to 2400‰ (Figure 3.5c). The 50% saturation agricultural soil was the least enriched and the 90% saturation agricultural soil was the most enriched among the four soils. The 90% saturation agricultural soil was significantly more enriched than the 85% saturation subalpine soil ($p = 0.0074$) and the 50% saturation agricultural soil ($p = 0.0095$), but there was no difference between the 90% saturation agricultural soil and the 95% saturation subalpine soil (Figure 3.5c).

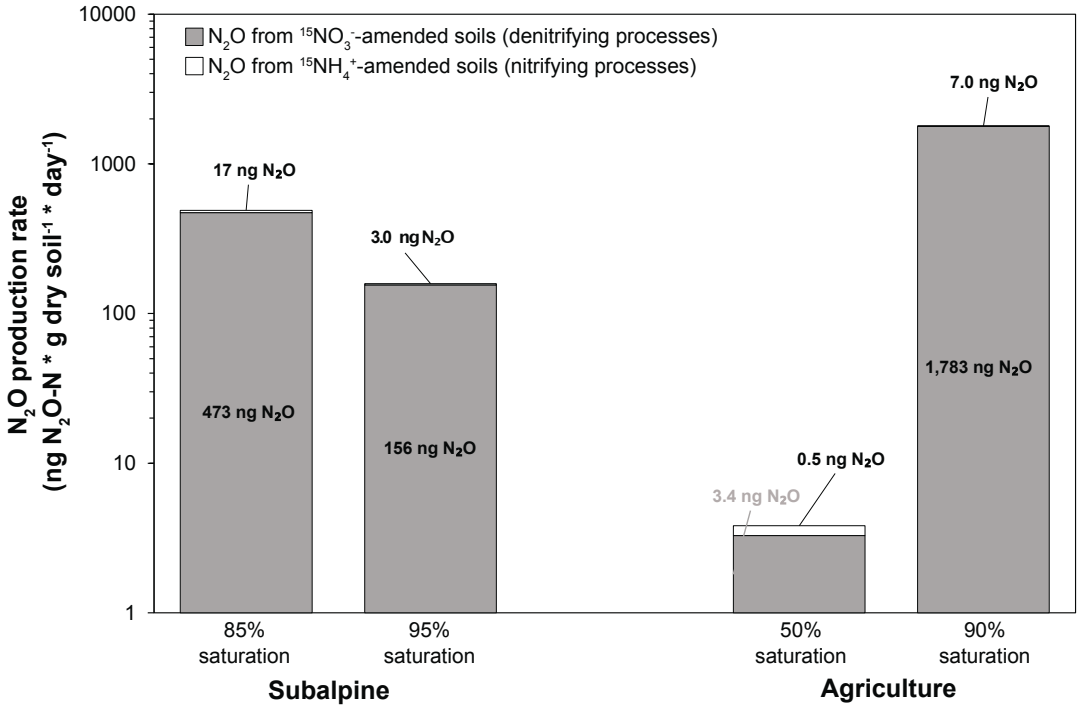

Figure 3.6. N_2O production rates partitioned by $^{15}NH_4^+$-oxidizing vs. $^{15}NO_3^-$–reducing pathways. In most cases, the majority of emitted N_2O is generated from microbial NO_3^- metabolism, although a detectable fraction of emitted N_2O is generated via microbial NH_4^+ metabolism in the $^{15}NH_4^+$-amended 50% saturation agricultural soil. In all cases, n = 4, except n = 3 for the $^{15}NO_3^-$-amended 50% saturation agricultural soil.

I also calculated the total N_2O production rate for each soil partitioned by N_2O emitted from $^{15}NO_3^-$ or $^{15}NH_4^+$-amended soil. I determined the N_2O production rate from NO_3^- reduction by multiplying the fraction of $^{15}N_2O$ emitted from $^{15}NO_3^-$-amended soils by the mean N_2O production rate from each pair of $^{15}NO_3$ and $^{15}NH_4^+$-amended soils. To determine the N_2O production rate from NH_4^+ oxidation, I subtracted the amount of N_2O produced from NO_3^- reduction from the abovementioned mean N_2O production rate. I averaged the N_2O production rates for each soil because there were no differences in production rate between the same soils held at the same saturation (see Section 4.3.1). This analysis further illustrates that most emitted N_2O came from NO_3^- reduction, with a minute fraction of emitted N_2O coming from NH_4^+ oxidation (Figure 3.6).

4.3.3 Isotopic enrichment in the $\delta^{15}N^{\alpha}$ vs. $\delta^{15}N^{\beta}$ position of the emitted N_2O

The location of isotopic enrichment (α-position or β-position) in the emitted N_2O varied among soils and by type of isotopic amendment. I present this data by quantifying the percent of emitted N_2O enriched in the β-position ($^{15}N – N – O$) from each soil by calculating the atom percent enrichment (APE) in each isotopomer, using Equations 6 and 7, where $AP^{15}N^{x}$ is the $AP^{15}N^{\alpha}$ or $^{15}N^{\beta}$, and AP_{std} corresponds to the AP of $^{15}N/(^{15}N+^{14}N)$ in N_2-Air (i.e., 0.003663):

$$(\mathbf{6})\ APE\ in\ \beta\ position = AP^{15}N^{\beta} - AP_{std}$$

$$APE\ in\ \alpha\ position = AP^{15}N^{\alpha} - AP_{std}$$

$$(\mathbf{7})\ Fraction\ of\ enriched\ ^{15}N\ in\ \beta\ position = \frac{APE\ \beta\ position}{APE\ \beta\ position + APE\ \alpha\ position}$$

On the converse, the fraction of N_2O enriched in the α-position (N – ^{15}N – O) from each soil would be 1 - fraction β-position enrichment. The reason I chose to present this data as percent β-position enrichment is because soils most frequently emitted more β-position $^{15}N_2O$ relative to α-position $^{15}N_2O$, so it seemed more appropriate to put the equation in terms of β-position enrichment.

The majority of the emitted enriched N_2O was derived from the $^{15}NO_3^-$-amended soils (Figure 3.6). Information about the α and β-position enrichment from the $^{15}NH_4^+$-amended soils is available in Appendix 2 (Appendix 2 Figure 2). In the $^{15}NO_3^-$-amended soils, the 90% saturation agricultural soil emitted significantly more N_2O enriched in the β-position than the other three soils ($p < 0.001$ in all cases; Figure 3.7, Appendix 2 Table 3). The 90% saturation agricultural soil emitted 60% of β-position-enriched N_2O, whereas the 50% saturation agricultural soil, the 85% saturation subalpine soil, and the 95% saturation subalpine soil emitted 54, 55, and 54% β-position-enriched N_2O (Figure 3.7). One-sample t-tests compared each soil's fraction of emitted $^{15}N^{\beta}$ to 50%; all soils emitted significantly more than 50% β-position-enriched N_2O ($p < 0.05$ in all cases). This indicates there is preferential enrichment occurring for the β-position. If preferential enrichment were not occurring, I would observe a 50-50% distribution of ^{15}N between the α-position and the β-position.

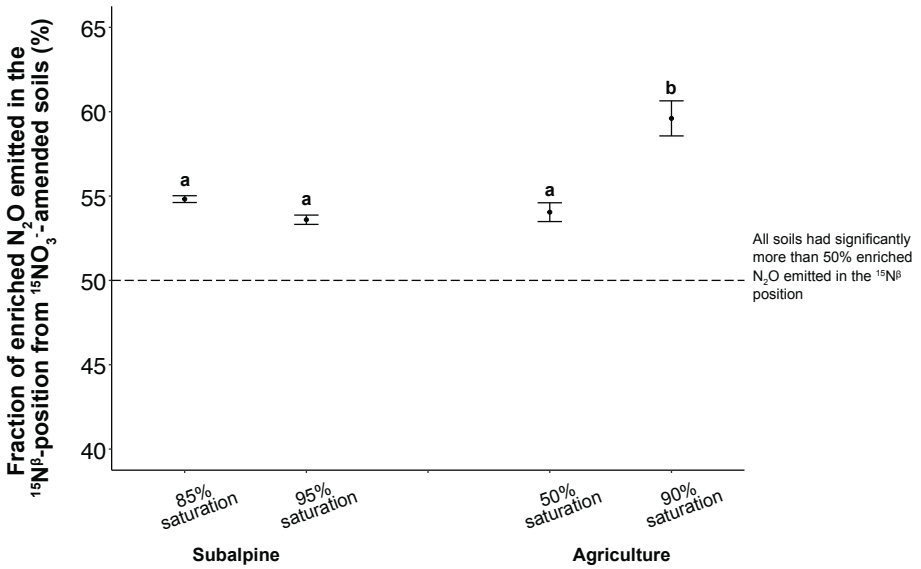

Figure 3.7. Percent of emitted N_2O enriched in the β-position (^{15}N—N—O) from each $^{15}NO_3^-$-amended soil. In all cases, n = 4, except n = 3 for the $^{15}NO_3^-$-amended 50% saturation agricultural soil. Bars represent a 95% CI around the mean. For all soils, significantly more than half of the enriched N_2O emitted was enriched in the β-position (all percentages significantly above 50% dotted line). Different letters illustrate significantly different means. *Note: the percent β-position enriched N_2O was only considered for the $^{15}NO_3^-$-amended soils because those soils emitted most of the isotopically enriched N_2O.*

5. Discussion

By incubating two distinct soils under both natural abundance and enriched conditions, I sought to better disentangle among N_2O-generating source processes in moist to wet soils (50-95% saturation). In this case, pairing methods revealed that both bacterial and fungal denitrification were the primary N_2O-generating source processes in all soils from 50-95% saturation. In addition, I made unique observations of β-position-specific enriched isotopomers, which both raise questions about biogeochemical pathways and intriguingly, could suggest a means of identifying co-denitrification, an important and currently understudied microbial process.

5.1 Modelling N_2O production rate

The general response of my natural abundance incubated soils to variation in soil moisture is consistent with previous studies, such that N_2O production rates showed a strong threshold behavior with much higher rates of emissions at higher soil moistures (Figure 3.2; Parton et al. 1996, Del Grosso et al. 2000, Li and Aber 2000, Parton et al. 2001, Ni et al. 2011, Taylor et al. 2017, Ji et al. 2018, Song et al. 2019). By applying a logistic regression to my N_2O production rate data, I can extract useful parameters about N_2O production capacity from these diverse soils (Table 3.4).

My findings are consistent with classic interpretations of microbial N_2O metabolism, wherein the transition from aerobic to anerobic metabolism is consistent with a shift from low N_2O flux to higher N_2O flux, and this is largely dictated by soil WFPS (Firestone and Davidson 1989, Li and Aber 2000, Butterbach-Bahl et al. 2013, Congreves et al. 2019). Although I used percent soil saturation, not WFPS, my findings align with Davidson (1993) who illustrated that from WFPS 60 to ~85%, most of the N-gas flux is emitted as N_2O. Similarly, I observed a stark transition from low N_2O emissions rates to high N_2O emission rates at ~60% soil saturation (Figure 3.2). It is worth noting that the maximum N_2O production rates differed widely among soil treatments. These differences are likely modulated by other variables that affect total NO_3^- reduction rate, such as soil NO_3^- or OC (Firestone and Davidson 1989; Figure 3.2, Table 3.1, Table 3.3).

5.2 Denitrification as the dominant N_2O-generating process

All isotopically enriched soils emitted N_2O almost exclusively from NO_3^- reduction, rather than from NH_4^+ oxidation, indicating that some combination of bacterial and/or fungal denitrification generated the observed N_2O (Figure 3.6). This aligns with the literature and my

natural abundance findings for three reasons. First, previous studies show that wetter, anoxic soils use NO_3^- as substrate for denitrification (Rohe et al. 2017, Congreves et al. 2019). Second, the accepted range of bacterial denitrification SP goes from -11 to 15‰, and most of my natural abundance SPs fell within this range across all soil saturations (Figure 3.3, Sutka et al. 2006, Well and Flessa 2009, Ostrom et al. 2010, Opdyke et al. 2009, Butterbach-Bahl et al. 2013, Hu et al. 2015, Rohe et al. 2017). Third, although I measured some SPs that were high (ranging from ~30 to 60‰), I also measured $^{15}N_2O$ emitted almost exclusively from $^{15}NO_3^-$-amended soils, rather than from $^{15}NH_4^+$-amended soils (Figure 3.5a, 3.5c). This supports fungal denitrification as the source of the N_2O (discussed in detail in 5.3 below), rather than a different biotic process like nitrifier-denitrification, where $^{15}N_2O$ from $^{15}NH_4^+$-amended soils would have been observed (Figure 3.5b; Wrage-Mönnig et al. 2018).

In sum, using these paired natural abundance and enriched isotopic methods helped us identify the importance of denitrification, be it bacterial or fungal, in two distinct soils, even under less wet conditions (e.g. 50-60% saturation). Recent studies have shown the ubiquity of denitrification across soil saturations, which my work finds as well (Opdyke et al. 2009, Ostrom et al. 2010, Groffman 2012, Fang et al. 2015, Thilakarathna and Hernandez-Ramirez 2021, Harris et al. 2021). It is notable that denitrification drives N_2O emissions over a broad range of soil moistures because this process tends to have greater N_2O production per unit N metabolized than other microbial N-transformations (Inatomi et al. 2019, Yoon et al. 2019, Wang et al. 2021). Thus, understanding why denitrification is so pervasive will be important future work.

5.3 Potential evidence of fungal denitrification

In general, my use of ^{15}N-labelled inorganic substrates to create enriched incubations corroborate, and bolster, my findings from the natural abundance incubations. Also, despite the

one-month time difference between enriched and natural abundance assays, it appears that the soils were behaving similarly, even after sieving and creating artificial incubation conditions. For example, soil NH_4^+ and NO_3^- levels were very similar over time (see Tables 3.2-3.3), and N_2O production rates were comparable as well (Figure 3.2, Figure 3.4).

For soils incubated under natural abundance conditions, I observed a decline in SP with increasing soil saturation (Figure 3.3). This pattern is clear, both within and across soils, despite the small sample size (Figure 3.3). Numerous studies interpret this decrease in SP with increasing soil moisture as indicating a transition from nitrification to denitrification (Bergstermann et al. 2011, Denk et al. 2017, Congreves et al. 2019, Ding et al. 2019). However, my enriched data demonstrate unambiguously that denitrification was the dominant source of N_2O (Figure 3.5, Figure 3.6).

Thus, although I observed atypically high SPs for some of the 50% saturation soils, I think these values are indicative of fungal denitrification. For my 50% saturation soils, I observed a SP of 65‰ for the HNHW soil and 56‰ for one of the LNLW soils, but mostly, I observed SPs lower than those for HNLW, LNHW, and LNLW soils (ranging from 7 to 28‰, Figure 3.3). Higher SP values can be indicative of fungal denitrification (~20 to 45‰), but my measured SPs fall above that reported range. Recently, Wong et al. (2020) reported similarly high SP values (83‰ ± 25‰) in marine sediments and posit that multiple biotic and abiotic processes proceeding through multiple cycles could account for such enrichment. Since I have no evidence for abiotic reactions, and since all agricultural soils had comparable fungi:bacteria ratios, it is plausible that in the 50% saturation HNHW and LNLW soils, reprocessing of fungal (and to some extent bacterial) denitrification contributed to these larger SP values (Table 3.3, Figure 3.3).

I also see generally more enriched SP values for HNHW and subalpine soils across all saturations (Figure 3.3). In the subalpine soil, I was able to measure biologically plausible SP values starting at 60% saturation, when denitrification is well-documented to be important (Groffman 2012, Fang et al. 2015, Cardenas et al. 2017, Schlüter et al. 2019, Thilarkarathna and Hernandez-Ramirez 2021). Fungal denitrification could be responsible for the more enriched SP values I measured from these soils. Perhaps in the HNHW and subalpine soils the fungal community contributed more to denitrification than the bacterial community, although I did not measure denitrification enzyme activity from my soils to verify this (Butterbach-Bahl et al. 2013). However, my enriched dataset helps support my proposal that fungal dentrification is occurring in the HNHW and subalpine soils across all saturations (see Section 5.2).

5.4 Position-specific enrichment in isotopically labelled soils

By isotopically labelling soils with $^{15}NH_4^+$ or $^{15}NO_3^-$, I was able to determine, and report for the first time, position-specific ^{15}N-enrichment in the emitted N_2O from incubations. The majority of the emitted N_2O was from $^{15}NO_3^-$-amended soils, as I discussed above, but within that emitted N_2O, 54-60% of the ^{15}N appeared in the β-position (Figure 3.7). This begs the question: what can this strong degree of position-specific enrichment tell us? It would be ideal if isotopically enriched isotopomers and SP could be informative of microbial N_2O-generating pathways because these position-specific enriched signatures have far more robust signal:noise ratios compared to position-specific natural abundance signatures (Wagner-Riddle et al. 2008; Zhang et al. 2015, Snider et al. 2017).

Currently, I do not have an explanation for these strong β-position-specific signatures from the enriched incubations, but three possibilities emerge. First, an inverse isotope effect, like Yang et al. (2014) observed, wherein the β-position N-atom binds more strongly to the active site

on a denitrification enzyme, could have resulted in greater β-position enrichment in the emitted N_2O. Second, this could be an indication of microbial N-transformations we have not yet discovered or do not yet fully understand biochemically. Future research should evaluate whether greater enrichment in the β-position occurs reliably under particular conditions. If strong patterns in position-specific enrichment are broadly observed, then this measure, like SP, could become another tool for understanding which microbial processes give rise to N_2O. Finally, it is possible that this strong position-specific enrichment is indicative of the infrequently studied microbial process co-denitrification, wherein the N for the denitrification reaction is obtained from two different sources. In co-denitrification, typically one N atom is derived from an organic source and another N atom is derived from NO or NO_2^- (Spott et al. 2011, Clough et al. 2017). Conceivably, either of these N sources (NO or N_2O) could become increasingly enriched during the stepwise denitrification process in a closed incubation system, and potentially be responsible for the β-position specific enrichment pattern I observed in the emitted $^{15}N_2O$ (Spott et al. 2011).

While this phenomenon I observed certainly warrants further study, the possibility of being able to identify co-denitrification is important to emphasize. According to Baggs (2011), co-denitrification has the potential to produce two molecules of N_2O for every two molecules of NO_3^- reduced, owing to co-substrate utilization. During conventional denitrification, one molecule of N_2O is produced for every two molecules of NO_3^- reduced. Thus, by failing to measure co-denitrification we could be underestimating denitrifier-produced N_2O by a factor of two, which could have critical implications for managing the N_2O budget (Baggs 2011).

5.5 Concluding remarks

I sought to better understand how incubating the same soils under natural abundance and isotopically enriched conditions can better inform our ability to study microbial N_2O-generating

processes. My study revealed that fungal and bacterial denitrification was the primary source of N_2O in all soils from 50-95% saturation. Further, I observed persistent β-position enrichment in the N_2O emitted from $^{15}NO_3^-$-amended soils, which could be indicative of co-denitrification, although this warrants further study. Thus, while pairing natural abundance and enriched methods did not reveal a *diversity* of N_2O-generating processes, I used these paired methods to discern among *diverse* denitrification pathways. As such, my work revealed the ubiquity of denitrification among the soils I tested at a range of different soil saturations.

Scientific research has made ample strides over the past ~30 years to improving our understanding of the microbial source processes responsible for N_2O emissions, and these strides are largely attributed to more precise instrumentation and improved methodologies (Snider et al. 2015, Ostrom et al. 2017, Ostrom et al. 2018, Yu et al. 2020, Ostrom et al. 2021). While I acknowledge that it can be logistically challenging for labs to perform natural abundance and isotopically enriched experiments in conjunction, my study illustrates that it can help to more finely discern among N_2O-generating source processes, like different forms of denitrification. Thus, I encourage future studies to continue pairing natural abundance and enriched measures of N_2O stable isotopes. I also encourage researchers to assess position-specific N_2O enrichment, as this may be yet another emergent property of the N_2O molecule that could help to reveal co-denitrification or a yet-identified microbial N-transformation.

CHAPTER 3 REFERENCES

Aber, J. D., K. J. Nadelhoffer, P. Steudler, and J. M. Melillo (1989), Nitrogen Saturation in Northern Forest Ecosystems, *Bioscience*, *39*(6), 378–386, doi:10.2307/1311067.

Aber, J., W. McDowell, K. Nadelhoffer, a Magill, G. Berntson, M. Kamakea, S. McNulty, W. Currie, L. Rustad, and I. Fernandez (1998), Nitrogen saturation in temperate forest ecosystems - Hypotheses revisited, *Bioscience*, *48*(11), 921–934, doi:10.2307/1313296.

Alvarez, R. A., S. W. Pacala, J. J. Winebrake, W. L. Chameides, and S. P. Hamburg (2012), Greater focus needed on methane leakage from natural gas infrastructure, (17), doi:10.1073/pnas.1202407109.

Andriukonis, E., and E. Gorokhova (2017), Kinetic 15N-isotope effects on algal growth, *Sci. Rep.*, *7*(March), 1–9, doi:10.1038/srep44181.

Baggs, E. M. (2008), A review of stable isotope techniques for N2O source partitioning in soils: recent progress, remaining challenges, and future considerations, *Rapid Commun. Mass Spectrom.*, *22*(22), 1664–1672, doi:10.1002/rcm.

Baggs, E. M. (2011), Soil microbial sources of nitrous oxide: Recent advances in knowledge, emerging challenges and future direction, *Curr. Opin. Environ. Sustain.*, *3*(5), 321–327, doi:10.1016/j.cosust.2011.08.011.

Ball, P. N., M. D. MacKenzie, T. H. DeLuca, and W. E. H. Montana (2010), Wildfire and Charcoal Enhance Nitrification and Ammonium-Oxidizing Bacterial Abundance in Dry Montane Forest Soils, *J. Environ. Qual.*, *39*(4), 1243–1253, doi:10.2134/jeq2009.0082.

Barnard, R., P. W. Leadley, and B. A. Hungate (2005), Global change, nitrification, and denitrification: A review, *Global Biogeochem. Cycles*, *19*(1), 1–13, doi:10.1029/2004GB002282.

Baron, J. S., H. M. Rueth, A. M. Wolfe, K. R. Nydick, E. J. Allstott, J. T. Minear, and B. Moraska (2000), Ecosystem responses to nitrogen deposition in the Colorado Front Range, *Ecosystems*, *3*(4), 352–368, doi:10.1007/s100210000032.

Bergstermann, A., L. Cárdenas, R. Bol, L. Gilliam, K. Goulding, A. Meijide, D. Scholefield, A. Vallejo, and R. Well (2011), Effect of antecedent soil moisture conditions on emissions and isotopologue distribution of N2O during denitrification, *Soil Biol. Biochem.*, *43*(2), 240–250, doi:10.1016/j.soilbio.2010.10.003.

Boot, C. M., E. K. Hall, K. Denef, and J. S. Baron (2016), Long-term reactive nitrogen loading alters soil carbon and microbial community properties in a subalpine forest ecosystem, *Soil Biol. Biochem.*, *92*, 211–220, doi:10.1016/j.soilbio.2015.10.002.

Butterbach-Bahl, K., E. M. Baggs, M. Dannenmann, R. Kiese, and S. Zechmeister-Boltenstern (2013), Nitrous oxide emissions from soils: how well do we understand the processes and their controls?, *Philos. Trans. R. Soc. London.*, *368*(1621), 20130122, doi:10.1098/rstb.2013.0122.

Cardenas, L. M., R. Bol, D. Lewicka-Szczebak, A. S. Gregory, G. P. Matthews, W. R. Whalley, T. H. Misselbrook, D. Scholefield, and R. Well (2017), Effect of soil saturation on denitrification in a grassland soil, *Biogeosciences Discuss.*, (1989), 1–51, doi:10.5194/bg-2016-556.

Chen, H., D. Williams, J. T. Walker, and W. Shi (2016), Probing the biological sources of soil N2O emissions by quantum cascade laser-based15N isotopocule analysis, *Soil Biol. Biochem.*, *100*, 175–181, doi:10.1016/j.soilbio.2016.06.015.
Ciais, P. et al. (2013), The physical science basis. Contribution of working group I to the fifth assessment report of the intergovernmental panel on climate change, *Chang. IPCC Clim.*, 465–570, doi:10.1017/CBO9781107415324.015.
Clough, T. J. et al. (2017), Influence of soil moisture on codenitrification fluxes from a urea-affected pasture soil, *Sci. Rep.*, *7*(1), 1–12, doi:10.1038/s41598-017-02278-y.
Congreves, K. A., T. Phan, and R. E. Farrell (2019), A new look at an old concept: Using 15N2O isotopomers to understand the relationship between soil moisture and N2O production pathways, *Soil*, *5*(2), 265–274, doi:10.5194/soil-5-265-2019.
Davidson E.A. (1993) Soil Water Content and the Ratio of Nitrous Oxide to Nitric Oxide Emitted from Soil. In: Oremland R.S. (eds) Biogeochemistry of Global Change. Springer, Boston, MA. https://doi.org/10.1007/978-1-4615-2812-8_20.
Davidson, E. A. (2009), The contribution of manure and fertilizer nitrogen to atmospheric nitrous oxide since 1860, *Nat. Geosci.*, *2*(9), 659–662, doi:10.1038/ngeo608.
Decock, C., and J. Six (2013), How reliable is the intramolecular distribution of 15N in N2O to source partition N2O emitted from soil?, *Soil Biol. Biochem.*, *65*(2), 114–127, doi:10.1016/j.soilbio.2013.05.012.
Del Grosso, S. J., W. J. Parton, A. R. Mosier, D. S. Ojima, A. E. Kulmala, and S. Phongpan (2000), General model for N 2 O and N 2 gas emissions from soils due to dentrification, *Global Biogeochem. Cycles*, *14*(4), 1045–1060, doi:10.1029/1999GB001225.
Denk, T. R. A., J. Mohn, C. Decock, D. Lewicka-Szczebak, E. Harris, K. Butterbach-Bahl, R. Kiese, and B. Wolf (2017), The nitrogen cycle: A review of isotope effects and isotope modeling approaches, *Soil Biol. Biochem.*, *105*, 121–137, doi:10.1016/j.soilbio.2016.11.015.
Denk, T. R. A., D. Kraus, R. Kiese, K. Butterbach-Bahl, and B. Wolf (2019), Constraining N cycling in the ecosystem model LandscapeDNDC with the stable isotope model SIMONE, *Ecology*, *100*(5), 1–15, doi:10.1002/ecy.2675.
Ding, J., F. Fang, W. Lin, X. Qiang, C. Xu, L. Mao, Q. Li, X. Zhang, and Y. Li (2019), N 2 O emissions and source partitioning using stable isotopes under furrow and drip irrigation in vegetable field of North China, *Sci. Total Environ.*, *665*, 709–717, doi:10.1016/j.scitotenv.2019.02.053.
Fang, Y. et al. (2015), Microbial denitrification dominates nitrate losses from forest ecosystems, *Proc. Natl. Acad. Sci. U. S. A.*, *112*(5), 1470–1474, doi:10.1073/pnas.1416776112.
Farquharson, R., and J. Baldock (2008), Concepts in modelling N2O emissions from land use, *Plant Soil*, *309*(1–2), 147–167, doi:10.1007/s11104-007-9485-0.
Fenn, M. E. et al. (2018), Nitrogen Excess in North American Ecosystems : Predisposing Factors, Ecosystem Responses, and Management Strategies *Ecological Applications*, *8*(3), 706-733.
Firestone, M. K., and E. A. Davidson (1989), Microbiologial Basis of NO and N20 production and consumption in soil, *Exch. Trace Gases between Terr. Ecosyst. Atmos.*, (January 1989), 7–21, doi:10.1017/CBO9781107415324.004.
Groffman, P. M. (2012), Terrestrial denitrification: Challenges and opportunities, *Ecol. Process.*, *1*(1), 1–11, doi:10.1186/2192-1709-1-11.

Harris, S. J. et al. (2020), N2O isotopocule measurements using laser spectroscopy: Analyzer characterization and intercomparison, *Atmos. Meas. Tech.*, *13*(5), 2797–2831, doi:10.5194/amt-13-2797-2020.

Heath, J., and J. S. Baron (2014), Climate, Not Atmospheric Deposition, Drives the Biogeochemical Mass-Balance of a Mountain Watershed, *Aquat. Geochemistry*, *20*(2–3), 167–181, doi:10.1007/s10498-013-9199-2.

Hu, H. W., D. Chen, and J. Z. He (2015), Microbial regulation of terrestrial nitrous oxide formation: Understanding the biological pathways for prediction of emission rates, *FEMS Microbiol. Rev.*, *39*(5), 729–749, doi:10.1093/femsre/fuv021.

Ibraim, E., E. Harris, S. Eyer, B. Tuzson, L. Emmenegger, J. Six, and J. Mohn (2018), Development of a field-deployable method for simultaneous, real-time measurements of the four most abundant N2O isotopocules, *Isotopes Environ. Health Stud.*, *54*(1), 1–15, doi:10.1080/10256016.2017.1345902.

Jenny H. (1980) Ecosystems and Soils. In: The Soil Resource. Ecological Studies (Analysis and Synthesis), vol 37. Springer, New York, NY. https://doi.org/10.1007/978-1-4612-6112-4_1.

Ji, Q., E. Buitenhuis, P. Suntharalingam, J. L. Sarmiento, and B. B. Ward (2018), Global Nitrous Oxide Production Determined by Oxygen Sensitivity of Nitrification and Denitrification, *Global Biogeochem. Cycles*, *32*(12), 1790–1802, doi:10.1029/2018GB005887.

Köster, J. R., R. Well, B. Tuzson, R. Bol, K. Dittert, A. Giesemann, L. Emmenegger, A. Manninen, L. Cárdenas, and J. Mohn (2013), Novel laser spectroscopic technique for continuous analysis of N 2O isotopomers - Application and intercomparison with isotope ratio mass spectrometry, *Rapid Commun. Mass Spectrom.*, *27*(1), 216–222, doi:10.1002/rcm.6434.

Lewicka-Szczebak, D., R. Well, R. Bol, A. S. Gregory, G. P. Matthews, T. Misselbrook, W. R. Whalley, and L. M. Cardenas (2015), Isotope fractionation factors controlling isotopocule signatures of soil-emitted N2O produced by denitrification processes of various rates, *Rapid Commun. Mass Spectrom.*, *29*(3), 269–282, doi:10.1002/rcm.7102.

Lewicka-Szczebak, D., M. Piotr Lewicki, and R. Well (2020), N2O isotope approaches for source partitioning of N2O production and estimation of N2O reduction-validation with the 15N gas-flux method in laboratory and field studies, *Biogeosciences*, *17*(22), 5513–5537, doi:10.5194/bg-17-5513-2020.

Li, C., J. Aber, F. Stange, K. Butterbach-Bahl, and H. Papen (2000), A process-oriented model of N2O and NO emissions from forest soils: 1. Model development, *J. Geophys. Res. Atmos.*, *105*(D4), 4369–4384, doi:10.1029/1999JD900949.

Li, Q., F. Wang, Q. Yu, W. Yan, X. Li, and S. Lv (2019), Dominance of nitrous oxide production by nitrification and denitrification in the shallow Chaohu Lake, Eastern China: Insight from isotopic characteristics of dissolved nitrous oxide, *Environ. Pollut.*, *255*, 113212, doi:10.1016/j.envpol.2019.113212.

Long, A., J. Heitman, C. Tobias, R. Philips, and B. Song (2013), Co-occurring anammox, denitrification, and codenitrification in agricultural soils, *Appl. Environ. Microbiol.*, *79*(1), 168–176, doi:10.1128/AEM.02520-12.

Löscher, C. R., A. Kock, M. Könneke, J. Laroche, H. W. Bange, and R. A. Schmitz (2012), Production of oceanic nitrous oxide by ammonia-oxidizing archaea, *Biogeosciences*, *9*(7), 2419–2429, doi:10.5194/bg-9-2419-2012.

Maeda, K., A. Spor, V. Edel-Hermann, C. Heraud, M.-C. Breuil, F. Bizouard, S. Toyoda, N. Yoshida, C. Steinberg, and L. Philippot (2015), N2O production, a widespread trait in fungi, *Sci. Rep.*, *5*(1), 9697, doi:10.1038/srep09697.

Mathieu, O., J. Lévêque, C. Hénault, M. J. Milloux, F. Bizouard, and F. Andreux (2006), Emissions and spatial variability of N2O, N2 and nitrous oxide mole fraction at the field scale, revealed with 15N isotopic techniques, *Soil Biol. Biochem.*, *38*(5), 941–951, doi:10.1016/j.soilbio.2005.08.010.

McTigue, N. D., W. S. Gardner, K. H. Dunton, and A. K. Hardison (2016), Biotic and abiotic controls on co-occurring nitrogen cycling processes in shallow Arctic shelf sediments, *Nat. Commun.*, *7*, 13145, doi:10.1038/ncomms13145.

Menyailo, O. V., and B. A. Hungate (2006), Stable isotope discrimination during soil denitrification: Production and consumption of nitrous oxide, *Global Biogeochem. Cycles*, *20*(3), doi:10.1029/2005GB002527.

Mohn, J. et al. (2014), Interlaboratory assessment of nitrous oxide isotopomer analysis by isotope ratio mass spectrometry and laser spectroscopy: Current status and perspectives, *Rapid Commun. Mass Spectrom.*, *28*(18), 1995–2007, doi:10.1002/rcm.6982.

Ni, B. J., M. Ruscalleda, C. Pellicer-Nàcher, and B. F. Smets (2011), Modeling nitrous oxide production during biological nitrogen removal via nitrification and denitrification: Extensions to the general ASM models, *Environ. Sci. Technol.*, *45*(18), 7768–7776, doi:10.1021/es201489n.

Oleksy, I. A., W. S. Beck, R. W. Lammers, C. E. Steger, C. Wilson, K. Christianson, K. Vincent, G. Johnson, P. T. J. Johnson, and J. S. Baron (2020), The role of warm, dry summers and variation in snowpack on phytoplankton dynamics in mountain lakes, *Ecology*, *101*(10), 1–12, doi:10.1002/ecy.3132.

Opdyke, M. R., N. E. Ostrom, and P. H. Ostrom (2009), Evidence for the predominance of denitrification as a source of N 2O in temperate agricultural soils based on isotopologue measurements, *Global Biogeochem. Cycles*, *23*(4), 1–10, doi:10.1029/2009GB003523.

Ostrom, N. E., R. Sutka, P. H. Ostrom, A. S. Grandy, K. M. Huizinga, H. Gandhi, J. C. von Fischer, and G. P. Robertson (2010), Isotopologue data reveal bacterial denitrification as the primary source of N2O during a high flux event following cultivation of a native temperate grassland, *Soil Biol. Biochem.*, *42*(3), 499–506, doi:10.1016/j.soilbio.2009.12.003.

Ostrom, N. E., and P. H. Ostrom (2012), Handbook of Environmental Isotope Geochemistry, , doi:10.1007/978-3-642-10637-8.

Ostrom, N. E., and P. H. Ostrom (2017), Mining the isotopic complexity of nitrous oxide: a review of challenges and opportunities, *Biogeochemistry*, *132*(3), 359–372, doi:10.1007/s10533-017-0301-5.

Ostrom, N. E. et al. (2018), Preliminary assessment of stable nitrogen and oxygen isotopic composition of USGS51 and USGS52 nitrous oxide reference gases and perspectives on calibration needs, *Rapid Commun. Mass Spectrom.*, *32*(15), 1207–1214, doi:10.1002/rcm.8157.

Palacin-Lizarbe, C., L. Camarero, S. Hallin, C. M. Jones, J. Cáliz, E. O. Casamayor, and J. Catalan (2019), The DNRA-denitrification dichotomy differentiates nitrogen transformation pathways in mountain lake benthic habitats, *Front. Microbiol.*, *10*(JUN), 1–15, doi:10.3389/fmicb.2019.01229.

Park, S., T. Perez, K. A. Boering, S. E. Trumbore, J. Gil, S. Marquina, and S. C. Tyler (2011), Can N2O stable isotopes and isotopomers be useful tools to characterize sources and

microbial pathways of N2O production and consumption in tropical soils?, *Global Biogeochem. Cycles*, *25*(1), 1–16, doi:10.1029/2009GB003615.
Park, S. et al. (2012), Trends and seasonal cycles in the isotopic composition of nitrous oxide since 1940, *Nat. Geosci.*, *5*(4), 261–265, doi:10.1038/ngeo1421.
Parton, W. J., A. R. Mosier, D. S. Ojima, D. W. Valentine, D. S. Schime, K. Weier, and A. E. Kulmala (1996), Generalized model for N2 and N2O production from nitrification and denitrification, *Global Biogeochem. Cycles*, *10*(3), 401–412, doi:10.1029/96GB01455.
Parton, W. J., E. a. Holland, S. J. Del Grosso, M. D. Hartman, R. E. Martin, a. R. Mosier, D. S. Ojima, and D. S. Schimel (2001), Generalized model for NOx and N2O emissions from soils, *J. Geophys. Res.*, *106*(2), 17403, doi:10.1029/2001JD900101.
Perez, T., D. Garcia-Montiel, S. E. Trumbore, S. C. Tyler, P. De Camargo, M. Moreira, M. Piccolo, and C. Cerri (2006), Nitrous oxide nitrification and denitrification 15N enrichment factors from Amazon forest soils, , *16*(6), 2153–2167.
Ravishankara, A. R., J. S. Daniel, and R. W. Portmann (2009), Nitrous oxide (N2O): The dominant ozone-depleting substance emitted in the 21st century, *Science (80-.).*, *326*(5949), 123–125, doi:10.1126/science.1176985.
Rector, C., K. R. Brye, J. Humphreys, R. J. Norman, E. E. Gbur, J. T. Hardke, C. Willett, and M. A. Evans-white (2018), Regional N 2 O emissions and global warming potential as affected by water management and rice cultivar on an Al fi sol in Arkansas , USA, *Geoderma Reg.*, *14*, e00170, doi:10.1016/j.geodrs.2018.e00170.
Rohe, L., R. Well, and D. Lewicka-Szczebak (2017), Use of oxygen isotopes to differentiate between nitrous oxide produced by fungi or bacteria during denitrification, *Rapid Commun. Mass Spectrom.*, *31*(16), 1297–1312, doi:10.1002/rcm.7909.
Rohe, L., T. Oppermann, R. Well, and M. A. Horn (2020), Nitrite induced transcription of p450nor during denitrification by Fusarium oxysporum correlates with the production of N2O with a high 15N site preference, *Soil Biol. Biochem.*, *151*(July), 108043, doi:10.1016/j.soilbio.2020.108043.
Russow, R., C. F. Stange, and H. U. Neue (2009), Role of nitrite and nitric oxide in the processes of nitrification and denitrification in soil: Results from 15N tracer experiments, *Soil Biol. Biochem.*, *41*(4), 785–795, doi:10.1016/j.soilbio.2009.01.017.
Rütting, T., P. Boeckx, C. Müller, and L. Klemedtsson (2011), Assessment of the importance of dissimilatory nitrate reduction to ammonium for the terrestrial nitrogen cycle, *Biogeosciences*, *8*(7), 1779–1791, doi:10.5194/bg-8-1779-2011.
Sanford, R. A. et al. (2012), Unexpected nondenitrifier nitrous oxide reductase gene diversity and abundance in soils, *Proc. Natl. Acad. Sci. U. S. A.*, *109*(48), 19709–19714, doi:10.1073/pnas.1211238109.
Schmidt, C. S., D. J. Richardson, and E. M. Baggs (2011), Constraining the conditions conducive to dissimilatory nitrate reduction to ammonium in temperate arable soils, *Soil Biol. Biochem.*, *43*(7), 1607–1611, doi:10.1016/j.soilbio.2011.02.015.
Smith, K. A. (2017), Changing views of nitrous oxide emissions from agricultural soil: key controlling processes and assessment at different spatial scales, *Eur. J. Soil Sci.*, *68*(2), 137–155, doi:10.1111/ejss.12409.
Schlüter, S., J. Zawallich, H. J. Vogel, and P. Dörsch (2019), Physical constraints for respiration in microbial hotspots in soil and their importance for denitrification, *Biogeosciences*, *16*(18), 3665–3675, doi:10.5194/bg-16-3665-2019.
Snider, D. M. (2011), A characterization of the controls of the nitrogen and oxygen isotope ratios

of biologically-produced nitrous oxide and nitrate in soils, (Doctoral dissertation). Retrieved from UWSpace. (https://uwspace.uwaterloo.ca/bitstream/handle/10012/6053/Snider_David.pdf?sequence=1&isAllowed=y) Waterloo, Ontario, Canada: University of Waterloo.

Snider, D., K. Thompson, C. Wagner-Riddle, J. Spoelstra, and K. Dunfield (2015), Molecular techniques and stable isotope ratios at natural abundance give complementary inferences about N2O production pathways in an agricultural soil following a rainfall event, *Soil Biol. Biochem.*, *88*, 197–213, doi:10.1016/j.soilbio.2015.05.021.

Snider, D. M., C. Wagner-Riddle, and J. Spoelstra (2017), Stable Isotopes Reveal Rapid Cycling of Soil Nitrogen after Manure Application, *J. Environ. Qual.*, *46*(2), 261–271, doi:10.2134/jeq2016.07.0253.

Song, X., X. Ju, C. F. E. Topp, and R. M. Rees (2019), Oxygen Regulates Nitrous Oxide Production Directly in Agricultural Soils, *Environ. Sci. Technol.*, *53*(21), 12539–12547, doi:10.1021/acs.est.9b03089.

Spott, O., R. Russow, and C. F. Stange (2011), Formation of hybrid N2O and hybrid N2 due to codenitrification: First review of a barely considered process of microbially mediated N-nitrosation, *Soil Biol. Biochem.*, *43*(10), 1995–2011, doi:10.1016/j.soilbio.2011.06.014.

Stuchiner, E. R., Z. D. Weller, and J. C. Fischer (2020), An approach for calibrating laser-based N 2 O isotopic analyzers for soil biogeochemistry research , *Rapid Commun. Mass Spectrom.*, (June 2020), 1–14, doi:10.1002/rcm.8978.

Sutka, R. L., N. E. Ostrom, P. H. Ostrom, J. A. Breznak, H. Gandhi, A. J. Pitt, and F. Li (2006), Distinguishing Nitrous Oxide Production from Nitrification and Denitrification on the Basis of Isotopomer Abundances, *Appl. Environ. Microbiol.*, *72*(1), 638–644, doi:10.1128/AEM.72.1.638.

Taylor, A. E., A. T. Giguere, C. M. Zoebelein, D. D. Myrold, and P. J. Bottomley (2017), Modeling of soil nitrification responses to temperature reveals thermodynamic differences between ammonia-oxidizing activity of archaea and bacteria, *ISME J.*, *11*(4), 896–908, doi:10.1038/ismej.2016.179.

Thilakarathna, S. K., and G. Hernandez-Ramirez (2021), Primings of soil organic matter and denitrification mediate the effects of moisture on nitrous oxide production, *Soil Biol. Biochem.*, *155*(February), 108166, doi:10.1016/j.soilbio.2021.108166.

Toyoda, S., H. Mutobe, H. Yamagishi, N. Yoshida, and Y. Tanji (2005), Fractionation of N2O isotopomers during production by denitrifier, *Soil Biol. Biochem.*, *37*(8), 1535–1545, doi:10.1016/j.soilbio.2005.01.009.

Toyoda, S., N. Yoshida, and K. Koba (2015), Isotopocule analysis of biologically produced nitrous oxide in various environments, *Mass Spectrom. Rev.*, *36*, 135–160, doi:10.1002/mas.

Trout, T. J., and W. C. Bausch (2017), USDA-ARS Colorado maize water productivity data set, *Irrig. Sci.*, *35*(3), 241–249, doi:10.1007/s00271-017-0537-9.

Van Groenigen, J. W., D. Huygens, P. Boeckx, T. W. Kuyper, I. M. Lubbers, T. Rütting, and P. M. Groffman (2015), The soil n cycle: New insights and key challenges, *Soil*, *1*(1), 235–256, doi:10.5194/soil-1-235-2015.

Vieten, B., T. Blunier, A. Neftel, C. Alewell, and F. Conen (2007), Fractionation factors for stable isotopes of N and O during N2O reduction in soil depend on reaction rate constant, *Rapid Commun. Mass Spectrom.*, *21*, 846–850, doi:10.1002/rcm.2915.

Wagner-Riddle, C., Q. C. Hu, E. van Bochove, and S. Jayasundara (2008), Linking Nitrous Oxide Flux During Spring Thaw to Nitrate Denitrification in the Soil Profile, *Soil Sci. Soc. Am. J.*, *72*(4), 908–916, doi:10.2136/sssaj2007.0353.

Well, R., I. Kurganova, V. L. De Gerenyu, and H. Flessa (2006), Isotopomer signatures of soil-emitted N2O under different moisture conditions - A microcosm study with arable loess soil, *Soil Biol. Biochem.*, *38*(9), 2923–2933, doi:10.1016/j.soilbio.2006.05.003.

Wen, Y., Z. Chen, M. Dannenmann, A. Carminati, G. Willibald, R. Kiese, B. Wolf, E. Veldkamp, K. Butterbach-Bahl, and M. D. Corre (2016), Disentangling gross N2O production and consumption in soil, *Sci. Rep.*, *6*(October), 1–8, doi:10.1038/srep36517.

Wenk, C. B. et al. (2016), Differential N2O dynamics in two oxygen-deficient lake basins revealed by stable isotope and isotopomer distributions, *Limnol. Oceanogr.*, *61*(5), 1735–1749, doi:10.1002/lno.10329.

Weinmann, T. (2020), Subalpine forest ecosystem responses to long-term nitrogen loading at Loch Vale Watershed, Colorado, USA (Doctoral dissertation). Retrieved from ProQuest. (https://www.proquest.com/docview/2423018123/FCFEBB9B6B934EB5PQ/5?accountid=10223) Fort Collins, Colorado, USA: Colorado State University.

Wrage, N., J. Lauf, A. del Prado, M. Pinto, S. Pietrzak, S. Yamulki, O. Oenema, and G. Gebauer (2004), Distinguishing sources of N2O in European grasslands by stable isotope analysis, *Rapid Commun. Mass Spectrom.*, *18*(11), 1201–1207, doi:10.1002/rcm.1461.

Wrage-Mönnig, N., M. A. Horn, R. Well, C. Müller, G. Velthof, and O. Oenema (2018), The role of nitrifier denitrification in the production of nitrous oxide revisited, *Soil Biol. Biochem.*, *123*(April), A3–A16, doi:10.1016/j.soilbio.2018.03.020.

Wong, W. W., M. F. Lehmann, T. Kuhn, C. Frame, S. C. Poh, I. Cartwright, and P. L. M. Cook (2020), Nitrogen and oxygen isotopomeric constraints on the sources of nitrous oxide and the role of submarine groundwater discharge in a temperate eutrophic salt-wedge estuary, , 1–15, doi:10.1002/lno.11664.

Wu, D., J. R. Köster, L. M. Cárdenas, N. Brüggemann, D. Lewicka-Szczebak, and R. Bol (2016), N2O source partitioning in soils using 15N site preference values corrected for the N2O reduction effect, *Rapid Commun. Mass Spectrom.*, *30*(5), 620–626, doi:10.1002/rcm.7493.

Wu, D., L. M. Cárdenas, S. Calvet, N. Brüggemann, N. Loick, S. Liu, and R. Bol (2017), The effect of nitrification inhibitor on N2O, NO and N2 emissions under different soil moisture levels in a permanent grassland soil, *Soil Biol. Biochem.*, *113*, 153–160, doi:10.1016/j.soilbio.2017.06.007.

Wu, D., R. Well, L. M. Cárdenas, R. Fuß, D. Lewicka-Szczebak, J. R. Köster, N. Brüggemann, and R. Bol (2019), Quantifying N2O reduction to N2 during denitrification in soils via isotopic mapping approach: Model evaluation and uncertainty analysis, *Environ. Res.*, *179*(August), doi:10.1016/j.envres.2019.108806.

Xia, Z., H. Xu, G. Chen, D. Dong, E. Bai, and L. Luo (2013), Soil N2O production and the δ15N-N2O value: Their relationship with nitrifying/denitrifying bacteria and archaea during a growing season of soybean in northeast China, *Eur. J. Soil Biol.*, *58*, 73–80, doi:10.1016/j.ejsobi.2013.05.008.

Yamamoto, A., H. Akiyama, Y. Nakajima, and Y. T. Hoshino (2017), Estimate of bacterial and fungal N2O production processes after crop residue input and fertilizer application to an agricultural field by15N isotopomer analysis, *Soil Biol. Biochem.*, *108*, 9–16, doi:10.1016/j.soilbio.2017.01.015.

Yang, H., H. Gandhi, N. E. Ostrom, and E. L. Hegg (2014), Isotopic fractionation by a fungal P450 nitric oxide reductase during the production of N2O, *Environ. Sci. Technol.*, *48*(18), 10707–10715, doi:10.1021/es501912d.

Yu, L. et al. (2020), What can we learn from N2O isotope data? - Analytics, processes and modelling , *Rapid Commun. Mass Spectrom.*, (June), 1–14, doi:10.1002/rcm.8858.

Yoshida, N., and S. Toyoda (2000), Constraining the atmospheric N2O budget from intramolecular site preference in N2O isotopomers, *Nature*, *405*(6784), 330–4, doi:10.1038/35012558.

Zhang, J., T. Lan, C. Müller, and Z. Cai (2015), Dissimilatory nitrate reduction to ammonium (DNRA) plays an important role in soil nitrogen conservation in neutral and alkaline but not acidic rice soil, *J. Soils Sediments*, *15*(3), 523–531, doi:10.1007/s11368-014-1037-7.

Zhang, W., Y. Li, C. Xu, Q. Li, and W. Lin (2016), Isotope signatures of N 2 O emitted from vegetable soil: Ammonia oxidation drives N 2 O production in NH 4+-fertilized soil of North China, *Sci. Rep.*, *6*(April), 1–10, doi:10.1038/srep29257.

Zhang, H., and K. Yemoto (2018), UAS-based remote sensing applications on the Northern Colorado Limited Irrigation Research Farm, *Int. J. Precis. Agric. Aviat.*, *1*(1), 1–10, doi:10.33440/j.ijpaa.20190202.50.

CHAPTER 4: USING ISOTOPE POOL DILUTION TO UNDERSTAND HOW ORGANIC CARBON ADDITIONS AFFECT N_2O CONSUMPTION IN DIVERSE SOILS

1. Summary

Nitrous oxide (N_2O) is a formidable greenhouse gas with a warming potential ~300x greater than CO_2. However, its emissions to the atmosphere have gone largely unchecked because the microbial and environmental controls that govern N_2O emissions have proven difficult to manage. The microbial process N_2O consumption is the only know biotic pathway that can remove N_2O from soil pores and can reduce net N_2O fluxes. Consequently, manipulating soils to increase N_2O consumption by organic carbon (OC) additions has steadily gained interest. However, the response of N_2O emission to different OC additions are inconsistent, and it is often unclear if lower N_2O emissions are due to increased consumption, decreased production, or both. Thus, simplified and systematic studies are needed to evaluate the efficacy of different OC additions on N_2O consumption.

I aimed to manipulate N_2O consumption by amending soils with OC molecules (succinate, acetate, propionate) more directly available to denitrifiers rather than to fermenters. I hypothesized that N_2O consumption is OC-limited, and I predicted that these denitrifier-targeted additions would lead to enhanced N_2O consumption and increased nosZ gene abundance. I incubated diverse soils in the laboratory and performed an isotope pool dilution assay to disentangle microbial N_2O emissions from consumption. I found that amending soils with OC increased gross N_2O consumption in six of the eight soils tested. Furthermore, three of the eight soils showed **I**ncreased N_2O **C**onsumption and **D**ecreased N_2O **E**missions (ICDE), a phenomenon I introduce in this study as an N_2O management ideal. I now hypothesize that

microbial N_2O consumption is regulated by the capacity for a soil to expand its regions of anoxia, and that is mediated by the addition of electron donors. I suggest future studies prioritize methodical assessment of different, specific, OC-additions to determine which additions help show ICDE in different soils.

2. Introduction

Nitrous oxide (N_2O) is a potent greenhouse gas (GHG) that has a 100-year warming potential 298x greater than carbon dioxide (CO_2), and it is the primary stratospheric ozone depleting substance (Ravishinkara et al. 2009, Ciais et al. 2013). Over the past 40 years, anthropogenic N_2O emissions have increased 30%, primarily due to inorganic nitrogen (N) additions to croplands (Tian et al. 2020). Unfortunately, it has been challenging to reduce N_2O emissions by cutting N inputs because N-fertilizer use is viewed as intrinsic to meeting crop yield demands (Reay et al. 2012, Smith 2017, Houser and Stuart 2020, Kanter et al. 2020b).

Ideally, the biogeochemical processes that regulate N_2O emission from croplands could be managed to diminish N_2O emissions. However, N_2O management has been challenged by the underlying diversity and complexity of soil N transformations associated with N_2O production (Butterbach-Bahl et al. 2013), and by the differing sensitivity of these processes to state factors (Domeignoz-Horta et al. 2017), transient effects like moisture and temperature (Schindlbacher et al. 2004, Luo et al. 2013), management history (Krause et al. 2017), and details of the N_2O production intervention (Subbarao et al. 2006, Lam et al. 2017, Zhou et al. 2017, Borchard et al. 2019, Hellman et al. 2019, Lazcano et al. 2021).

The observation of N_2O uptake from soils, as measured by gas flux chambers (Chapuis-Lardy et al. 2007) has focused attention on the process of N_2O consumption in soils, and it highlighted the possibility that N_2O emissions may be cut by managing the N_2O consumption

process (Figure 4.2, Yoon et al. 2019). The only known biological pathway for N_2O consumption occurs in denitrifying bacteria where the NosZ enzyme catalyzes the respiratory reduction of N_2O to N_2 (Richardson et al. 2009, Hallin et al. 2018). Soil metagenomic studies of the nosZ gene suggest that the N_2O consuming community is diverse and abundant (Jones et al. 2013, Jones et al. 2014, Bakken and Frostegård 2017). But despite this conceptual potential for managing N_2O consumption, Stein (2020) notes in a recent review that significant knowledge gaps prevent us from predicting the response of N_2O consumption to manipulation or controlling it at the scale of ecosystems.

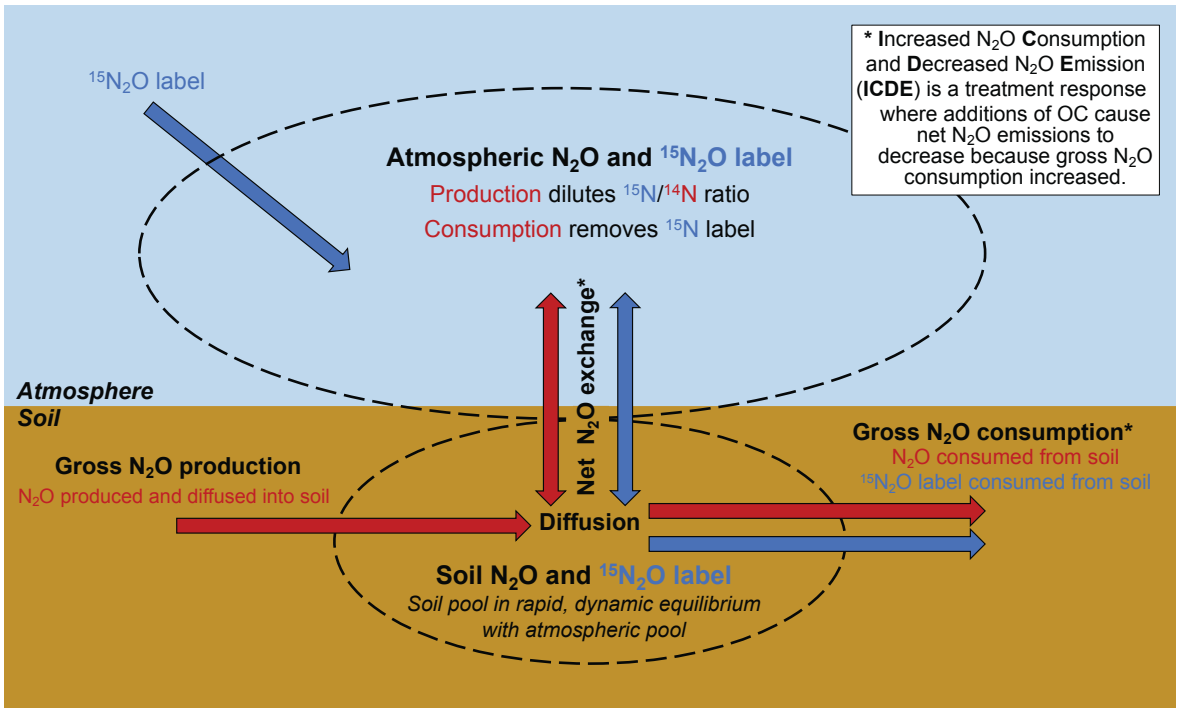

Figure 4.1. To disentangle the kinetics of N_2O production, consumption, and net emission, I used isotope pool dilution, an assay where isotopically enriched $^{15}N_2O$ is injected into the headspace of a closed incubation system and then the label $^{15}N_2O$ disappearance is monitored over time. Soil and atmospheric gases (pools bounded by dotted outlines) are in dynamic equilibrium, maintained by diffusion and gas concentration gradients induced by soil biology over the 48-hr incubation period of the study. Thus, the N_2O and label $^{15}N_2O$ concentrations measured in the headspace of the incubation system were ultimately driven by biological processes of N_2O production and consumption in the soil. Red arrows indicate fluxes that affect the bulk N_2O pool while blue arrows indicate fluxes that affect the label $^{15}N_2O$. In this study, I quantify gross N_2O consumption by tracking the disappearance of label $^{15}N_2O$ over time. I also quantify net emission as the change in bulk N_2O concentration over time.

In my experiment, I sought to stimulate N_2O consumption and thereby reduce net N_2O emissions. To enhance N_2O consumption, I added OC to soils and compared the N_2O consumption rates and net N_2O emission rates in control vs. manipulated soils. In response to OC-amendment, I looked for **I**ncreased gross N_2O **C**onsumption and **D**ecreased net N_2O **E**missions (ICDE) in soils. From a GHG management perspective, it would be ideal to induce ICDE in any soil. Here I explore how amending soils with organic carbon (OC) provides an electron donor source for enhanced $N_2O \rightarrow N_2$ reduction, which corresponds to N_2O consumption. When some soils show an ICDE response, but others do not, I examine the factors that explain the response.

One major area of uncertainty about stimulating N_2O consumption is how altering organic matter supply might affect the overall N_2O soil biogeochemistry. Organic matter additions are the focus of many N_2O management studies (Stevenson et al. 2011, Sutton-Grier et

al. 2011, Senbayram et al. 2012, Wu et al. 2018, Hellman et al. 2019, Lazcano et al. 2021, Wang et al. 2021a). N_2O consumption is primarily an anaerobic, respiratory pathway (Hein and Jörg 2019, Shan et al. 2021), and so there exists an environmental correlation where N_2O consumption rates are highest where both O_2 concentrations are low and organic matter abundance is high (Senbayram et al. 2012, Wu et al. 2013, Conthe et al. 2018, Wu et al. 2018). However, studies have found that the net emission of N_2O can go either up or down, depending on the soil and the nature of the organic matter addition. For example, manure additions may create more anoxic conditions, but these additions also provide nitrogen, leading to potential stimulation of N_2O production (Butterbach-Bahl and Danemman 2011, Duan et al. 2019). Additionally, sugar additions (e.g., glucose) have most commonly caused increased N_2O emissions and reduced nosZ abundance (Millar et al. 2009, Morley and Baggs 2010, Mitchell et al. 2013, Barrett et al. 2016, although they have also contributed to anoxia and a reduction in N_2O emissions from soil microcosms (Sánchez-Martín et al. 2008). It is becoming clear that simplified and systematic studies are needed to evaluate the efficacy of different organic carbon additions on N_2O consumption.

A second major area of uncertainty arises from the challenge of measuring N_2O production and consumption. When studies find differing N_2O emission responses to organic matter addition, it is often not clear if the differences arise from changes in N_2O production, N_2O consumption or both (Butterbach-Bahl and Danemman 2011, Zhu et al. 2015, McMillan et al. 2016, Conthe et al. 2019, Duan et al. 2019, Wang et al. 2019, Shan et al. 2021). Ideally, management intervention would induce **I**ncreased N_2O **C**onsumption and **D**ecreased N_2O **E**missions (ICDE, Figure 4.1), but other outcomes are, of course, possible. The use of labeled $^{15}N_2O$ in an isotope pool dilution assay is a gold standard that allows direct quantification of N_2O

production and consumption (Figure 4.1, Chapuis-Lardy et al. 2007, Yang et al. 2011). Although isotopic analyses have historically been costly, required significantly elevated N_2O concentrations (Clough et al. 2006), and slow sample throughput (Ostrom and Ostrom 2017), new laser-based N_2O isotopic analyzers are effective at near-ambient N_2O concentrations, with much faster throughput and minimal sample preparation (Stuchiner et al. 2020).

The ability to rapidly and systematically screen the effects of various organic carbon (OC) additions on N_2O consumption rates opens a new pathway for improved management of N_2O consumption. Here, I sought to induce N_2O consumption in soils by providing the microbial communities with additions of OC. Based on previous work (Hedin et al. 1998, Ostrom et al. 2002) that stimulated N_2O consumption through the addition of OC compounds known to be used by denitrifiers (acetate, succinate, propionate), I hypothesized that N_2O consumption is generally OC limited. In this experiment, I aimed to manipulate N_2O consumption by amending soils with an abundance of the abovementioned electron donors that are more exclusively available to denitrifiers, rather than to fermenters. I predicted that these targeted additions would stimulate nosZ abundance and lead to enhanced N_2O consumption (Kuypers et al. 2018). To test this, I incubated diverse soils collected from Colorado, New Mexico, and Minnesota in the laboratory (1) to see how amending them with denitrifier-specific OC compounds would broadly affect N_2O production and consumption among soils, and (2) to see how underlying features of the different soils would impact their capacity to consume N_2O. All soils were held at 60% water saturation, amended with non-fermentable organic acids (acetate, succinate, propionate), and incubated in the laboratory for 48 hr. I used $^{15}N_2O$ isotope pool dilution to disentangle microbial N_2O emissions from consumption (Figure 4.1). I also measured a suite of soil properties and microbial N-cycling gene abundances to examine which of these factors individually and

collectively helped to explain the soil N_2O behavior I observed. To my knowledge, no other study has yet sought to intentionally manipulate N_2O consumption and quantify that effect using $^{15}N_2O$ isotope pool dilution. However, understanding how to stimulate N_2O consumption could have important implications for managing N_2O emissions from soils, particularly in agricultural systems.

3. Materials and Methods

3.1 Field sampling and soil characterization

Soils were collected from eight locations in the United States (Table 4.1). Four soils were collected in Colorado, one soil was collected in New Mexico, and two soils were collected in Minnesota. Site and soil-specific properties are summarized in Table 4.1. All soils were collected within July-August 2019. Throughout the remainder of the article, soils will be referred to by their site name in Table 4.1.

Table 4.1. Summary of environments where soils were collected and features of all soils used in the incubation experiment. MAT, MAP, soil classifications, and horizons were determined using the United States Department of Agriculture Natural Resources Conservation Service Soil Resource Reports.

Site name	Location	Site name	GPS coordinates	MAT (°C)	MAP (mm)	Soil classification	Soil horizon
Shortgrass Steppe	Nunn, CO	Shortgrass prairie	40.80458, -104.71565	11	381	Alluvial Nunn, fine clayey loam	Ap/Bt
Limited Irrigation Research Farm	Greeley, CO	Colorado cornfield	40.44852, -104.63897	9.5	373	Ustic Haplargids Olney fine sandy loam	A
Sevilleta Grassland	Socorro, NM	Desert grassland	34.34914, -106.88624	16	229	Mesic Ustic Haplocalcids, loamy-skeletal, carbonatic	A/C
Colorado State University	Fort Collins, CO	Urban Lawn	40.57770, -105.07775	10	408	Fort Collins loam	Ap/Bt
Sky Pond	Rocky Mountain National Park, CO	Alpine meadow	40.27971, -105.66886	1.4	1050	Cryochrepts, Cryumbrepts Rocky sandy loam	O/A/Bw
Loch Vale	Rocky Mountain National Park, CO	Subalpine forest	40.29649, -105.64612	1.4	1050	Cryic spodosols Rocky sandy loam	O/A
Wellrose Farms	Elrosa, MN	Minnesota cornfield	45.60081, -95.01333	5.5	721	Mesic typic Udoll friable silty loam	A
Fenske Lake Cabins	Ely, MN	Coniferous forest	47.99823, -91.91292	4	797	Udic Eveleth-Eagelsnest-Conic complex, rocky loam	A/Bw

3.2 Soil collection and analyses

All soils were collected from the top ~20 cm of the soil profile. Soils were collected using a 5cm-diameter soil auger. The sites Shortgrass Steppe, Limited Irrigation Research Farm, Sevilleta Grassland, Colorado State University, and Wellrose Farms all had either designated plots or sampling areas (e.g., a lawn, a specific cornfield), so within those designated areas ten soil cores were collected randomly. The sites Sky Pond, Loch Vale, and Fenske Lake Cabins represented broader geographic areas (e.g., a forest), so ten soil cores were collected at randomly assigned GPS points within ~150 m of the GPS coordinates for the site (Table 4.1).

Cores were bulked into gallon Ziploc bags, placed on ice in the field to minimize microbial activity, and then refrigerated at 4 °C upon arrival to the laboratory. Soils collected outside of Colorado were shipped overnight to Colorado State University on ice, sieved to 2mm and homogenized within 72 hr after sampling. Soils collected in Colorado were sieved to 2mm and homogenized within 24 hr after sampling. Processed soils were frozen in gallon Ziploc bags at -20 °C. All incubations and analyses were performed within two months of soil collection.

Prior to freezing soils, I measured soil inorganic N (IN) via KCl extractions and calculated soil gravimetric water content (GWC). I also measured soil IN concentrations after all soils had been incubated. Ammonium (NH_4^+) and NO_3^- were extracted from soils in a 5:1 2M KCl to soil mixture. Mixtures were shaken at 250 rpm for 60 minutes, settled for 60 minutes, and then gravity filtered. Extracts were analyzed colorimetrically with an Alpkem FIA wet chemistry system (O.I. Analytical, College Station TX). I determined gravimetric water content (GWC) by drying 10 g soil subsamples to a constant weight at 105 °C.

Frozen soils were thawed to measure soil pH, SOC, and SON. I measured soil pH from slurries of 10:1 deionized (DI) water to soil with a benchtop meter (Thermo Scientific Orion Star™ A211 Benchtop pH Meter, Waltham, MA, USA). Frozen soil subsamples were dried in a 60 °C oven, ground to powder on a table roller, and then combusted for SOC and SON analysis with a LECO Tru-Spec CN analyzer (Leco Corp., St. Joseph, MI, USA). Soils did not contain appreciable inorganic C.

3.3 Determination of soil saturation

For all incubations, I held soils at 60% soil saturation. To determine how much water to add to each soil to achieve this saturation, I determined the maximum water holding capacity (WHC) for each soil. First, I amended thawed subsamples of frozen, field-moist soil with DI water until fully saturated. Then, I dried these subsamples to a constant weight at 105 °C and calculated saturated water content (SWC) by dividing the g water in the subsample by the subsample dry soil mass. I used this metric rather than % water-filled pore space (WFPS) because in sieving my soils I broke down all soil pore structures. Finally, to determine the g of water to add to a given soil, I used Equation 1, where g soil corresponds to the g soil incubated, and 0.6 corresponds to the target percent saturation (60%):

$$g\ H_2O\ to\ add = g\ soil\ x\ ((SWC\ x\ 0.6) - soil\ GWC)) \qquad (1)$$

3.4 Soil incubations

3.4.1 Preparation of organic carbon solution

I prepared an aqueous OC amendment for all treated soils. Equal quantities on a % mass C basis of powdered sodium succinate, sodium acetate, and sodium propionate were dissolved into DI water and diluted serially (two dilutions) to a final concentration of 6.28 mg/L. All

organic compounds were obtained from Sigma Aldrich (St. Louis, MO, USA). Aqueous solutions were stored at 4 °C when not in use.

The organic acids used are all non-fermentable, naturally occurring, and have previously been determined by Hedin et al. (1998) to impact denitrifier metabolism. I determined the concentration for the OC-amendment by calculating the stoichiometric amount of C required to reduce all the IN in a subsample from the Limited Irrigation Research Farm that was collected prior to my full soil sampling campaign (Table 4.1). I chose to use that soil for the IN benchmark because I knew this soil would have a high IN concentration, and I wanted to ensure that my OC-amendment would provide an ample electron donor supply for microbial metabolism in all the amended soils.

3.4.2 Soil amendments and incubation setup

Soils were separated into either Control, or OC-amended (+OC) groups. For all incubations, the frozen soil equivalent of 75g dry soil was weighed into 0.5 L Ball jars and refrigerated overnight to thaw. Prior to treatment, all soils were removed from the refrigerator and warmed to room temperature over ~1 hr. To bring all soils to 60% saturation, Control soils were amended with DI water and +OC soils were amended with DI water and 1mL of the +OC solution. Either amendment was distributed by pipette over the soils. After all liquid was added to a given soil, it was thoroughly mixed to ensure sufficient distribution of OC (if applicable) and homogenous saturation.

After all soils were treated, jars were sealed for incubation. In Stuchiner and von Fischer (unpublished manuscript in revision with JGR: Biogeosciences, *see Chapter 3*) I provide a detailed description of my incubation apparatus, which includes a 1L Tedlar gas bag attached to

the jar headspace to allow for removal of a large quantity of air for subsequent [N_2O] and isotopic analysis with my laser-based analyzer (see 2.4.3 for details). Prior to incubation, I flushed and filled all incubation apparatuses from a cylinder of custom-blend air intended to closely emulate Earth's atmosphere (2ppm CH_4, 0.450ppm N_2O, 21% O_2, and N_2 to balance) but without CO_2 and water vapor, as these gases contribute to optical peak broadening effects (Bowling et al. 2005, Ostrom and Ostrom 2017, Stuchiner et al. 2020). After incubation vessels were flushed and filled, I used a 3mL syringe to inject 1 mL of 99 atom percent (AP) $^{15}N_2O$ into each headspace for isotope pool dilution (details in Section 3.4.4). The syringe was pumped multiple times to ensure that all labelled gas was injected into the incubation vessel.

I performed time zero (T_0) and time 48 (T_{48}) measurements to enable a 48 hr assay duration. Soils were incubated on a lab countertop at room temperature (24 °C) for either 60 minutes (T_0, to allow for homogenization of headspace air following $^{15}N_2O$ addition) or 49 hr (T_{48}). At the end of the incubation period, I mixed each jar and gas bag's air by attaching a 60 mL syringe to the jar's gas sampling port and, by opening the stopcock valve connecting the jar headspace to the gas bag, I pumped the syringe for ~ 60 seconds to homogenize the jar headspace and Tedlar gas bag (Stuchiner and von Fischer unpublished manuscript in revision with JGR: Biogeosciences, *see associated Methods file*). At the time of sampling, I connected my incubation apparatus directly to the gas analyzer-scrubber system (see 2.4.3 for details). As the analyzer removed air from the jar headspace, air was simultaneously removed from gas bag, thus keeping the jar air pressure at atmospheric pressure.

3.4.3 Measurements of N_2O and CO_2 concentration, and N_2O isotopic composition

After 60 minutes (T_0) or 49 hours (T_{48}), incubation vessels were analyzed for N_2O concentration and isotopic composition by a laser-based Los Gatos Research (LGR) N_2O

isotopic analyzer (Los Gatos Research N_2O Isotopic Analyzer model 914–0027; ABB-Los Gatos Research, Mountain View, CA, USA). Gas was sampled from each incubation vessel for 12-15 minutes (or until the N_2O concentration stabilized) at a flowrate of 42 mL/min into the analyzer. I removed CO_2, water vapor and volatile organics from the sample air using a Nafion-Carbosorb-Silica gel scrubbing system. Removing these gases minimizes the optical peak-broadening effects inherent to laser-based analyzers (Stuchiner et al. 2020).

All raw concentration data for each N_2O sample was exported to Excel (version 16.52), where it was trimmed to only include stabilized N_2O isotopocule readings (the final ~5 minutes of sampling). These values were used to calculate average N_2O and isotopomer concentrations. All reported concentrations were then corrected against calibrations using the model and approach described in Stuchiner et al. (2020).

I measured accumulated CO_2 in the T_{48} incubation jars to characterize microbial respiration. Air samples of 3mL were drawn with a 3mL syringe from remaining headspace air in the incubation jars at the end of the T_{48} N_2O sampling. Samples were analyzed on a laser-based Los Gatos Research Greenhouse Gas Analyzer (Los Gatos Research Greenhouse Gas Analyzer model 908-0007-001; ABB-Los Gatos Research, Mountain View, CA, USA). Sample air was admitted to the analyzer by injecting the 3mL air samples into a continuous flow of zero-grade air (80:20 N_2:O_2 blend, Airgas Industries) that connected to the analyzer via an open split. All baseline GHG concentrations were <10ppm, and each injected sample yielded a brief CO_2 concentration peak. The height (i.e., maximum concentration) of these peaks were calibrated with a four-point calibration curve generated with CO_2 standards from Airgas (1023, 5000, 10000, 60000ppm CO_2) that were also injected into the analyzer when zero-grade air was flowing through it.

3.4.4 Flux calculations and isotope pool dilution

I calculated net N_2O emission using measures of the headspace N_2O concentration and calculated gross N_2O consumption using isotope pool dilution (Kirkham and Bartholomew 1954, von Fischer and Hedin 2002). Net N_2O flux was calculated from the difference in N_2O concentration between T_0 and T_{48} and is presented in units ng N_2O-N/g dry soil/day.

Gross N_2O consumption is quantified based on the disappearance of ^{15}N-labeled N_2O. I follow the convention of von Fischer and Hedin (2002) which considers N_2O production rate to be relatively constant over the measurement interval but N_2O consumption to be a first-order function of N_2O concentration. Thus, I adopt their equation 4 and modify it as:

$$F = \frac{d[N_2O]}{dt} = P - k[N_2O].$$

Where F is the net flux rate, $[N_2O]$ is the N_2O concentration in the jar headspace, P is the production rate, and k is the first-order consumption rate constant. Note that the gross consumption rate is the product of k and the N_2O concentration. A focus in my study was quantifying the consumption rate, which is essentially measuring the uptake constant, k. The amount of labeled N_2O falls exponentially over time following Equation 2,

$$^{*}N_2O(t) = {}^{*}N_2O_0 e^{-kt} \qquad (2)$$

Which is equivalent to Equation 3,

$$\ln {}^{*}N_2O\ (t) = \ln\ {}^{*}N_2O_0 - k \bullet t \qquad (3)$$

Where $*N_2O(t)$ is the amount of labeled N_2O at time t. Substituting $*N_2O_{(48)}$ and t = 48, the solution for k is:

$$k = \frac{\ln {}^{*}N_2O_0 - \ln {}^{*}N_2O_{(48)}}{48} \qquad (4)$$

I calculated *N_2O, the amount of labeled N_2O in the incubation jar headspace, as the product of the total headspace N_2O concentration and the AP excess (APE) $^{15}N^{bulk}$ in the N_2O.

Determination of the APE follows a series of calculations. First, after N_2O and its isotopomers were calibrated using equations from Stuchiner et al. (2020), I determined $^{15}N^{bulk}$ by calculating the average concentration of $^{15}N^{\alpha}$ and $^{15}N^{\beta}$ using Equation 5:

$$^{15}\mathrm{N}^{\mathrm{bulk}} = \frac{[\,^{14}N^{15}N^{16}O] + [\,^{15}N^{14}N^{16}O]}{2} \qquad (5)$$

Next, I subtracted (5) from the total N_2O concentration for a given sample to calculate the light ($^{14}N^{14}N^{16}O$) fraction of emitted N_2O. Then I calculated the atom percent of the heavy isotope (AP) for each sample using Equation 6:

$$AP = \frac{^{15}\mathrm{N}^{\mathrm{bulk}}}{^{15}\mathrm{N}^{\mathrm{bulk}} + \,^{14}N^{14}N^{16}O} \qquad (6)$$

Then, I subtracted the AP of natural abundance $^{15}N_2O$ from the observed AP to obtain the APE of $^{15}N_2O$ present in the incubation headspace. I assumed a natural abundance $\delta^{15}N$ of N_2O to be -35‰, which is equivalent to AP of 0.3535% (Hu et al. 2015).

These excess $^{15}N_2O$ concentrations were used in Equation 4 to calculate k, the first order rate constant for N_2O consumption. Gross N_2O consumption rate was then calculated by multiplying each k value by 0.332, the mean atmospheric N_2O concentration in parts per million (ppm) in 2019 (www.N2Olevels.org). Each gross consumption rate was expressed in units ng N_2O-N/g dry soil/day.

3.4.5 Leak test of incubation apparatus

A separate test assessed the gastight seals of the incubation vessels. Twelve incubation vessels were flushed and filled with zero-grade air and injected with 1 mL of 99 AP $^{15}N^{15}N^{16}O$

into the headspace of each jar using a 3 mL syringe. After mixing the jar and gas bag air thoroughly, this raised the N_2O concentration and the $\delta^{15}N^{bulk}$ on average to ~500ppb and ~6300‰, respectively. Six vessels were sampled for N_2O and isotopomer concentrations at T_0 and the remaining six vessels were sampled at T_{48}. All samples were measured on my LGR N_2O isotopic analyzer. T-tests revealed that changes from T_0 to T_{48} in total N_2O concentration were not significant, while changes in concentration of enriched $^{15}N_2O$ was less than 2.3% for $\delta^{15}N^{\alpha}$ and $\delta^{15}N^{\beta}$.

3.4.6 Post-incubation soil and genetic measurements

After all gas had been sampled for the T_{48} incubations, soil replicates from each group were bulked into a Ziploc bag and re-homogenized. Soil IN was measured immediately thereafter, as in Section 3.2. Two-gram subsamples from each treatment group were frozen at -80 °C in preparation for microbial genetic analysis, and remaining soils were frozen at -20 °C.

To measure the abundances of key N-cycling genes (nifH, nirK, clade I nosZ), I extracted DNA from soils that had been frozen at -80 °C using a Qiagen Powersoil Pro kit according to the manufacturer's instructions (Qiagen, Germantown, MD, USA). The nifH gene encodes the enzyme that catalyzes N-fixation, the nirK gene encodes the enzyme that catalyzes reduction of nitrite (NO_2^-) to nitric oxide (NO) and is thus characteristic of incomplete denitrification, and the nosZ gene encodes the enzyme that catalyzes reduction of N_2O to N_2 and is thus characteristic of complete denitrification (Sanford et al. 2012, Domeignoz-Horta et al. 2015, Kuypers et al. 2018). I acknowledge that nirS is also measured to represent incomplete denitrification (Sanford et al. 2012), however cost constraints prevented us from quantifying that gene. The quality (A260/A280) and concentration from each DNA sample was determined spectrophotometrically

using a NanoDrop (Thermo Scientific, Waltham, MA, USA). All samples were diluted to 10 ng/μL and then I characterized the abundances of the abovementioned N-cycling genes using qPCR analysis. All qPCR reactions were performed in 96-well plates using an ABI Prism 7500 Sequence detection system (Applied Biosystems, Foster City, CA, USA). The following thermal cycling program was used for all genes: 95 °C for 15 s, 63 to 58 °C for 30 s (-1 °C by cycle), 72 °C for 30 s, 80 °C for 15 s, 6 cycles, as in Trivedi et al. (2012). For each soil sample, qPCR amplification was performed for each N-cycling gene four times. Gene abundances (e.g., gene copy number) were determined by using simple linear regressions that related the cycle threshold (Ct) value for each sample to known Ct values from a standard curve. Standard curves for each gene were generated by preparing an 8-fold serial dilution of plasmid that contained the gene of interest.

I acknowledge that clade II nosZ has been identified as an important gene in the $N_2O \rightarrow N_2$ reduction step in the denitrification pathway (Jones et al. 2014, Almaraz et al. 2020, Chee-Sanford et al. 2020). However, due to financial constraints and a lack of primers I could not quantify clade II nosZ gene abundances in this study.

3.5 Data analyses

3.5.1 Calculation of OC:Control ratios

To determine the effect of the +OC treatment, I compared +OC vs control for net N_2O emissions, gross N_2O consumption, soil NO_3^- and NH_4^+ concentrations, microbially emitted [CO_2], and the gene abundances of nifH, nirK, and clade I nosZ for all soils at the conclusion of incubations. To quantify the effect of OC-amendment, I calculated response ratios as the +OC:Control ratio for each variable measured. Because the +OC and Control replicates for a

given soil were not paired, I calculated the mean for the Control for each property, and then I divided each +OC value by the mean Control value. Thus, for a ratio >1 the +OC treatment increased that property, while for a ratio <1 the +OC treatment decreased that property. When applicable, +OC:Control response ratios were used in all statistical analyses.

3.5.2 Statistical analyses

All raw data was collected and collated in Excel, and then all statistical analyses were performed in RStudio (version 4.0.2 (2020-06-22) – "Taking Off Again" © 2020 The R Foundation for Statistical Computing). Differences among initial soil NO_3^- and NH_4^+ concentrations were determined using one-way ANOVAs. Associations among all inherent soil properties and +OC:Control ratios and ICDE were examined using a MANOVA (Box 1), with subsequent one-way ANOVAs performed to assess differences among all soils for each property individually. Residuals were examined for departure from normality. All N_2O production and consumption data from all soil incubations were log-transformed to meet assumptions of normality in residuals.

I also performed a Principal Components Analysis (PCA) to examine the associations among variables and ICDE. I used the package `factoextra` to visualize the results of the PCA and I used the package `missMDA` to impute the dataset. To determine if there were significant associations among properties and ICDE I performed t-tests comparing the Yes ICDE vs. No ICDE coordinate loadings for PCs 1-4.

4. Results

4.1 N_2O emission and consumption rates

OC additions simulated gross N_2O consumption in six of the eight incubated soils (Figure 4.2). This includes the alpine meadow, Colorado cornfield, desert grassland, Minnesota cornfield, shortgrass prairie, and subalpine forest. However, soils differed in whether +OC led to an increase vs. decrease in net N_2O emissions. The alpine meadow, Minnesota cornfield, and subalpine forest soils all had increased N_2O emissions in +OC compared to Control soils, whereas the Colorado cornfield, desert grassland, and shortgrass prairie soils all had decreased N_2O emissions in +OC compared to Control soils. Consequently, these latter three soils showed ICDE (Box 1). Only the coniferous forest decreased in both net emissions and gross consumption following OC-amendment. Note that the urban lawn soil is not included in Figure 4.2 because no gross consumption was observed; only the urban lawn had increased net emissions and no gross consumption following OC-amendment (data not shown). On average, among the seven soils plotted in Figure 4.2, there was a 366% increase in N_2O consumption following OC-amendment, and a 250% increase in N_2O emissions following OC-amendment.

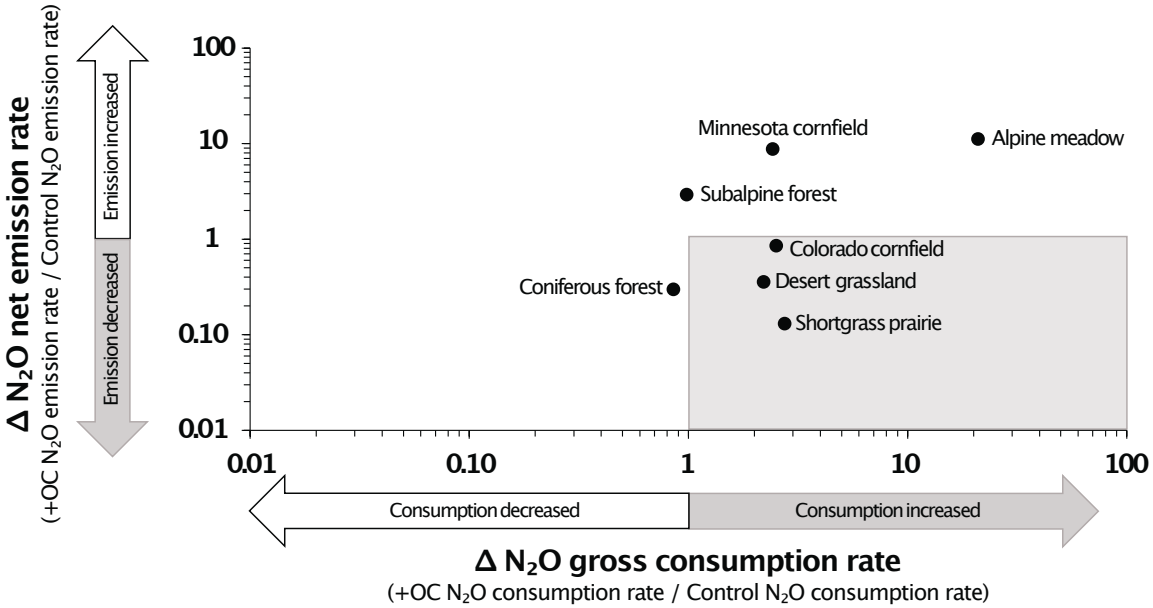

Figure 4.2. Change in (or "Δ") net N_2O emission vs. gross N_2O consumption rates for all soils excluding the Urban Lawn soils, in which no N_2O consumption was observed following +OC amendment. Δ values were calculated as +OC:Control response ratios for gross consumption rate and net emission rate (both rates are in ng N_2O-N/g dry soil/day). Soils included in the grey box had **I**ncreased N_2O **C**onsumption and **D**ecreased N_2O **E**missions (ICDE). For net N_2O emission, n = 6 in all cases except the alpine meadow, in which n = 12. For gross N_2O consumption, n = 12 for the alpine meadow, n = 5 for the Minnesota cornfield, n = 2 for the coniferous forest, and in all other cases n = 6.

4.2 Differences among soil properties and microbial gene abundances

I performed a MANOVA regressing all the soil and microbial properties I measured vs. the ICDE categories (hereafter categorized as "Yes ICDE" or "No ICDE"). The MANOVA revealed that at least one of the properties impacted whether a soil showed ICDE or not ($p < 0.0001$). To better discern which properties were important drivers of ICDE, I performed subsequent one-way ANOVAs to assess differences among soils for each property individually. As illustrated in Fig 2, all properties were highly significantly different among soils ($p < 0.0001$, Figure 4.3A-4.2F) except for the microbial gene abundances ($p = 0.095$ for Δ nosZ:nirK and $p = 0.148$ for Δ nifH, Figure 4.3G and 4.3H, respectively).

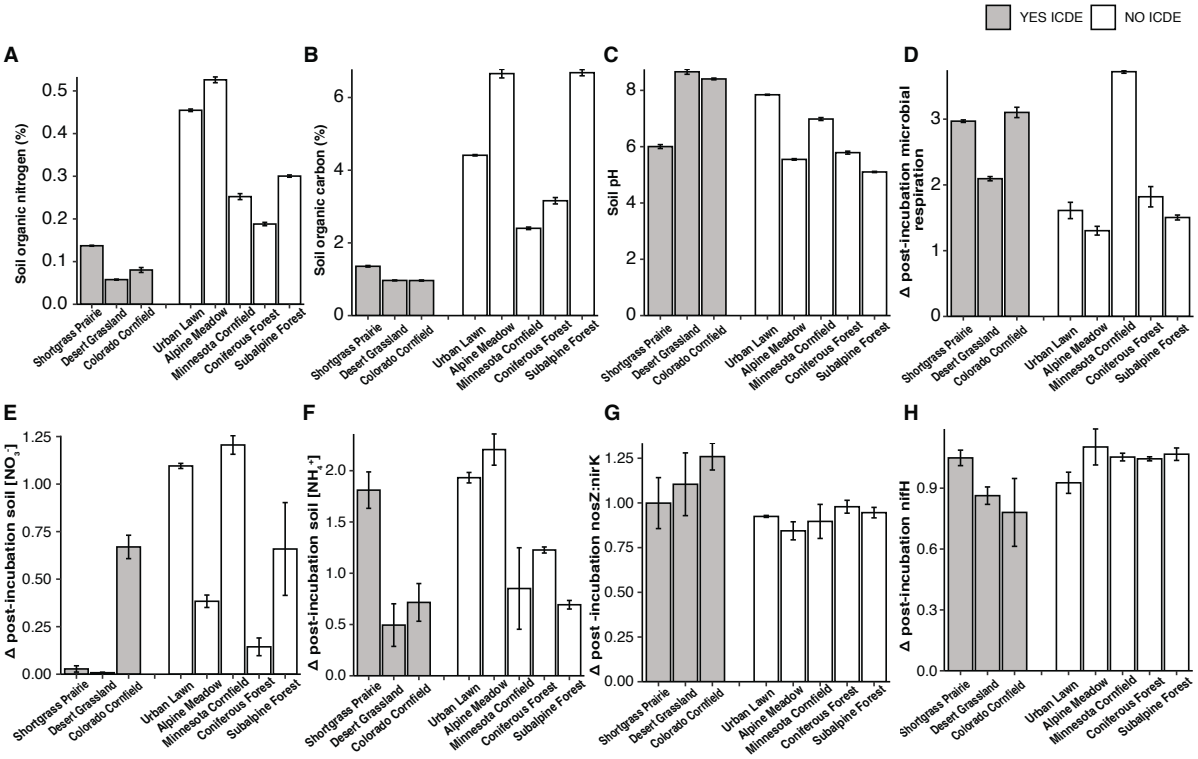

Figure 4.3. Panels **A-H** show the soil properties or microbial genes abundances among all soils tested, with panels in order from most (**A**) to least (**H**) significance in one-way ANOVA for soil. Panels **A-C** are direct measures of soil properties that were measured prior to the incubation experiments, whereas panels **D-H** are all Δ values for +OC:Control soil properties and N-cycling gene abundances. The Δ nosZ:nirK (panel **G**) is a ratio-of-ratios, in which the nosZ:nirK ratio for +OC soils is divided by the nosZ:nirK ratio for the Control soils. I partitioned soils by Yes ICDE (grey bars) vs. No ICDE (white bars) groupings to highlight properties that Yes ICDE had in common and how collectively Yes ICDE vs. No ICDE differed in their properties. Error bars are ± one SE from the mean. Please see Appendix 3 Table 1 for n-values and units for each property.

ANOVAs indicate that soils had significant differences in IN pools prior to incubation. There was a significant difference among all soils for NH_4^+ ($p < 0.0001$) and NO_3^- ($p < 0.0001$) concentrations (Figure 4.4). Tukey pairwise comparisons revealed that there were multiple significant differences among soil NH_4^+ concentrations pre-incubation, whereas there were fewer differences among soil NO_3^- concentrations pre-incubation (Figure 4.4). However, the differences among NO_3^- concentrations were more pronounced, with the Minnesota cornfield having the highest soil NO_3^- concentration ($p < 0.0001$ in all cases), the Colorado cornfield having the second highest soil NO_3^- concentration ($p < 0.001$ in all cases), and the Urban lawn

having the third highest soil NO_3^- concentration ($p < 0.001$ for all comparisons except $p = 0.0001$ for Urban Lawn vs. Desert grassland and $p = 0.0076$ for Urban Lawn vs. Alpine meadow, Figure 4.4).

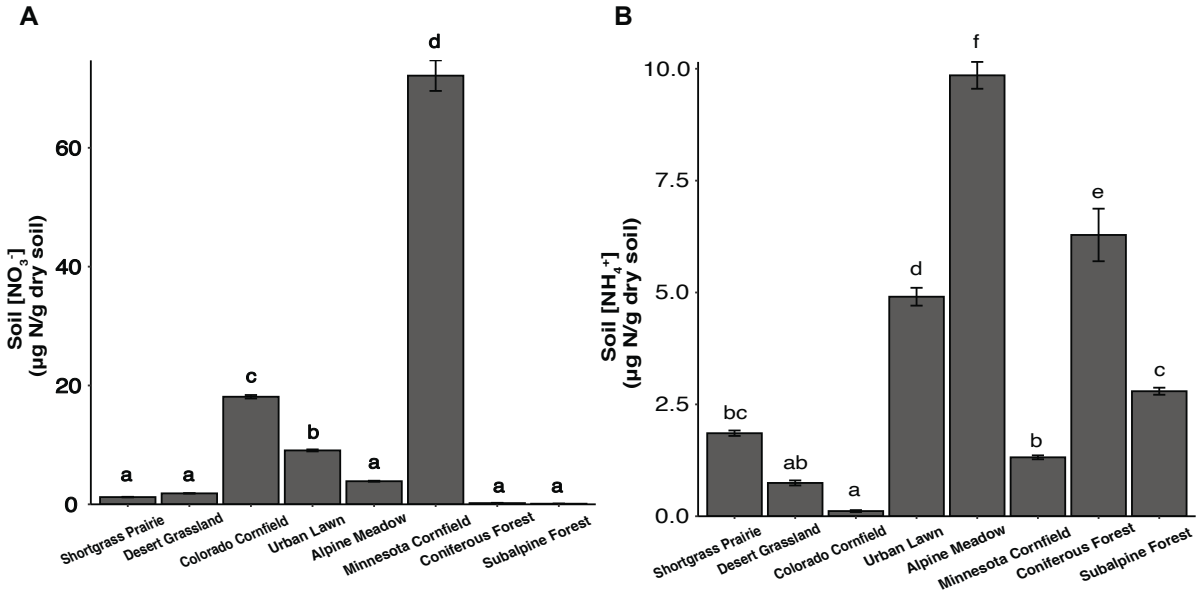

Figure 4.4. Initial NO_3^- (panel **A**) and NH_4^+ (panel **B**) concentrations in soils prior to incubations. Soil extractable NO_3^- and NH_4^+ were measured within 24-72 hr of field sampling. Letters correspond to significantly different mean concentrations. In all cases, n = 4, and error bars are ± one SE from the mean.

4.3 Associations between predictor variables and ICDE

My PCA grouped variables to reveal associations among predictor variables and ICDE. Principal component (PC) 1 explained more than 50% of the variation among the variables, whereas PC2 explained approximately 17% of the variation among the variables (Figure 4.5). While PC1 accounted for the most associations among variables and ICDE, I ranked the loadings associated to each predictor variable for PCs 1-4. These loadings and rankings are summarized in Table 4.2.

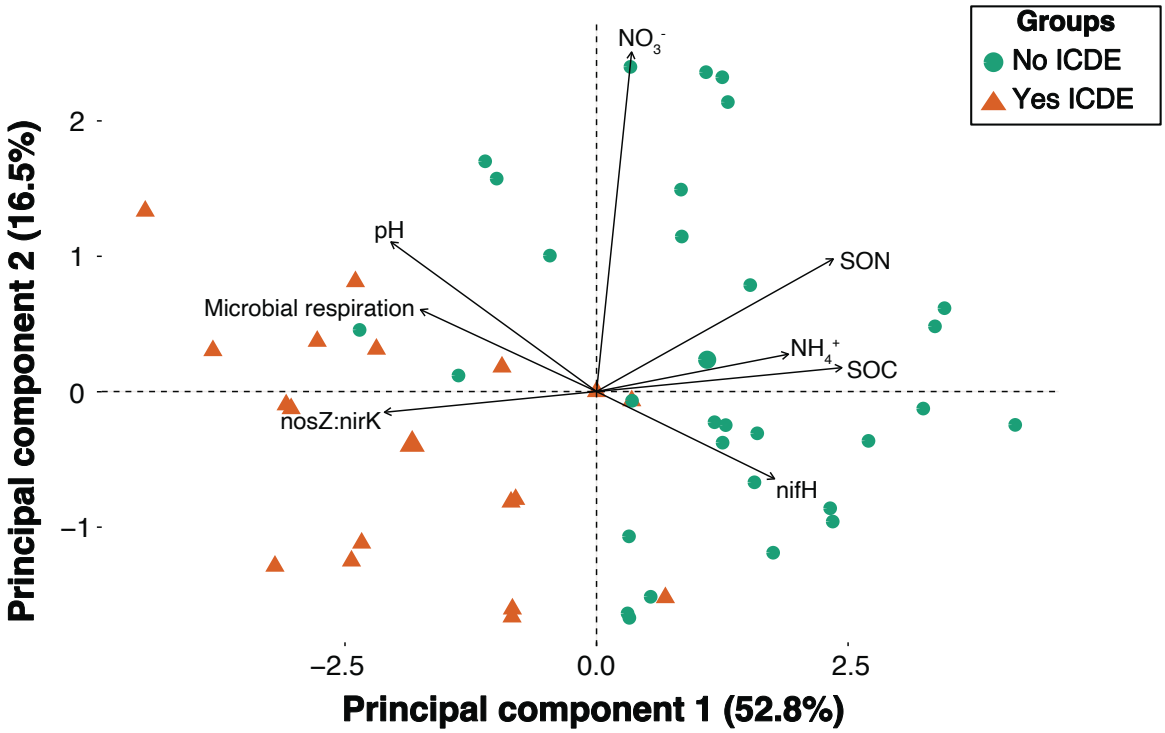

Figure 4.5. Loading and biplot for PCA. Orange triangles correspond to Yes ICDE soils, whereas green circles correspond to No ICDE soils. See Appendix 3 Table 1 for n-values for each variable.

Table 4.2. Predictor variables, their associated p-values from individual ANOVAs, and loadings for each variable for principal components (PCs) 1-4. Each loading has a corresponding rank associated with it, and ranks are ordered by the loading absolute values, or magnitude of loading. Ranks are listed next to their loading value in parentheses. Variables are listed in the table in order of significant differences among soils, from most significant difference to least significant difference. Significant association with ICDE for each ranking were calculated using two-sample t-tests (Appendix 3 Figure 1). The first three predictors were all direct measures of soil properties that were measured prior to the incubation experiments. The last five predictors are all Δ values for +OC:Control soil properties and N-cycling gene abundances.

Predictor	**p-value (from ANOVAs)**	**PC1: rank (loading)**	**PC2: rank (loading)**	**PC3: rank (loading)**	**PC4: rank (loading)**
Significant association with Yes/No ICDE?	NA	**Yes** $p < 0.0001$	**No** $p = 0.07$	**No** $p = 0.74$	**No** $p = 0.09$
SON	< 0.0001 ***	**2 (0.43)**	**3 (0.32)**	6 (-0.20)	6 (-0.08)
SOC	< 0.0001 ***	**1 (0.44)**	7 (0.06)	5 (-0.21)	**2 (0.35)**
pH	< 0.0001 ***	**4 (-0.37)**	**2 (0.36)**	**4 (-0.25)**	**4 (-0.24)**
Δ Microbial respiration	< 0.0001 ***	7(-0.32)	5 (0.20)	**1 (0.63)**	5 (-0.17)
Δ Soil NO_3^-	< 0.0001 ***	8 (0.06)	**1 (0.82)**	7 (0.18)	**3 (0.25)**
Δ Soil NH_4^+	< 0.0001 ***	5 (0.35)	6 (0.09)	8 (-0.05)	**1 (-0.84)**
Δ nosZ:nirK	0.095	**3 (-0.38)**	8 (-0.05)	**3 (-0.30)**	7 (-0.03)
Δ nifH	0.148	6 (0.32)	**4 (-0.21)**	**2 (0.57)**	8 (0.01)

Further, t-tests comparing Yes vs. No ICDE coordinates for the different soils illustrated there was a significant association with ICDE for PC1, but not for PC2 (Table 4.2). However, the association with ICDE for PC2 was borderline significant ($p = 0.07$). Plots associated with t-tests can be found in Appendix 3 (Appendix 3 Figure 1). From PC1, the loadings indicate that Yes ICDE soils associated most strongly with low SOC, low SON, high Δ nosZ:nirK, and high soil pH (Table 4.2). The Yes ICDE soils also associated with low Δ soil NH_4^+, low Δ nifH abundance, and high Δ microbial respiration on PC1, but associated very weakly with Δ soil NO_3^- (Table 4.2). However, Δ soil NO_3^- was the most strongly loaded variable on PC2, and the Yes ICDE soils associated most strongly with low Δ soil NO_3^- (Figure 4.5, Table 4.2).

5. Discussion

I sought to stimulate N_2O consumption in diverse soils by adding OC to manipulate the reducing potential of these soils. I hypothesized that providing excess electron donors to soil microbes would stimulate $N_2O \rightarrow N_2$ reduction by inducing denitrifiers to use N_2O as a terminal electron acceptor (Firestone and Davidson 1989, Hedin et al. 1998, Ostrom et al. 2002). My hypothesis was supported, in that amending soils with OC stimulated N_2O consumption in most of the soils tested (six out of eight soils). However, the joint response of consumption and N_2O emission differed among soils. Three soils showed ICDE while other soils increased N_2O consumption, but also increased N_2O emissions (Figure 4.2). My data on various soil and microbial genetic properties provide some insights into the dynamics of N_2O metabolism that I observed. With an improved understanding, I hope this and future studies following this approach will enable better prediction of a soil's potential for N_2O consumption, based on its properties and microbial gene abundances. Net uptake of N_2O from the atmosphere has been documented in gas flux chamber studies for decades (Chapius-Lardy 2007, Schlesinger 2013,

Almaraz et al. 2020), but only recently has N_2O consumption been recognized as a force that regulates net N_2O emissions (Shan et al. 2021). My findings likely have implications for explaining these field-scale observations.

My interpretation of ICDE rests heavily on the concept of soil redox dynamics, both at the bulk soil scale and across soil anoxic microsites. From a bulk redox perspective, the energetic metabolism of soil microbes requires both electron donors (usually some form of OC) and electron acceptors, such as O_2, NO_3^-, MnO_2, Fe^{2+}, SO_4^{2-}, CO_2, etc. These electron acceptors exist on a "ladder" that ranks their energetic favorability from greatest to least, with the oxidation of O_2 being the most energetically favorable and the oxidation of CO_2 being the least energetically favorable (Hedin et al. 1998). A given soil can range from being electron donor limited (typically oxic environments) to electron acceptor limited (typically anoxic environments). Interestingly, N_2O reduction falls between NO_3^- and MnO_2 reduction on the redox ladder.

Because of this sequencing, I originally hypothesized that further additions of OC (e.g., electron donors) would both drive O_2 consumption, creating a greater soil volume where N_2O reduction could occur (Wu et al. 2013, Sihi et al. 2020), and also stimulate the metabolism of denitrifiers directly by adding substrates known to be used by those bacteria. Decreased N_2O emissions in response to OC-amendment has been observed in previous studies. For example, Cavigelli & Robertson (2001) found that the N_2O:N_2 production ratio for pure cultures of denitrifying bacteria fell as the supply ratio of OC:NO_3^- became greater. Likewise, along a redox gradient at a soil-stream interface, Hedin et al. (1998) saw C additions lead to lower N_2O emissions. However, I now hypothesize that adding OC to soils might not increase N_2O consumption *unless* the added electron donors expand anoxic regions in the soil where N_2O consumption is thermodynamically favorable. I predict that such an enhancement of N_2O

consumption will depend on the physical and biogeochemical features of the soil such as aggregation, pore structure, and microscale hotspots of respiration.

5.1 N_2O consumption rate increased in response to +OC treatment

Gross N_2O consumption rate increased in response to +OC treatment in most but not all the soils tested (Figure 4.2). Differences in redox potential among the soils may have contributed to some of the differential emission and consumption behaviors I observed (Senbayram et al. 2012, Wang et al. 2021b, Cheng et al. 2017, Włodarczyk et al. 2021). One possible explanation is that the soils that showed ICDE became sufficiently reducing in response to OC-amendment. If the OC-amendment enabled electron donor supply to exceed electron acceptor NO_3^- supply, the soil microbes would have the redox capacity to fully deplete the NO_3^- pool for energy metabolism (Taylor and Townsend 2010). As a result, microbes would need to use N_2O as an alternative electron acceptor, which would stimulate complete denitrification and consequently, ICDE. Previous work also supports this explanation. Under specific OC amendments, soil NO_3^- concentration and N_2O emissions have been shown to decrease, indicating more complete denitrification (Hill et al. 2000, Gillam et al. 2007, Dodla et al. 2008, Senbayram et al. 2012, Lan et al. 2017, Wang et al. 2021b). Furthermore, the differential balance of electron donors and acceptors among the soils I tested is likely regulated by other features in the soil (Neubauer et al. 2005, Gu and Riley 2010, Sutton-Grier et al. 2011, Jamali et al. 2016). The soils that showed ICDE differed notably from the soils that did not in specific properties (Figure 4.2, Figure 4.5). I argue in the next section that these properties contribute to why soils did or did not show ICDE.

5.2 Assessing soil properties to predict ICDE

From a management perspective, it would be ideal to predict which soils are more likely to respond to +OC treatment with ICDE. In general, the soils with ICDE had markedly lower

SOM, and in response to OC-amendment, had greater depletion of soil NO_3^-, larger increases in soil microbial respiration, and bigger increases in the ratio of nosZ:nirK genes (Figure 4.2). These findings support my initial hypothesis, N_2O consumption is limited by reductants, and it supports my follow-up hypothesis, that for C additions to induce ICDE, the additions need to expand the N_2O reducing regions in the soil without over-stimulating N_2O production via denitrification. I posit the soils that showed ICDE were OM-limited, and the OC-amendment induced heightened microbial activity, and altered the soil redox environment in a way that both drove net NO_3^- consumption and increased gross N_2O consumption (Figures 4.2 and 4.3). This notion is supported by the PCA, which heavily weighted SOC, SON, microbial respiration, and nosZ:nirK with the soils that showed ICDE along PC1 (Figure 4.5), and other studies (Miller et al. 2009, Buchen et al. 2019, Guo et al. 2020, Gallarotti et al. 2021, Voigt et al. 2021). The significant role of pH in affecting N_2O consumption, as revealed in PC1 and the pH one-way ANOVA, is consistent with the effect of high pH being more favorable for NosZ enzyme activity (Figures 4.3 and 4.5; Richardson et al. 2009, Blum et al 2018).

Soils that did not show ICDE were characterized by high SOM, and in response to OC-amendment, had variable changes in soil NO_3^- and in soil microbial respiration, and little change in the ratio of nosZ:nirK genes, findings that were supported in individual one-way ANOVAs (Figure 4.3) and in the cumulative PCA (Figure 4.5). These findings also support my hypothesis, showing ICDE hinged on electron donor-acceptor balance. For example, the Minnesota cornfield and the Urban lawn, the soils with the first and third highest initial soil NO_3^- concentrations, respectively, both increased N_2O consumption, increased N_2O emissions, and increased soil NO_3^- concentrations following OC-amendment (Figure 4.2, Figure 4.3). It is possible that the OC additions helped to create suboxic and anoxic microsites in these soils to host incomplete and

complete denitrification, which perhaps prompted nitrification in more aerobic areas of the soil to fulfill metabolic demand for electron acceptors (Stevenson et al. 2011, Wu et al. 2018, Surey et al. 2020). Microbes in soils with high NO_3^- concentrations have been shown to suppress clade I nosZ transcription, which could help explain why the Minnesota cornfield and Urban lawn soils had increased NO_3^- concentrations following OC-amendment (Hallin et al. 2018). This could also help explain why all soils that did not show ICDE had less pronounced shifts in abundances of nosZ and nirK compared to the soils that showed ICDE (Figure 4.2, Hallin et al. 2018). Furthermore, all the soils that did not show ICDE tended to have higher initial soil NH_4^+ concentrations (Figure 4.4). These soils would have had enhanced capacity for nitrification in oxic soil loci, and consequently, less NO_3^- limitation to denitrification, which was demonstrated by those soils having generally higher NO_3^- concentrations following OC-amendment (Figure 4.3, Figure 4.4, Darrah et al. 1987, Jiang et al. 2011). Lastly, all the soils that did not show ICDE had markedly higher SOM compared to the soils that showed ICDE (Figure 4.2). When soil microbes are less resource limited, both by electron donors and acceptors, they do not need to be as efficient metabolically, which can result in more denitrification overall (Senbayram et al. 2012, Scheer et al. 2020, Surey et al. 2020). This may explain why multiple soils had increased N_2O consumption *and* increased N_2O emissions.

5.3 Carbon limitation threshold to ICDE

From my findings, I present a conceptual framework to explain how +OC treatment stimulated ICDE (Figure 4.6). Broadly, to stimulate gross N_2O consumption, soil microbes must surpass a C-limitation threshold to induce sufficient anoxia for N_2O consumption to occur. I posit this is how SOC-poor soils showed ICDE in my soil incubations. Conversely, the other soils that did not show ICDE had higher SOC and might not have been (as) reductant limited. As

a result, those soils might have been less responsive to the OC-amendment (Figure 4.2, Figure 4.6).

How might the soils that did not show ICDE respond to an even larger OC-amendment? I hypothesize that the electron donor supply must create sufficiently reducing conditions to show ICDE. If supported, this suggests that the soils that did not show ICDE were still reductant (e.g., OC) limited. This raises the question, where does the OC-limitation threshold lie for different soils, and how can we predict it? What other variables mediate this threshold? Being able to identify the amount of OC a soil requires to induce ICDE, and if in fact that soil is a good candidate for +OC treatment (e.g., what is its aggregation potential?) could be useful for screening soils as targets for N_2O consumption management.

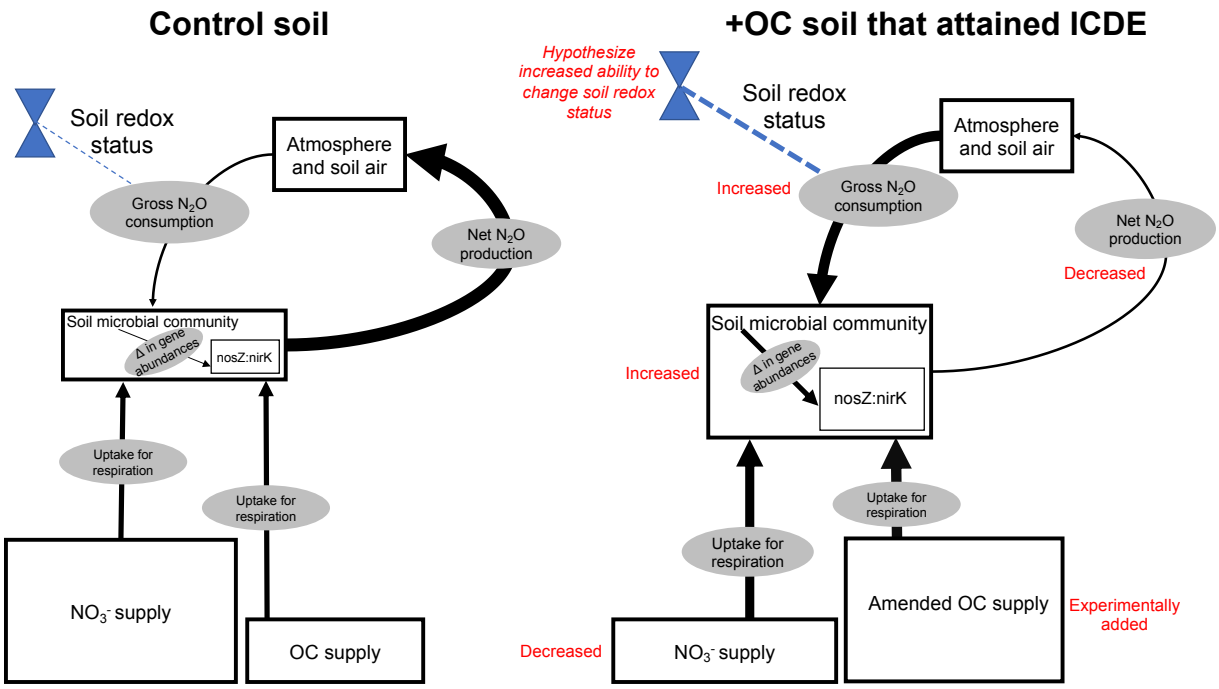

Figure 4.6. Conceptual diagram compare-contrasting a Control soil to its OC-amended counterpart that showed ICDE. Boxes correspond to pools, arrows correspond to fluxes, and ovals describe the fluxes. Blue valves correspond to the ability for a soil to change its redox status (mediated by aggregation, pore structure, microscale hotspots of respiration, etc.). Red text next to pools, fluxes, or valves provide details for how they change in response to +OC treatment or provide a hypothesized change. I hypothesize soils that showed ICDE overcame an OC-limitation and were freed from electron donor limitations to increase microbial activity and subsequently change the soil redox environment. These changes contributed to increased transcription of nosZ relative to nirK, thus driving an increase in gross N_2O consumption. The blue dotted line illustrates the capacity in the soil to enable N_2O consumption, and the thickness of the line indicates if the capacity is high or low. I posit the soils that showed ICDE had high capacity to expand regions of anoxia where N_2O consumption was thermodynamically favorable. The sizes of pools and fluxes are not to scale, but rather illustrate general changes in pool sizes or process rates.

5.4 Future work

As with many soil assays, there is debate about the nature of gross rates of gas metabolism that is quantified by isotope pool dilution (Wen et al. 2016). Future work could reveal much about how soil gas concentration gradients are maintained, and what "communication" of information is revealed through isotope additions to jar headspace. I measured net N_2O emissions, which accounts for the N_2O that gets emitted from the soil into the

jar headspace, but clearly there can be both production and consumption of gases that are not directly quantified in this assay. For example, produced N_2O could get trapped in a soil pore and never diffuse to the jar headspace, or it could be retained in an anoxic microsite. As a result, emitted N_2O could get consumed in the same anoxic microsite it never leaves, or intriguingly, it could get produced and consumed by the same soil microbe (Lycus et al. 2018). Thus, it is possible I could be underestimating both gross N_2O production and consumption. Wen et al. (2016) argue that gas flow soil cores better account for anoxic microsite N_2O production and consumption than isotope pool dilution. However, I performed the pool dilution assay in a closed system for 48 hrs, which I argue is sufficient time for $^{15}N_2O$ label to diffuse throughout the soil and enable measuring most of the gross production and consumption (von Fischer and Hedin 2002). Addressing these methodological discussions will be necessary for understanding what drives the balance between N_2O production and consumption in soils (Yang et al. 2016).

It also remains unresolved how the +OC treatment impacts other soil microbial community responses. Specifically, I did not examine how amending soils with OC affected CH_4 emissions, or if CO_2 emissions from microbial respiration offset N_2O consumption (Li et al. 2005, Zaehle et al. 2011, Zhou et al. 2017). While I expect that amending soils with my +OC treatment would stimulate microbial respiration, it would be ideal if the +OC treatment also stimulated an ICDE-induced net N_2O reduction to offset any CO_2 or CH_4 emissions from +OC treatment. However, addressing that question directly will require follow-up work. Additionally, as we continue to explore the potential of using organic amendments to decrease net N_2O emissions, it will be important to better understand which specific additions are most effective at reducing net emissions. Studies have illustrated that certain OC amendments can increase net N_2O emissions (Guenet et al. 2020). To use these amendments successfully, it will be crucial to

better understand which organic amendments to use or avoid on different soils, as it is possible amendments may differ in their efficacy by soil type (Guenet et al. 2020). Managing N_2O consumption could be a frontier for GHG management, particularly in agroecosystems. These systems are projected to become an increasingly important source of GHGs as the human population grows, so developing strategies to curtail their emissions while sustainably feeding people will be instrumental for the future (Battye et al. 2017, Bakken and Frostegård 2020, Kanter et al. 2020a).

CHAPTER 4 REFERENCES

Almaraz, M., Wong, M. Y., & Yang, W. H. (2020). Looking back to look ahead: a vision for soil denitrification research. *Ecology*, *101*(1), 1–10. https://doi.org/10.1002/ecy.2917

Bakken, L. R., & Frostegård, Å. (2017). Sources and sinks for N2O, can microbiologist help to mitigate N2O emissions? *Environmental Microbiology*, *19*(12), 4801–4805. https://doi.org/10.1111/1462-2920.13978

Bakken, L. R., & Frostegård, Å. (2020). Emerging options for mitigating N2O emissions from food production by manipulating the soil microbiota. *Current Opinion in Environmental Sustainability*, *47*, 89–94. https://doi.org/10.1016/j.cosust.2020.08.010

Barrett, M., Khalil, M. I., Jahangir, M. M. R., Lee, C., Cardenas, L. M., Collins, G., … O'Flaherty, V. (2016). Carbon amendment and soil depth affect the distribution and abundance of denitrifiers in agricultural soils. *Environmental Science and Pollution Research*, *23*(8), 7899–7910. https://doi.org/10.1007/s11356-015-6030-1

Battye, W., Aneja, V. P., & Schlesinger, W. H. (2017). Is nitrogen the next carbon? *Global Biogeochemical Cycles*, *30*, 1000–1014. https://doi.org/10.1002/eft2.235

Blum, J. M., Su, Q., Ma, Y., Valverde-Pérez, B., Domingo-Félez, C., Jensen, M. M., & Smets, B. F. (2018). The pH dependency of N-converting enzymatic processes, pathways and microbes: effect on net N2O production. *Environmental Microbiology*, *20*(5), 1623–1640. https://doi.org/10.1111/1462-2920.14063

Borchard, N., Schirrmann, M., Cayuela, M. L., Kammann, C., Wrage-Mönnig, N., Estavillo, J. M., … Novak, J. (2019). Biochar, soil and land-use interactions that reduce nitrate leaching and N2O emissions: A meta-analysis. *Science of the Total Environment*, *651*, 2354–2364. https://doi.org/10.1016/j.scitotenv.2018.10.060

Bowling, D. R., Burns, S. P., Conway, T. J., Monson, R. K., & White, J. W. C. (2005). Extensive observations of CO2 carbon isotope content in and above a high-elevation subalpine forest. *Global Biogeochemical Cycles*, *19*(3), 1–15. https://doi.org/10.1029/2004GB002394

Buchen, C., Roobroeck, D., Augustin, J., Behrendt, U., Boeckx, P., & Ulrich, A. (2019). High N 2 O consumption potential of weakly disturbed fen mires with dissimilar denitrifier community structure. *Soil Biology and Biochemistry*, *130*(July 2018), 63–72. https://doi.org/10.1016/j.soilbio.2018.12.001

Butterbach-Bahl, K., & Dannenmann, M. (2011). Denitrification and associated soil N2O emissions due to agricultural activities in a changing climate. *Current Opinion in Environmental Sustainability*, *3*(5), 389–395. https://doi.org/10.1016/j.cosust.2011.08.004

Cavigelli, M. A., & Robertson, G. P. (2001). Role of denitrifier diversity in rates of nitrous oxide consumption in a terrestrial ecosystem. *Soil Biology and Biochemistry*, *33*(3), 297–310. https://doi.org/10.1016/S0038-0717(00)00141-3

Cavigelli, M. A., & Robertson, G. P. (2000). The functional significance of denitrifier community composition in a terrestrial ecosystem. *Ecology*, *81*(5), 1402–1414. https://doi.org/10.1890/0012-9658(2000)081[1402:TFSODC]2.0.CO;2

Chapuis-Lardy, L., Wrage, N., Metay, A., Chotte, J. L., & Bernoux, M. (2007). Soils, a sink for N2O? A review. *Global Change Biology*, *13*(1), 1–17. https://doi.org/10.1111/j.1365-2486.2006.01280.x

Chee-Sanford, J. C., Connor, L., Krichels, A., Yang, W. H., & Sanford, R. A. (2020). Hierarchical detection of diverse Clade II (atypical) nosZ genes using new primer sets for classical- and multiplex PCR array applications. *Journal of Microbiological Methods*, *172*(March), 105908. https://doi.org/10.1016/j.mimet.2020.105908

Conthe, M., Lycus, P., Arntzen, M., Ramos da Silva, A., Frostegård, Å., Bakken, L. R., … van Loosdrecht, M. C. M. (2019). Denitrification as an N2O sink. *Water Research*, *151*, 381–387. https://doi.org/10.1016/j.watres.2018.11.087

Conthe, M., Parchen, C., Stouten, G., Kleerebezem, R., & van Loosdrecht, M. C. M. (2018). O2 versus N2O respiration in a continuous microbial enrichment. *Applied Microbiology and Biotechnology*, *102*(20), 8943–8950. https://doi.org/10.1007/s00253-018-9247-3

Darrah, P. R., Nye, P. H., & White, R. E. (1987). The effect of high solute concentrations on nitrification rates in soil. *Plant and Soil*, *97*(1), 37–45. https://doi.org/10.1007/BF02149821

Domeignoz-Horta, L. A., Spor, A., Bru, D., Breuil, M. C., Bizouard, F., Léonard, J., & Philippot, L. (2015). The diversity of the N2O reducers matters for the N2O:N2 denitrification end-product ratio across an annual and a perennial cropping system. *Frontiers in Microbiology*, *6*(SEP). https://doi.org/10.3389/fmicb.2015.00971

Duan, P., Zhang, Q., Zhang, X., & Xiong, Z. (2019). Mechanisms of mitigating nitrous oxide emissions from vegetable soil varied with manure, biochar and nitrification inhibitors. *Agricultural and Forest Meteorology*, *278*(December 2018), 107672. https://doi.org/10.1016/j.agrformet.2019.107672

Firestone, M. K., & Davidson, E. A. (1989). Microbiologial Basis of NO and N20 production and consumption in soil. *Exchange of Trace Gases between Terrestrial Ecosystems and the Atmosphere*, (January 1989), 7–21. https://doi.org/10.1017/CBO9781107415324.004

Gallarotti, N., Barthel, M., Verhoeven, E., Pereira, E. I. P., Bauters, M., Baumgartner, S., … Six, J. (2021). In-depth analysis of N2O fluxes in tropical forest soils of the Congo Basin combining isotope and functional gene analysis. *ISME Journal*. https://doi.org/10.1038/s41396-021-01004-x

Gillam, K. M., Zebarth, B. J., & Burton, D. L. (2008). Nitrous oxide emissions from denitrification and the partitioning of gaseous losses as affected by nitrate and carbon addition and soil aeration. *Canadian Journal of Soil Science*, *88*(2), 133–143. https://doi.org/10.4141/CJSS06005

Groffman, P. M., Altabet, M. a., Bohlke, J. K., Butterbach-Bahl, K., David, M. B., Firestone, M. K., … Voyteck, M. a. (2006). Methods for Measuring Denitrification : *Ecological Applications*, *16*(December), 2091–2122.

Guenet, B., Gabrielle, B., Chenu, C., Arrouays, D., Balesdent, J., Bernoux, M., … Pellerin, S. (2021). Can N 2 O emissions offset the benefits from soil organic carbon storage ?, (August 2020), 237–256. https://doi.org/10.1111/gcb.15342

Guo, B., Zheng, X., Yu, J., Ding, H., Pan, B., Luo, S., & Zhang, Y. (2020). Dissolved organic carbon enhances both soil N2O production and uptake. *Global Ecology and Conservation*, *24*, e01264. https://doi.org/10.1016/j.gecco.2020.e01264

Hallin, S., Philippot, L., Löffler, F. E., Sanford, R. A., & Jones, C. M. (2018). Genomics and Ecology of Novel N 2 O-Reducing Microorganisms. *Trends in Microbiology*, *26*(1), 43–55. https://doi.org/10.1016/j.tim.2017.07.003

Hedin, L. O., Von Fischer, J. C., Ostrom, N. E., Kennedy, B. P., Brown, M. G., & Philip Robertson, G. (1998). Thermodynamic constraints on nitrogen transformations and other

biogeochemical processes at soil-stream interfaces. *Ecology*, *79*(2), 684–703. https://doi.org/10.1890/0012-9658(1998)079[0684:TCONAO]2.0.CO;2

Hellman, M., Bonilla-Rosso, G., Widerlund, A., Juhanson, J., & Hallin, S. (2019). External carbon addition for enhancing denitrification modifies bacterial community composition and affects CH4 and N2O production in sub-arctic mining pond sediments. *Water Research*, *158*(2), 22–33. https://doi.org/10.1016/j.watres.2019.04.007

Hill, A. R., Devito, K. J., & Campagnolo, S. (2000). Subsurface denitrification in a forest riparian zone : Interactions between hydrology and supplies of nitrate and organic carbon, (Hill 1996), 193–223.

Houser, M., & Stuart, D. (2020). An accelerating treadmill and an overlooked contradiction in industrial agriculture: Climate change and nitrogen fertilizer. *Journal of Agrarian Change*, *20*(2), 215–237. https://doi.org/10.1111/joac.12341

Jamali, H., Quayle, W., Scheer, C., Rowlings, D., & Baldock, J. (2016). Effect of soil texture and wheat plants on N2O fluxes: A lysimeter study. *Agricultural and Forest Meteorology*, *223*(2), 17–29. https://doi.org/10.1016/j.agrformet.2016.03.022

Jiang, X., Ma, Y., Yuan, J., Wright, A. L., & Li, H. (2011). Soil particle surface electrochemical property effects on abundance of ammonia-oxidizing bacteria and ammonia-oxidizing archaea, NH4+ activity, and net nitrification in an acid soil. *Soil Biology and Biochemistry*, *43*(11), 2215–2221. https://doi.org/10.1016/j.soilbio.2011.07.014

Jones, C. M., Graf, D. R. H., Bru, D., Philippot, L., & Hallin, S. (2013). The unaccounted yet abundant nitrous oxide-reducing microbial community: A potential nitrous oxide sink. *ISME Journal*, *7*(2), 417–426. https://doi.org/10.1038/ismej.2012.125

Jones, C. M., Spor, A., Brennan, F. P., Breuil, M. C., Bru, D., Lemanceau, P., … Philippot, L. (2014). Recently identified microbial guild mediates soil N2O sink capacity. *Nature Climate Change*, *4*(9), 801–805. https://doi.org/10.1038/nclimate2301

[a]Kanter, D. R., Del Grosso, S., Scheer, C., Pelster, D. E., & Galloway, J. N. (2020). Why future nitrogen research needs the social sciences. *Current Opinion in Environmental Sustainability*, *47*, 54–60. https://doi.org/10.1016/j.cosust.2020.07.002

[b]Kanter, D. R., Ogle, S. M., & Winiwarter, W. (2020). Building on Paris: integrating nitrous oxide mitigation into future climate policy. *Current Opinion in Environmental Sustainability*, *47*, 7–12. https://doi.org/10.1016/j.cosust.2020.04.005

Kuypers, M. M. M., Marchant, H. K., & Kartal, B. (2018). The microbial nitrogen-cycling network. *Nature Reviews Microbiology*, *16*(5), 263–276. https://doi.org/10.1038/nrmicro.2018.9

Lam, S. K., Suter, H., Mosier, A. R., & Chen, D. (2017). Using nitrification inhibitors to mitigate agricultural N2O emission: a double-edged sword? *Global Change Biology*, *23*(2), 485–489. https://doi.org/10.1111/gcb.13338

Lazcano, C., Zhu-Barker, X., & Decock, C. (2021). Effects of organic fertilizers on the soil microorganisms responsible for n2o emissions: A review. *Microorganisms*, *9*(5), 1–18. https://doi.org/10.3390/microorganisms9050983

Li, C., Frolking, S., & Butterbach-Bahl, K. (2005). Carbon sequestration in arable soils is likely to increase nitrous oxide emissions, offsetting reductions in climate radiative forcing. *Climatic Change*, *72*(3), 321–338. https://doi.org/10.1007/s10584-005-6791-5

Lycus, P., Soriano-Laguna, M. J., Kjos, M., Richardson, D. J., Gates, A. J., Milligan, D. A., … Bakken, L. R. (2018). A bet-hedging strategy for denitrifying bacteria curtails their release

of N2O. *Proceedings of the National Academy of Sciences of the United States of America*, *115*(46), 11820–11825. https://doi.org/10.1073/pnas.1805000115

McMillan, A. M. S., Pal, P., Phillips, R. L., Palmada, T., Berben, P. H., Jha, N., … Luo, J. (2016). Can pH amendments in grazed pastures help reduce N2O emissions from denitrification? - The effects of liming and urine addition on the completion of denitrification in fluvial and volcanic soils. *Soil Biology and Biochemistry*, *93*, 90–104. https://doi.org/10.1016/j.soilbio.2015.10.013

Miller, M. N., Zebarth, B. J., Dandie, C. E., Burton, D. L., Goyer, C., & Trevors, J. T. (2009). Influence of Liquid Manure on Soil Denitrifier Abundance, Denitrification, and Nitrous Oxide Emissions. *Soil Science Society of America Journal*, *73*(3), 760–768. https://doi.org/10.2136/sssaj2008.0059

Mitchell, D. C., Castellano, M. J., Sawyer, J. E., & Pantoja, J. (2013). Cover Crop Effects on Nitrous Oxide Emissions: Role of Mineralizable Carbon. *Soil Science Society of America Journal*, *77*(5), 1765–1773. https://doi.org/10.2136/sssaj2013.02.0074

Morley, N., & Baggs, E. M. (2010). Carbon and oxygen controls on N2O and N2 production during nitrate reduction. *Soil Biology and Biochemistry*, *42*(10), 1864–1871. https://doi.org/10.1016/j.soilbio.2010.07.008

Neubauer, S. C., Givler, K., Valentine, S. K., & Megonigal, J. P. (2005). Seasonal patterns and plant-mediated controls of subsurface wetland biogeochemistry. *Ecology*, *86*(12), 3334–3344. https://doi.org/10.1890/04-1951

Ostrom, N. E., Hedin, L. O., Von Fischer, J. C., & Robertson, G. P. (2002). Nitrogen transformations and NO3- removal at a soil-stream interface: A stable isotope approach. *Ecological Applications*, *12*(4), 1027–1043. https://doi.org/10.1890/1051-0761(2002)012[1027:ntanra]2.0.co;2

Ostrom, N. E., & Ostrom, P. H. (2017). Mining the isotopic complexity of nitrous oxide: a review of challenges and opportunities. *Biogeochemistry*, *132*(3), 359–372. https://doi.org/10.1007/s10533-017-0301-5

Reay, D. S., Davidson, E. a., Smith, K. a., Smith, P., Melillo, J. M., Dentener, F., & Crutzen, P. J. (2012). Global agriculture and nitrous oxide emissions. *Nature Climate Change*, *2*(6), 410–416. https://doi.org/10.1038/nclimate1458

Richardson, D., Felgate, H., Watmough, N., Thomson, A., & Baggs, E. (2009). Mitigating release of the potent greenhouse gas N2O from the nitrogen cycle - could enzymic regulation hold the key? *Trends in Biotechnology*, *27*(7), 388–397. https://doi.org/10.1016/j.tibtech.2009.03.009

Sánchez-Martín, L., Vallejo, A., Dick, J., & M Skiba, U. (2008). The influence of soluble carbon and fertilizer nitrogen on nitric oxide and nitrous oxide emissions from two contrasting agricultural soils. *Soil Biology and Biochemistry*, *40*(1), 142–151. https://doi.org/10.1016/j.soilbio.2007.07.016

Sanford, R. A., Wagner, D. D., Wu, Q., Chee-Sanford, J. C., Thomas, S. H., Cruz-García, C., … Löffler, F. E. (2012). Unexpected nondenitrifier nitrous oxide reductase gene diversity and abundance in soils. *Proceedings of the National Academy of Sciences of the United States of America*, *109*(48), 19709–19714. https://doi.org/10.1073/pnas.1211238109

Scheer, C., Fuchs, K., Pelster, D. E., & Butterbach-Bahl, K. (2020). Estimating global terrestrial denitrification from measured N2O:(N2O + N2) product ratios. *Current Opinion in Environmental Sustainability*, *47*, 72–80. https://doi.org/10.1016/j.cosust.2020.07.005

Schlesinger, W. H. (2013). An estimate of the global sink for nitrous oxide in soils. *Global Change Biology*, *19*(10), 2929–2931. https://doi.org/10.1111/gcb.12239

Senbayram, M., Chen, R., Budai, A., Bakken, L., & Dittert, K. (2012). N 2O emission and the N 2O/(N 2O+N 2) product ratio of denitrification as controlled by available carbon substrates and nitrate concentrations. *Agriculture, Ecosystems and Environment*, *147*(1), 4–12. https://doi.org/10.1016/j.agee.2011.06.022

Shan, J., Sanford, R. A., Chee-Sanford, J., Ooi, S. K., Löffler, F. E., Konstantinidis, K. T., & Yang, W. H. (2021). Beyond denitrification: The role of microbial diversity in controlling nitrous oxide reduction and soil nitrous oxide emissions. *Global Change Biology*, (October 2020), 1–15. https://doi.org/10.1111/gcb.15545

Sihi, D., Davidson, E. A., & Savage, K. E. (2020). Simultaneous numerical representation of soil microsite production and consumption of carbon dioxide , methane , and nitrous oxide using probability distribution functions, (August 2019), 200–218. https://doi.org/10.1111/gcb.14855

Smith, K. A. (2017). Changing views of nitrous oxide emissions from agricultural soil: key controlling processes and assessment at different spatial scales. *European Journal of Soil Science*, *68*(2), 137–155. https://doi.org/10.1111/ejss.12409

Stein, L. Y. (2020). The Long-Term Relationship between Microbial Metabolism and Greenhouse Gases. *Trends in Microbiology*, *28*(6), 500–511. https://doi.org/10.1016/j.tim.2020.01.006

Stevenson, B. A., Schipper, L. A., McGill, A., & Clark, D. (2011). Denitrification and Availability of Carbon and Nitrogen in a Well-drained Pasture Soil Amended with Particulate Organic Carbon. *Journal of Environmental Quality*, *40*(3), 923–930. https://doi.org/10.2134/jeq2010.0463

Stuchiner, E. R., Weller, Z. D., & Fischer, J. C. (2020). An approach for calibrating laser-based N 2 O isotopic analyzers for soil biogeochemistry research . *Rapid Communications in Mass Spectrometry*, (June 2020), 1–14. https://doi.org/10.1002/rcm.8978

Subbarao, G., Ito, O., Sahrawat, K., Berry, W., Nakahara, K., Ishikawa, T., … Rao, I. (2006). Scope and strategies for regulation of nitrification in agricultural systems - Challenges and opportunities. *Critical Reviews in Plant Sciences*, *25*(4), 303–335. https://doi.org/10.1080/07352680600794232

Sutton-Grier, A. E., Keller, J. K., Koch, R., Gilmour, C., & Megonigal, J. P. (2011). Electron donors and acceptors influence anaerobic soil organic matter mineralization in tidal marshes. *Soil Biology and Biochemistry*, *43*(7), 1576–1583. https://doi.org/10.1016/j.soilbio.2011.04.008

Taylor, P. G., & Townsend, A. R. (2010). Stoichiometric control of organic carbon – nitrate relationships from soils to the sea. *Nature*, *464*(April), 1178–1181. https://doi.org/10.1038/nature08985

Trivedi, P., He, Z., Van Nostrand, J. D., Albrigo, G., Zhou, J., & Wang, N. (2012). Huanglongbing alters the structure and functional diversity of microbial communities associated with citrus rhizosphere. *ISME Journal*, *6*(2), 363–383. https://doi.org/10.1038/ismej.2011.100

Wang, B., Brewer, P. E., Shugart, H. H., Lerdau, M. T., & Allison, S. D. (2019). Soil aggregates as biogeochemical reactors and implications for soil–atmosphere exchange of greenhouse gases—A concept. *Global Change Biology*, *25*(2), 373–385. https://doi.org/10.1111/gcb.14515

[a]Wang, C., Amon, B., Schulz, K., & Mehdi, B. (2021). Factors That Influence Nitrous Oxide Emissions from Agricultural Soils as Well as Their Representation in Simulation Models: A Review. *Agronomy*, *11*(4), 770. https://doi.org/10.3390/agronomy11040770

[b]Wang, J., Chen, Z., Xu, C., Elrys, A. S., Shen, F., Cheng, Y., & Chang, S. X. (2021). Organic amendment enhanced microbial nitrate immobilization with negligible denitrification nitrogen loss in an upland soil. *Environmental Pollution*, *288*(3), 117721. https://doi.org/10.1016/j.envpol.2021.117721

Wen, Y., Chen, Z., Dannenmann, M., Carminati, A., Willibald, G., Kiese, R., … Corre, M. D. (2016). Disentangling gross N2O production and consumption in soil. *Scientific Reports*, *6*(October), 1–8. https://doi.org/10.1038/srep36517

Włodarczyk, T., Brzezińska, M., Stępniewski, W., & Majewska, U. (2021). Sequence and preference in the use of electron acceptors in flooded agricultural soils, (3), 61–71. https://doi.org/10.31545/intagr/132372

Wu, D., Dong, W., Oenema, O., Wang, Y., Trebs, I., & Hu, C. (2013). N2O consumption by low-nitrogen soil and its regulation by water and oxygen. *Soil Biology and Biochemistry*, *60*, 165–172. https://doi.org/10.1016/j.soilbio.2013.01.028

Wu, D., Wei, Z., Well, R., Shan, J., Yan, X., Bol, R., & Senbayram, M. (2018). Straw amendment with nitrate-N decreased N2O/(N2O+N2) ratio but increased soil N2O emission: A case study of direct soil-born N2 measurements. *Soil Biology and Biochemistry*, *127*(October), 301–304. https://doi.org/10.1016/j.soilbio.2018.10.002

Yang, W. H., Teh, Y. A., & Silver, W. L. (2011). A test of a field-based 15N-nitrous oxide pool dilution technique to measure gross N2O production in soil. *Global Change Biology*, *17*(12), 3577–3588. https://doi.org/10.1111/j.1365-2486.2011.02481.x

Yang, W. H., & Silver, W. L. (2016). Net soil-atmosphere fluxes mask patterns in gross production and consumption of nitrous oxide and methane in a managed ecosystem. *Biogeosciences*, *13*(5), 1705–1715. https://doi.org/10.5194/bg-13-1705-2016

Zaehle, S., Ciais, P., Friend, A. D., & Prieur, V. (2011). Carbon benefits of anthropogenic reactive nitrogen offset by nitrous oxide emissions. *Nature Geoscience*, *4*(9), 601–605. https://doi.org/10.1038/ngeo1207

Zhang, X., Liu, W., Schloter, M., Zhang, G., Chen, Q., Huang, J., … Han, X. (2013). Response of the Abundance of Key Soil Microbial Nitrogen-Cycling Genes to Multi-Factorial Global Changes. *PLoS ONE*, *8*(10), 2–11. https://doi.org/10.1371/journal.pone.0076500

Zhou, M., Zhu, B., Wang, S., Zhu, X., Vereecken, H., & Brüggemann, N. (2017). Stimulation of N2O emission by manure application to agricultural soils may largely offset carbon benefits: a global meta-analysis. *Global Change Biology*, *23*(10), 4068–4083. https://doi.org/10.1111/gcb.13648

Zhu, K., Bruun, S., Larsen, M., Glud, R. N., & Jensen, L. S. (2015). Heterogeneity of O2 dynamics in soil amended with animal manure and implications for greenhouse gas emissions. *Soil Biology and Biochemistry*, *84*, 96–106. https://doi.org/10.1016/j.soilbio.2015.02.012

CHAPTER 5: OVERCOMING C LIMITATION TO STIMULATE N_2O CONSUMPTION IN DIVERSE SOILS BY "THREADING THE NEEDLE" THROUGH COMPLEXITIES OF SOIL C AND N DYNAMICS

1. Introduction

Nitrous oxide (N_2O) is a potent greenhouse gas that is emitted from diffuse natural and anthropogenic sources, but most N_2O is emitted from soils (Tian et al. 2020). Approximately 50% of soil N_2O emissions come from agricultural soils, owing to excess nitrogen (N) fertilizer use to meet crop yield demands (Reay et al. 2012, Smith 2017, Houser and Stuart 2020). Thus, managing N_2O emissions, especially from the agricultural sector, has become an increasingly important area of research. However, studies have primarily focused on understanding the biotic processes that drive N_2O production, rather than N_2O consumption (Subbarao et al. 2006, Van Meter et al. 2016, Bakken and Frostegard 2017, Lam et al. 2017). While soil field studies using gas flux chambers have observed negative N_2O fluxes for decades (Chapuis-Lardy et al. 2007), only recently has N_2O consumption been recognized as a force that helps regulate net N_2O emissions (Yang et al. 2016). N_2O consumption is the only known biotic process that removes N_2O from soil pores, whereby microbes reduce N_2O to N_2 biochemically (Chapuis-Lardy et al. 2007, Yang and Silver 2016). Net N_2O emissions are the balance of N_2O production and consumption, and when N_2O consumption rate exceeds production rate, negative fluxes occur, which is desirable from a greenhouse gas (GHG) management perspective. Indeed, researchers have become more interested in better understanding what drives N_2O consumption in soils over the past decade (Schlesinger et al. 2013). It would be ideal to learn what stimulates N_2O consumption because then N_2O could be managed after it has already been produced.

Previous work has shown that N_2O consumption is usually driven by sufficient supply of electron donors, such as organic carbon (OC), in soils (Mitchell et al. 2013, Wen et al. 2017, Zhou et al. 2017, Guo et al. 2020, Highton et al. 2020). When soils are amended with OC, it can have a two-pronged effect: (1) the OC provides an electron donor source for the microbial reduction of N-oxides, and (2) the OC contributes to anoxia, either by physically creating anoxic microsites, or by driving microbial respiration, such that microbes will use alternative electron acceptors to O_2 (such as N_2O). A variety of different OC amendments have been applied to soils to examine the N_2O flux response, and typically one of three outcomes occur: net N_2O emissions decrease, the N_2O:N_2 product ratio decreases, or N_2O emissions increase (Schulz et al. 2017, Wu et al. 2018, Duan et al. 2019). But it is typically unclear if changes in N_2O flux are mediated by increases in N_2O consumption, decreases in N_2O emissions, or both (Butterbach-Bahl and Danemman 2011, Mitchell et al. 2013, Zhu et al. 2015, McMillan et al. 2016, Wu et al. 2018, Conthe et al. 2019, Duan et al. 2019, Wang et al. 2019).

Studies have also focused on the presence of clade I and clade II nosZ gene abundance in soils since that gene encodes the enzyme (NosZ) responsible for $N_2O \rightarrow N_2$ reduction. In fact, nosZ gene abundance has recently been described as a proxy for N_2O consumption potential in soils (Buchen et al. 2019, Highton et al. 2020). Several drivers have emerged that are important for regulating the abundance of nosZ, including soil OC (SOC), inorganic N (IN), and soil pH, however studies differ in their conclusions about the importance of a given driver for clade I vs. clade II nosZ abundance (Schulz et al. 2017, Conthe et al. 2018, Hein and Simon 2019, Guo et al. 2020). This is further complicated by the fact that clade I nosZ has been studied for decades in what is now referred to as "canonical" denitrification (Shan et al. 2021), whereas clade II nosZ was only discovered in 2012 (Sanford et al. 2012). Additionally, the suite of primers necessary to

amplify all the subclades of clade II nosZ were only made recently available (Chee-Sanford et al. 2020). Consequently, there have been very few field and microcosm-based studies to explore clade II nosZ *in situ* (Christensen et al. 2021, Shan et al. 2021). It remains unclear if clade I and clade II nosZ abundances are modulated in the same way by the same drivers, and it remains unclear if/how these genes work in consort to contribute to N_2O consumption in soils. Furthermore, studies assessing how OC additions differentially impact clade I and clade II nosZ are needed.

In Chapter 4, I found that adding specific OC molecules (succinate, acetate, propionate) to soils caused **I**ncreased N_2O **C**onsumption and **D**ecreased N_2O **E**missions (ICDE) for some, but not all, soils. I determined that in OC-poor soils, the OC additions stimulated an increase in clade I nosZ abundance by providing microbes with the electron donors necessary to consume N_2O. I hypothesized the reason those soils showed ICDE while other soils did not was because the OC addition liberated the soil microbes to expand their reducing regions and support N_2O consumption. However, these findings shed light on the complicating factor of soil redox heterogeneity, in that not all reducing regions in soil are favorable for N_2O consumption. For example, soils with high NO_3^- that become more reducing in response to OC addition could increase N_2O production. And so, the challenge becomes balancing the creation of anoxic sites, but *not* suboxic sites that will favor N_2O production.

Previous work and my Chapter 4 study help bring into focus all that we have learned about N_2O consumption, but also all that remains unclear. This body of work has revealed several key outstanding questions: (1) What are the best organic amendments to stimulate N_2O consumption in soils, and does this vary by soil? (2) What drives the abundances of clade I and clade II nosZ in soils, and do their drivers differ? (3) Can we harness the collective information

about N_2O consumption to make broad management decisions for stimulating N_2O consumption in soils? In this study, I amended soils with different concentrations (low, medium, and high) of the OC amendment I used in Chapter 4. While this experiment aimed to address the broad abovementioned questions, it specifically also sought to address my follow-up questions from the previous study: will progressively larger additions of OC expand anoxic regions in soil that are thermodynamically favorable for N_2O consumption? Or alternatively, is there an OC availability threshold that soils must surpass, and does this threshold differ by soil type?

Here, I incubated seven diverse soils collected from Colorado and New Mexico in the lab at 60% soil saturation for 48 hrs, and I used ^{15}N isotope pool dilution to separately quantify N_2O emissions and consumption. To gain a better understanding of the underlying soil and microbial properties driving N_2O production and consumption, I measured a variety of soil properties and multiple N-cycling genes, notably including clade II nosZ. Few studies have been conducted that assess the behavior of this gene *in situ*, and I predict that quantifying it will help to elucidate more clearly what drives N_2O consumption across soils. In sum, continuing to broaden the scope of how I interpret and understand N_2O consumption can move us closer to stimulating this process for N_2O emissions management.

2. Materials and Methods

2.1 Field sampling and soil characterization

Soils were collected from seven locations in Colorado and New Mexico, United States of America (Table 5.1). Five soils were collected in Colorado, and the other two soils were collected in New Mexico. All soil and site properties are summarized in Table 5.1. All soils were collected in July 2020, and hereafter soils will be referred to by their site name in Table 5.1.

Table 5.1. Summary of environments and physical and chemical properties of collected soils. MAT, MAP, soil classifications, and horizons were determined using the United States Department of Agriculture Natural Resources Conservation Service Soil Resource Reports.

Site name	Location	Site name	GPS coordinates	MAT (°C)	MAP (mm)	Soil classification	Horizon
Agricultural Research, Development, and Education Center	Fort Collins, CO	Conventional cornfield	40.65160, -104.99881	8.3	381	Fort Collins loam, Pleistocene or older, alluvium and/or eolian deposits	Ap/Bt1
Jornada Experimental Range	Las Cruces, NM	Desert shrubland	32.54346, -106.85956	17	254	Wink-Harrisburg association, mixed calcareous coarse-loamy alluvium	H1/H2
Limited Irrigation Research Farm	Greeley, CO	Limited irrigation cornfield	40.44852, -104.63897	9.5	373	Ustic Haplargids Olney fine sandy loam	A
Loch Vale	Rocky Mountain National Park, CO	Subalpine forest	40.29649, -105.64612	1.4	1050	Cryic spodosols Rocky sandy loam	O/A
Sevilleta Grassland	Socorro, NM	Desert grassland	34.34914, -106.88624	16	229	Mesic Ustic Haplocalcids, loamy-skeletal, carbonatic	A/C
Shortgrass Steppe	Nunn, CO	Shortgrass prairie	40.80458, -104.71565	11	381	Alluvial Nunn, fine clayey loam	Ap/Bt
Sky Pond	Rocky Mountain National Park, CO	Alpine meadow	40.27971, -105.66886	1.4	1050	Cryochrepts, Cryumbrepts Rocky sandy loam	O/A/Bw

2.2 Soil collection and analyses

All soils were collected from the top ~20 cm of the soil profile using a 5cm-diameter soil auger. The sites Shortgrass Steppe, Limited Irrigation Research Farm, Agricultural Research, Development, and Education Center, Jornada Experimental Range, and Sevilleta Grassland all had designated areas to sample within (e.g., a specific field), so within those designated areas ten soil cores were collected randomly. The sites Sky Pond and Loch Vale represented broader geographic areas (e.g., a forest), so ten soil cores were collected at randomly assigned GPS points within ~150 m of the GPS coordinates for the site (Table 5.1).

Cores were bulked into gallon Ziploc bags, placed on ice in the field to minimize microbial activity, and then refrigerated at 4 °C upon arrival to the laboratory. Soils collected outside of Colorado were driven back to Colorado State University on ice, sieved to 2mm and homogenized within 72 hr after sampling. Soils collected in Colorado were sieved to 2mm and homogenized within 24 hr after sampling. Processed soils were frozen in gallon Ziploc bags at -20 °C. All incubations and analyses were performed within two months of soil collection.

I measured inorganic N (IN) via KCl extractions and calculated gravimetric water content (GWC) for all soils prior to freezing. I also measured soil IN concentrations after all soils had

been incubated. Ammonium (NH_4^+) and NO_3^- extraction and analysis procedures were the same as in Chapter 4. Determination of gravimetric water content (GWC) were the same as in Chapter 4.

Frozen soils were thawed to measure soil pH, SOC, and SON. I measured soil pH using the same procedure from Chapter 4, and SOC and SON measurements were performed externally with a LECO Tru-Spec CN analyzer (Leco Corp., St. Joseph, MI, USA) at Ward Laboratories in Kearney, NE. Frozen soil subsamples were dried in a 60 °C oven, and ground to powder on a table roller at Colorado State University prior to shipment to Ward Laboratory.

Frozen soils were shipped directly to Ward Laboratories for soil texture analysis by hydrometer.

2.3 Determination of soil saturation

For all incubations, I held soils at 60% soil saturation. I determined how much water to add to each soil to achieve this saturation using the same procedure as in Chapter 4. Briefly, I calculated saturated water content (SWC) by dividing the g water in soil subsamples at maximum water holding capacity (WHC) by the subsample dry soil mass. I used this metric rather than % water-filled pore space (WFPS) because in sieving my soils I broke down all soil pore structures. Finally, to determine the g of water to add to a given soil, I used Equation 1, where g soil corresponds to the g soil incubated, and 0.6 corresponds to the target percent saturation (60%):

$$g\ H_2O\ to\ add = g\ soil\ x\ ((SWC\ x\ 0.6) - soil\ GWC)) \qquad (1)$$

2.4 Soil incubations

2.4.1 Preparation of organic carbon solutions

I prepared three aqueous OC amendments for all treated soils. Equal quantities on a % mass C basis of powdered sodium succinate, sodium acetate, and sodium propionate were dissolved into DI water and diluted serially (two dilutions) to a final concentration of 6.28 mg/L (Low OC), 12.56 mg/L (Medium OC), and 18.84 mg/L (High OC). All organic compounds were obtained from Sigma Aldrich (St. Louis, MO, USA). Aqueous solutions were stored at 4 °C when not in use.

The organic acids used are all non-fermentable, naturally occurring, and have previously been determined by Hedin et al. (1998) to impact denitrifier metabolism. I determined the concentration for the Low OC-amendment previously (see Chapter 4, Section 3.4.). In this study, I chose to double and triple that amendment concentration for continuity, rather than determining a different series of OC-levels.

2.4.2 Soil amendments and incubation setup

Soils were separated into either Control, Low OC, Medium OC, or High OC (hereafter all OC-amended soils referred to as +OC soils). As in Chapter 4, for each sample, the frozen soil equivalent of 75g dry soil was weighed into 0.5 L Ball jars, refrigerated overnight to thaw, warmed to room temperature prior to treatment, and then brough to 60% saturation. Briefly, Control soils were amended with DI water and +OC soils were amended with DI water and 1mL of the appropriate +OC solution. Either amendment was distributed by pipette over the soils, and then thoroughly mixed to ensure sufficient distribution of OC (if applicable) and homogenous saturation.

After all soils were treated, jars were sealed for incubation. In Stuchiner and von Fischer (unpublished manuscript in revision with JGR: Biogeosciences, *see Chapter 3*) I provide a detailed description of my incubation apparatus, which includes a 1L Tedlar gas bag attached to the jar headspace to allow for removal of a large quantity of air for subsequent [N_2O] and isotopic analysis with the laser-based analyzer (see 2.4.3 for details). I prepared incubation apparatuses the same as in Chapter 4, by flushing and filling all apparats from a cylinder of custom-blend air intended to closely emulate Earth's atmosphere, and then injecting 1mL of 99 atom percent (AP) $^{15}N_2O$ into each jar's headspace for isotope pool dilution (details in Section 2.4.4).

I performed time zero (T_0) and time 48 (T_{48}) measurements to enable a 48 hr assay duration (see Chapter 4, Section 3.4.2 for details). Soils were incubated on a lab countertop at room temperature (24 °C) for either 60 minutes (T_0), or 49 hr (T_{48}). At the end of the incubation period, I mixed each jar and gas bag's air thoroughly (Stuchiner and von Fischer unpublished manuscript in revision with JGR: Biogeosciences, *see Chapter 3*). At the time of sampling, I connected each incubation apparatus directly to the gas analyzer-scrubber system (see 2.4.3 for details). The analyzer removed air from the jar headspace and gas bag simultaneously, thus keeping the jar air pressure at atmospheric pressure.

2.4.3 Measurements of N_2O and CO_2 concentration, and N_2O isotopic composition

After 60 minutes (T_0) or 49 hours (T_{48}), incubation vessels were analyzed for N_2O concentration and isotopic composition by a laser-based Los Gatos Research (LGR) N_2O isotopic analyzer (Los Gatos Research N_2O Isotopic Analyzer model 914–0027; ABB-Los Gatos Research, Mountain View, CA, USA) as in Chapter 4.

All raw concentration data for each N_2O sample was exported to Excel (version 16.52), where it was trimmed to only include stabilized N_2O isotopocule readings (the final ~5 minutes of sampling). These values were used to calculate average N_2O and isotopomer concentrations. All reported concentrations were then corrected against calibrations using the model and approach described in Stuchiner et al. (2020).

I measured accumulated CO_2 in T_0 and T_{48} incubation jars to characterize microbial respiration. Air samples of 3mL were drawn with a 3mL syringe from remaining headspace air in the incubation jars at the end of N_2O sampling. Samples were analyzed on a laser-based Los Gatos Research Greenhouse Gas Analyzer using the procedure described in Chapter 4 (Los Gatos Research Greenhouse Gas Analyzer model 908-0007-001; ABB-Los Gatos Research, Mountain View, CA, USA). Briefly, each sample was injected into a continuous flow of zero-grade air (80:20 N_2:O_2 blend, Airgas Industries) that connected to the analyzer via an open split, and each injected sample yielded a brief CO_2 concentration peak. The height (i.e., maximum concentration) of these peaks were calibrated with a four-point calibration curve using the same standards as in Chapter 4.

A previous test assessed the gastight seals of the incubation vessels (see Chapter 4, Section 3.4.5). Briefly, 12 incubation vessels were flushed and filled with zero-grade air and then injected with 1 mL of 99 AP $^{15}N^{15}N^{16}O$. Six vessels were sampled for N_2O and isotopomer concentrations at T_0 and the remaining six vessels were sampled at T_{48}, and t-tests revealed that changes from T_0 to T_{48} in total N_2O concentration were not significant, while changes in concentration of enriched ^5N_2O was less than 2.3% for $\delta^{15}N^{\alpha}$ and $\delta^{15}N^{\beta}$.

2.4.4 Flux calculations and isotope pool dilution

I calculated net N_2O emission using measures of the headspace N_2O concentration and calculated gross N_2O consumption using isotope pool dilution (Kirkham and Bartholomew 1954, von Fischer and Hedin 2002). Net N_2O flux was calculated from the difference in N_2O concentration between T_0 and T_{48} and is presented in units ng N_2O-N/g dry soil/day. I describe the calculations used to obtain these net and gross fluxes in detail in Chapter 4.

2.4.5 Post-incubation soil and genetic measurements

After all gas had been sampled for the T_{48} incubations, soil replicates from each group were bulked into a Ziploc bag, re-homogenized, and soil IN was measured immediately thereafter (see Chapter 4, section 3.2, and this chapter section 2.2. for details). Like in Chapter 4, two-gram subsamples from each treatment group were frozen at -80 °C in preparation for microbial genetic analysis, and remaining soils were frozen at -20 °C.

To measure the abundances of key N-cycling genes (nifH, nirK, nirS, clade I nosZ, clade II nosZ), and microbial community genes (16S ribosomal RNA, rRNA, 18S rRNA) I extracted DNA from soils that had been frozen at -80 °C using a Qiagen Powersoil Pro kit according to the manufacturer's instructions (Qiagen, Germantown, MD, USA). The genes 16S rRNA and 18S rRNA are commonly used indicators of bacterial (16S rRNA) and fungal (18S rRNA) gene abundances. Furthermore, I use 16S rRNA gene abundances to standardize the abundances of all other genes (Henry et al. 2006). The nifH gene encodes the enzyme that catalyzes N-fixation (Kuypers et al. 2018). The nirK and the nirS genes encode the enzyme that catalyzes reduction of nitrite (NO_2^-) to nitric oxide (NO) and is thus characteristic of incomplete denitrification, with the notable difference that microbes harboring nirK often lack clade I nosZ, whereas microbes harboring nirS are more likely to have clade I nosZ (Sanford et al. 2012, Graf et al. 2014). The

clade I nosZ gene encodes the enzyme that catalyzes reduction of N_2O to N_2 and is thus characteristic of complete canonical denitrification, whereas clade II nosZ includes a suite of subclades and also encodes the enzyme that catalyzes reduction of N_2O to N_2, but potentially under more diverse circumstances than clade I nosZ (Sanford et al. 2012, Domeignoz-Horta et al. 2015, Shan et al. 2021).

The quality (A260/A280) and concentration from each DNA sample was determined spectrophotometrically using a NanoDrop (Thermo Scientific, Waltham, MA, USA). All genetic measurements were performed as in Chapter 4. Briefly, samples were diluted to 10 ng/μL and then I characterized the abundances of the abovementioned genes using qPCR analysis as in Trivedi et al. (2012) for all genes excluding clade II nosZ.

For clade II nosZ, I characterized the abundances of clade II nosZ subclades A, B, and C as in Chee-Sanford et al. (2020). While Chee-Sanford et al. (2020) describes eight subclades (A-H), I was only able to successfully amplify subclade A-C, as this is a novel gene to quantify, and its amplification pipeline is still being refined.

For each soil sample, I performed qPCR amplification four to six times for each gene, as occasionally samples did not amplify. Gene abundances (e.g., gene copy number) were determined by using simple linear regressions that related the cycle threshold (Ct) value for each sample to known Ct values from a standard curve. I calculated a mean gene abundance for clade II nosZ by averaging the gene abundances of subclades A-C.

2.5 Data analyses

2.5.1 Calculation of +OC treatments:Control ratios

To determine the effect of the +OC treatments, I compared each +OC treatment response (e.g., responses for Low, Medium, and High OC) vs. control for net N_2O emissions, gross N_2O

consumption, soil NO_3^- and NH_4^+ concentrations, microbially emitted [CO_2], and the gene abundances of nifH, nirS, nirK, clade I nosZ, and clade II nosZ. for all soils at the conclusion of incubations. I quantified the effect of each OC-treatment as in Chapter 4. Briefly, I calculated response ratios of each variable measured by dividing the +OC value for a given property by the weighted average for the Control of that same property. If a ratio was > 1 the +OC treatment increased that property, and if a ratio was <1 the +OC treatment decreased that property. I used +OC:Control response ratios in all statistical analyses when applicable.

2.5.2 Statistical analyses

All raw data was collected, collated, and reorganized in Excel, and then all statistical analyses were performed in RStudio (version 4.0.2 (2020-06-22) – "Taking Off Again" © 2020 The R Foundation for Statistical Computing). Differences between pre-OC addition soil NO_3^- and post OC-addition soil NO_3^- were determined using one-way ANOVAs. The same test was used for pre- vs. post-OC addition soil NH_4^+. I also performed one-way ANOVAs to compare SOC, SON, and soil pH among all pre-incubation soils. Two-way ANOVAs were used to compare among soil and microbial community responses to the different OC-amendments following incubation, including microbial respiration, clade I nosZ abundance, and clade II nosZ abundance. I also used simple linear regression analysis to identify correlations between +OC:Control N_2O emissions or consumption and +OC:Control microbial respiration. I examined residuals for departure from normality and determined that all N_2O production and consumption data should be log-transformed to meet assumptions of normality.

Associations among microbial N-cycling gene ratios (+OC:Control ratios) and N_2O flux responses were examined using a MANOVA. Follow-up one-way ANOVAs were performed to identify differences among all the OC-amended soils for each N-cycling gene. To visualize these

associations, I performed a Principal Components Analysis (PCA) to see how the N-cycling gene abundance ratios associated with the different N_2O flux responses. I used the package `missMDA` to impute the dataset for the PCA, and I used the package `factoextra` to visualize the PCA results.

3. Results

3.1 N_2O *flux responses to +OC treatments*

The different +OC treatments stimulated a range of N_2O flux responses across the different soils (Figure 5.1). Within soils from a given site, all soils typically responded to +OC treatment, regardless of amendment level, in the same way. Eleven of the +OC soils increased N_2O consumption in response to treatment, and ten of the +OC soils decreased N_2O consumption in response to treatment (Figure 5.1). Four soils showed ICDE, including all the desert shrubland soils, and the desert grassland Low OC-amended soil. Nine soils showed **I**ncreased N_2O **C**onsumption and **I**ncreased N_2O **E**mission (ICIE), including all the limited irrigation corn field soils, all the alpine meadow soils, and the conventional cornfield medium OC-amended soil. Eight soils showed **D**ecreased N_2O **C**onsumption and **D**ecreased N_2O **E**mission (DCDE), including all the desert grassland soils, all the subalpine forest soils, and the desert grassland High and Medium OC-amended soils. Finally, two soils, the conventional cornfield Low and High OC-amended soils, showed **D**ecreased N_2O **C**onsumption and **I**ncreased N_2O **E**mission (DCIE; Figure 5.1).

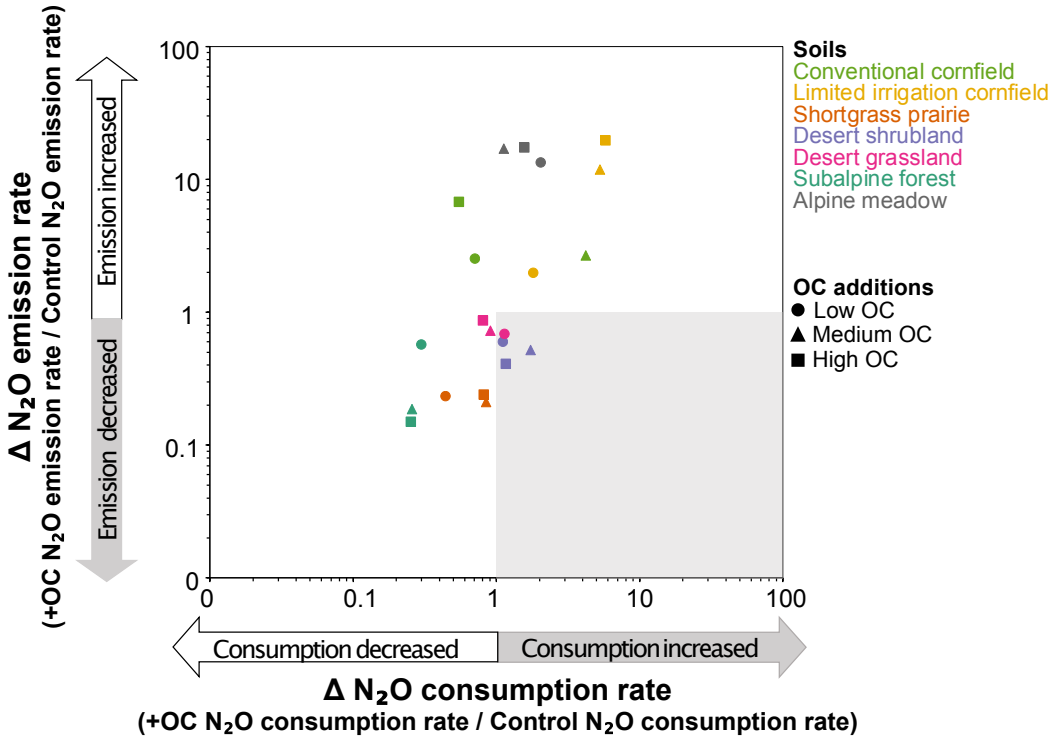

Figure 5.1. Change in (or "Δ") net N_2O emission vs. gross N_2O consumption rates for all soils. Colors correspond to the different soils, and shapes correspond to the +OC treatment. Δ values were calculated by dividing +OC N_2O emission or consumption rates by Control N_2O emission or consumption rates. The grey box highlights region where soils can show ICDE, a GHG management ideal. In all cases, n = 6 for Control N_2O emission rates, and for Control N_2O consumption rates n = 6 for the desert grassland, limited irrigation cornfield, and subalpine forest, but n = 4 for the convention cornfield and shortgrass prairie, and n = 5 for the desert shrubland and the alpine meadow. For N_2O emission ratios, n = 6 for all soils except n = 2 for conventional cornfield medium OC, n = 5 for desert grassland high and medium OC, n = 5 for subalpine forest Low OC, and n = 5 for desert grassland Low OC. For N_2O consumption ratios, n = 2 for all conventional cornfield soils, n = 5 for desert shrubland low and high OC-amended soils and n = 6 for desert shrubland medium OC-amended soils, n = 5 for subalpine forest medium and high OC-amended soils and n = 6 for subalpine forest low OC-amended soils, n = 6 for desert grassland medium and high OC-amended soils and n = 4 for desert grassland low OC-amended soils, and n = 5 for desert grassland medium and high OC-amended soils and n = 6 for desert grassland low OC-amended soils.

3.2 Microbial respiration and respiration-N_2O flux relationships

3.2.1 Microbial respiration

There were significant site, treatment, and site by treatment interaction effects for microbial respiration +OC vs. Control ratios following incubation ($p < 0.0001$ in all cases), as

revealed by a two-way ANOVA (Figure 5.2). Subsequent site and site by treatment pairwise comparisons showed that these responses varied by N_2O flux category, and somewhat within soil type (Figure 5.2).

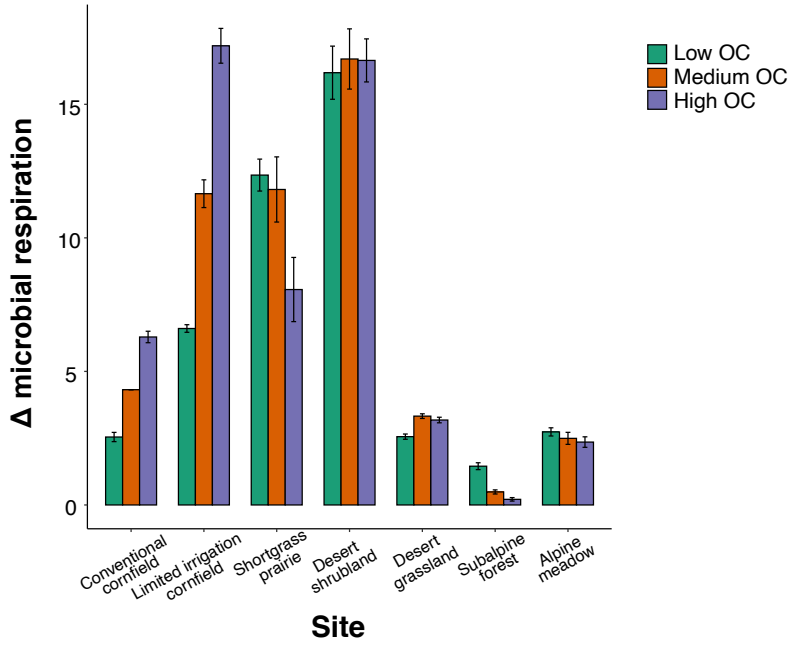

Figure 5.2. Microbial respiration ratios across all soils and +OC treatments. The Δ values were calculated by dividing +OC microbial respiration by Control microbial respiration. In all cases n = 6, except n = 2 for the Convention cornfield Medium OC-amended soil. Error bars are ± one SE from the mean.

ICDE soils

All desert shrubland soils showed comparable microbial respiration regardless of treatment, and the desert grassland Low OC soil did not differ from the desert grassland Medium or High OC soils. The desert shrubland soils collectively have notably higher Δ respiration values than all others ($p < 0.0001$ in all cases).

ICIE soils

Respiration progressively increased with successive OC additions for the limited irrigation cornfield soils ($p < 0.0001$ in all cases), and the conventional cornfield Medium OC

soil had a higher Δ respiration ratio than Low and High OC-amended soils, although not significantly. Dissimilarly, respiration progressively decreased for the alpine meadow soil, although not appreciably (no significant differences).

DCDE soils

Respiration progressively decreased for the shortgrass prairie soils and for the subalpine forest soils, however only the High OC-amended shortgrass prairie soil was significantly different from the Medium and Low ($p < 0.0001$ in both cases), and there were no significant differences among the subalpine forest soils. The desert grassland Medium and High OC-amended soils did not differ from each other.

DCIE soils

Respiration progressively increased with successive OC additions for the conventional cornfield Low and High OC additions, however only Low and High significantly differed from each other ($p < 0.0001$) and neither significantly differed from the conventional cornfield Medium OC soil.

3.2.2 Microbial respiration vs. N_2O fluxes

Simple linear regression analyses revealed there were relationships between the microbial respiration ratios and certain N_2O flux ratios.

There were no correlations between respiration ratio and the N_2O emission ratio, across all soils or by OC-amendment level (Figure 5.3). Although there was a negative relationship between the Low OC Δ N_2O emission rate and Δ respiration rate, it was not significant (Figure 5.3).

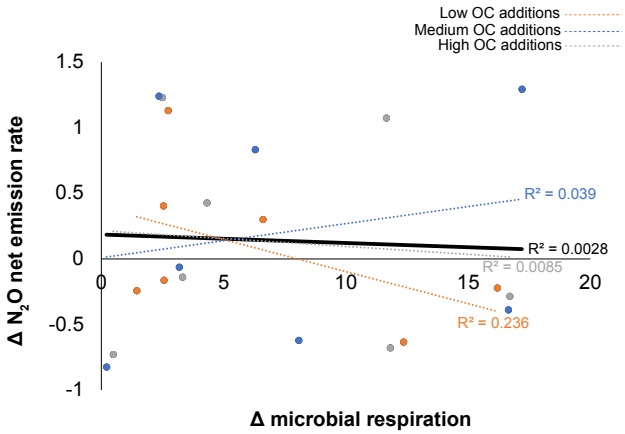

Figure 5.3. Relationship between Δ N_2O emission rate and Δ microbial respiration. All values are means obtained after 48 hr soil incubations. There were no significant correlations between Δ N_2O emissions and Δ microbial respiration across all soils or across Low, Medium, or High OC-amended soils alone. N = 21 for total Δ N_2O emission rate and total Δ microbial respiration, and n = 7 for each OC-amendment level.

Conversely, there was a positive correlation ($R^2 = 0.19$) between the N_2O consumption ratio and the microbial respiration ratio across all OC additions, with the intercept and the slope both significantly different from zero ($p < 0.0001$ and $p = 0.05$, respectively), indicating a significant positive correlation (Figure 5.4). However, there was no significant relationships between Δ N_2O consumption and Δ microbial respiration for the only the Low, Medium, or High OC soils. There were apparent positive correlations for the Medium and High OC relationships ($R^2 = 0.19$ and 0.49, respectively), but neither correlation was significant. That said, the slope was borderline significantly different from zero ($p = 0.08$) for High OC, suggesting a near significant positive correlation for those soils (Figure 5.4).

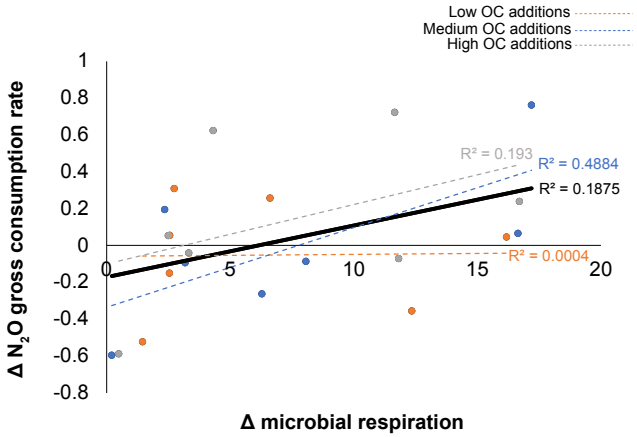

Figure 5.4. Relationship between Δ N_2O consumption rate and Δ microbial respiration. All values are means obtained after 48 hr soil incubations. There was a significant correlation between Δ N_2O consumption and Δ microbial respiration across all soils (black line, p = 0.05), but there were not significant correlations between Δ N_2O consumption and Δ microbial respiration across Low, Medium, or High OC-amended soils alone, although the correlation for High OC soils (blue dotted line) was borderline significant (p = 0.08). N = 21 for total Δ N_2O emission rate and total Δ microbial respiration, and n = 7 for each OC-amendment level.

3.3 Changes in soil IN from pre to post incubation

One-way ANOVAs revealed differences within each soil from before and after incubations and among the +OC treated soils vs. the control soils for both NH_4^+ and NO_3^- (Figure 5.5).

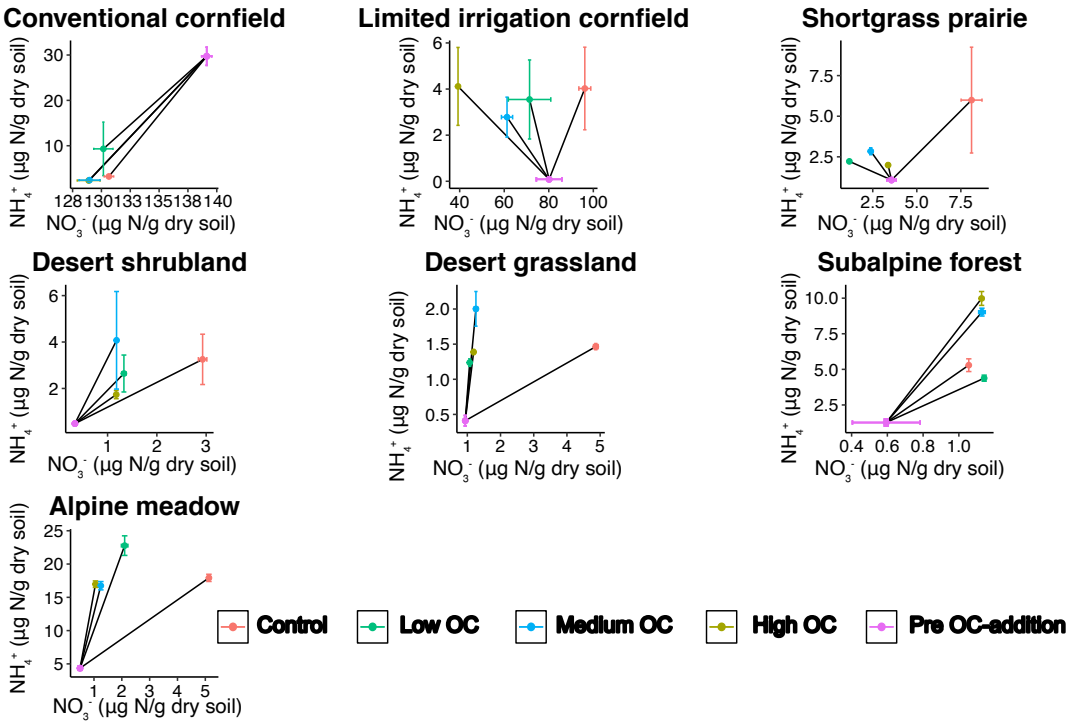

Figure 5.5. Relationships between soil NH_4^+ and NO_3^- concentrations from before OC-additions and after OC-additions (post 48 hr incubations). For the pre soils, IN was extracted with 24-72 hrs of sampling, and for the OC-amended soils, IN was extracted immediately following incubation. For pre OC-addition soils, n = 4 in all cases, and for all OC-amended and Control soils, n = 3. Error bars are ± one SE from the mean.

ICDE soils

The desert shrubland did not have any significant differences in soil NH_4^+ concentration among any of the soil, but all the post OC-addition soils differed from the pre-OC addition soils for NO_3^- ($p < 0.0001$, Figure 5.5). The desert grassland Low OC-amended soil differed from the pre-OC amendment soil ($p = 0.002$) and from the Medium OC-amended soil ($p = 0.006$) for NH_4^+, but for NO_3^- only the Low OC-amended soil differed from the Control soil ($p < 0.0001$, Figure 5.5).

ICIE soils

The conventional cornfield Medium OC soil NH_4^+ and NO_3^- concentrations significantly differed from the pre-OC NH_4^+ and NO_3^- concentrations ($p = 0.0001$ and $p < 0.0001$,

respectively, Figure 5.5). The limited irrigation cornfield had no differences among any NH_4^+ concentrations, but there were multiple differences among the NO_3^- concentrations. The High OC soil differed from the pre-OC soil and the Low OC soil ($p = 0.0013$, $p = 0.0125$, respectively). The Medium and High OC soils were also both significantly different from the Control ($p = 0.007$ and $p = 0.0001$, respectively), whereas the Low OC soil is borderline significantly different from the control ($p = 0.06$). For the alpine meadow NH_4^+ concentrations, all the soils significantly differed from the pre-OC soils ($p < 0.0001$ in all cases), and all the post-incubation soils significantly different from the Low OC soil ($p = 0.007$, $p = 0.0013$, and $p = 0.0018$ for Control, Medium, and High OC-amendment, respectively). The NO_3^- concentrations for all the post-OC addition alpine meadow soils significantly differed from the pre-OC addition soils ($p < 0.0001$ in all cases $p = 0.0001$ for the High OC soil). All the OC-amended soils significantly differed from the Control ($p < 0.0001$ in all cases, Figure 5.5).

DCDE soils

For the subalpine forest soil NH_4^+ levels, all the OC-amended soils significantly differed from the pre-amendment soil ($p < 0.001$ in all cases except $p = 0.0002$ for the Low OC soil, Figure 5.5.). Furthermore, the Medium and High OC-amended soils differed from the Control soil ($p < 0.001$ in both cases), but the Low OC soil did not differ from the control. For NO_3^- levels, all the treated soils significantly differed from the pre-OC addition soils ($p = 0.03$, $p = 0.03$, and $p = 0.03$ for Low, Medium, and High, respectively), and the Control was borderline significantly different from the pre-OC addition soils ($p = 0.07$).

The desert grassland Medium and High OC soils both significantly differed in NH_4^+ from the pre-OC soil ($p < 0.0001$, and $p = 0.0005$ for Medium and High, respectively). Both soils and the Control significantly differed in NO_3^- compared to the pre-OC soil ($p < 0.0001$, $p = 0.0005$, p

= 0.004 for Control, Medium, High, respectively). Additionally, the Medium and High soils both differed from the Control soil ($p < 0.0001$).

For the shortgrass prairie, there were no differences in NH_4^+ among any of the soils. There were differences in soil NO_3^- between the pre-OC soil and the Control and Low OC soils ($p < 0.0001$ and $p = 0.0008$ for Control and Low, respectively), and the with Medium OC soil was borderline significantly different from the pre-OC soil ($p = 0.0834$). All of the +OC soils had significantly different NO_3^- levels from the Control ($p < 0.0001$ in all cases, Figure 5.5).

DCIE soils

For the conventional cornfield, NH_4^+ levels differed for the pre-OC to post Low and High OC-amended soils ($p = 0.0013$ for Low and $p = 0.0001$ for High, respectively, Figure 5.5.). Similarly, NO_3^- levels differed from the pre-OC to post Low and High OC-amended soils ($p < 0.0001$ in both cases).

3.4. Soil genetics

A MANOVA revealed that particular N-cycling genes associated with certain soil flux responses ($p < 0.0001$), as the PCA also illustrates (Figure 5.6). Subsequent one-way ANOVAs revealed that all genes significantly differed among the soils and treatments ($p < 0.001$ for all genes except clade II nosZ average, where $p = 0.013$).

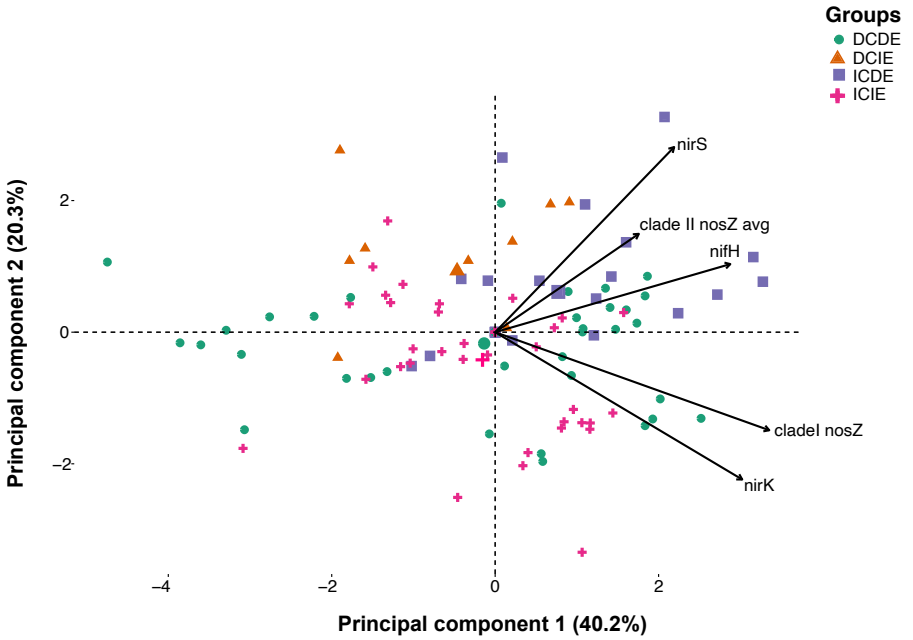

Figure 5.6. Loading and biplot for PCA. Different symbols correspond to different N_2O flux groups. See Appendix 4 Table 2 for original n-values for each variable, n = 6 for all imputed variables.

The PCA illustrates that the gene response ratios (+OC gene abundance divided by Control gene abundance) tended to cluster along PC1 and PC2 (Figure 5.6). The response ratios for nifH, nirS, and clade II nosZ loaded mainly with ICDE and DCDE soils, whereas nirK and clade I nosZ loaded primarily with DCDE and ICIE soils. More specifically, nirK and clade I nosZ loaded most strongly with the subalpine forest and alpine meadow soils, and nifH, nirS, and clade II nosZ loaded most strongly with the desert shrubland and desert grassland soils. None of the N-cycling genes loaded strongly with the conventional cornfield, limited irrigation cornfield, or shortgrass prairie (Figure 5.6).

Clade I nosZ gene abundances increased with increasing OC addition within soils, and a two-way ANOVA found differences within and among soils, as well (Figure 5.7). I performed this test without interaction effects due to the low statistical power from my number of replicates per sample. For clade I, the two-way ANOVA revealed there were significant site and treatment

effects among the soils and their nosZ abundance ($p < 0.0001$ in both cases). Pairwise comparisons illustrated that there were multiple differences within specific soils. The desert shrubland Low OC soil was significantly different from the Medium OC soil ($p = 0.05$) and from the High OC soil ($p = 0.0024$). The desert grassland Low OC soil was significantly different from the High OC soil ($p = 0.034$). Finally, most of the subalpine forest soils significantly differed from each other, with the Low OC soil differing from the High OC soil ($p < 0.0001$), and Medium OC soil differing from High OC soil ($p = 0.015$; Figure 5.7).

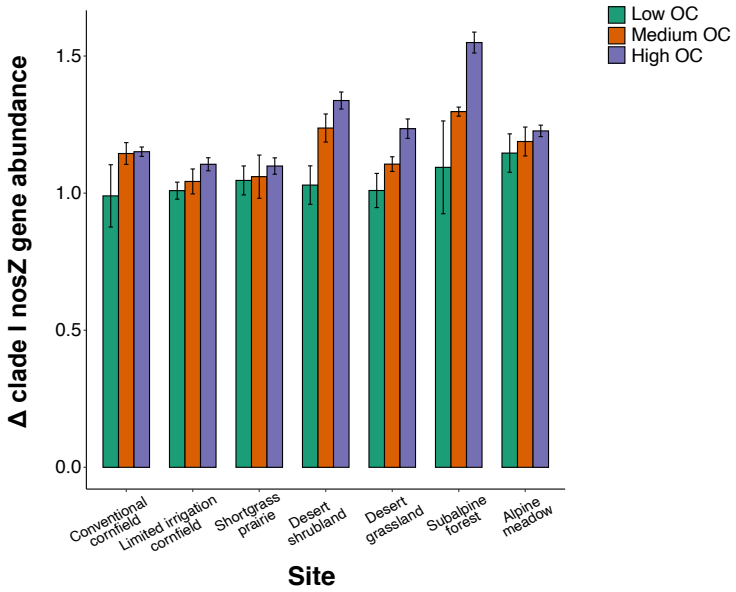

Figure 5.7. Δ clade I nosZ gene abundance by site and by +OC treatment. These Δ values were calculated by dividing the +OC nosZ gene abundances by the Control nosZ gene abundance. In all cases, n = 4 and error bars are ± one SE from the mean.

In contrast, the clade II nosZ two-way ANOVA with interaction effects (n-values were bigger for these samples) showed a significant soil effect ($p = 0.008$), but no treatment effect or site by treatment effect (Figure 5.8). This illustrates that differences among the soils drove the differences in clade II nosZ gene abundance, regardless of +OC treatment. Pairwise comparisons illustrated that within soils, only the desert grassland soils differed between each other. The Low

OC soil differed from the Medium ($p = 0.02$) and from the High OC soil ($p = 0.033$), but the Medium and High OC soils did not differ from each other.

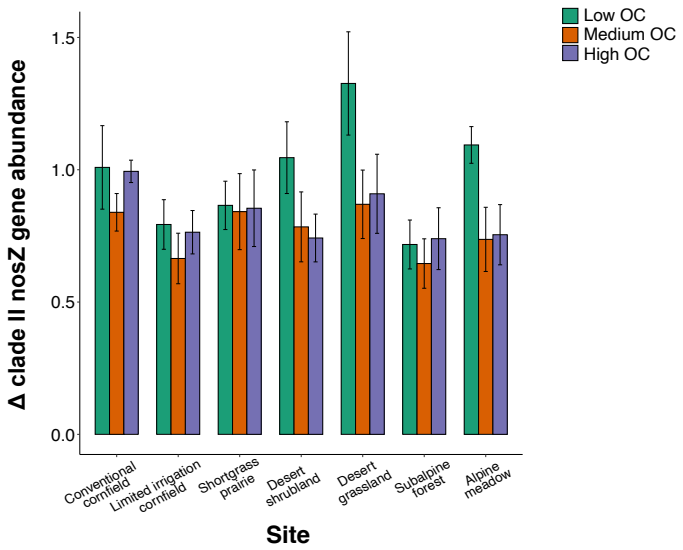

Figure 5.8. Δ clade II nosZ gene abundance by site and by +OC treatment. These Δ values were calculated by determining the mean gene abundance for clade II nosZ by averaging subclades A, B, and C. Then, that mean was divided by the Control clade II nosZ gene abundance. See Appendix 4 Table 1 for n-values, and error bars are ± one SE from the mean.

3.5. Soil properties

Direct measures of soil properties revealed many differences among the soils in texture, SOC, SON, and soil pH. The soil texture analyses are summarized Table 5.2. In general, the largest fraction of all soils was sand, but the conventional cornfield soil also had a notably large clay fraction (Table 5.2).

Table 5.2. Soil texture measures for soil from each site. These direct measures of soil properties were measured prior to the incubation experiments. For each soil, one 500 g sample was used to measure soil texture by hydrometer.

Site name	Soil texture	Sand (%)	Silt (%)	Clay (%)
Conventional cornfield	Clay Loam	39	29	32
Limited irrigation cornfield	Loamy Sand	75	13	12
Shortgrass prairie	Sandy Loam	66	18	16
Desert shrubland	Sandy Loam	86	6	8
Desert grassland	Sandy Loam	66	20	14
Subalpine forest	Sandy Loam	63	25	12
Alpine meadow	Sandy Loam	59	33	8

A one-way ANOVA revealed a significant difference among all soils in % SOC and % SON ($p < 0.0001$ in both cases, Figure 5.9). For SOC, follow-up Tukey pairwise comparisons showed that most soils were significantly different from each other, with $p < 0.0001$ in most cases, except $p = 0.0009$ and $p = 0.004$ for desert shrubland vs. limited irrigation cornfield and for desert grassland vs. shortgrass prairie, respectively (Figure 5.9a). For SON, follow-up Tukey pairwise comparisons also showed significant differences among most soils ($p < 0.0001$ in most cases, except $p = 0.013$, $p = 0.02$, and $p = 0.0001$ for desert grassland vs. limited irrigation cornfield, desert grassland vs. desert shrubland, and desert shrubland vs. shortgrass prairie, respectively, Figure 5.9b).

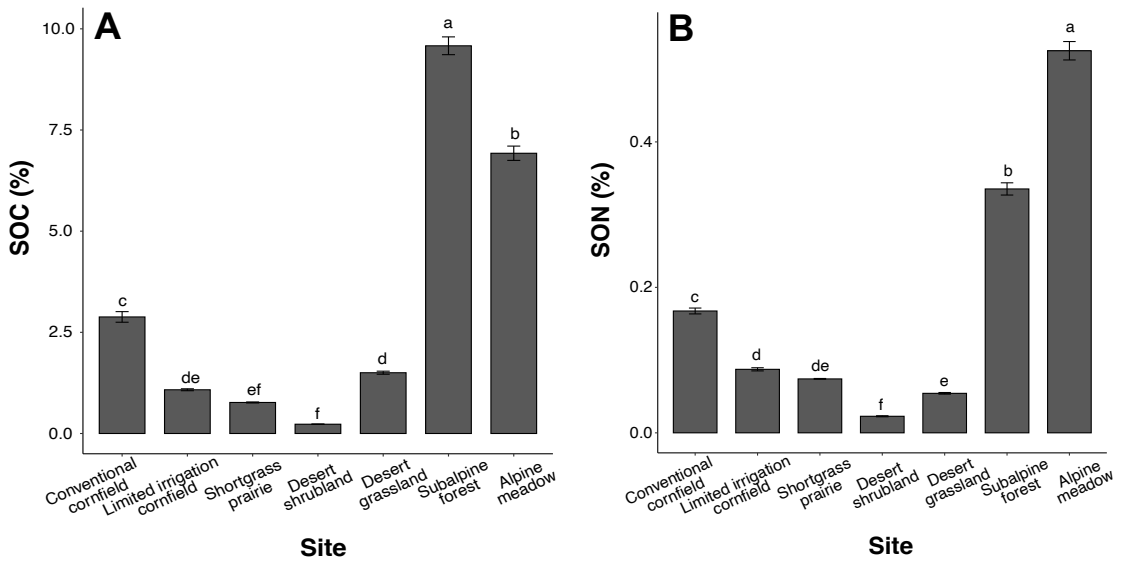

Figure 5.9. SOC (panel **A**) and SON (panel **B**) by soil type. These direct measurements were taken prior to soil incubation. Letters indicate significantly different mean values, and n = 4 in all cases. Error bares are ± one SE from the mean.

Finally, a one-way ANOVA revealed significant differences in pH among all soils ($p < 0.0001$; Figure 5.10). One-way ANOVA revealed a significant difference among the soils ($p < 0.0001$). Follow-up Tukey pairwise comparisons showed there were significant differences among all soils ($p < 0.0001$ in all cases), except there was a borderline significant difference between the limited irrigation cornfield and desert shrubland soil pH ($p = 0.06$).

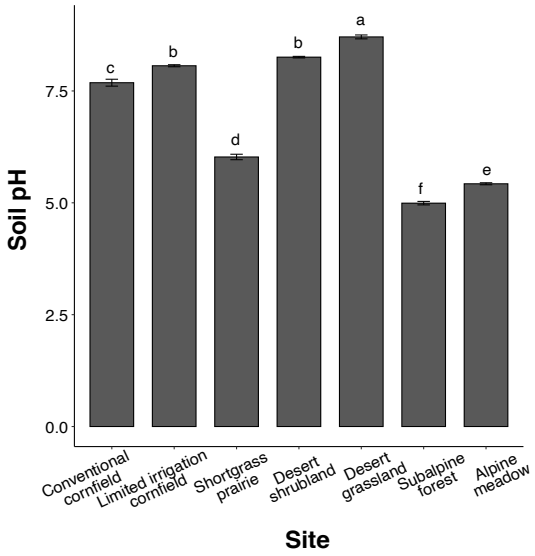

Figure 5.10. Soil pH by soil type. These direct measures of soil properties were measured prior to the incubation experiments. Letters correspond to significantly different pH values. In all cases, n = 9, and error bars are ± one SE from the mean.

4. Discussion

In this study, I incubated diverse soils under a range of OC concentration amendments to see how these treatments effect N_2O production and consumption, and how these responses are mediated by soil and microbial community properties. I sought to address the question: does amending soil with increasing concentrations of OC contribute to microbes surpassing a C-limitation threshold and creating reducing regions in soil that are thermodynamically favorable for N_2O consumption? I predicted that as soils became less reductant limited, they would have increased capacity for N_2O consumption such that all soils could show ICDE. While the results from this study did not fully support my prediction (Figure 5.1), I have gained instead a more nuanced understanding of the drivers of microbial N_2O consumption, and this can be beneficial for future N_2O consumption management strategies.

Primarily, it is too simplistic to consider an entire soil microcosm, even at the scale of a 0.5 L jar, susceptible to one OC threshold. Soils are not homogeneous, and unsaturated soils can have many anoxic microsites that OC amendment cannot readily penetrate (Ebrahimi et al. 2016). Additionally, aggregate sizes differ among and within soils, and these different sizes can impact substrate and gas diffusion rates, thus impacting OC delivery to anoxic aggregate centers (Schlüter et al. 2018). Indeed, soil heterogeneity contributes to many possible N_2O production or consumption outcomes because across tiny spatial scales, no two environments are the same (Harms et al. 2009). More specifically, the soil redox conditions that affect N_2O consumption also affect N_2O production (Palta et al. 2014, Badagliacca et al. 2018, Luo et al. 2021). For example, when soils become more reducing, that can contribute to NO_3^- reduction, rather than N_2O reduction (Palta et al. 2014). These differences in microbial N-transformations can be mediated by soil properties that contribute to substrate availability, microbial enzyme activity, or O_2 availability, such as NO_3^- (Friedl et al. 2020), pH (Blum et al. 2018), and soil texture (Table 5.2; Keiluweit et al. 2017). Invariably, this suite of conditions becomes complex, and challenges our efforts to manage N_2O emissions by focusing only on N_2O consumption. However, to better understand N_2O consumption management options, we must be able to make sense of the diverse N_2O flux responses to OC additions (Figure 5.1).

4.1 Drivers of N_2O consumption disagree with previous studies

N_2O consumption *can* be stimulated via OC additions to diminish N_2O emissions, but the drivers behind this stimulation are not straightforward. N_2O consumption increased in 11 out of 28 treatment soils, but while proximal soil and microbial measurements support previous trends, they also illuminate discrepancies between my findings and other studies.

My study revealed an association between Δ N_2O consumption and Δ microbial respiration (Figure 5.4). In response to +OC treatment, microbial respiration increased, although there was some variation with how much respiration increased with successive +OC treatments (Figure 5.2). This heightened microbial activity likely depleted soil O_2 and contributed to an increased volume of reducing regions (Stevenson et al. 2011, Wu et al. 2013, Wang et al. 2021), which created more sites for N_2O consumption in particular soils (Table 5.2; Ribas et al. 2019). I do not see the same association between N_2O emissions and microbial respiration (Figure 5.3), which indicates that the added OC has a stronger effect on N_2O consumption than N_2O emission. This contradicts Yang and Silver's (2016) findings. In a northern California cornfield, they found that the greatest predictor of N_2O production and consumption was microbial respiration, likely because it is a proxy for labile C availability for denitrification. However, my findings suggest that if microbial respiration is correlated with consumption but not emissions perhaps these denitrifier-targeted amendments are specifically targeting N_2O reducers, rather than N_2O producers and reducers.

My analyses of clade I and clade II nosZ gene abundance somewhat align with this notion (Figures 5.7 and 5.8). Across all soils, clade I nosZ gene abundance increased with successively increasing OC additions. The treatment effect was significant ($p < 0.0001$), which supports this broad trend, although there were not always significant differences in gene abundance within a given soil type (Figure 5.7). Previous studies have illustrated a positive relationship between clade I nosZ abundance and SOC (Barrett et al. 2016, Wang et al. 2020), and while previous work (Luo et al. 2021) has also illustrated a positive relationship between clade II nosZ abundance and SOC, in my study clade II nosZ was less responsive to OC additions than clade I nosZ (Figure 5.8). Previous work has also shown a correlation between

increased N_2O uptake and increased clade I (Barett et al. 2016) and clade II (Xu et al. 2020) nosZ abundance. Interestingly, in my study it also was not always the soils that showed the greatest increases in nosZ following OC-amendment (Figures 5.7 and 5.8) that showed the greatest increases in N_2O consumption (Figure 5.1). This indicates that perhaps the soils that consumed the most N_2O already had abundant clade I and II nosZ genes, so abundances did not change appreciably in response to added OC.

Together these findings, (1) associations between Δ microbial respiration and Δ N_2O consumption but not Δ emissions, and (2) a lack of associations between Δ nosZ gene abundances and Δ N_2O consumption, call several mechanistic drivers of N_2O consumption into question. My results indicate that certain OC additions specifically contribute to N_2O consumption, not N_2O production, and my results also indicate that increases in nosZ might not be as important predictors of N_2O consumption as previously thought (e.g., Buchen et al. 2019). These discrepancies could be important for explaining and anticipating N_2O consumption behaviors in soils and future studies should see if these trends hold in other soils or in field settings.

4.2 Drivers of ICDE in soils

From a management perspective, it is important to understand why some situations led to the desired outcome of ICDE, particularly if the drivers of increased consumption and decreased emissions deviated from previous trends. These deviations could be useful for expanding understanding of N_2O flux responses to different OC treatments.

The desert shrubland and desert grassland-Low OC soils all showed ICDE, and these soils were generally characterized by small changes in soil IN (Figure 5.5), associations with

nirS, nifH, and clade II nosZ (Figure 5.6), some increases in clade I nosZ (both soils; Figure 5.7) and clade II nosZ (only desert grassland-Low OC; Figure 5.8), low SOC and SON (Figure 5.9), and high soil pH (Figure 5.10). The general lack of change in IN for ICDE soils indicates that either available NO_3^- was getting rapidly reduced as it was getting nitrified, or the low NO_3^- availability is what precipitated increased N_2O consumption (Senbayram et al. 2019).

Furthermore, it is interesting that these soils associated with Δ nirS and Δ clade II nosZ gene abundances (Figure 5.6). Although nirS is a gene associated with N_2O production, microbes harboring nirS typically also harbor clade I nosZ (Graf et al. 2014, Shan et al. 2021). Even though all soils that showed ICDE also showed increases in clade I nosZ, those soils associated with nirS, but not with clade I nosZ (Figure 5.6). Rather, the ICDE soils associated with clade II nosZ (Figure 5.6), even though only the desert grassland-Low OC soil showed an increase in clade II nosZ (Figure 5.8). Collectively, these findings support that these "atypical" denitrifiers (those harboring clade II nosZ, Sanford et al. 2012) are an important mediator of soil N_2O sink capacity (Jones et al. 2013, Jones et al. 2014), and that they might have been abundant in these soils irrespective of OC amendment. Conthe et al. (2018) describe that clade II N_2O reducers are more likely to be in soils with fewer episodic N_2O emission pulses, like desert soils, where they can constantly serve as background reducers. Thus, it makes sense that the two desert soils would be associated with clade II nosZ. Additionally, perhaps the association with nirS illustrates an N_2O reduction potential, wherein if a large fraction of the microbial community harbors nirS, then they *can* stimulate N_2O consumption by increasing clade I nosZ gene abundance in response to +OC treatment (Figure 5.7).

The interaction between these genes and soil pH partly contradicts previous findings (Figure 5.10). Luo et al. (2021) reported that clade II nosZ was negatively correlated with soil

pH, but these desert soils have the two highest pHs of all the soils tested (Figure 5.10). However, it is understood that the NosZ enzyme, transcribed from clade I nosZ, has increased activity under higher pH (Richardson et al. 2009). Perhaps, given the largely unexplored clade II nosZ gene, it is possible that denitrification enzymes produced from certain microbes harboring this gene perform better at higher pH.

Finally, both the desert shrubland and grassland soils had the lowest SOC and SON percentages among all soils (Figure 5.9). Following certain +OC treatments, some of the ICDE soils showed significant increases in clade I or clade II nosZ abundance. The literature has been largely in agreement about the positive association between OC additions and nosZ abundance, so my findings align with expectations (Barrett et al. 2016, Buchen et al. 2019, Duan et al. 2019, Dai et al. 2019, Aamer et al. 2020, Guo et al. 2020). However, the increases I observed did not occur for all ICDE soils, and not necessarily all increases were large. This harks back to the notion in Section 4.1 that perhaps the relationship between N_2O consumption and nosZ gene abundance is less straightforward than previously thought.

Collectively, the soils that showed ICDE had very specific soil C and N circumstances that likely contributed to their unique microbial genetic compositions and N_2O flux responses. However, if other soils do not "thread the needle" in the same specific way, it remains to be seen if they *can* show ICDE. Addressing this will require follow-up work. Future studies could examine how inherent soil C and N status interact with different OC amendments to effect N_2O flux.

4.3 Other N_2O flux responses

Although most of the soils I incubated did not show ICDE, it is still important to understand their behaviors; their responses to the +OC treatment could be useful for N_2O management strategies. Indeed, seven soils showed ICIE, eight soils showed DCDE, and two soils showed DCIE (Figure 5.1). From a management perspective, the ICIE and DCDE soils are of interest because N_2O consumption increased markedly in some ICIE soils, and while the DCDE soils did not increase N_2O consumption, they did decrease N_2O emissions.

The majority of ICIE soils (limited irrigation cornfield and alpine meadow soils) were characterized by moderate to minimal changes in NO_3^- and increases in NH_4^+ (Figure 5.5), and comparable increases in clade I and clade II nosZ (Figures 5.7 and 5.8). However, the soils largely differed in their Δ respiration, which genes they associated with (Figure 5.6), SOC and SON (Figure 5.9), and soil pH (Figure 5.10). The conventional cornfield-Medium OC soil also exhibited unique responses to +OC treatment. The similarities and differences among these soils are puzzling, as I would expect some unifying features to contribute to the same N_2O flux response, as I observed with the ICDE soils.

For the limited irrigation cornfield and alpine meadow soil IN responses, it is also puzzling that NH_4^+ increased whereas NO_3^- did not, given that N_2O emissions increased in the ICIE soils (Senbayram et al. 2019). Wang et al. (2016) observed rapid NH_4^+ to NO_3^- conversion when they fertilized wheat crops with NH_4^+ fertilizer, so it is possible the NH_4^+ in these soils was rapidly nitrified and then rapidly reduced to N_2O or to N_2. Alternatively, the limited irrigation cornfield soils showed some substantial decreases in NO_3^- abundance from before vs. after +OC treatment, which aligns with literature expectations. Wen et al. (2017) observed a strong, positive correlation between N_2O production and consumption, and both processes were mediated by soil

NO_3^- availability, so perhaps the drawdown in soil NO_3^- supported N_2O production and consumption in the limited irrigation cornfield soils.

However, neither soil increased clade I nosZ abundance appreciably (Figure 5.7), though the alpine meadow-Low OC clade II nosZ abundance notably increased, but not significantly (Figure 5.8). This further suggests that certain soils already had the genetic capacity to reduce N_2O, regardless of +OC treatment, but it is strange that the alpine meadow soils positively associated with nirK and clade I nosZ, while the limited irrigation and conventional cornfield soils did not (Figure 5.6). I hypothesize that enzymes involved in incomplete and complete denitrification could help explain these outcomes, as perhaps enzyme activity was greater in these soils (Bakken et al. 2012). Perhaps in the more acidic alpine meadow soils (Figure 5.10) the nirK and clade I nosZ abundances were more important for showing ICIE than in the cornfields, where higher pH (Figure 5.10) might create more amenable conditions for denitrification enzymes (Blum et al. 2018). While studies examining N_2O production and consumption typically measure N-cycling gene abundances, perhaps future work should consider incorporating denitrification enzyme activity, as it might be an important explanatory variable.

The majority of DCDE soils (shortgrass prairie and subalpine forest soils), were characterized by successively decreasing microbial respiration with increased OC amendments (Figure 5.2), minimal changes in soil NO_3^- but increases in soil NH_4^+ (Figure 5.5), minimal changes in clade II nosZ gene abundance (Figure 5.8), and lower soil pH (Figure 5.10). However, the soils differed in that the subalpine forest soils associated with nirK and clade I nosZ while the shortgrass prairie soils did not (Figure 5.6), the subalpine forest soils showed increased clade I nosZ while the shortgrass prairie soils did not, and the subalpine forest soils had markedly higher SOC and SON that the shortgrass prairie soils (Figure 5.9).

The subalpine forest is an interesting situation, in that those soils are characterized by high organic matter (Figure 5.9), low soil NO_3^- (Figure 5.5), and associate with denitrifying genes (Figure 5.6), suggesting they should be good candidates for ICDE (Miller et al. 2009, Mitchell et al. 2013, Wu et al. 2018, Duan et al. 2019). However, it is notable that the subalpine forest Δ microbial respiration was so small compared to other soils (Figure 5.2). I hypothesize the OC additions could have had an acidifying effect on the subalpine forest soils. The +OC treatment is a blend of organic acids and adding sufficiently high concentrations of those acids to soils with an already low pH (~5 for the subalpine soils) could have reduced pH to the point where microbial activity was depressed and also denitrification enzyme activities for nirK and clade I nosZ were depressed (Richardson et al. 2009, Bakken et al. 2012).

It is not immediately clear why the shortgrass prairie soils showed DCDE (Figure 5.1). Generally, it appears that soil and microbial properties were less stimulated by any of the +OC treatments. Or if properties did not exhibit a large Δ increase, they decreased, such as soil NO_3^- (Figure 5.5) or clade II nosZ gene abundance (Figure 5.8). This highlights the possibility that some soils might not necessarily be ideal candidates for OC amendments to stimulate N_2O consumption, as they just might not be responsive to amendment.

4.4 Reducing N_2O emissions other ways?

While the intention of this study was to further explore the potential of inducing ICDE in diverse soils, it is intriguing to consider that this work generated alternative possibilities to ICDE for decreasing N_2O emissions. ICIE soils did increase N_2O consumption markedly, although they increased emissions markedly, too. It would be ideal if we could develop a way to increase N_2O consumption *more* than N_2O emissions. To my knowledge, this has never been observed in soils, but it may be possible through bioengineering the NosZ enzyme, an emerging area of research

(Stein 2020). Furthermore, while DCDE soils did not show the outcome I predicted, it could still be viewed as a management "win" if N_2O emissions decreased. The subalpine forest soil indicated that +OC treatment likely depressed soil pH, contributing to reduced microbial activity and denitrification enzyme activity. Conversely, the shortgrass prairie soil indicated that it was not responsive to +OC treatment. While I would not necessarily advocate for pickling soils to decrease N_2O emissions, certain soils could be good candidates for OC additions to decrease overall denitrification activities. It remains to be seen if this will have adverse effects on soil properties or microbial community composition, which warrants future studies. However, while this study may show that OC amendments are not necessarily a ubiquitous solution to decreasing N_2O emissions, there are evidently multiple paths forward.

CHAPTER 5 REFERENCES

Aamer, M., Shaaban, M., Hassan, M. U., Guoqin, H., Ying, L., Hai Ying, T., … Peng, Z. (2020). Biochar mitigates the N2O emissions from acidic soil by increasing the nosZ and nirK gene abundance and soil pH. *Journal of Environmental Management*, *255*(November 2019), 109891. https://doi.org/10.1016/j.jenvman.2019.109891

Badagliacca, G., Benítez, E., Amato, G., Badalucco, L., Giambalvo, D., Laudicina, V. A., & Ruisi, P. (2018). Long-term no-tillage application increases soil organic carbon, nitrous oxide emissions and faba bean (Vicia faba L.) yields under rain-fed Mediterranean conditions. *Science of the Total Environment*, *639*, 350–359. https://doi.org/10.1016/j.scitotenv.2018.05.157

Bakken, L. R., Bergaust, L., Liu, B., & Frostegård, Å. (2012). Regulation of denitrification at the cellular level: A clue to the understanding of N2O emissions from soils. *Philosophical Transactions of the Royal Society B: Biological Sciences*, *367*(1593), 1226–1234. https://doi.org/10.1098/rstb.2011.0321

Bakken, L. R., & Frostegård, Å. (2017). Sources and sinks for N2O, can microbiologist help to mitigate N2O emissions? *Environmental Microbiology*, *19*(12), 4801–4805. https://doi.org/10.1111/1462-2920.13978

Barrett, M., Khalil, M. I., Jahangir, M. M. R., Lee, C., Cardenas, L. M., Collins, G., … O'Flaherty, V. (2016). Carbon amendment and soil depth affect the distribution and abundance of denitrifiers in agricultural soils. *Environmental Science and Pollution Research*, *23*(8), 7899–7910. https://doi.org/10.1007/s11356-015-6030-1

Buchen, C., Roobroeck, D., Augustin, J., Behrendt, U., Boeckx, P., & Ulrich, A. (2019). High N 2 O consumption potential of weakly disturbed fen mires with dissimilar denitrifier community structure. *Soil Biology and Biochemistry*, *130*(July 2018), 63–72. https://doi.org/10.1016/j.soilbio.2018.12.001

Butterbach-Bahl, K., & Dannenmann, M. (2011). Denitrification and associated soil N2O emissions due to agricultural activities in a changing climate. *Current Opinion in Environmental Sustainability*, *3*(5), 389–395. https://doi.org/10.1016/j.cosust.2011.08.004

Chapuis-Lardy, L., Wrage, N., Metay, A., Chotte, J. L., & Bernoux, M. (2007). Soils, a sink for N2O? A review. *Global Change Biology*, *13*(1), 1–17. https://doi.org/10.1111/j.1365-2486.2006.01280.x

Chee-Sanford, J. C., Connor, L., Krichels, A., Yang, W. H., & Sanford, R. A. (2020). Hierarchical detection of diverse Clade II (atypical) nosZ genes using new primer sets for classical- and multiplex PCR array applications. *Journal of Microbiological Methods*, *172*(March), 105908. https://doi.org/10.1016/j.mimet.2020.105908

Christensen, S., Gera Hol, W. H., Kurm, V., & Vestergård, M. (2021). Increased likelihood of high nitrous oxide (N2o) exchange in soils at reduced microbial diversity. *Sustainability (Switzerland)*, *13*(4), 1–8. https://doi.org/10.3390/su13041685

Conthe, M., Parchen, C., Stouten, G., Kleerebezem, R., & van Loosdrecht, M. C. M. (2018). O2 versus N2O respiration in a continuous microbial enrichment. *Applied Microbiology and Biotechnology*, *102*(20), 8943–8950. https://doi.org/10.1007/s00253-018-9247-3

Conthe, M., Wittorf, L., Kuenen, J. G., Kleerebezem, R., Van Loosdrecht, M. C. M., & Hallin, S. (2018). Life on N2O: Deciphering the ecophysiology of N2O respiring bacterial

communities in a continuous culture. *ISME Journal*, *12*(4), 1142–1153. https://doi.org/10.1038/s41396-018-0063-7

Conthe, M., Lycus, P., Arntzen, M., Ramos da Silva, A., Frostegård, Å., Bakken, L. R., … van Loosdrecht, M. C. M. (2019). Denitrification as an N2O sink. *Water Research*, *151*, 381–387. https://doi.org/10.1016/j.watres.2018.11.087

Dai, Z., Li, Y., Zhang, X., Wu, J., Luo, Y., Kuzyakov, Y., … Xu, J. (2019). Easily mineralizable carbon in manure-based biochar added to a soil influences N 2 O emissions and microbial-N cycling genes. *Land Degradation and Development*, *30*(4), 406–416. https://doi.org/10.1002/ldr.3230

Duan, P., Zhang, Q., Zhang, X., & Xiong, Z. (2019). Mechanisms of mitigating nitrous oxide emissions from vegetable soil varied with manure, biochar and nitrification inhibitors. *Agricultural and Forest Meteorology*, *278*(December 2018), 107672. https://doi.org/10.1016/j.agrformet.2019.107672

Ebrahimi, A., & Or, D. (2016). Microbial community dynamics in soil aggregates shape biogeochemical gas fluxes from soil profiles - upscaling an aggregate biophysical model. *Global Change Biology*, *22*(9), 3141–3156. https://doi.org/10.1111/gcb.13345

Friedl, J., Scheer, C., De Rosa, D., Müller, C., Grace, P. R., & Rowlings, D. W. (2021). Sources of nitrous oxide from intensively managed pasture soils: The hole in the pipe. *Environmental Research Letters*, *16*(6). https://doi.org/10.1088/1748-9326/abfde7

Guo, B., Zheng, X., Yu, J., Ding, H., Pan, B., Luo, S., & Zhang, Y. (2020). Dissolved organic carbon enhances both soil N2O production and uptake. *Global Ecology and Conservation*, *24*, e01264. https://doi.org/10.1016/j.gecco.2020.e01264

Harms, T. K., Wentz, E. A., & Grimm, N. B. (2009). Spatial heterogeneity of denitrification in semi-arid floodplains. *Ecosystems*, *12*(1), 129–143. https://doi.org/10.1007/s10021-008-9212-6

Hein, S., & Simon, J. (2019). Bacterial nitrous oxide respiration: electron transport chains and copper transfer reactions. *Advances in Microbial Physiology*, *75*, 137–175. https://doi.org/10.1016/bs.ampbs.2019.07.001

Henderson, S. L., Dandie, C. E., Patten, C. L., Zebarth, B. J., Burton, D. L., Trevors, J. T., & Goyer, C. (2010). Changes in denitrifier abundance, denitrification gene mRNA levels, nitrous oxide emissions, and denitrification in anoxic soil microcosms amended with glucose and plant residues. *Applied and Environmental Microbiology*, *76*(7), 2155–2164. https://doi.org/10.1128/AEM.02993-09

Henry, S., Bru, D., Stres, B., Hallet, S., & Philippot, L. (2006). Quantitative detection of the nosZ gene, encoding nitrous oxide reductase, and comparison of the abundances of 16S rRNA, narG, nirK, and nosZ genes in soils. *Applied and Environmental Microbiology*, *72*(8), 5181–5189. https://doi.org/10.1128/AEM.00231-06

Highton, M. P., Bakken, L. R., Dörsch, P., Wakelin, S., de Klein, C. A. M., Molstad, L., & Morales, S. E. (2020). Soil N2O emission potential falls along a denitrification phenotype gradient linked to differences in microbiome, rainfall and carbon availability. *Soil Biology and Biochemistry*, *150*(September). https://doi.org/10.1016/j.soilbio.2020.108004

Houser, M., & Stuart, D. (2020). An accelerating treadmill and an overlooked contradiction in industrial agriculture: Climate change and nitrogen fertilizer. *Journal of Agrarian Change*, *20*(2), 215–237. https://doi.org/10.1111/joac.12341

Jones, C. M., Graf, D. R. H., Bru, D., Philippot, L., & Hallin, S. (2013). The unaccounted yet abundant nitrous oxide-reducing microbial community: A potential nitrous oxide sink. *ISME Journal*, *7*(2), 417–426. https://doi.org/10.1038/ismej.2012.125

Keiluweit, M., Gee, K., Denney, A., & Fendorf, S. (2018). Anoxic microsites in upland soils dominantly controlled by clay content. *Soil Biology and Biochemistry*, *118*(December 2017), 42–50. https://doi.org/10.1016/j.soilbio.2017.12.002

Lam, S. K., Suter, H., Mosier, A. R., & Chen, D. (2017). Using nitrification inhibitors to mitigate agricultural N2O emission: a double-edged sword? *Global Change Biology*, *23*(2), 485–489. https://doi.org/10.1111/gcb.13338

Liang, L. L., Eberwein, J. R., Allsman, L. A., Grantz, D. A., & Jenerette, G. D. (2015). Regulation of CO2 and N2O fluxes by coupled carbon and nitrogen availability. *Environmental Research Letters*, *10*(3). https://doi.org/10.1088/1748-9326/10/3/034008

Luo, X., Zeng, L., Wang, L., Qian, H., Hou, C., Wen, S., … Chen, W. (2021). Abundance for subgroups of denitrifiers in soil aggregates asscociates with denitrifying enzyme activities under different fertilization regimes. *Applied Soil Ecology*, *166*(March), 103983. https://doi.org/10.1016/j.apsoil.2021.103983

McMillan, A. M. S., Pal, P., Phillips, R. L., Palmada, T., Berben, P. H., Jha, N., … Luo, J. (2016). Can pH amendments in grazed pastures help reduce N2O emissions from denitrification? - The effects of liming and urine addition on the completion of denitrification in fluvial and volcanic soils. *Soil Biology and Biochemistry*, *93*, 90–104. https://doi.org/10.1016/j.soilbio.2015.10.013

Miller, M. N., Zebarth, B. J., Dandie, C. E., Burton, D. L., Goyer, C., & Trevors, J. T. (2009). Influence of Liquid Manure on Soil Denitrifier Abundance, Denitrification, and Nitrous Oxide Emissions. *Soil Science Society of America Journal*, *73*(3), 760–768. https://doi.org/10.2136/sssaj2008.0059

Mitchell, D. C., Castellano, M. J., Sawyer, J. E., & Pantoja, J. (2013). Cover Crop Effects on Nitrous Oxide Emissions: Role of Mineralizable Carbon. *Soil Science Society of America Journal*, *77*(5), 1765–1773. https://doi.org/10.2136/sssaj2013.02.0074

Palta, M. M., Ehrenfeld, J. G., & Groffman, P. M. (2014). "Hotspots" and "Hot Moments" of Denitrification in Urban Brownfield Wetlands. *Ecosystems*, *17*(7), 1121–1137. https://doi.org/10.1007/s10021-014-9778-0

Reay, D. S., Davidson, E. a., Smith, K. a., Smith, P., Melillo, J. M., Dentener, F., & Crutzen, P. J. (2012). Global agriculture and nitrous oxide emissions. *Nature Climate Change*, *2*(6), 410–416. https://doi.org/10.1038/nclimate1458

Ribas, A., Mattana, S., Llurba, R., Debouk, H., Sebastià, M. T., & Domene, X. (2019). Biochar application and summer temperatures reduce N2O and enhance CH4 emissions in a Mediterranean agroecosystem: Role of biologically-induced anoxic microsites. *Science of the Total Environment*, *685*, 1075–1086. https://doi.org/10.1016/j.scitotenv.2019.06.277

Roman-Perez, C. C., & Hernandez-Ramirez, G. (2021). Sources and priming of nitrous oxide production across a range of moisture contents in a soil with high organic matter. *Journal of Environmental Quality*, *50*(1), 94–109. https://doi.org/10.1002/jeq2.20172

Sanford, R. A., Wagner, D. D., Wu, Q., Chee-Sanford, J. C., Thomas, S. H., Cruz-García, C., … Löffler, F. E. (2012). Unexpected nondenitrifier nitrous oxide reductase gene diversity and abundance in soils. *Proceedings of the National Academy of Sciences of the United States of America*, *109*(48), 19709–19714. https://doi.org/10.1073/pnas.1211238109

Schlesinger, W. H. (2013). An estimate of the global sink for nitrous oxide in soils. *Global Change Biology*, *19*(10), 2929–2931. https://doi.org/10.1111/gcb.12239
Schlüter, S., Henjes, S., Zawallich, J., Bergaust, L., Horn, M., Ippisch, O., … Dörsch, P. (2018). Denitrification in soil aggregate analogues-effect of aggregate size and oxygen diffusion. *Frontiers in Environmental Science*, *6*(APR), 1–10. https://doi.org/10.3389/fenvs.2018.00017
Schlüter, S., Zawallich, J., Vogel, H. J., & Dörsch, P. (2019). Physical constraints for respiration in microbial hotspots in soil and their importance for denitrification. *Biogeosciences*, *16*(18), 3665–3675. https://doi.org/10.5194/bg-16-3665-2019
Schulz, S., Kölbl, A., Ebli, M., Buegger, F., Schloter, M., & Fiedler, S. (2017). Field-Scale Pattern of Denitrifying Microorganisms and N2O Emission Rates Indicate a High Potential for Complete Denitrification in an Agriculturally Used Organic Soil. *Microbial Ecology*, *74*(4), 765–770. https://doi.org/10.1007/s00248-017-0991-1
Senbayram, M., Budai, A., Bol, R., Chadwick, D., Marton, L., Gündogan, R., & Wu, D. (2019). Soil NO 3− level and O 2 availability are key factors in controlling N 2 O reduction to N 2 following long-term liming of an acidic sandy soil. *Soil Biology and Biochemistry*, *132*(3), 165–173. https://doi.org/10.1016/j.soilbio.2019.02.009
Shan, J., Sanford, R. A., Chee-Sanford, J., Ooi, S. K., Löffler, F. E., Konstantinidis, K. T., & Yang, W. H. (2021). Beyond denitrification: The role of microbial diversity in controlling nitrous oxide reduction and soil nitrous oxide emissions. *Global Change Biology*, (October 2020), 1–15. https://doi.org/10.1111/gcb.15545
Smith, K. A. (2017). Changing views of nitrous oxide emissions from agricultural soil: key controlling processes and assessment at different spatial scales. *European Journal of Soil Science*, *68*(2), 137–155. https://doi.org/10.1111/ejss.12409
Stein, L. Y. (2020). The Long-Term Relationship between Microbial Metabolism and Greenhouse Gases. *Trends in Microbiology*, *28*(6), 500–511. https://doi.org/10.1016/j.tim.2020.01.006
Stuchiner, E. R., Weller, Z. D., & Fischer, J. C. (2020). An approach for calibrating laser-based N 2 O isotopic analyzers for soil biogeochemistry research . *Rapid Communications in Mass Spectrometry*, (June 2020), 1–14. https://doi.org/10.1002/rcm.8978
Subbarao, G., Ito, O., Sahrawat, K., Berry, W., Nakahara, K., Ishikawa, T., … Rao, I. (2006). Scope and strategies for regulation of nitrification in agricultural systems - Challenges and opportunities. *Critical Reviews in Plant Sciences*, *25*(4), 303–335. https://doi.org/10.1080/07352680600794232
Thilakarathna, S. K., & Hernandez-Ramirez, G. (2021). How does management legacy, nitrogen addition, and nitrification inhibition affect soil organic matter priming and nitrous oxide production? *Journal of Environmental Quality*, *50*(1), 78–93. https://doi.org/10.1002/jeq2.20168
Van Meter, K. J., Basu, N. B., Veenstra, J. J., & Burras, C. L. (2016). The nitrogen legacy: Emerging evidence of nitrogen accumulation in anthropogenic landscapes. *Environmental Research Letters*, *11*(3). https://doi.org/10.1088/1748-9326/11/3/035014
Wang, N., Luo, J. L., Juhasz, A. L., Li, H. B., & Yu, J. G. (2020). Straw decreased N2O emissions from flooded paddy soils via altering denitrifying bacterial community compositions and soil organic carbon fractions. *FEMS Microbiology Ecology*, *96*(5), 1–11. https://doi.org/10.1093/femsec/fiaa046

Wang, Z. H., Miao, Y. fang, & Li, S. X. (2016). Wheat responses to ammonium and nitrate N applied at different sown and input times. *Field Crops Research*, *199*, 10–20. https://doi.org/10.1016/j.fcr.2016.09.002

Wang, B., Brewer, P. E., Shugart, H. H., Lerdau, M. T., & Allison, S. D. (2019). Soil aggregates as biogeochemical reactors and implications for soil–atmosphere exchange of greenhouse gases—A concept. *Global Change Biology*, *25*(2), 373–385. https://doi.org/10.1111/gcb.14515

Wen, Y., Chen, Z., Dannenmann, M., Carminati, A., Willibald, G., Kiese, R., … Corre, M. D. (2016). Disentangling gross N2O production and consumption in soil. *Scientific Reports*, *6*(October), 1–8. https://doi.org/10.1038/srep36517

Wu, D., Wei, Z., Well, R., Shan, J., Yan, X., Bol, R., & Senbayram, M. (2018). Straw amendment with nitrate-N decreased N2O/(N2O+N2) ratio but increased soil N2O emission: A case study of direct soil-born N2 measurements. *Soil Biology and Biochemistry*, *127*(October), 301–304. https://doi.org/10.1016/j.soilbio.2018.10.002

Xu, X., Liu, Y., Singh, B. P., Yang, Q., Zhang, Q., Wang, H., … Li, Y. (2020). NosZ clade II rather than clade I determine in situ N2O emissions with different fertilizer types under simulated climate change and its legacy. *Soil Biology and Biochemistry*, *150*(August), 107974. https://doi.org/10.1016/j.soilbio.2020.107974

Zhou, M., Zhu, B., Wang, S., Zhu, X., Vereecken, H., & Brüggemann, N. (2017). Stimulation of N2O emission by manure application to agricultural soils may largely offset carbon benefits: a global meta-analysis. *Global Change Biology*, *23*(10), 4068–4083. https://doi.org/10.1111/gcb.13648

Zhu, K., Bruun, S., Larsen, M., Glud, R. N., & Jensen, L. S. (2015). Heterogeneity of O2 dynamics in soil amended with animal manure and implications for greenhouse gas emissions. *Soil Biology and Biochemistry*, *84*, 96–106. https://doi.org/10.1016/j.soilbio.2015.02.012

CHAPTER 6: SUMMARY AND CONCLUSIONS

The purpose of this dissertation was to expand our understanding of the drivers of N_2O production and consumption in soils. N_2O emissions present a critical threat to the warming of earth's atmosphere (Tian et al. 2020) and to the depletion of earth's stratospheric ozone layer (Ravishankara et al. 2009). Being able to understand the soil and microbial properties that control net N_2O fluxes will be crucial to a more sustainable future. In this dissertation, I sought to address three broad questions: (1) What strategies do we have to robustly measure N_2O production and consumption processes? (2) What are the most important processes driving N_2O fluxes from soils? (3) How can we effectively manage N_2O emissions, given its diffuse and diverse sources?

I addressed the first question in Chapter 2 by developing a calibration algorithm for a laser-based N_2O isotopic analyzer. These analyzers are easy to use, high throughput, relatively inexpensive (Stuchiner et al. 2020), and have the potential to be field-deployable (Ibraim et al. 2018), which could allow for high precision *in situ* measurements like never before. However, the primary deterrent standing in their way is calibration and analytical precision challenges (Ostrom and Ostrom 2017). The calibration algorithm I developed helps mitigate these challenges and can serve as a roadmap for other labs to use laser-based methods to measure N_2O production and consumption processes.

I addressed the second question in Chapter 3, where I used a paired natural abundance and isotopic enrichment approach to disentangle among N_2O-generating source processes in different soils. I found that denitrification, be it fungal or bacterial, was the dominant N_2O-generating source process in all soils across all experimental conditions. These findings have

implications for how we prioritize managing N_2O emissions moving forward. It could be that management efforts should prioritize controlling denitrification, given that my work (Stuchiner et al., in review), and a growing body of literature (Ostrom et al. 2010, Baggs 2011, Fang et al. 2015, Krause et al. 2017, Harris et al. 2021), suggests that other N_2O production processes make far smaller contributions to net N_2O emissions.

I also addressed the second question in Chapters 4 and 5, where I examined the properties that drive N_2O consumption using an isotope pool dilution assay (von Fischer and Hedin 2002, Yang et al. 2011). In Chapter 4 I developed a novel framework for anticipating ICDE in soils. I hypothesized that as soils are freed from electron donor limitation via OC amendment, soil microbes will expand regions of anoxia that are thermodynamically favorable for N_2O consumption. In Chapter 5, I sought to expand upon this idea by amending soils with successively increasing levels of OC to help all tested soils show ICDE. However, I learned that inducing ICDE requires a delicate balance of soil and microbial dynamics. But I also gained greater understanding of the important drivers of N_2O consumption and importantly, clade II nosZ, a novel and minimally studied N_2O reducing gene. This work revealed to me a broader range of possible strategies for decreasing N_2O emissions by N_2O consumption, even if the primary method is not necessarily ICDE.

The third question, how can we effectively manage N_2O emissions, I sought to jointly address in all my research chapters, but this is an ongoing, and nuanced, question. First and foremost, N_2O management will improve when we have heightened capacity to precisely, and efficiently, measure N_2O production and consumption processes. My work developing a calibration algorithm for a laser-based N_2O isotopic analyzer brings us one step closer to achieving that goal. We also need to prioritize management efforts to focus on the most

important sources of N_2O. My work in Chapter 3, and the work of others, indicates that denitrification is the primary source of N_2O from soils (Ostrom et al. 2010, Baggs 2011, Fang et al. 2015, Krause et al. 2017, Harris et al. 2021). Additionally, agricultural soils are the largest source of soil-emitted N_2O (Reay et al. 2012, Smith 2017, Houser and Stuart 2020, Kanter et al. 2020). While agricultural management efforts have mainly prioritized improving fertilization regimes (Bakken and Frostegard 2017) or developing nitrification inhibitors for crop soils (Subbarao et al. 2006, Van Meter et al. 2016, Lam et al. 2017), it could be the more important process to manage is denitrification. I sought to address the denitrification management issue in Chapters 4 and 5 by working to better understand the drivers of N_2O consumption. It turns out that soil redox heterogeneity creates a really complicated suite of factors to consider in order to effectively stimulate N_2O consumption in soils. This suggests that we might need a more coordinated effort to systematically address the drivers and roadblocks to N_2O consumption, such that we can effectively regulate this process and manage net N_2O fluxes.

Recently, Almaraz et al. (2020) proposed the development of a Global Denitrification Research Network, a network that coordinates multi-site experiments and ensures consistent data collection protocols for research continuity. This network would be modelled after the Nutrient Network (NutNet) and involve a broad and interdisciplinary group of researchers spanning many institutions with lab capacities to perform sophisticated denitrification studies. Ideally, efforts like these interdisciplinary and coordinated collaborations to improve understanding of the denitrification pathway will be crucial to N_2O management. Denitrification is the primary driver of N_2O emissions, *and* the sole biotic pathway for N_2O removal. It seems that the most effective path forward will be thoroughly plumbing the complexity of denitrification. Only then can we best understand how to reduce emissions and stimulation N_2O consumption.

CHAPTER 6 REFERENCES

Almaraz, M., Wong, M. Y., & Yang, W. H. (2020). Looking back to look ahead: a vision for soil denitrification research. *Ecology*, *101*(1), 1–10. https://doi.org/10.1002/ecy.2917

Bakken, L. R., & Frostegård, Å. (2017). Sources and sinks for N2O, can microbiologist help to mitigate N2O emissions? *Environmental Microbiology*, *19*(12), 4801–4805. https://doi.org/10.1111/1462-2920.13978

Fang, Y., Koba, K., Makabe, A., Takahashi, C., Zhu, W., Hayashi, T., … Yoh, M. (2015). Microbial denitrification dominates nitrate losses from forest ecosystems. *Proceedings of the National Academy of Sciences of the United States of America*, *112*(5), 1470–1474. https://doi.org/10.1073/pnas.1416776112

Harris, E., Diaz-Pines, E., Stoll, E., Schloter, M., Schulz, S., Duffner, C., … Bahn, M. (2021). Denitrifying pathways dominate nitrous oxide emissions from managed grassland during drought and rewetting. *Science Advances*, *7*(6). https://doi.org/10.1126/sciadv.abb7118

Houser, M., & Stuart, D. (2020). An accelerating treadmill and an overlooked contradiction in industrial agriculture: Climate change and nitrogen fertilizer. *Journal of Agrarian Change*, *20*(2), 215–237. https://doi.org/10.1111/joac.12341

Kanter, D. R., Ogle, S. M., & Winiwarter, W. (2020). Building on Paris: integrating nitrous oxide mitigation into future climate policy. *Current Opinion in Environmental Sustainability*, *47*, 7–12. https://doi.org/10.1016/j.cosust.2020.04.005

Krause, H. M., Thonar, C., Eschenbach, W., Well, R., Mäder, P., Behrens, S., … Gattinger, A. (2017). Long term farming systems affect soils potential for N2O production and reduction processes under denitrifying conditions. *Soil Biology and Biochemistry*, *114*, 31–41. https://doi.org/10.1016/j.soilbio.2017.06.025

Lam, S. K., Suter, H., Mosier, A. R., & Chen, D. (2017). Using nitrification inhibitors to mitigate agricultural N2O emission: a double-edged sword? *Global Change Biology*, *23*(2), 485–489. https://doi.org/10.1111/gcb.13338

Ostrom, N. E., Sutka, R., Ostrom, P. H., Grandy, A. S., Huizinga, K. M., Gandhi, H., … Robertson, G. P. (2010). Isotopologue data reveal bacterial denitrification as the primary source of N2O during a high flux event following cultivation of a native temperate grassland. *Soil Biology and Biochemistry*, *42*(3), 499–506. https://doi.org/10.1016/j.soilbio.2009.12.003

Reay, D. S., Davidson, E. a., Smith, K. a., Smith, P., Melillo, J. M., Dentener, F., & Crutzen, P. J. (2012). Global agriculture and nitrous oxide emissions. *Nature Climate Change*, *2*(6), 410–416. https://doi.org/10.1038/nclimate1458

Smith, K. A. (2017). Changing views of nitrous oxide emissions from agricultural soil: key controlling processes and assessment at different spatial scales. *European Journal of Soil Science*, *68*(2), 137–155. https://doi.org/10.1111/ejss.12409

Stuchiner, E. R., Weller, Z. D., & Fischer, J. C. (2020). An approach for calibrating laser-based N 2 O isotopic analyzers for soil biogeochemistry research . *Rapid Communications in Mass Spectrometry*, (June 2020), 1–14. https://doi.org/10.1002/rcm.8978

Subbarao, G., Ito, O., Sahrawat, K., Berry, W., Nakahara, K., Ishikawa, T., … Rao, I. (2006). Scope and strategies for regulation of nitrification in agricultural systems - Challenges and

opportunities. *Critical Reviews in Plant Sciences*, *25*(4), 303–335. https://doi.org/10.1080/07352680600794232

Tian, H., Xu, R., Canadell, J. G., Thompson, R. L., Winiwarter, W., Suntharalingam, P., … Yao, Y. (2020). A comprehensive quantification of global nitrous oxide sources and sinks. *Nature*, *586*(7828), 248–256. https://doi.org/10.1038/s41586-020-2780-0

Van Meter, K. J., Basu, N. B., Veenstra, J. J., & Burras, C. L. (2016). The nitrogen legacy: Emerging evidence of nitrogen accumulation in anthropogenic landscapes. *Environmental Research Letters*, *11*(3). https://doi.org/10.1088/1748-9326/11/3/035014

von Fischer, J. C., & Hedin, L. O. (2002). Separating methane production and consumption with a field-based isotope pool dilution technique. *Global Biogeochemical Cycles*, *16*(3), 8-1-8–13. https://doi.org/10.1029/2001gb001448

Yang, W. H., Teh, Y. A., & Silver, W. L. (2011). A test of a field-based 15N-nitrous oxide pool dilution technique to measure gross N2O production in soil. *Global Change Biology*, *17*(12), 3577–3588. https://doi.org/10.1111/j.1365-2486.2011.02481.

APPENDICES

APPENDIX 1 CHAPTER 2

Gas scrubbing system:

Below is a detailed description of the parts used in the gas scrubbing set-up that was described in Section 3.4. This set-up was adapted from Nathanial Ostrom and Hasand Gandhi (pers. comm.).

A series of traps is used to scrub the sample stream of CO_2, water vapor and other impurities. The traps are placed in the following sequence:

Sample bag/incubation jar → in-line particulate filter (7 micron) → Nafion Dryer → CO_2 sorbent trap → Silica gel/Activated charcoal →in-line particulate filter (7 micron) → LGR inlet

The following list details the specific traps used, and we have also included some more information about preparing the Silica gel/Activated charcoal trap for use:

1. Nafion Dryer: PERMA PURE LLC (732) 244-0010 (item # 1.00MD-110-144P-4, 144" Dryer 1/4 Poly Fit/Shell). Drying gas was UHP N_2 flowing at ~400 mL/minute.

2. CO_2 sorbent trap: 30 cm long Pyrex tube (3/8" OD, ¼" ID) filled with 25 cm of sorbent (Carbosorb, Elemental Microanalysis, item # B1237). Material is secured with a 2.5 cm plug of glass wool at both ends of tube.

3. Silica gel/Activated charcoal: 40 cm long Pyrex tube (3/8" OD, ¼" ID) filled with ~9 cm of activated charcoal (Sigma Aldrich, 242233-250G) and ~25 cm of silica gel, pore size 60A, 200-400 mesh particle size (Sigma Aldrich 288594-500G). The silica gel was conditioned by wrapping the silica gel portion of the tube with a heating tape and heating it to ~180°C while flowing UHP N_2 through the tube at ~100 mL/minute. The silica gel is conditioned (e.g., heated with UHP N_2 flowing through) for 24 hours, and then cooled for two hours under a UHP N_2 flow of ~100 mL/minute. Swagelok valves at the ends of this trap allow us to move and store the trap after conditioning. The ends are plugged with 2.5 cm of glass wool. See the picture below:

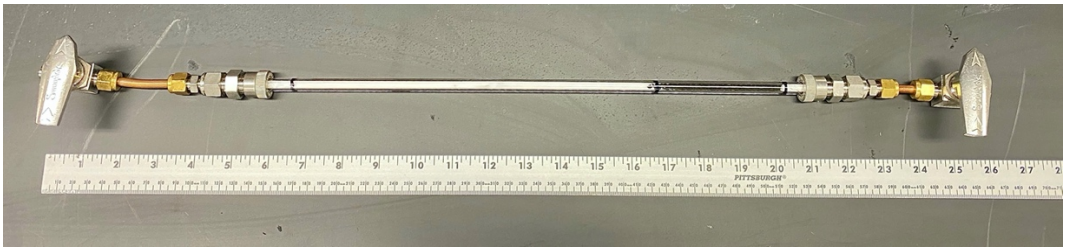

Appendix 1 Figure 1. Image of the silica gel & activated charcoal scrubber.

4. in-line particulate filter (7 micron, Swagelok, part number: SS-4F-7)

Dilution of primary standard (USGS52) for laboratory use:

The USGS52 primary standard was prepared for laboratory use by diluting it into commercially prepared zero-grade air (synthetic 80:20 N_2:O_2 blend, Airgas Inc., Radford, VA, USA). The standard was shipped to us sealed in a ~15cm long, ¼" diameter borosilicate glass tube. Dilution was achieved by breaking the glass tube of standard inside an evacuated 20-L portable air tank purchased from Harbor Freight Tools (Calabasas, CA, USA), which was sealed with a valve and accessed with ¼" Swagelok fittings.

To release the standard gas into the tank, the glass tube of the standard was first taped to a ~30 cm length of string and the tube and string were carefully lowered into the portable air tank. The tank was then evacuated to <400 microns. After the tank's valves were sealed, the tank was shaken vigorously until the glass tube containing the standard was heard to break. Finally, ~110 STP L of a commercially prepared cylinder of zero-grade air from Airgas Inc. was admitted and that gas was allowed to flow into the tank containing the standard until it was pressurized to 350 kPa. A metal frit filter (~1-micron nominal size) prevents glass fragments from exiting the standard gas tank.

Preparation of gas bags:

Standards of differing [N_2O] were prepared in gas bags. An Alicat Scientific mass flow controller (MFC) was programmed to administer zero-grade air (an 80:20 N_2 and O_2 blend) to

each gas bag at a rate of 1 standard L/min (SLPM). These MFCs can be programmed to administer gas mixtures (such as the zero-grade air described) over a 0-10 SLPM range. To fill the gas bag with 1 standard L, the valves connecting the zero-grade air cylinder to the MFC to the gas bag were opened and a stopwatch was set for 60 seconds. In some instances, it made more sense to fill a gas bag with 0.5 L of zero-air, in which case the stopwatch was set for 30 seconds. After the desired time period all the valves were closed and the opening to the gas bag (gas bags are outfitted with a two-way stopcock) was sealed. A syringe was then filled directly from the cylinder containing either primary or secondary standard and the desired amount of standard was injected into the gas bag. After that, the bags are ready for use.

Table 1 below details the amount of zero-grade air, standard, and the syringe volume (for the standard) required to prepare gas bags of the different N_2O concentrations that were used to develop the calibration algorithm. The volumes of zero-grade air and standard to use were determined with the following equation:

$$C_3 = (C_1V_1 * C_2V_2)/(V_1+V_2)$$

where C_3 is the final concentration in the gas bag, C_1 and V_1 are the concentration and volume of the primary or secondary standard, respectively, and C_2 and V_2 are the concentration and volume, respectively, of the zero-grade air.

Appendix 1 Table 1. Dilution of the 500ppm secondary standard into gas bags for calibrations.

[N_2O] in gas bag	Volume of zero-grade air added to bag (L)	Volume of 500 ppm standard added to bag (mL)	Syringe(s) used to add standard
300ppm	0.5	750	1-L, 60-mL syringes
280ppm	0.5	637	1-L, 60-mL syringes
240ppm	0.5	462	1-L, 60-mL, and 3-mL syringes
220ppm	0.5	393	1-L, 60-mL syringes
200ppm	0.5	334	1-L, 60-mL syringes
180ppm	0.5	282	1-L, 60-mL syringes
140ppm	1	389	1-L, 60-mL syringes
130ppm	1	352	1-L, 60-mL syringes
120ppm	1	316	1-L, 60-mL syringes
115ppm	1	299	1-L, 60-mL syringes
100pm	1	250	1-L, 60-mL syringes
90ppm	1	220	1-L, 30-mL syringes
80ppm	1	191	1-L, 60-mL syringes
70ppm	1	163	1-L, 60-mL, and 3-mL syringes
60ppm	1	136.5	1-L, 60-mL, and 1-mL syringes
50ppm	1	112	60-mL syringe
40ppm	1	87	60-mL syringe
30ppm	1	64	60-mL syringe, 3-mL syringes
20ppm	1	42	30-mL syringe
15ppm	1	31	30-mL, 3-mL syringes
10ppm	1	20.5	30-mL, 1-mL syringes
8ppm	1	16.3	30-mL, 1-mL syringes
5ppm	1	10.2	30-mL, 1-mL syringes
2ppm	1	4.1	30-mL, 1-mL syringes
1ppm	1	2.1	30-mL, 1-mL syringes
0.8ppm	1	1.6	30-mL, 1-mL syringes
0.4ppm	1	0.8	1-mL syringe
0.3ppm	1	0.6	1-mL syringe

[N_2O] residual percentage error:

Figure 2 shows histograms of the residual percentage error tended to be greater in the corrected low and high N_2O concentration values for the primary standard, rather than for the secondary standard (see Section 5.1).

We hypothesize that the greater percentage error in the corrected low and high primary standard N_2O values is because we prepared the primary standard in the lab rather than obtaining a commercially prepared standard, such as our secondary standard, which came from Airgas.

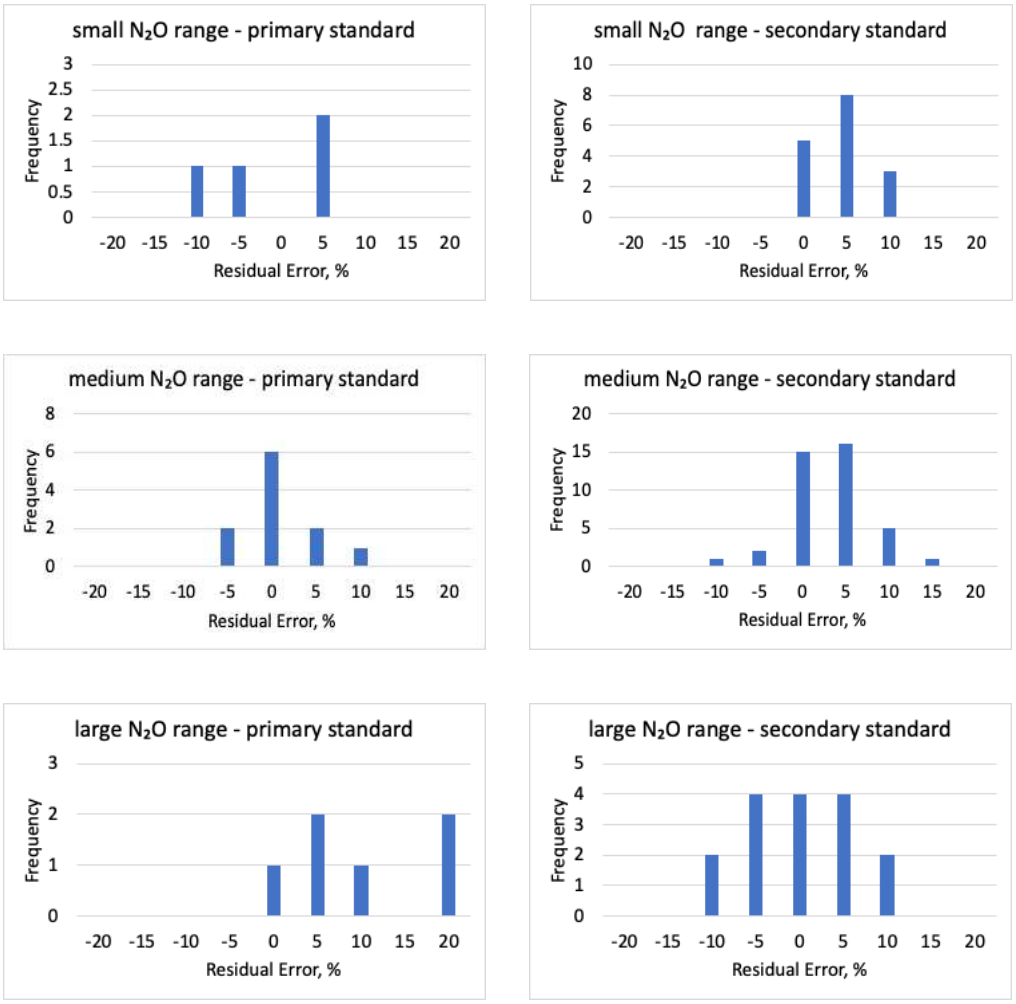

Appendix 1 Figure 2. Histograms of percentage residual error in standards across concentration ranges. There tends to be more error in the primary standard at low and high [N_2O].

APPENDIX 2 CHAPTER 3

Appendix 2 Text 1

Methods for measuring soil properties

Prior to freezing soils, we performed KCl extractions and calculated soil gravimetric water content. To quantify soil NH_4^+ and NO_3^- levels, we mixed 10 g soil subsamples with 50 mL 2M KCl, and they were shaken at 250 rpm for 1 hr, settled overnight, and then gravity filtered. Extracts were frozen and thereafter analyzed colorimetrically using an Alpkem FIA wet chemistry system (O.I. Analytical, College Station TX). We determined gravimetric water content by drying subsamples to a constant weight in a 105 °C oven.

After soils had been frozen, we measured soil pH, soil organic C and N (SOC and SON), and soil microbial biomass C and N (MBC and MBN). We created slurries of 1:10 soil to DI water and then measured soil pH with a benchtop meter (Thermo Scientific Orion Star™ A211 Benchtop pH Meter, Waltham, MA, USA). Frozen soil subsamples were dried in a 60 °C oven and then ground for SOC and SON analysis with a LECO Tru-Spec CN analyzer (Leco Corp., St. Joseph, MI, USA). Microbial biomass was extracted from 20 g frozen soil subsamples in 100 mL 0.5M K_2SO_4, and then solubilized in 1% chloroform. MBC and MBN were measured using a Shimadzu Total Organic Carbon analyzer that also measures ON (Shimadzu Scientific Instruments, Wood Dale, IL, USA). MBC and MBN were calculated as the differences between 1% chloroform slurry C or N and the extractable OC or ON concentration. SOC, SON, MBC, and MBN were only measured for soils collected in June 2018.

Frozen soils were overnight shipped on ice to Ward Laboratories Inc. (Kearney, NE, USA), where soil phospholipid fatty acids (PLFAs) were extracted, saponified, and methylated

to form fatty acid methyl esters (FAMEs) as in Allison et al. 2007. FAMEs were then identified and quantified using a capillary gas chromatograph. Ward Laboratories summed individual FAMEs into the following functional groups: Gram + bacteria, Gram – bacteria, arbuscular mycorrhizal fungi, saprophytes, protozoa, and undifferentiated using methods as in Allison et al. 2007, and afterwards we estimated total fungi:bacteria ratios for each soil.

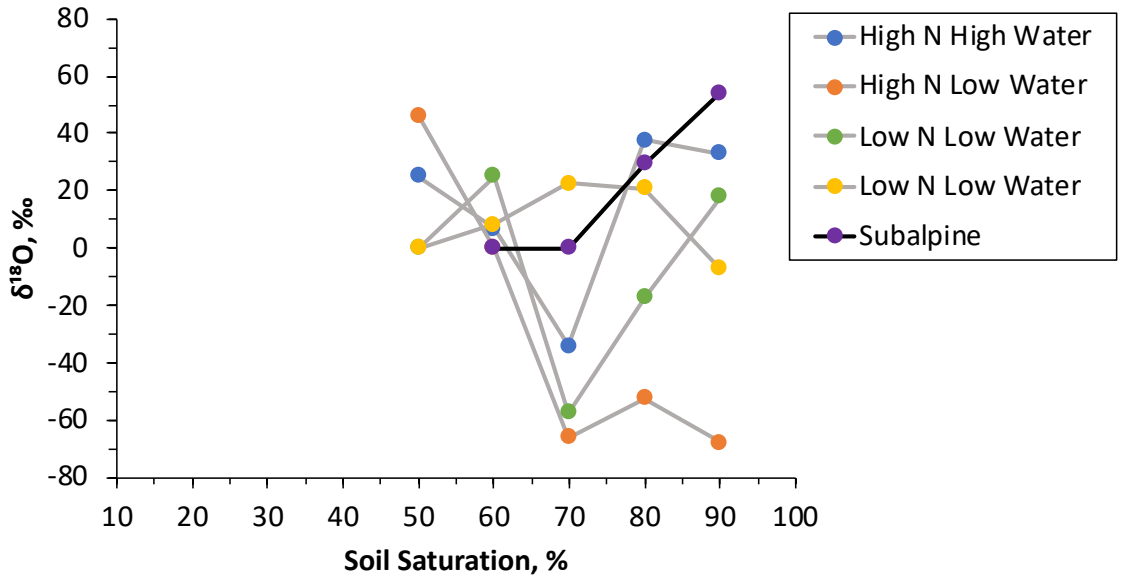

Appendix 2 Figure 1. $\delta^{18}O$ values for each soil held at the different soil saturations during the natural abundance incubations.

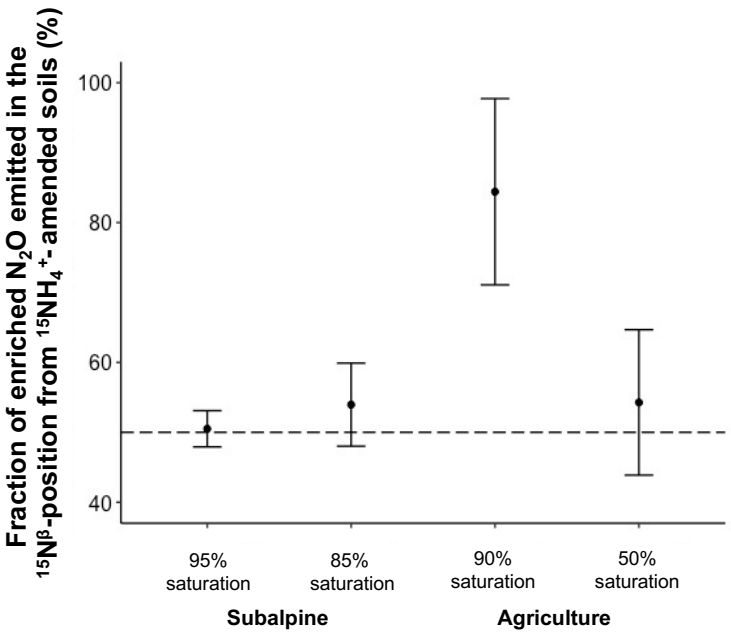

Appendix 2 Figure 2. Percent of emitted N_2O enriched in the β-position ($^{15}N—N—O$) from each $^{15}NH_4^+$-amended soil. Because very little of the emitted N_2O arose from $^{15}NH_4^+$ transformations (see Figure 5 in main text) we focused our analyses primarily on the $^{15}NO_3^-$ transformations, but it is worth noting that the β-position enrichment is more variable in the $^{15}NH_4^+$-amended soils, and there might be a yet-discovered biological reason for this. In all cases n = 4, and bars represent a 95% CI around the mean. The dotted line crosses at 50%, illustrating that unlike the $^{15}NO_3^-$-amended soils, the $^{15}NH_4^+$-amended soils did not show as coherent differences in emitted N_2O enriched in the α vs. β position.

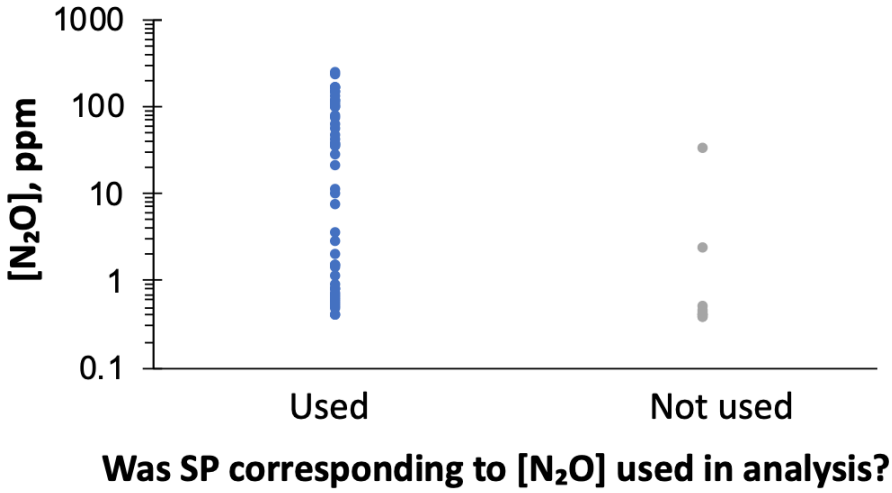

Appendix 2 Figure 3. The [N_2O] that correspond to used and not used SP values for our natural abundance dataset. For the natural abundance dataset, each reported SP has a corresponding [N_2O], but as Stuchiner et al. (2020) stipulates, sometimes if [N_2O] is very low or an instrument error occurs, SP values can get reported that are biologically implausible. Mean [N_2O] for the used SP values was ~52ppm, whereas mean [N_2O] for the not used SP values was ~3.8ppm. Only biologically plausible (see Methods 3.2.2) SP values were included in our data analysis, and this figure illustrates the [N_2O] at which SP values were used or not. While some low [N_2O] SP values were used, most of the unused SP values are from soils that emitted low concentrations of N_2O (< 2ppm). However, there is one instance where a soil emitted ~32 ppm but the reported SP value was -76‰ (see Appendix 2 Table 1), which we deem biologically implausible based on reported literature values plus uncertainty (Hu et al. 2015). *Note the log-transformed y-axis*.

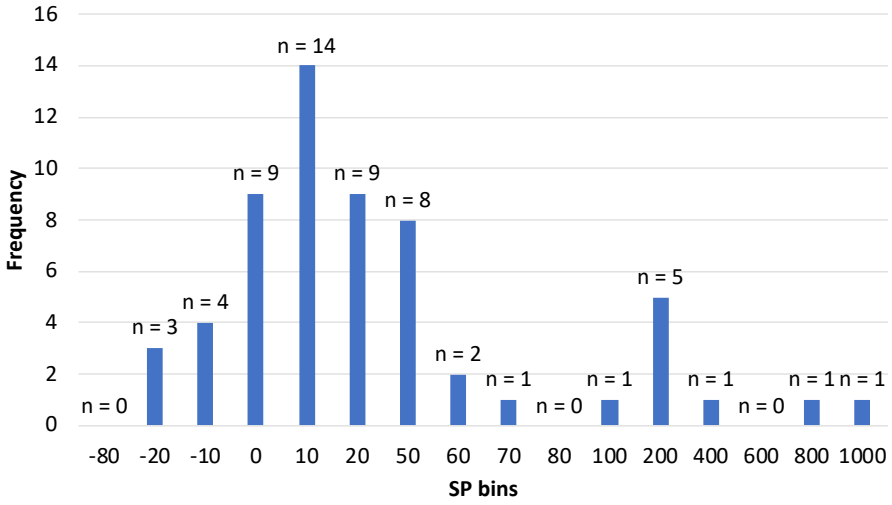

Appendix 2 Figure 4. The frequency at which our LGR N_2O isotopic analyzer reported SP values in certain ranges from our natural abundance dataset. Most SP values ranged from -20 to 80‰.

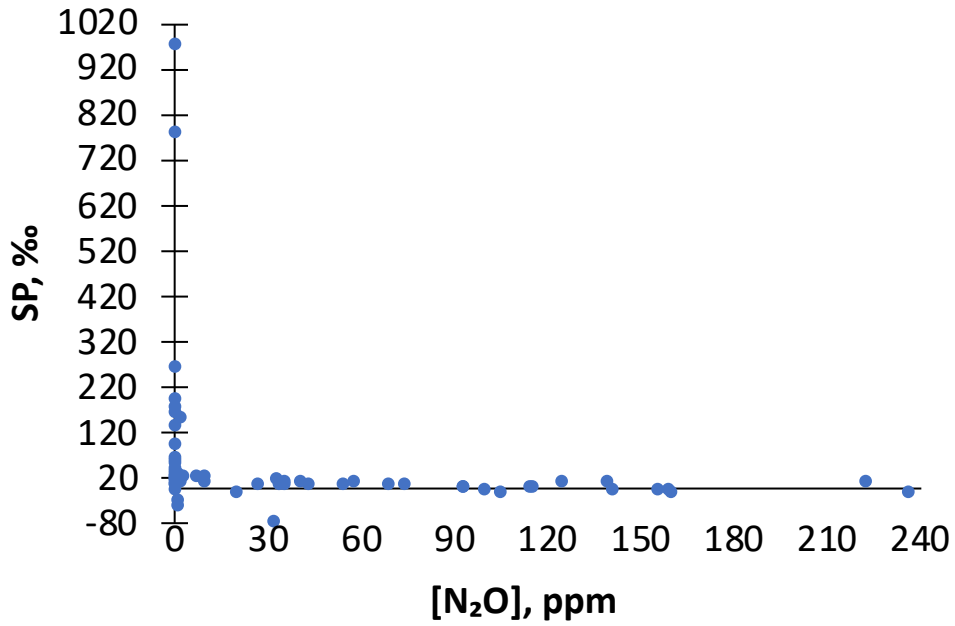

Appendix 2 Figure 5. SP vs. N_2O concentration for our natural abundance dataset. This illustrates that we see anomalously high SP values almost exclusively at the lowest N_2O concentrations, which aligns with what we find in Stuchiner et al. (2020). Consequently, we excluded these values from our analysis.

Appendix 2 Table 1. All SP data from soils held at 50% saturation and higher. We constrained our range of useable SP values from -40 to 65‰ to include any reported literature values plus uncertainty (Hu et al. 2015). Excluded SP values were biologically infeasible, likely due to low N_2O concentration or instrument error. Highlighted values were excluded from analysis. This data is also represented in Appendix 2 Figure 3 to illustrate that most of the unused data had low [N_2O], which can result in implausible isotopomer readings (Stuchiner et al. 2020).

Site	Soil	Soil saturation (%)	Headspace N_2O concentration (ppm)	SP (‰)
Agriculture	HNHW	50	0.38	780.4
Agriculture	HNHW	50	0.58	64.7
Agriculture	HNHW	50	0.40	263.1
Agriculture	HNLW	50	0.48	-6.6
Agriculture	HNLW	50	0.79	20.9
Agriculture	LNHW	50	0.52	6.4
Agriculture	LNHW	50	0.61	31.3
Agriculture	LNHW	50	0.56	18.2
Agriculture	LNLW	50	0.45	52.7
Agriculture	LNLW	50	0.63	4.0
Agriculture	HNHW	60	0.38	970.7
Agriculture	HNHW	60	0.76	56.9
Agriculture	HNHW	60	0.44	131.3
Agriculture	HNLW	60	0.70	17.1
Agriculture	HNLW	60	1.47	-31.6
Agriculture	LNHW	60	20.37	-16.0
Agriculture	LNHW	60	7.18	21.1
Agriculture	LNHW	60	1.35	-40.8
Agriculture	LNLW	60	0.88	3.2
Agriculture	LNLW	60	1.45	20.2
Agriculture	HNHW	70	9.79	21.6
Agriculture	HNHW	70	1.90	29.2
Agriculture	HNHW	70	10.50	11.3
Agriculture	HNLW	70	32.80	-76.0
Agriculture	HNLW	70	36.24	6.9
Agriculture	LNHW	70	41.23	7.3
Agriculture	LNHW	70	99.99	-9.6
Agriculture	LNHW	70	36.06	4.1
Agriculture	LNLW	70	58.47	6.8
Agriculture	LNLW	70	69.83	4.2
Agriculture	HNHW	80	139.90	10.9
Agriculture	HNHW	80	33.58	14.9
Agriculture	HNHW	80	93.50	-1.1
Agriculture	HNLW	80	114.75	-2.9
Agriculture	HNLW	80	156.22	-9.9
Agriculture	LNHW	80	159.64	-8.5
Agriculture	LNHW	80	105.59	-11.5
Agriculture	LNHW	80	34.19	1.8
Agriculture	LNLW	80	160.12	-13.4
Agriculture	LNLW	80	54.75	5.9
Agriculture	HNHW	90	223.16	6.7
Agriculture	HNHW	90	125.46	11.6
Agriculture	HNHW	90	141.80	-9.8
Agriculture	HNLW	90	115.61	-4.1
Agriculture	HNLW	90	93.26	-1.4
Agriculture	LNHW	90	237.22	-15.8
Agriculture	LNHW	90	44.01	2.6
Agriculture	LNLW	90	74.38	1.8
Agriculture	LNLW	90	27.26	4.7
Subalpine	Subalpine	50	0.42	89.0
Subalpine	Subalpine	50	0.37	189.1
Subalpine	Subalpine	60	0.37	161.6
Subalpine	Subalpine	60	0.39	38.3
Subalpine	Subalpine	70	0.39	28.4
Subalpine	Subalpine	70	0.49	172.8
Subalpine	Subalpine	80	2.70	12.0
Subalpine	Subalpine	80	2.23	148.1
Subalpine	Subalpine	90	3.46	19.1
Subalpine	Subalpine	90	1.06	14.9

Appendix 2 Table 2. Sample size information for all the natural abundance soil incubations. Note that for soil saturations 10-40%, n =3 in all cases, but none of these saturations were included in the SP analysis because [N_2O] was too low to yield reliable SP values (all [N_2O] < 0.7 ppm). Only soil saturations from the final SP analysis were included in this table (which is why only 60-90% saturation incubations are included for the subalpine soil). The reason why n < 3 for certain 50-90% soil saturations is because SP values were removed if they were deemed biologically implausible (see Methods 2.2.2 for details regarding SP removal criteria).

Site	Soil type	Soil saturation (%)	Sample size (n)
Agriculture	HNHW	50	1
		60	1
		70	3
		80	3
		90	3
Agriculture	HNLW	50	2
		60	2
		70	1
		80	2
		90	2
Agriculture	LNHW	50	3
		60	3
		70	3
		80	3
		90	2
Agriculture	LNLW	50	2
		60	2
		70	2
		80	2
		90	2
Subalpine	Subalpine	60	1
		70	1
		80	1
		90	2

Appendix 2 Table 3. The $\delta^{15}N^{\alpha}$, $\delta^{15}N^{\beta}$, and SP values for the $^{15}NO_3^-$-amended soils. Note that because most emitted N_2O was enriched in the β-position, the resulting SP values are far more negative than natural abundance-level fractionation expectations. *Note: because the enriched incubations only used one soil type from each site, soil type also corresponds to source location in this case.*

Soil type	Soil saturation (%)	$\delta^{15}N^{\alpha}$ (‰)	$\delta^{15}N^{\beta}$ (‰)	SP (‰)
HNHW	90	2310.88	3648.99	-1338.11
HNHW	90	1790.23	2559.24	-769.01
HNHW	90	1867.93	2761.41	-893.48
HNHW	90	1805.16	2601.24	-796.09
HNHW	50	746.87	859.32	-112.45
HNHW	50	737.05	873.08	-136.03
HNHW	50	539.46	644.63	-105.17
Subalpine	95	924.07	1077.49	-157.93
Subalpine	95	795.14	928.94	-139.14
Subalpine	95	2213.36	2530.91	-358.42
Subalpine	95	2203.63	2529.63	-361.19
Subalpine	85	736.65	886.74	-152.37
Subalpine	85	728.04	879.53	-153.68
Subalpine	85	704.61	863.63	-161.01
Subalpine	85	673.78	821.53	-149.67

Appendix 2 Table 4. The amount of $^{15}NO_3^-$ and $^{15}NH_4^+$ added to the subalpine and agricultural soils. We include the g of each tracer dissolved into a specific amount of DI water. For the different soils, the amount of stable isotope tracer is diluted into a different volume of water to accommodate the amount of water we needed to add to each soil to bring the soil to its desired saturation (see Methods 3.1.3 for details). Stable isotope solutions were made by dissolving powdered stable isotope tracer ($Na^{15}NO_3^-$ and $^{15}NH_4^+Cl$) in DI water and serially diluting each tracer to the desired concentration (double the ^{15}N pool size for $^{15}NO_3^-$ and $^{15}NH_4^+$ in each soil, see Methods 3.2.1 for details).

	Subalpine soil (g tracer added)	HNHW Agriculture soil (g tracer added)
$^{15}NH_4Cl$	1.16E-06	8.44E-07
$Na^{15}NO_3$	3.13E-07	2.46E-05

	Subalpine soil (mL DI water used to dissolve tracer)	HNHW Agriculture soil (mL DI water used to dissolve tracer)
$^{15}NH_4Cl$	10	4
$Na^{15}NO_3$	10	4

APPENDIX 3 CHAPTER 4

Appendix 3 Table 1. Numbers of replicates (n) for all soil and microbial genetic properties measured before or after soil incubations (all properties from Figure 4.2 in Chapter 4). Unless otherwise stated, n-values are the same for a given property across all soils tested. The n-values for all properties measured before incubations correspond to technical replicates from each bulked and homogenized soil. The n-values for all properties measured after incubation correspond to technical replicates from bulked and homogenized soils from incubation jars from the same treatment. For example, the contents from all the +OC Shortgrass prairie jars would be combined into one Ziploc bag and homogenized, whereas the contents from all the Control Shortgrass prairie jars would be combined into one Ziploc bag and homogenized, and so on for all the other soils tested. *Note: soil NO_3^- and NH_4^+ concentrations are measured before and after incubations. The before-incubations n-values are included in Figure 4.3 in the main text of this paper, whereas the after-incubations n-values are included here.*

Property measured	**Units of measured property**	**n-value**	**Measured before or after soil incubations?**
Soil organic carbon (SOC)	Percent, %	5, except n = 4 for: - Minnesota cornfield - Coniferous forest	Before
Soil organic nitrogen (SON)	Percent, %	5, except n = 4 for: - Minnesota cornfield - Coniferous forest	Before
Soil pH	Percent H^+	5	Before
Microbial respiration	μg CO_2-C * g $soil^{-1}$ day^{-1}	6	After
Soil [NO_3^-]	μg N * g dry $soil^{-1}$ day^{-1}	3	After
Soil [NH_4^+]	μg N * g dry $soil^{-1}$ day^{-1}	3	After
nosZ:nirK	Ratio (of log_{10} gene copy numbers)	4	After
nifH	Log_{10} gene copy number	3, except n = 4 for: - +OC Colorado cornfield - Control Coniferous forest - Control Alpine meadow - +OC Urban Lawn - Control Urban Lawn	After

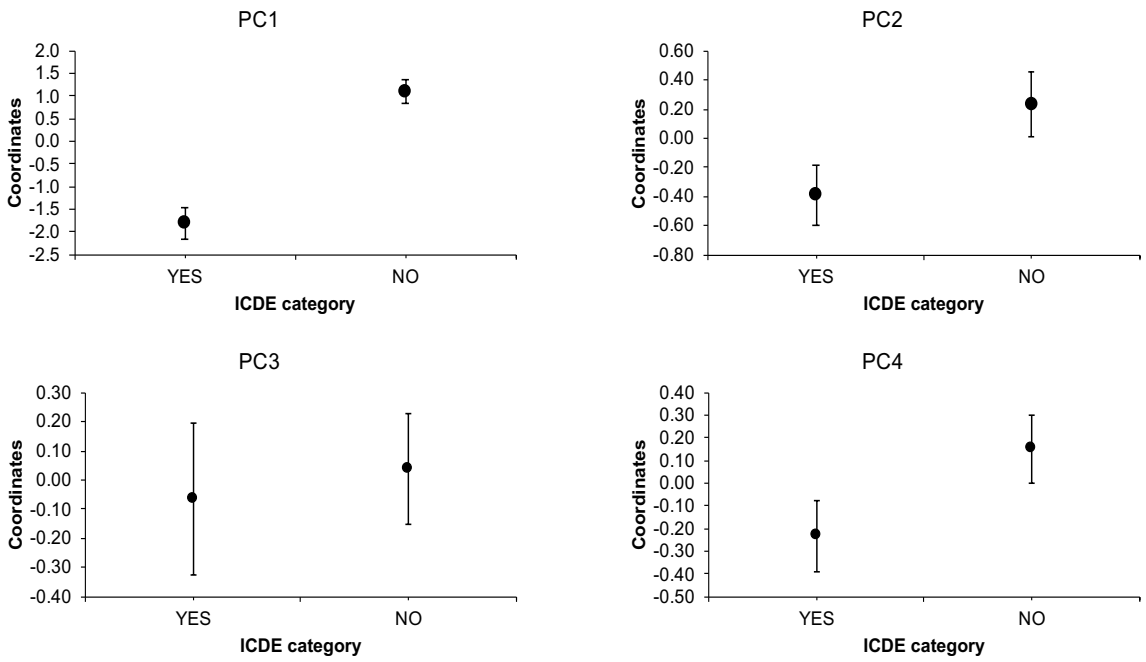

Appendix 3 Figure 1. T-tests comparing Yes vs. No ICDE mean coordinate loadings among the properties used in the Principal Components Analysis (PCA) in this study. Only PC1 yielded significant differences in mean loading for Yes vs. No ICDE ($p < 0.0001$), however PC2 yielded borderline significant differences in mean loading for Yes vs. No ICDE ($p = 0.07$). In all cases $n = 18$ for Yes ICDE coordinates, and $n = 30$ for No ICDE coordinates. Error bars are ± one SE from the mean.

APPENDIX 4 CHAPTER 5

Appendix 4 Table 1. These are the n-values for the clade II nosZ Δ values used in the PCA (Figure 5 in the main text).

Soil	N-value for PCA
Conventional cornfield-Low OC	4
Conventional cornfield-Medium OC	5
Conventional cornfield-High OC	5
Limited irrigation cornfield-Low OC	4
Limited irrigation cornfield-Medium OC	5
Limited irrigation cornfield-High OC	5
Shortgrass prairie-Low OC	4
Shortgrass prairie-Medium OC	4
Shortgrass prairie-High OC	5
Desert shrubland-Low OC	4
Desert shrubland-Medium OC	4
Desert shrubland-High OC	4
Desert grassland-Low OC	5
Desert grassland-Medium OC	4
Desert grassland-High OC	4
Subalpine forest-Low OC	4
Subalpine forest-Medium OC	4
Subalpine forest-High OC	5
Alpine meadow-Low OC	4
Alpine meadow-Medium OC	5
Alpine meadow-High OC	5

Appendix 4 Table 2. The n-values for Δ clade II nosZ gene abundances.

Soil	N-value for PCA
Conventional cornfield-Low OC	11
Conventional cornfield-Medium OC	12
Conventional cornfield-High OC	13
Limited irrigation cornfield-Low OC	11
Limited irrigation cornfield-Medium OC	14
Limited irrigation cornfield-High OC	13
Shortgrass prairie-Low OC	11
Shortgrass prairie-Medium OC	12
Shortgrass prairie-High OC	13
Desert shrubland-Low OC	12
Desert shrubland-Medium OC	12
Desert shrubland-High OC	12
Desert grassland-Low OC	13
Desert grassland-Medium OC	12
Desert grassland-High OC	12
Subalpine forest-Low OC	11
Subalpine forest-Medium OC	11
Subalpine forest-High OC	13
Alpine meadow-Low OC	10
Alpine meadow-Medium OC	12
Alpine meadow-High OC	13